TARGETING INDOLEAMINE 2,3-DIOXYGENASES AND TRYPTOPHAN DIOXYGENASE FOR CANCER IMMUNOTHERAPY

EDITED BY: Lieve Brochez, Alexander J. Muller, Dirk Schadendorf Schadendorf, George C. Prendergast and Vibeke Kruse

PUBLISHED IN: Frontiers in Immunology and Frontiers in Oncology

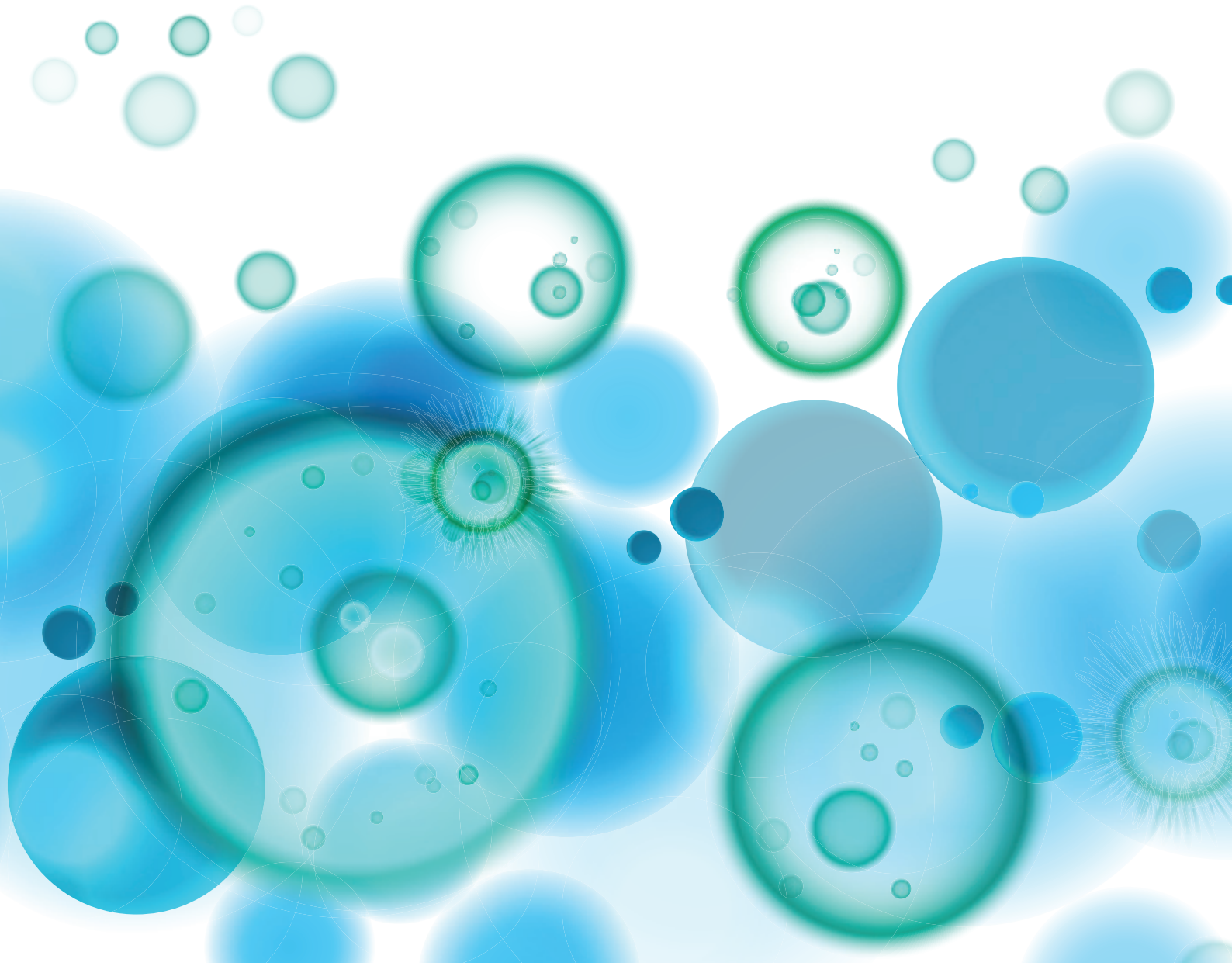

frontiers Research Topics

frontiers

ISSN 1664-8714
ISBN 978-2-88974-297-4
DOI 10.3389/978-2-88974-297-4

About Frontiers

Frontiers is more than just an open-access publisher of scholarly articles: it is a pioneering approach to the world of academia, radically improving the way scholarly research is managed. The grand vision of Frontiers is a world where all people have an equal opportunity to seek, share and generate knowledge. Frontiers provides immediate and permanent online open access to all its publications, but this alone is not enough to realize our grand goals.

Frontiers Journal Series

The Frontiers Journal Series is a multi-tier and interdisciplinary set of open-access, online journals, promising a paradigm shift from the current review, selection and dissemination processes in academic publishing. All Frontiers journals are driven by researchers for researchers; therefore, they constitute a service to the scholarly community. At the same time, the Frontiers Journal Series operates on a revolutionary invention, the tiered publishing system, initially addressing specific communities of scholars, and gradually climbing up to broader public understanding, thus serving the interests of the lay society, too.

Dedication to Quality

Each Frontiers article is a landmark of the highest quality, thanks to genuinely collaborative interactions between authors and review editors, who include some of the world's best academicians. Research must be certified by peers before entering a stream of knowledge that may eventually reach the public - and shape society; therefore, Frontiers only applies the most rigorous and unbiased reviews.
Frontiers revolutionizes research publishing by freely delivering the most outstanding research, evaluated with no bias from both the academic and social point of view. By applying the most advanced information technologies, Frontiers is catapulting scholarly publishing into a new generation.

What are Frontiers Research Topics?

Frontiers Research Topics are very popular trademarks of the Frontiers Journals Series: they are collections of at least ten articles, all centered on a particular subject. With their unique mix of varied contributions from Original Research to Review Articles, Frontiers Research Topics unify the most influential researchers, the latest key findings and historical advances in a hot research area! Find out more on how to host your own Frontiers Research Topic or contribute to one as an author by contacting the Frontiers Editorial Office: frontiersin.org/about/contact

TARGETING INDOLEAMINE 2,3-DIOXYGENASES AND TRYPTOPHAN DIOXYGENASE FOR CANCER IMMUNOTHERAPY

Topic Editors:
Lieve Brochez, Ghent University, Belgium
Alexander J. Muller, Lankenau Institute for Medical Research, United States
Dirk Schadendorf Schadendorf, Essen University Hospital, Germany
George C. Prendergast, Lankenau Institute for Medical Research, United States
Vibeke Kruse, Ghent University Hospital, Belgium

Topic Editor Dr. Alexander J. Muller receives financial support by IO Biotech company. All other Topic Editors declare no competing interests with regards to the Research Topic subject.

Citation: Brochez, L., Muller, A. J., Schadendorf, D. S., Prendergast, G. C., Kruse, V., eds. (2022). Targeting Indoleamine 2,3-dioxygenases and Tryptophan Dioxygenase for Cancer Immunotherapy. Lausanne: Frontiers Media SA.
doi: 10.3389/978-2-88974-297-4

Table of Contents

frontiers in Immunology

EDITORIAL
published: 06 December 2021
doi: 10.3389/fimmu.2021.789473

Editorial: Targeting Indoleamine 2,3-dioxygenases and Tryptophan Dioxygenase for Cancer Immunotherapy

Lieve Brochez[1], Vibeke Kruse[2], Dirk Schadendorf[3], Alexander J. Muller[4] and George C. Prendergast[4]**

[1] Department of Dermatology, University Hospital Ghent and Cancer Research Institute Ghent (CRIG), Ghent, Belgium, [2] Department of Medical Oncology, University Hospital Ghent and Cancer Research Institute Ghent (CRIG), Ghent, Belgium, [3] Department of Dermatology and Comprehensive Cancer Center, University Hospital Essen, Essen, Germany, [4] Lankenau Institute for Medical Research, Wynnewood, PA, United States

Keywords: IDO, TDO, cancer immunology, immunotherapy, immunometabolism

OPEN ACCESS

Edited and reviewed by:
Katy Rezvani,
University of Texas MD Anderson Cancer Center, United States

****Correspondence:***
Lieve Brochez
lieve.brochez@ugent.be
George C. Prendergast
prendergast@limr.org

Specialty section:
This article was submitted to Cancer Immunity and Immunotherapy, a section of the journal Frontiers in Immunology

Received: *05 October 2021*
Accepted: *19 October 2021*
Published: *06 December 2021*

Citation:
Brochez L, Kruse V, Schadendorf D, Muller AJ and Prendergast GC (2021) Editorial: Targeting Indoleamine 2,3-dioxygenases and Tryptophan Dioxygenase for Cancer Immunotherapy. Front. Immunol. 12:789473. doi: 10.3389/fimmu.2021.789473

Editorial on the Research Topic

Targeting Indoleamine 2,3-dioxygenases and Tryptophan Dioxygenase for Cancer Immunotherapy

Immunometabolism is emerging as a core element in cancer, both in the pathophysiological equation that yields malignancy and in the therapeutic equation that yields curative efficacy. In particular, the tryptophan catabolic enzyme IDO1 has attracted much attention as a functional biomarker and therapeutic target in many cancers, with increasing notice of TDO, IDO2 (IDO/TDO enzymes), along with TPH and IL4I1 as additional tryptophan-degrading enzymes that drive malignancy and impede therapy *via* enzymatic and non-enzymatic processes like IDO1. A rapidly growing literature reveals multiple mechanisms through which these bad actors subvert tumor microenvironments to drive disease, most notably by tolerizing the immune system to tumor antigens, but also by enhancing tumor-feeding inflammatory signals and abnormal vascular networks. While initially focused on IDO1, which multiple studies have correlated with negative clinical outcomes (1), the full scope of drug discovery and development efforts now encompasses all these tryptophan-degrading enzymes, reinforced in part in 2018 by the negative readout of a large but flawed Phase 3 trial of the IDO1-selective inhibitor epacadostat in combination with the PD1 antibody pembrolizumab in stage IV melanoma (2). It is clear further insights into the expression and function of IDO1 and other tryptophan-degrading enzymes is needed in cancer.

This Research Topic includes two reviews on IDO/TDO enzymes in cancer. Zhai et al. survey IDO1-mediated immunosuppression in advanced brain tumors (glioblastomas), where IDO1 elevation synergizes with naturally occurring elevation of IDO1 in the central nervous system during aging. Notably, findings presented argue that immunotherapeutic efficacy in this setting requires neutralization of both the enzyme-dependent and enzyme-independent functions of IDO1. While enzyme inhibitors lack dual-targeting capability, vaccine approaches to eliminate IDO1 protein may be useful in this challenging disease setting (3, 4). Meireson et al. reviewed induction mechanisms and distinct functions of IDO1 in different compartments of the tumor microenvironment, including tumor cells, tumor stromal fibroblasts, endothelial, immune and

mesenchymal cells, and peripheral blood. This group has recently published data on the clinical importance of IDO1 expression and its IFNγ-induced upregulation in peripheral blood monocytes in early stage melanoma (5).

Genetic experiments in mice support the likelihood that IDO1 functions in both tumor cells and stromal immune cells to drive immunosuppression (6). A recent extension of these genetic studies suggests that IDO1 may drive metastatic growth by enabling tumor neovascularization, through an innate inflammatory pathway distinct from adaptive immune control (7, 8). The complexity revealed in diverse patterns of IDO1 expression in human tumors may impact how IDO1 blockade influences therapeutic responses in different drug combination contexts.

This Research Topic also includes six research reports on IDO/TDO enzymes in cancer, four of which address the potential prognostic utility of IDO/TDO expression in various disease settings. Herrera-Rios et al. studied IDO1 expression in brain metastases of human melanoma. As noted by Zhai et al., the immunosuppressive properties of brain parenchyma differ from the rest of the body. Here a comparative tissue analysis identified macrophages/microglia as the major source of IDO1 expression, which was observed to correlate with a specific reduction in cytotoxic CD8+ T cells. Thüring et al. conducted a pilot clinical study of IDO1 gene expression in urine obtained from prostate cancer patients undergoing radical prostatectomy, where they observed evidence of a correlation with Gleason progression score. In human hepatocellular carcinoma, Chinnadurai et al. implicated IDO1 and PD-L1 as players in T cell suppression in this setting by investigating RNA expression of IDO/TDO and a set of B7 ligands. Lastly, in a retrospective study of non-small cell lung cancer (NSCLC), Mandarano et al. report a correlation between elevated levels of IDO2 and poor prognosis, a finding recently confirmed by another group (9).

Two studies in this Research Topic probed the relationship between IDO/TDO enzymes and therapeutic response. In the Lewis model of lung cancer, Zhang et al. combined a targeted IDO1 siRNA with photothermal therapy (PTT), an irradiative modality that may engage an abscopal mechanism of antitumor immunity. Using a nanocarrier approach to coordinately deliver the siRNA and enable tumor heating, the authors observed that IDO1 downregulation stimulated antitumor immunity in combination with PTT (which appears to act by stimulating tumor cell apoptosis). These findings extend the evidence that the efficacy of specific anti-cancer regimens such as PTT can be improved by IDO1 blockade (1, 10). Botticelli et al. studied patients with NSCLC, renal cell carcinoma (RCC) or head and neck squamous carcinoma (HNSCC) who were treated with anti-PD1 after failing first-line therapy. Their findings suggested a correlation between elevated serum Kyn/Trp ratio and early progressors in squamous and non-squamous NSCLC. Further, they observed a trend toward longer progression-free survival when the serum Kyn/Trp ratio was determined to be at normal baseline levels. These observations align with other findings where baseline Kyn/Trp levels, but also increased levels at week 4 of anti-PD1 immunotherapy, were associated with decreased survival in melanoma and renal cell carcinoma (11). In the study from Botticelli et al., while some correlation to gender, site of metastasis, NSCLC and squamous histology was observed, the suggestive data obtained will require follow up in larger studies. Contextually focused studies such as these are critical to informing how treatments targeting IDO/TDO enzymes can be best leveraged for future clinical success.

AUTHOR CONTRIBUTIONS

GP and LB composed the text. All authors contributed to the article and approved the submitted version.

FUNDING

GP acknowledges generous support for IDO/TDO studies over nearly two decades by NIH grants R01 CA109542, R01 CA191191 and R21 CA 159337 and support from the U.S. Department of Defense Breast Cancer Research Program, American Lung Association, Dan and Florence Green Foundation, Charlotte Geyer Foundation, Pardee Foundation, W.W. Smith Trust, New Link Genetics Corporation, Lankenau Medical Center Foundation and Main Line Health. This funding was not related to the writing of this Editorial. This research program has benefited from long-standing productive collaborations with Alexander Muller, James DuHadaway, Lisa Laury-Kleintop and Laura Mandik-Nayak and many others at Lankenau. LB: Part of this research was supported by 'Kom Op tegen Kanker' (Stand up against Cancer).

ACKNOWLEDGMENTS

LB is a skin cancer specialist at the Ghent University Hospital and the Cancer Research Institute Ghent (CRIG) with interest in translational cancer immunology and a special focus on IDO.

REFERENCES

1. Brochez L, Chevolet I, Kruse V. The Rationale of Indoleamine 2,3-Dioxygenase Inhibition for Cancer Therapy. *Eur J Cancer* (2017) 76:167–82. doi: 10.1016/j.ejca.2017.01.011
2. Muller AJ, Manfredi MG, Zakharia Y, Prendergast GC. Inhibiting IDO Pathways to Treat Cancer: Lessons From the ECHO-301 Trial and Beyond. *Semin Immunopathol* (2019) 41:41–8. doi: 10.1007/s00281-018-0702-0
3. Dey S, Sutanto-Ward E, Kopp KL, DuHadaway J, Mondal A, Ghaban D, et al. Peptide Vaccination Directed Against IDO1-Expressing Immune Cells Elicits CD8(+) and CD4(+) T-Cell-Mediated Antitumor Immunity and Enhanced Anti-PD1 Responses. *J Immunother Cancer* (2020) 8:e000605. doi: 10.1136/jitc-2020-000605
4. Andersen MH, Svane IM. Indoleamine 2,3-Dioxygenase Vaccination. *Oncoimmunology* (2015) 4:e983770. doi: 10.4161/2162402X.2014.983770
5. Meireson A, Ferdinande L, Haspeslagh M, Hennart B, Allorge D, Ost P, et al. Clinical Relevance of Serum Kyn/Trp Ratio and Basal and IFNgamma-

Upregulated IDO1 Expression in Peripheral Monocytes in Early Stage Melanoma. *Front Immunol* (2021) 12:736498. doi: 10.3389/fimmu.2021.736498
6. Muller AJ, DuHadaway JB, Chang MY, Ramalingam A, Sutanto-Ward E, Boulden J, et al. Non-Hematopoietic Expression of IDO Is Integrally Required for Inflammatory Tumor Promotion. *Cancer Immunol Immunother* (2010) 59:1655–63. doi: 10.1007/s00262-010-0891-4
7. Mondal A, Smith C, DuHadaway JB, Sutanto-Ward E, Prendergast GC, Bravo-Nuevo A, et al. IDO1 Is an Integral Mediator of Inflammatory Neovascularization. *EBioMedicine* (2016) 14:74–82. doi: 10.1016/j.ebiom.2016.11.013
8. Dey S, Mondal A, DuHadaway JB, Sutanto-Ward E, Laury-Kleintop LD, Thomas S, et al. IDO1 Signaling Through GCN2 in a Subpopulation of Gr-1 (+) Cells Shifts the IFNgamma/IL6 Balance to Promote Neovascularization. *Cancer Immunol Res* (2021) 9:514–28. doi: 10.1158/2326-6066.CIR-20-0226
9. Ma W, Liang J, Liu J, Tian D, Chen Z. Establishment and Validation of an Eight-Gene Metabolic-Related Prognostic Signature Model for Lung Adenocarcinoma. *Aging (Albany NY)* (2021) 13:8688–705. doi: 10.18632/aging.202681
10. Muller AJ, Prendergast GC. Marrying Immunotherapy With Chemotherapy: Why Say IDO? *Cancer Res* (2005) 65:8065–8. doi: 10.1158/0008-5472.CAN-05-2213
11. Li H, Bullock K, Gurjao C, Braun D, Shukla SA, Bosse D, et al. Metabolomic Adaptations and Correlates of Survival to Immune Checkpoint Blockade. *Nat Commun* (2019) 10:4346. doi: 10.1038/s41467-019-12361-9

Conflict of Interest: LB has participated in an advisory board to Incyte Inc. on epacadostat in melanoma and was invited to give a MSL seminar to Incyte Inc. on IDO (2017). GP declares a conflict of interest due to his role as a co-inventor in the discovery and development of IDO/TDO inhibitor technologies patented by the Lankenau Institute for Medical Research and licensed to Duet Therapeutics, Inc., a private company for which he serves presently as a scientific advisor.

The remaining authors declare that the research was conducted in the absence of any commercial or financial relationships that could be construed as a potential conflict of interest.

Publisher's Note: All claims expressed in this article are solely those of the authors and do not necessarily represent those of their affiliated organizations, or those of the publisher, the editors and the reviewers. Any product that may be evaluated in this article, or claim that may be made by its manufacturer, is not guaranteed or endorsed by the publisher.

frontiers in Immunology

ORIGINAL RESEARCH
published: 05 February 2020
doi: 10.3389/fimmu.2020.00120

Macrophages/Microglia Represent the Major Source of Indolamine 2,3-Dioxygenase Expression in Melanoma Metastases of the Brain

Dayana Herrera-Rios[1,2†], Sadaf S. Mughal[3†], Sarah Teuber-Hanselmann[4], Daniela Pierscianek[2,5], Antje Sucker[1,2], Philipp Jansen[1,2], Tobias Schimming[1,2], Joachim Klode[1,2], Julia Reifenberger[6], Jörg Felsberg[7], Kathy Keyvani[4], Benedikt Brors[3], Ulrich Sure[2,5], Guido Reifenberger[2,7], Dirk Schadendorf[1,2] and Iris Helfrich[1,2]*

[1] Skin Cancer Unit of the Dermatology Department, Medical Faculty, West German Cancer Center, University Duisburg-Essen, Essen, Germany, [2] German Cancer Consortium (DKTK), Partner Site Essen/Düsseldorf, Essen, Germany, [3] Division of Applied Bioinfomatics, German Cancer Research Center (DKFZ), Heidelberg, Germany, [4] Medical Faculty, West German Cancer Center, Institute of Neuropathology, University Duisburg-Essen, Essen, Germany, [5] Department of Neurosurgery, Medical Faculty, West German Cancer Center, University Duisburg-Essen, Essen, Germany, [6] Department of Dermatology, Medical Faculty, Heinrich Heine University, Düsseldorf, Germany, [7] Medical Faculty, Institute of Neuropathology, Heinrich Heine University, Düsseldorf, Germany

OPEN ACCESS

Edited by:
Zlatko Trajanoski, Innsbruck Medical University, Austria

Reviewed by:
María Marcela Barrio, Fundación Cáncer, Argentina
Per thor Straten, Herlev Hospital, Denmark

***Correspondence:**
Iris Helfrich
iris.helfrich@uk-essen.de

[†] *These authors have contributed equally to this work*

Specialty section:
This article was submitted to Cancer Immunity and Immunotherapy, a section of the journal Frontiers in Immunology

Received: *03 September 2019*
Accepted: *16 January 2020*
Published: *05 February 2020*

Citation:
Herrera-Rios D, Mughal SS, Teuber-Hanselmann S, Pierscianek D, Sucker A, Jansen P, Schimming T, Klode J, Reifenberger J, Felsberg J, Keyvani K, Brors B, Sure U, Reifenberger G, Schadendorf D and Helfrich I (2020) Macrophages/Microglia Represent the Major Source of Indolamine 2,3-Dioxygenase Expression in Melanoma Metastases of the Brain. Front. Immunol. 11:120. doi: 10.3389/fimmu.2020.00120

The manifestation of brain metastases in patients with advanced melanoma is a common event that limits patient's survival and quality of life. The immunosuppressive properties of the brain parenchyma are very different compared to the rest of the body, making it plausible that the current success of cancer immunotherapies is specifically limited here. In melanoma brain metastases, the reciprocal interplay between immunosuppressive mediators such as indoleamine 2, 3-dioxygenase (IDO) or programmed cell death-ligand 1 (PD-L1) in the context of neoplastic transformation are far from being understood. Therefore, we analyzed the immunoreactive infiltrate (CD45, CD3, CD8, Forkhead box P3 [FoxP3], CD11c, CD23, CD123, CD68, Allograft Inflammatory factor 1[AIF-1]) and PD-L1 with respect to IDO expression and localization in melanoma brain metastases but also in matched metastases at extracranial sites to correlate intra- and interpatient data with therapy response and survival. Comparative tissue analysis identified macrophages/microglia as the major source of IDO expression in melanoma brain metastases. In contrast to the tumor infiltrating lymphocytes, melanoma cells *per se* exhibited low IDO expression levels paralleled by cell surface presentation of PD-L1 in intracranial metastases. Absolute numbers and pattern of IDO-expressing cells in metastases of the brain correlated with recruitment and localization of $CD8^+$ T cells, implicating dynamic impact on the regulation of T cell function in the brain parenchyma. However, paired analysis of matched intra- and extracranial metastases identified significantly lower fractions of cytotoxic $CD8^+$ T cells in intracranial metastases while all other immune cell populations remain unchanged. In line with the already established clinical benefit for PD-L1 expression in extracranial melanoma metastases, Kaplan-Meier analyses correlated PD-L1 expression in brain metastases with favorable

outcome in advanced melanoma patients undergoing immune checkpoint therapy. In summary, our data provide new insights into the landscape of immunosuppressive factors in melanoma brain metastases that may be useful in the implication of novel therapeutic strategies for patients undergoing cancer immunotherapy.

Keywords: melanoma, brain metastases, IDO, immune checkpoint molecules, tumor-associated macrophages, immunogenic microenvironment

INTRODUCTION

The recent clinical success of cancer immunotherapies in patients suffering from malignant melanoma and other cancer types has revolutionized the therapeutic landscape of metastatic cancer. A major breakthrough has been achieved by the release of T cells from a suppressive "immune checkpoint," thereby allowing effective anti-tumor responses (1–3). Numerous clinical studies in metastatic cancer, including malignant melanoma, demonstrate high efficacy and manageable toxicity by using FDA-approved immune checkpoint inhibitors against the cytotoxic T lymphocyte antigen-4 (CTLA-4) and/or programmed cell death 1 (PD-1)/PD-1 ligand (PD-L1) axis; thus, immunotherapy has rapidly become a standard treatment modality in oncology. Recent data correlated clinical benefit of PD1/PD-L1 immune checkpoint inhibition with the expression level of membrane-associated PD-L1 on tumor cells, commonly induced by Interferon-γ (IFN-γ)-mediated signaling (3). Interestingly, lymphocytes of the tumor microenvironment (TME) represent the major source of IFN-γ secretion (4–6). IFN-γ is also a strong inducer of indoleamine 2, 3-dioxygenase (IDO), an enzyme initiating the first and rate-limiting step of tryptophan degradation along the kynurenine pathway (7–9). In 2014, preclinical data identified IDO for its mechanistic synergy with immune checkpoint inhibitors (10). IDO was shown to be a facilitator of cancer development by its role to exert a strong immuno-suppressive effect through local inhibition of T lymphocytes or other immune cells, consequently contributing to tumor-protective immune suppression (11). It directs survival of CD4-positive T-helper cells and promotes regulatory T-cell differentiation (12). IDO is expressed in certain types of immune cells as well as in cancer cells, contributing substantially to immune evasion in the tumor microenvironment. However, it's "mode-of-action" is best characterized and understood in dentritic cells (13). Expression of IDO in primary melanomas and sentinal lymph nodes was identified as an independent negative prognostic factor for overall and relapse-free survival in melanoma patients (14–16). Interestingly, early clinical trials using the IDO inhibitor epacadostat in combination with immune checkpoint inhibitors targeting CTLA-4 (nivolumab) or PD-1 (ipilimumab or pembrolizumab) have reported higher response rates and longer progression free survival (PFS) when compared with checkpoint inhibitors alone (17, 18). However, recent data from a first phase III trial in patients with unresectable stage III or IV melanoma receiving epacadostat plus pembrolizumab or placebo plus pembrolizumab showed no clinical improvement for the addition of the IDO inhibitor to pembrolizumab (19). Nevertheless, efficient analyses of IDO downstream targets are lacking, as well as detailed validation trials addressing drug dosing, and therefore the usefulness of IDO inhibitors to enhance the efficacy of anti-PD-1 therapy remains unclear.

Since checkpoint inhibitors do not have to cross the blood-brain barrier (BBB) to execute activity and their effects extend over prolonged periods, potential clinical efficacy in the central nervous system (CNS) has been discussed. Metastasis to the brain is still a clinically challenging issue that may develop in up to 40% of patients with advanced disease (20) and metastatic spread is responsible for about 90% of cancer-related deaths across all entities (21). The incidence of brain metastases (BM) is rising partly due to improved visualization and diagnosis techniques but also caused by further development in systemic treatment approaches directing prolonged survival of cancer patients (22). Treatment options targeting established metastases in the CNS are rather limited, mainly caused by inefficient drug penetration across the BBB. Moreover, patients with BM are commonly excluded from clinical trials, including those investigating novel targeted therapies, as the limited survival associated with BM prevents reaching study endpoints. A multitude of cohort studies identified cutaneous melanoma as the third most common cause of BM development (23). BMs in malignant melanoma patients is frequent during disease progression, dominating prognosis and quality of life of affected patients (24–26). The incidence of overt BM at first presentation is about 20%, in advanced melanoma patients around 50% and even higher as autopsy studies reported frequencies of 55 up to 75% (27). Patients with BM from melanoma have a poor prognosis, resulting in median overall survival of 17–22 weeks (28, 29). In consequence, in 2017 the significance of BM presence was incorporated into the American Joint Committee on Cancer (AJCC) staging system as an independent prognostic factor in patients with malignant melanoma (30).

The understanding of the brain as an "immune-privileged" organ has recently changed due to detailed characterization of border-associated structures connecting the CNS with the periphery. Thus, in 2015 a functional draining lymphatic vascular system of the CNS has been described for the first time by different groups implicating the transport of brain-specific antigens into cervical lymph nodes (31, 32). Nevertheless, the entry of the CNS is strictly controlled by the BBB to protect the brain from neurotoxic mediators, but patrolling leukocytes such as $CD4^+$ and $CD8^+$ T cells and bone marrow-derived antigen-presenting DC have already been identified in the meninges and choroid plexus in pre-clinical models

and men (33, 34). Thus, some BM resected under ipilimumab therapy showed dense infiltration of $CD8^+$ cytotoxic tumor infiltrating lymphocytes (TILs) and $FoxP3^+$ regulatory T cells, indicating a triggered immune response under therapy (35). The immunosuppressive properties of the brain parenchyma, which is highly divergent compared to the rest of the body (36–38) could therefore strongly impact any local anti-tumor response. As such, the reciprocal interaction between tumor and immune cells as well as the association between the density and localization of lymphocytic infiltrates in melanoma BM is currently under investigation. Early results from ongoing trials indicate promising activity of immune checkpoint inhibitors by using anti-CTLA-4 (39), anti-PD-1 (40, 41) or a combination of both therapies (42) also in the CNS. Although intracranial response rates up to 47 % were achieved, this response was not translated into improved patients survival (42). As such, it has become clear, that neoplastic processes in the brain may induce prominent anti-tumor immune response. In consequence, IDO could function as a suitable target to enhance the efficacy of checkpoint therapy in the brain. However, the immunosuppressive mechanisms in BM are far away from been understood. Therefore, a deeper understanding of the cellular composition of the BM-associated TILs and its impact on immunosuppressive factors is necessary for developing novel therapeutic combination strategies against BM establishment and outgrowth. Nevertheless, the impact of IDO expression in the presence of tumor-infiltrating lymphocytes (TILs) and other immunoreactive inflammatory cells as macrophages/microglia or dendritic cells for the responsiveness to cancer immunotherapy is still elusive.

Thus, here we provide the landscape of IDO expression in coevolution with the immunogenic microenvironment in a large cohort of melanoma patients with BM, including patients with matched pairs of BM and extracranial melanoma metastases to correlate intra- and interpatient data with therapy response and survival.

MATERIALS AND METHODS

Patients and Patient-Derived Tissue Samples

We analyzed formalin-fixed and paraffin-embedded (FFPE) tissue samples from metastases of 72 patients with BM from malignant melanoma. For 19 patients, matched pairs of BM and metastases at extracranial sites were available that allowed for intra-individual comparative analyzes. In total, we included 74 intracranial and a set of 22 matched extracranial melanoma metastases in our study. Relevant clinical data of these patients are listed in **Table 1**. The cohort was collected as part of the "*Brain_Prevent*"consortium in Germany, including following sites: Department of Dermatology, Institute of Neuropathology, Department of Neurosurgery, all Essen and the Institute of Neuropathology and Department of Dermatology at the Heinrich-Heine University Düsseldorf, all Germany. In detail, tissue samples from intracranial melanoma metastases were retrieved from the tissue banks at the Institute of Neuropathology, University Hospital Essen, and the Institute of Neuropathology, Heinrich Heine University Düsseldorf, Germany. Extracranial metastases of corresponding patients ("matched-pair" samples) were provided by the Skin Cancer Biobank (SCABIO) of the Department of Dermatology, University Hospital Essen, or the Department of Dermatology, Heinrich Heine University Düsseldorf, Germany. All intracranial and extracranial melanoma metastases were histopathologically diagnosed (ST-H, TS, JR, KK, GR). Clinical data and follow-up information were obtained from the SCABIO or the West German Biobank (WBE) of the University Hospital Essen. Informed patient consent was obtained from all patients. The study was performed with approval by the ethics committee of the Medical Faculty, University Duisburg-Essen (ethics approvals no. 11-4715 and no. 15-6723-BO), and the ethics committee of the Medical Faculty, Heinrich Heine University Düsseldorf (ethics approval no. 5246).

Immunohistochemistry

Serial sections were prepared from formalin-fixed, paraffin-embedded tumor biopsy samples. Standard hematoxylin and eosin (H&E) staining was performed for visualization of the tissue morphology. For each biopsy the tumor area was marked as "Region Of Interest (ROI)" by the neuropathologist or the dermatopathologist. Immunohistochemistry was performed using primary antibodies against the following proteins: IDO (clone D5J4E, Cell Signaling Technology, Frankfurt am Main, Germany), CD45RO (clones 2B11 + PD7/26, Dako, Denmark), CD3 (clon SP7, DCS Innovative Diagnostik Systems, Hamburg, Germany), CD8 (clone C8/144B; Dako, Denmark), Foxp3 (clon 206D, BioLegend, Koblenz, Germany), PD-L1 (clone E1L3N, Cell Signaling Technology, Frankfurt am Main, Germany), AIF1 (Acris, Hamburg, Germany), and CD11c (clon 5D11, DCS Innovative Diagnostik Systems, Hamburg, Germany), CD68 (clone PG-M1, Dako, Denmark), CD23 (clone 1B12, Novocastra, Wetzlar, Germany), CD123 (clone 6H6, Abcam, Newcastle, UK). Staining was performed by using the Dako REAL detection system and the goat-on-rodent AP-polymer Kit (GAP514H, Biocare medical, Zytomed) on the Dako Autostainer 46 System followed by hematoxylin counterstaining (Dako, Denmark). To avoid staining specific variations, all sections per individual marker were stained in the same run on the autostainer. Slides were digitalized using Amperio AT2 (Leica Biosystems Imaging INC) at the WBE.

Quantitative Digital Pathology/Tissue Image Analysis

Protein expression analyses on a cell-to-cell basis was performed by using the Definiens Tissue Studio Software® (Definiens AG, München, Germany). Intratumoral analyses of each sample were made by using the marked ROI (tumor area) and this ROI was transferred to each individual staining per tissue sample for further histopathology-based analyses. Peritumoral analyses were made by analyzing the individual markers at the tumor margin of the stroma as already described (43). For each protein, individual parameters were established by using the corresponding IgG control for each primary antibody. We generated two tissue

TABLE 1 | Patients characteristics and clinical data.

Characteristics		
Patients, *n*		72
Matched-pair, *n*		19
Metastasis, *n*		
Intracranial		74
Extracranial		
Skin		19
Adrenal gland		2
Lymph node		1
Gender, *n*	**Age at first BM diagnosis (years ± *SD*)**	**Age at BM surgery (years ± *SD*)**
Female, 34	58 ± 14	58 ± 13
Male, 38	59 ± 15	59 ± 14
Therapy, *n* patients (%)		
Mono-CT		5 (6.9)
Mono-RT		7 (9.7)
Mono-IMT		2 (2.8)
CT+RT		12 (16.7)
CT+IMT		6 (8.3)
RT+IMT		6 (8.3)
CT+RT+IMT		13 (18.1)
Unknown		21 (29.2)
Number of brain metastasis, patients (%)		
1		53 (73.6)
2		9 (12.5)
3		6 (8.3)
4		2 (2.8)
5		1 (1.4)
6		1 (1.4)
Location of intracranial melanoma metastases, *n* = patients (%)		
Cerebrum		48 (16)
Cerebellum		6 (8)
Unknown		18 (25)
Clinical outcome, *n* (%)		
Alive		16 (22.2)
Dead		37 (51.4)
Unknown		19 (26.4)

CT, chemotherapy; RT, radiotherapy; IMT, immunotherapy.

sections on each slide which have been used to stain in parallel the IgG control and the primary antibody on the same section and in the same run of the Dako Autostainer. The "background" intensity given by the IgG control was used as threshold for each individual maker. For IDO expression level analysis we calculated the thresholds for following individual categories on the basis of the calculated mean: low (0.05), moderate (0.09) and high (0.3). The threshold for CD45 (0.03), CD3 (0.03), CD8 (0.1), Foxp3 (0.1), AIF (0.07), and CD11c (0.07) was calculated by discriminating false positive detection given by melanophages which we excluded by using the corresponding H&E sections. Areas without nuclei in between the tumor area (wholes, cuts, punch biopsies) were excluded in order to calculate the individual number of positive cells per total number of tumor cells.

Statistical Analysis

All statistical analyses were performed in R version 3.2.3. Survival analysis was calculated using the R packages survival (2.41–3) and survminer (0.4.3). The end of follow-up period of the study was December 2017. Two clinical survival outcome endpoints were chosen for the endpoints analysis: Overall Survival (OS) and Progression-Free Survival (PFS). The OS period was calculated from the date of initial diagnosis until the date of death from any cause. PFS was identified by using the period of time after date of initial melanoma diagnosis until the development of a brain metastasis. For univariate analysis, long-rank *p*-values were calculated. For multivariate analysis, Cox's proportional hazards models were used. Plots were generated using the ggplot2 (2.2.1). Multivariate Cox proportional hazards regression models were fit using function *coxph* and the forest plots were generated using the *ggforest* command. The Wilcoxon paired test was used to calculate the correlation of the infiltrates of immune cells in patient-matched brain and skin biopsies. A *p*-value correction was applied using the "holm" method. An adjusted *p*-value of 0.1 was considered significant. Spearman correlation was performed to check the relationship of total IDO expressing cells in ICM and ECM to the PD-L1 expression (intensity) status. Plots were drawn using ggplot2 package in R. The curve was smoothened using a linear regression (*lm*). A *post-hoc* Tukey HSD (Hosnest Significant Difference) followed by Anova was performed to test the pairwise correlation among the PD-L1 expression values and IDO states (total IDO expressing cells; high, medium and low intensity of IDO-positive cells).

RESULTS

Patient Cohort

In total, our study included 72 patients, 34 women, and 38 men, with an age of 58 ± 13 and 59 ± 15 years (mean ± SD), suffering from malignant melanoma and diagnosed for the development of brain metastases (for detailed description of the patient characteristics see **Table 1**). From 19 of these 72 patients "matched" biopsies were available from extracranial sides, thus allowing for intrapatient analyses. Out of 74 intracranial melanoma metastases from the 72 patients, 48 metastases were located in the cerebrum and six tumors were resected from the cerebellum, while information on supra- vs. infratentorial location was missing for 18 BM. The set of 22 "patient-matched" extracranial metastases from 19 patients included 19 cutaneous, two lymph node and one adrenal gland melanoma metastases (**Table 1**).

Distinct IDO Expression Patterns in Metastases of Malignant Melanoma

First, we detected cytoplasmic IDO expression in all 74 intracranial and 22 extracranial metastases of advanced melanoma patients (**Figure 1**). Interestingly, we observed

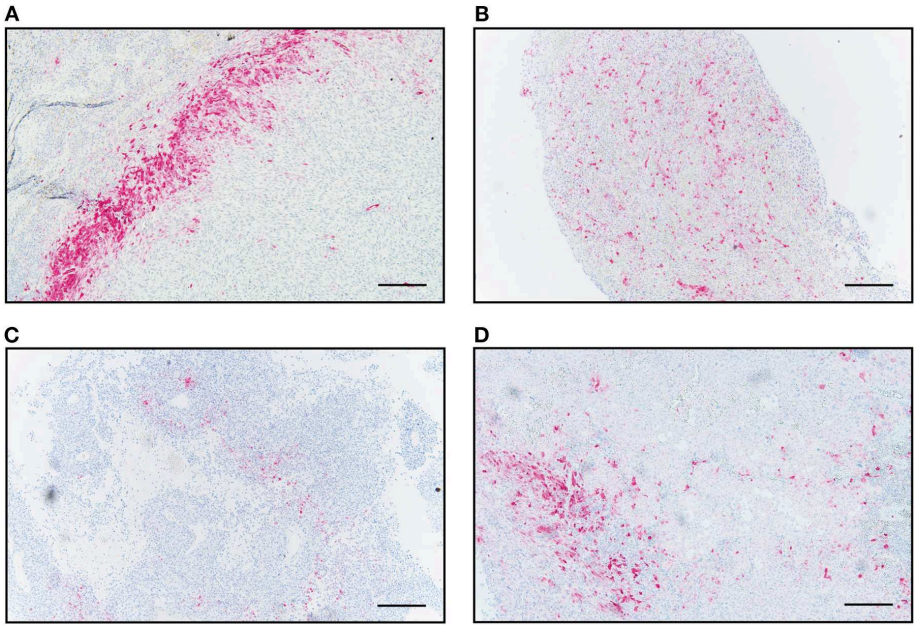

FIGURE 1 | Immunohistochemical and pathological analyses of IDO distribution in human melanoma metastases. Four distinct infiltration patterns of IDO-positive cells were predominantly detected independent of intracranial or extracranial origin. Representative images for the individual distribution patterns are presented in intracranial metastases. IDO-positive cells in a **(A)** "border-like," **(B)** "diffuse," **(C)** "partial rim" and **(D)** combined "partial rim plus diffuse" localization. Scale bar, 200 μm.

distinct patterns of IDO tissue distribution. One expression pattern we defined as "border-like" due to the exclusive location of IDO-positive cells at the invasive tumor-stroma interface, surrounding the tumor like a wall (**Figure 1A**). This pattern was detected in 3/74 (4%) intracranial and 4/22 (18.1%) extracranial metastases. The second expression pattern which we named "diffuse" was frequently seen in both metastatic tissue sites, i.e., was present in 59/74 (80%) intracranial and 8/22 (36.3%) extracranial metastases. This pattern corresponded to a widespread diffuse occurence of IDO^+ cells in the tumor mass (**Figure 1B**). The third pattern, which we described as "partial rim," corresponded to an interrupted border-like expression (**Figure 1C**). This pattern was found in 5/74 (7%) intracranial and 6/22 (27.3%) extracranial metastases. A fourth pattern combined the "partial rim" and the "diffuse" pattern and was detected in seven metastases of the CNS (9%) and 4 cases of extracranial sites (18.1%, **Figure 1D**).

Intratumoral Variability of IDO Expression Level Mediate PD-L1 Surface Expression

In addition to the distinct patterns of IDO immunopositivity in malignant melanoma metastases, we detected also an intratumoral heterogeneity for the IDO expression intensity, independent of the tissue origin (**Supplementary Figure 1**). By using quantitative digital pathology tissue diagnostics, we generated an individual cell-by-cell threshold for the immunohistochemistry-based IDO intensity level (**Figure 2A**). By using the "patient-matched" cohort of 19 patients, we detected—with exception of patient no. 16—that more than 50% of the IDO^+ tumor area was represented by melanoma cells expressing low levels of IDO and that only 10–20% of IDO^+ tumor area was represented by immune cells, which showed moderate or high expression intensity (**Figure 2B**). However, Kaplan-Meier analysis revealed that neither the IDO expression level nor the total number of IDO-positive cells in the distinct metastases impacted disease progression or survival of advanced melanoma patients (data not shown).

We next asked the question whether the immunosuppressive factor IDO directs the expression of other immunosuppressive molecules with regard to the PD-1/PD-L1 axis. Tukey HSD test was performed to test for significance. We found that only the tumor cell-associated IDO, represented by low IDO intensity, strongly correlates with PD-L1 surface expression ($p = 0.0006$) and, in consequence, that the number of IDO^+ tumor cells directs the intratumoral expression level of the immunosuppressive molecule PD-L1 ($p = 0.00015$, **Table 2**).

IDO Favors an Immunosuppressive Signature in Melanoma Brain Metastases Directing Efficacy of Cancer Immunotherapy

The current knowledge and understanding of cancer immunotherapy has changed dramatically during the last decades. Multiple clinical data let assume that the amount and also the localization of the lymphocytic infiltrate in different cancer entities directs the response to cancer immunotherapy. In 2014, Tumeh and colleagues could show that pre-existing $CD8^+$ T cells distinctly located at the invasive tumor front correlate with the expression of the immunosuppressive checkpoint molecules PD-1/PD-L1, predicting response to

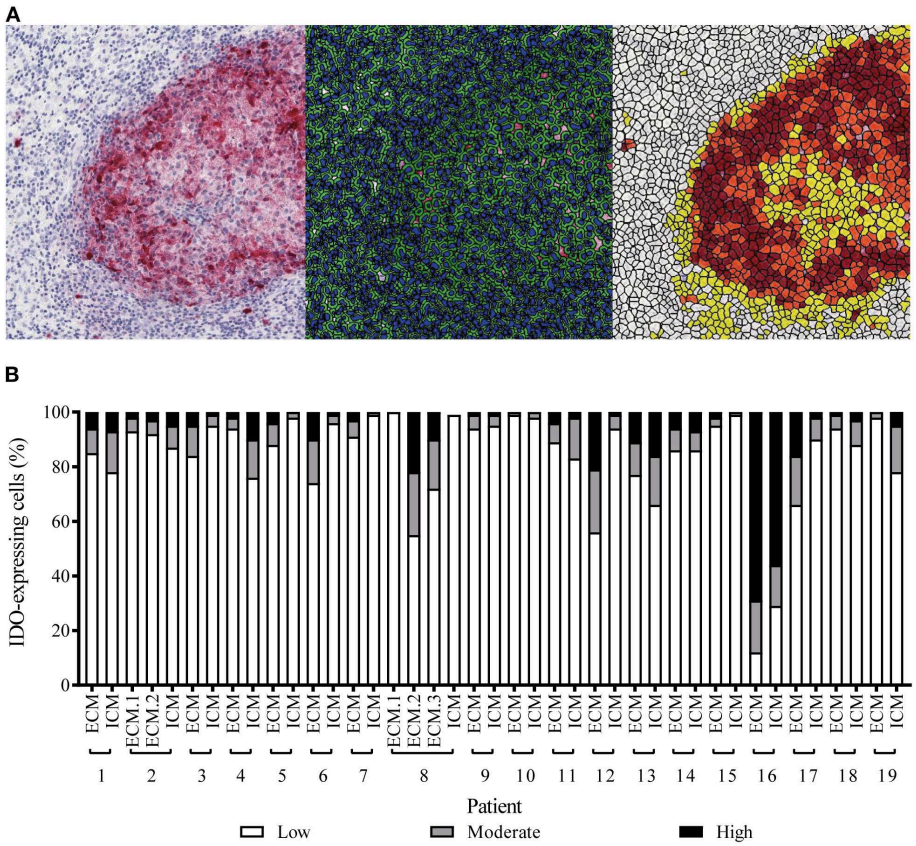

FIGURE 2 | Quantitative assessment of IDO-expression intensity in patient-matched melanoma metastases of intracranial and corresponding extracranial origin. **(A)** Representative images for immunohistochemical-based IDO-expression (left), parameter-based separation of cell-cell borders (middle), classification of high (brown), moderate (orange) and low (yellow) expression intensities or IDO-negative areas (white, right). **(B)** Statistically-based calculation for the intratumoral percentage of high (black), moderate (gray), low (white) IDO-expressing cells in intracranial (ICM) or extracranial (ECM) metastases of individual melanoma patients ($n = 19$).

immunotherapy in patients suffering from malignant melanoma (3). Because the detailed localization of IDO$^+$ cells in melanoma metastases of the brain and its impact on the recruitment of TILs is still elusive, we addressed this issue in our cohort of melanoma BM and matched extracranial melanoma metastases. We first called intra- and interpatient analyses by using our patient-matched cohort for the number of cells expressing IDO and markers of the lymphocytic infiltrate (CD45, CD3, FoxP3, CD8), PD-L1 and the Allograft inflammatory factor 1 (AIF-1), mainly expressed by macrophages/microglia. We detected a significant higher number of CD8$^+$ T cells in metastases of extracranial sites when compared to metastases of the CNS ($p = 0.016$), whereas all other markers remained unchanged represented (**Figure 3**). Interestingly, we found that the localization of IDO-positive cells is strongly paralleled with the localization of the lymphocytic infiltrate, with exception of FoxP3-positive regulatory T cells, which were also recruited into the tumor mass, but not localized in areas of high IDO-expression as exemplarily presented in **Supplementary Figure 2** in cutaneous melanoma metastases. Moreover, whereas we detected a balanced expression of IDO$^+$ cells in metastases of the brain ($p = 0.351$, **Figure 4A**) we found significantly higher fractions of IDO-expressing cells with intratumoral localization in extracranial metastases when compared to the peritumoral microenvironment ($p = 0.005$, **Figure 4B**).

TABLE 2 | Correlation of PD-L1 and IDO.

Number of cells	Adjusted *p*-value
Total IDO / PD-L1	0.00015
Low IDO / PD-L1	0.00066
Moderate IDO / PD-L1	0.11716
High IDO / PD-L1	0.06842

A post-hoc-Tuckey HSD (Honest Significant Difference) followed by anova was performed to test the pairwise comparisons among the PD-L1 expression values and IDO (Total number of IDO expressing cells, high, medium, and low IDO expressing cells). The 95% confidence for lower and upper intervals is mentioned together with the adjusted p-values.

The development of brain metastases is a significant cause of morbidity or mortality for patients with metastatic cancer, including melanoma. However, for still unclear clinical reasons some patients show a better outcome as others. By using a total of 38 cases, 13 patients who received standard care therapy and 17 cases which received immune checkpoint inhibitors alone or in combination with other therapies, showed a median survival of 228 vs. 336 days using the time of

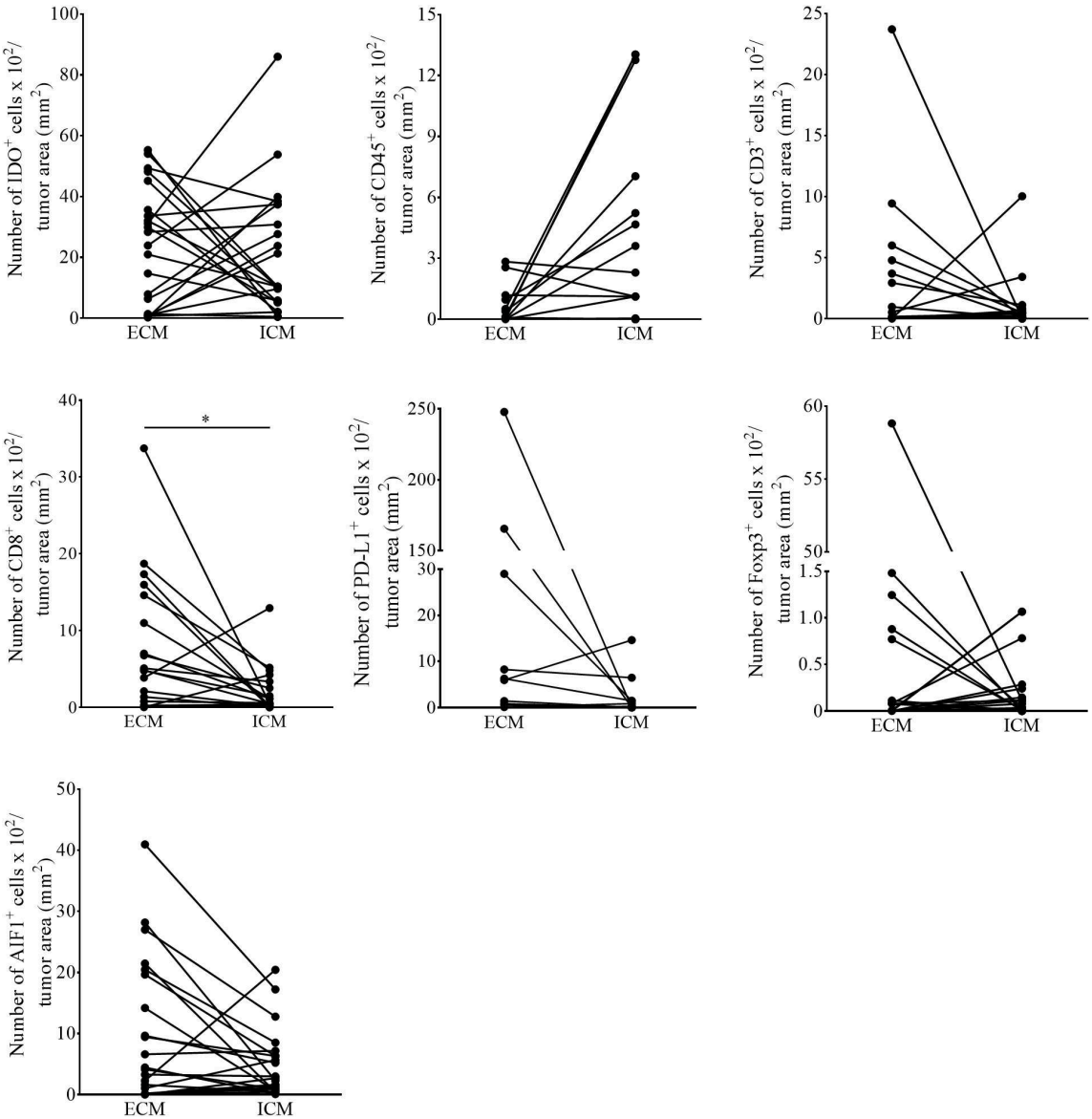

FIGURE 3 | Quantitative assessment for the number of immunoreactive cells in patient-matched melanoma metastases. The number of IDO, CD45, CD3, CD8, FoxP3, PD-L1, and AIF1 positive cells in intra- (ICM) and corresponding extracranial (ECM) metastases of individual melanoma patients ($n = 19$ patients, n ECM $= 22$, n ICM $=19$; $^*p < 0.05$).

first BM observation and date of death. Therefore, we asked whether the expression of IDO itself, independent of the cellular source, is associated with the recruitment of tumor infiltrating lymphocyte subsets and whether this immunoreactive infiltrate influences the clinical outcome of melanoma patients in our cohort.

We detected a strong correlation between IDO positivity and infiltration of $CD8^+$ cytotoxic T cells in intra- ($R = 0.34$, $p = 0.0032$) and extracranial ($R = 0.44$, $p = 0.0420$) metastases, whereas expression of IDO paralleled by the recruitment of regulatory T cells, as evidenced by CD3/FoxP3 immunostaining, was exclusively seen in metastases at extracranial sites ($R = 0.66$, $p = 0.0007$, **Figure 5**). However, preforming a multivariate Cox proportional hazards regression model we did not observe a significant association for disease progression with regard to the individual lymphocyte subtypes in metastases of the brain (**Supplementary Figure 3**). Interestingly, statistical analyses identified a significant positive correlation of IDO with PD-L1 expression which was solely detectable in metastases of intracranial sites ($R = 0.37$, $p = 0.0011$) predicting worse prognosis in these patients in the multivariate analyses ($p = 0.017$, **Figures 5**, **6**).

The recent success of cancer immunotherapy in different cancer entities by using the so called "checkpoint inhibitors"

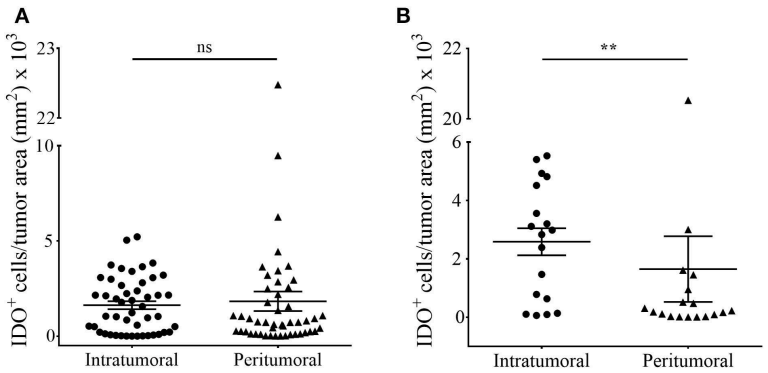

FIGURE 4 | Comparative analyses of intratumoral and peritumoral IDO-expression in human melanoma metastases of intracranial and extracranial origin. The total number of IDO-positive cells localized in the tumor (intratumoral) or around (peritumoral) in **(A)** ICM and **(B)** ECM was quantified in accordance to histopathological labeling of the tumor area by using the quantitative digital pathology tissue analysis system Definiens Tissue Studio (*n* ICM = 48/47 patients, *n* ECM = 18/16 patient, *n* matched-pairs = 16; $^{**}p < 0.05$). To ensure statistical balance between both parameters we excluded all patient samples from the analyses in the case of missing stroma in the individual tissue specimen.

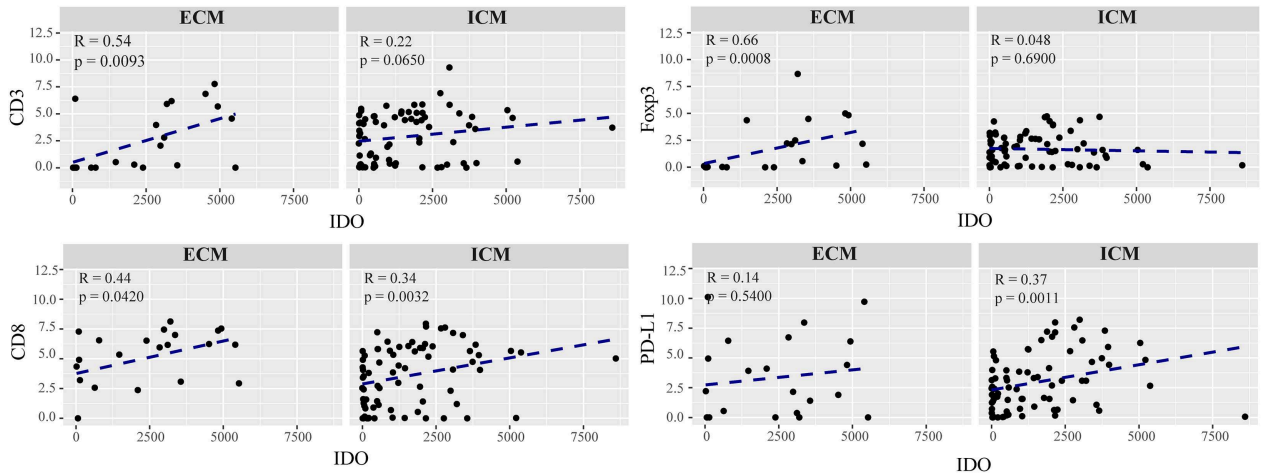

FIGURE 5 | Correlation of the immunoreactive infiltrate and IDO expression in extracranial and intracranial melanoma metastases. Each dot in the scatter plot represents an individual patient. The x-axis represents the total number of IDO expressing cells and the y-axis shows the expression of CD3, FoxP3, CD8, and PD-L1 represented in a logarithmic scale. ECM and ICM denotes the exracranial and intracranial melanoma metastases. Spearman correlations were performed and regression was calculted using (*lm*) function.

paralleled the expression of intratumoral PD-L1 with clinical response (3, 44). Thus, we analyzed whether patients with melanoma BM receiving checkpoint inhibitors as a monotherapy ($n = 2$) or in combination with chemotherapy ($n = 6$), radiotherapy ($n = 6$) or both ($n = 13$) at any time of disease might gain a clinical benefit from high PD-L1 expression in their brain metastases. A Kaplan-Meier survival analysis was performed and the patients were divided in two groups based on median PD-L1 expression. Whereas, the expression of the immune checkpoint molecule PD-L1 did not appear to have an impact on disease progression (log-rank $p = 0.16$, **Figure 7A**) it significantly affected patients survival (log-rank $p = 0.033$, **Figure 7B**). The 50% survival probabilities for the patients with low PD-L1 expression is 5 years whereas, patients with a high PD-L1 expression showed a 50% survival probability of 10 years. However, due to the limited number of patients, these results must be validated in a larger cohort of advanced melanoma patients with brain metastases undergoing checkpoint therapy.

High IDO Expression Level Are Primarily Represented by Macrophages/Microglia

In addition to tumor cells, expression of the immunomodulatory protein IDO by subpopulations of tumor-associated immune cells, e.g., dendritic cells, macrophages and B-lymphocytes, has been reported in different types of cancer (45–47). However, the major cellular source of IDO expression in intracranial melanoma metastases is still unknown. Since we found low IDO expression levels in melanoma cells of BM, we went further into the analysis of distinct subsets of monocytes by co-staining experiments including 10 selected cases each from our

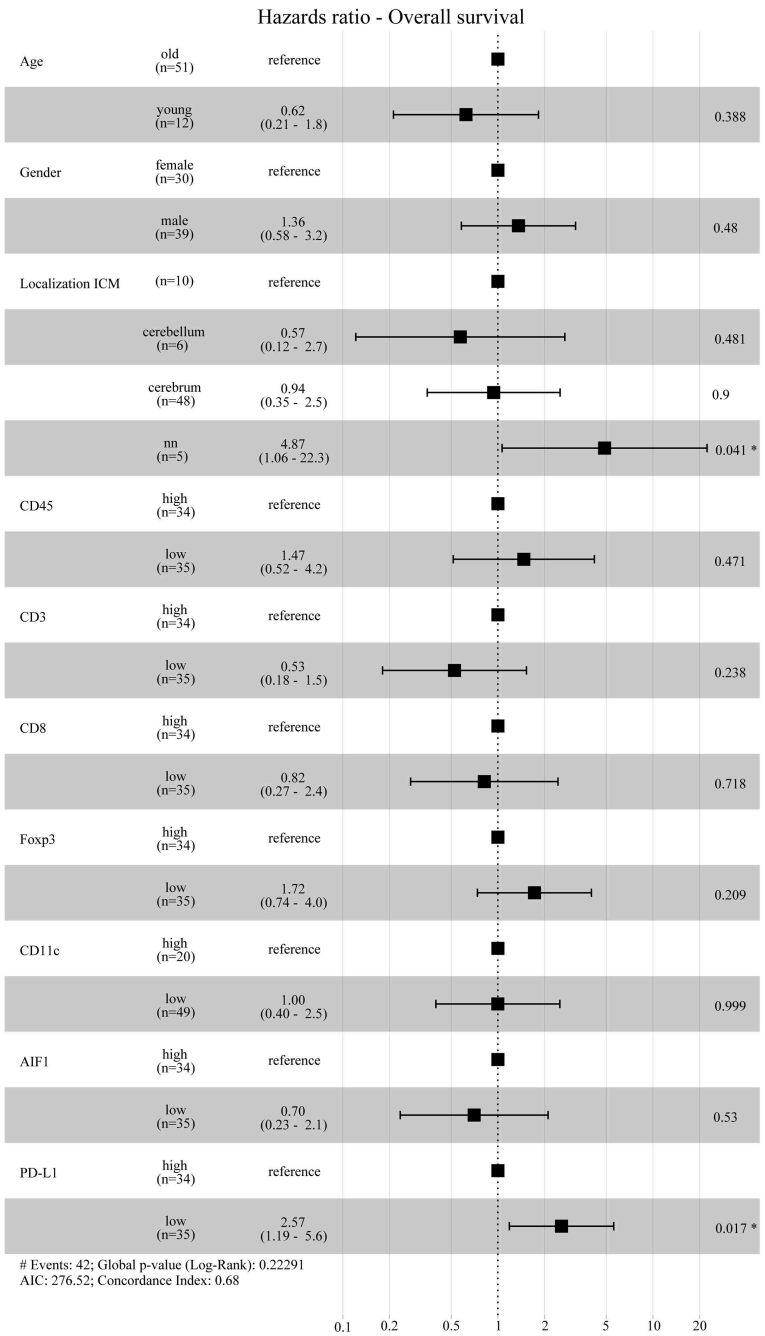

FIGURE 6 | Hazard ratio Overall survival. Forest plot for the cox proportional hazards model was calculated by using age, gender, localization of the ICM and immunoreactive infiltrates. The patients below 40 years of age at death were grouped in the "young" group and vice versa. For the immune cell infiltrates the patients were grouped into a "high" or "low-group" based on the median expression values. According to the multivariate model, low PD-L1 expressing patients have a significantly higher hazards ratio and thus poor overall survival compared to patients with high PD-L1 expression.

"matched-pair" cohort of patients with tissue from intracranial and extracranial melanoma metastases. To avoid false positive detection mediated by brownish melanophages or melanocytic tumor cells, we exclusively selected amelanotic tissue samples for these analyses. First, we addressed the expression of IDO in different subtypes of DCs by using specific antibodies against the integrin a-x (CD11c), the Fcε-Rezeptor II (CD23) expressed on follicular DC and the interleucin 3 receptor (CD123), represented in conventional DCs (cDCs) and plasmacytoid dendritic cells (pDCs) as presented in **Figure 8**. Nevertheless, it is important to note that all of these markers are also expressed by different subpopulations of monocytes and granulocytes, dependent on

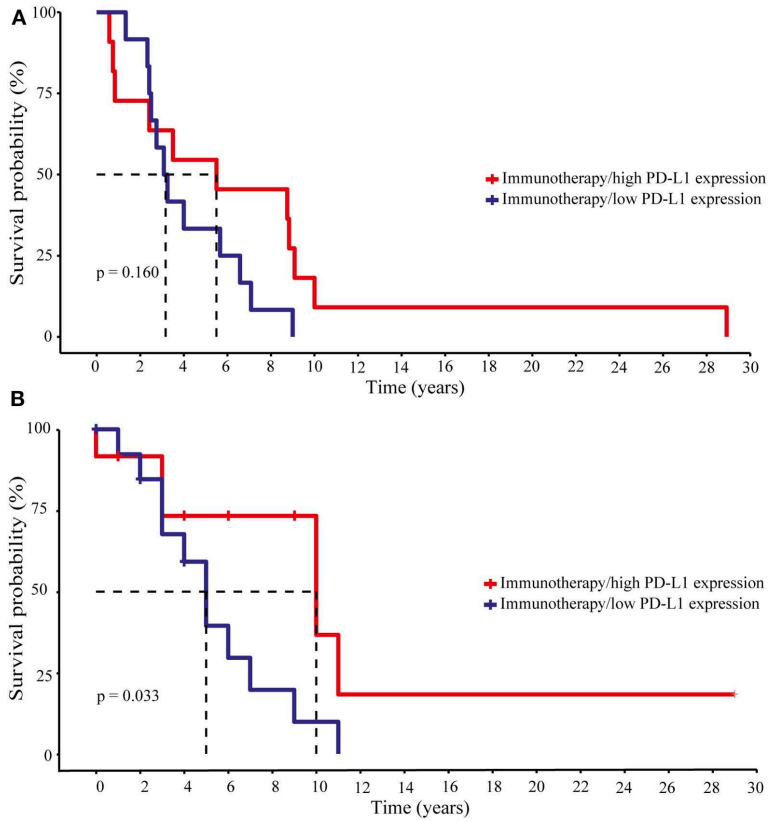

FIGURE 7 | Disease progression and survival analyses of melanoma patients under immunotherapy with respect to intracranial PD-L1 expression. Patients were divided into two groups, "high" and "low" PD-L1 expression due to the median PD-L1 expression level. **(A)** Progression-free survival. Long-rank test statistics show no differences in the progression-free survival for patients with high and low PD-L1 expression (Log-rank *p*-value 0.160). **(B)** Overall survival. According to the Kaplan–Meier curve patients with high PD-L1 had a greater benefit from immunotherapy and showed a better overall survival (Log-rank *p*-value 0.033). Dotted lines indicate the 50% survival probabilities for both groups.

their level of maturation and activation. Intratumoral CD11c expression was limited to brain metastases whereas only two cases showed co-expression of CD11c with IDO. We detected $IDO^+/CD23^+$ co-expression in 1/10 intra- and 2/10 extracranial metastases. Finally, $IDO^+/CD123^+$ double-positive cells could be detected in 9/10 brain metastases but only in 3/10 metastases at extracranial sites. Interestingly, IDO-positive CD23 and CD123 cells were histopathologically confirmed as macrophages. Double immunostaining for IDO with CD68, a protein that is highly expressed by cells of the monocyte lineage and tissue macrophages, or AIF-1, identified a strong infiltration by IDO^+ macrophages/microglia in all analyzed metastases independent of the tissue origin. In detail, 37 ± 2% (mean ± SD) or 48 ± 11% (mean ± SD) of $CD68^+$ macrophages and 17 ± 8% (mean ± SD) or 11 ± 3% (mean ± SD) of $AIF1^+$ macrophages/microglia co-expressed IDO in metastases of intracranial or extracranial sites, and presented high expression level by using the individual thresholds for IDO determined by the Definiens pathology software (**Figure 8**). Although the expression intensity of IDO in DCs subpopulations was comparable to that in macrophages/microglia, it became clear that the macrophage/microglia population in melanoma metastases is of greater importance due to the very limited presence of DCs in the tumors of our cohort.

DISCUSSION

Following non-small cell lung cancer (NSCLC) and breast cancer, melanoma is the third most common origin of metastases to the brain. However, they exhibit the highest risk for cerebral tropism of all cancer entities, reflected by a 50–75% chance for development of intracranial metastases in advanced melanoma patients (27, 48, 49). Altough the local treatment approaches using whole-brain radiation therapy, stereotactic radiosurgery and/or surgical resection remain important, the use of systemic therapies has initiated a new therapeutic area in the management of melanoma brain metastases. Despite recent advances in the systemic treatment of extracranial metastases by using BRAF-targeted therapy in patients harboring $BRAF^{V600E}$-mutant melanomas or inhibitors targeting immune checkpoint molecules, the treatment of melanoma brain metastases remains a major challenge. Multiple phase II and III studies have shown that ipilimumab and nivolumab are active in advanced melanoma

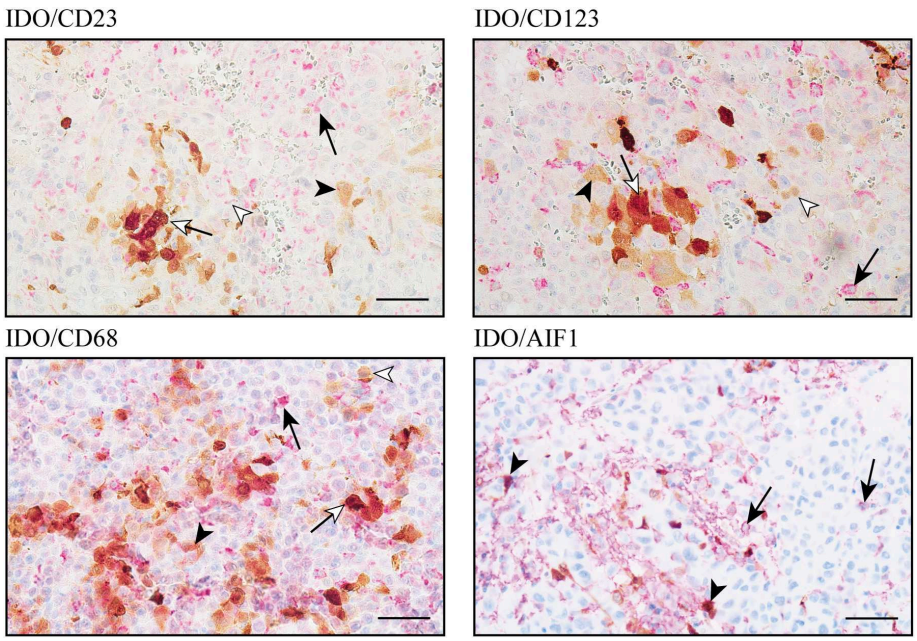

FIGURE 8 | IDO-expression on cellular components of the immunoreactive tumor infiltrate in melanoma metastases of the central nervous system. Immunohistochemical-based co-immunostaining for IDO (brown) and indicated makers for subpopulations of DC and macrophages/microglia (all in red) exemplarily shown in intracranial (right) metastases. Black arrowhead: IDO^+ macrophage; black arrow: single expression of the indicated markers (CD23, CD123, CD68, or AIF1); white arrow: co-expression of IDO plus indicated maker in macrophages, white arrowhead: single marker detection. Representative images were presented. Scale bar = 50 μm.

and that the combination therapies involving PD-1 or CTLA-4 inhibitors presented a superior efficacy when compared to the individual monotherapies (50–53). Nevertheless, only 40–45% of melanoma patients benefit from cancer immunotherapy *per se* (51).

Although the use of immune checkpoint inhibitors targeting PD-1 and/or CTLA-4 has nowadays become an established therapy in melanoma, it is still critical to transfer our knowledge from extracranial sites to intracranial melanoma lesions with respect to the unique "immune-specialized" microenvironment of the brain (54, 55). After extravasation of tumor cells into the brain parenchyma they enter a fundamentally different tissue environment with respect to the metabolic situation, the cellular compositions, the brain-specific extracellular matrix proteins and the immunoreactive heterogenous cell population with regard to the primary site of their origin (56). This appears particularly relevant in the context of immune cell activity against extravasated single cancer cells and micrometastases when the normal brain parenchyma, including the blood-brain barrier, is still largely intact. In line with this concept, melanoma patients developed remarkable high rates of BM during Ipilimumab in one study (57), which fits to the empirical impression of many clinical experts in the field. In contrast, brain macrometastases have been found to respond well to ipilimumab and other immune checkpoint inhibitors in subsets of patients (35, 58) which supports the general concept that preventing metastatic outgrowth is very different (biologically and therapeutically) from targeting large established macrometastases. However, limited clinical data are available adressing the activation of checkpoint inhibitors in the CNS. One of the first phase II studies evaluated the activity of ipilimumab in patients with melanoma brain metastases and enrolled 72 patients in a two-arm clinical trial (39). Fifty-one patients were neurologically asymptomatic and therefore did not receive any corticosteroids at time of enrollment (arm A), whereas 21 patients showed symptomatic disease and were on a stable dose of corticosteroids (arm B). This study achieved intracranial response rates of 16 and 5% in cohort A and B, respectively, and hence confirmed the activity of anti-PD-1 therapy in the CNS, but also highlighted the importance of being off corticosteroids at the time of therapy initiation. Multiple follow-up clinical trials addressed the activity of combination therapies targeting PD-1 and CTLA-4 vs. monotherapy in advanced melanoma patients (42, 59, 60). In summary, all achieved activities at the intracranial site, albeit to limited extents. Interestingly, novel data of the multicentre open-labeled randomized phase II trial NCT02374242 suggested a higher chance of long-term durable intracranial response by using the combination of ipilimumab and nivolumab in patients with asymptomatic untreated melanoma brain metastases (42). According to the current clinical data, own unpublished data by using the primary melanoma model MT/ret, which spontaneously induces multiple cutaneous melanoma and distant organ metastases, including the CNS, show that inhibition of the PD-1/PD-L1 axis resulted in diminished intracranial tumor load but failed to suppress the establishement of micrometastases in the CNS (Helfrich, unpublished data) (61, 62). These clinical data argue for a principle ability of immune checkpoint inhibitors to reach meaningful anticancer immunity in the brain, however, the current therapies seem to fail for their suppression of metastatic seeding of the CNS by cancer cells.

IDO expression and activity has been documented in several cancer entities and has been correlated with negative prognostic factors (9). Thus, it was only a question of time until first clinical trials combined IDO inhibitors like epacadostat or navoximod with inhibitors targeting the PD-1/PD-L1 axis or CTLA-4 in differnt tumor entities, including advanced melanoma (19, 63–66). Since all of this studies demonstrated acceptable safety, good tolerability, and pharmacological activity, there was no clear evindence of patients benefit when combined to PD-1/PD-L1 inhibitors. Nevertheless, IDO data with respect to the CNS metastases are missing.

In the present study, we analyzed tissue samples of 74 intracranial metastases from 72 advanced melanoma patients and 22 matched melanoma metastases at extracranial sites from 19 of the 72 patients. We specifically adressed the expression of immunosuppressive mediators such as IDO and PD-L1 in the context of the tumor-associated immunoreactive infiltrate. We found that IDO is expressed in different patterns in melanoma brain metastases indicating IDO expression as a marker of anti-tumor immune response. First, in contrast to data described by Krähenbühl et al. (16), who analyzed different primary cutaneous melanoma types and corresponding organ metastases (with exception of CNS metastases) in 43 patients undergoing cancer immunotherapy or targeted therapy and described IDO immunoreactivity in 17/43 pretreated samples, we found that IDO expression is highly consistant indicating IDO as a marker of anti-tumor immune response. Moreover, a strong correlation of IDO expression in peritumoral sites of the primary tumors has been linked to IDO expression in the sentinel lymph node, directing the numbers of intratumoral lymphocytes as a result of immune control (14). In contrast to CNS metastases, we found higher IDO-positive cell numbers in the tumor mass when compared with peritumoral localization in melanoma metastases at extracranial sites, which would fit to an ongoing anti-tumoral immune response, since high levels of IFN-γ are secreted during this process. In addition, our investigation revealed different distribution patters of IDO-positive cells in melanoma metastases, but these were independent of the metastatic origin. Interestingly, neither the localization nor the distribution pattern of IDO had an impact on patient outcome. However, the heterogeneous expression of the immunosupressive IDO which we detected both, within and between patients, may explain the high variation in the clincal response to IDO combination treatment (19, 63, 64).

Since several studies correlated high TIL levels with favorable outcome (67–69) our data are in line with the work of Harter et al. (37). Neither disease progression nor patient survival was affected by the number of TILs in melanoma brain metastases in our patient cohort *per se*. As TILs represent also the major source for the secretion of inflammatory stimuli such as IFN-γ and TNF-α (4, 70), resulting in activation of lymphocytes and induction of PD-L1 expression, we analyzed this aspect also in our tissue specimens. Interestingly, with regard to the expression of the immunosupressive molecule IDO, we found that IDO-positive cells correlated with the recruitment of $CD8^+$ T cells to the site of strongest IDO expression, which was paralleled by high expression of PD-L1, indicating a highly immunogenic situation modulated by cells with high IDO expression. Nevertheless, we need to consider that our cohort consists of patients who had received various mono- or combination therapies before resection of the investigated brain metastasis, possibly including pre-operative corticosteroid treatment, to minimize inflammatory side effects. Therefore, we are aware of the discussion that patient's therapy may affect the cellular component of immunoreactive populations, however, it has been shown that corticosteroids neither affect the TIL population nor the PD-L1 expression in melanoma brain metastases (38). Interestingly, IDO has also been considered for its negative impact by increasing the expression of $FoxP3^+$ on regulatory T cells (71, 72), a correlation which we also observed in extracranial metastases. However, melanoma brain metastases do not appear to show this reciprocal interplay. The heterogenous IDO expression of melanoma metastases which we described here on the basis of immunohistochemistry, prompted our further investigation on the cell types that represent the major producers of IDO in melanoma brain metastases. Although melanoma cells *per se* expressed IDO, but at low intensity when compared to expression levels in immune cells, our data clearly indicate the impact of macrophages/microglia on IDO expression in melanoma brain metastases. Despite functional knowledge of myeloid cells, e.g., microglia and tumor-associated marcrophages (TAMs), in normal tissue, primary tumors and metastases, insights into their molecular identity, and clinical impact in intracranial metastases are still limited. In general, microglia and TAMs represent the most abundant non-neoplastic cells in brain metastases (73). Despite the lack of clinical data for the impact of microglia density and brain-associated TAM infiltration for patients prognosis, some pre-clinical data implicate tumor-promoting functions (74–76). In addition, functional charaterization of IDO expression with regard to polarization and functionality of both cell types in brain metastases are missing so far. Since our data are solely based on the use of FFPE specimens, the activity of IDO in the tumor mass with regard to tryptophan catabolism *per se* but also the impact of IDO for the activity and polarization of macrophages/microglia in the brain remain to be analyzed in fresh-frozen tissue samples from melanoma brain metastases but also in preclinical mouse models. For example, therapeutic intervention in the MT/ret-transgenic mouse model of metastatic melanoma would allow to analyse the population of IDO-positive TAMs/microglia in detail for their surface marker expression under IDO-targeted therapy. These newly identified surface markers could represent potential novel targets to reach more meaningful activity with regard to melanoma immunotherapy, potentially including re-education of macrophages as a new therapeutic strategy (77).

DATA AVAILABILITY STATEMENT

The datasets generated for this study are available on request to the corresponding author.

ETHICS STATEMENT

Informed patient consent was obtained from all patients. The study was performed with approval by the ethics committee of the Medical Faculty, University Duisburg-Essen (ethics approvals no. 11-4715 and no. 15-6723-BO), and the ethics committee of the Medical Faculty, Heinrich Heine University Düsseldorf (ethics approval no. 5246).

AUTHOR CONTRIBUTIONS

IH, DS, and GR conceptualized and designed the study. DH-R and SM performed the experiments, generated, and analyzed data. SM and BB conceptualized and generated statistical analyses. ST-H, DP, AS, PJ, TS, JK, JF, KK, US, JR, GR, and DS collected and provided clinical material and data. GR and IH designed the selection of the patient cohort. IH conceptualized, coordinated, and directed the project. DH-R, SM, and IH wrote the manuscript. All authors performed manuscript review.

FUNDING

This work was supported in part by the German Cancer Aid (DKH, No. 70112507 to IH, DS, and GR), the German Research Foundation (DFG) - HE 5294/2-1 (KFO 337), the Hiege Stiftung gegen Hautkrebs, Monika Kutzner Stiftung (P#18) and Brigitte and Dr. Konstanze Wegener Stiftung (all to IH).

ACKNOWLEDGMENTS

We gratefully acknowledge I.-V. Westedt and M. Bau for the technical assistance.

SUPPLEMENTARY MATERIAL

The Supplementary Material for this article can be found online at: https://www.frontiersin.org/articles/10.3389/fimmu.2020.00120/full#supplementary-material

REFERENCES

1. Ribas A. Tumor immunotherapy directed at PD-1. *N Engl J Med.* (2012) 366:2517–9. doi: 10.1056/NEJMe1205943
2. Ribas A, Wolchok JD. Cancer immunotherapy using checkpoint blockade. *Science.* (2018) 359:1350–5. doi: 10.1126/science.aar4060
3. Tumeh PC, Harview CL, Yearley JH, Shintaku IP, Taylor EJ, Robert L, et al. PD-1 blockade induces responses by inhibiting adaptive immune resistance. *Nature.* (2014) 515:568–71. doi: 10.1038/nature13954
4. Dunn GP, Koebel CM, Schreiber RD. Interferons, immunity and cancer immunoediting. *Nat Rev Immunol.* (2006) 6:836–48. doi: 10.1038/nri1961
5. Deczkowska A, Baruch K, Schwartz M. Type I/II interferon balance in the regulation of brain physiology and pathology. *Trends Immunol.* (2016) 37:181–92. doi: 10.1016/j.it.2016.01.006
6. Mojic M, Takeda K, Hayakawa Y. The dark side of IFN-gamma: its role in promoting cancer immunoevasion. *Int J Mol Sci.* (2017) 19:e89. doi: 10.3390/ijms19010089
7. Taylor MW, Feng GS. Relationship between interferon-gamma, indoleamine 2,3-dioxygenase, and tryptophan catabolism. *FASEB J.* (1991) 5:2516–22. doi: 10.1096/fasebj.5.11.1907934
8. Spranger S, Spaapen RM, Zha Y, Williams J, Meng Y, Ha TT, et al. Up-regulation of PD-L1, IDO, and T(regs) in the melanoma tumor microenvironment is driven by CD8(+) T cells. *Sci Transl Med.* (2013) 5:200ra116. doi: 10.1126/scitranslmed.3006504
9. Brochez L, Chevolet I, Kruse V. The rationale of indoleamine 2,3-dioxygenase inhibition for cancer therapy. *Eur J Cancer.* (2017) 76:167–82. doi: 10.1016/j.ejca.2017.01.011
10. Spranger S, Koblish HK, Horton B, Scherle PA, Newton R, Gajewski TF. Mechanism of tumor rejection with doublets of CTLA-4, PD-1/PD-L1, or IDO blockade involves restored IL-2 production and proliferation of CD8+ T cells directly within the tumor microenvironment. *J Immunother Cancer.* (2014) 2:3. doi: 10.1186/2051-1426-2-3
11. Johnson TS, Munn DH. Host indoleamine 2,3-dioxygenase: contribution to systemic acquired tumor tolerance. *Immunol Invest.* (2012) 41:765–97. doi: 10.3109/08820139.2012.689405
12. Baban B, Chandler PR, Sharma MD, Pihkala J, Koni PA, Munn DH, et al. IDO activates regulatory T cells and blocks their conversion into Th17-like T cells. *J Immunol.* (2009) 183:2475–83. doi: 10.4049/jimmunol.0900986
13. Munn DH, Sharma MD, Lee JR, Jhaver KG, Johnson TS, Keskin DB, et al. Potential regulatory function of human dendritic cells expressing indoleamine 2,3-dioxygenase. *Science.* (2002) 297:1867–70. doi: 10.1126/science.1073514
14. Chevolet I, Speeckaert R, Haspeslagh M, Neyns B, Krüse V, Schreuer M, et al. Peritumoral indoleamine 2,3-dioxygenase expression in melanoma: an early marker of resistance to immune control? *Br J Dermatol.* (2014) 171:987–95. doi: 10.1111/bjd.13100
15. Speeckaert R, Vermaelen K, van Geel N, Autier P, Lambert J, Haspeslagh M, et al. Indoleamine 2,3-dioxygenase, a new prognostic marker in sentinel lymph nodes of melanoma patients. *Eur J Cancer.* (2012) 48:2004–11. doi: 10.1016/j.ejca.2011.09.007
16. Krähenbühl L, Goldinger SM, Mangana J, Kerl K, Chevolet I, Brochez L, et al. A longitudinal analysis of IDO and PDL1 expression during immune- or targeted therapy in advanced melanoma. *Neoplasia.* (2018) 20:218–25. doi: 10.1016/j.neo.2017.12.002
17. Gibney G, Hamid O, Lutzky J, Olszanski A, Gangadhar T, Gajewski T, et al. 511 Updated results from a phase 1/2 study of epacadostat (INCB024360) in combination with ipilimumab in patients with metastatic melanoma. *Eur J Cancer.* (2015) 51:S106–7. doi: 10.1016/S0959-8049(16)30312-4
18. Hamid O, Gajewski TF, Frankel AE, Bauer TM, Olszanski AJ, Luke JJ, et al. 1214OEpacadostat plus pembrolizumab in patients with advanced melanoma: phase 1 and 2 efficacy and safety results from ECHO-202/KEYNOTE-037. *Ann Oncol.* (2017) 28:mdx377.001. doi: 10.1093/annonc/mdx377.001
19. Long GV, Dummer R, Hamid O, Gajewski TF, Caglevic C, Dalle S, et al. Epacadostat plus pembrolizumab versus placebo plus pembrolizumab in patients with unresectable or metastatic melanoma (ECHO-301/KEYNOTE-252): a phase 3, randomised, double-blind study. *Lancet Oncol.* (2019) 20:1083–97. doi: 10.1016/S1470-2045(19)30274-8
20. Cagney DN, Martin AM, Catalano PJ, Redig AJ, Lin NU, Lee EQ, et al. Incidence and prognosis of patients with brain metastases at diagnosis of systemic malignancy: a population-based study. *Neuro Oncol.* (2017) 19:1511–21. doi: 10.1093/neuonc/nox077
21. Chaffer CL, Weinberg RA. A perspective on cancer cell metastasis. *Science.* (2011) 331:1559–64. doi: 10.1126/science.1203543
22. Tawbi HA, Boutros C, Kok D, Robert C, McArthur G. New era in the management of melanoma brain metastases. *Am Soc Clin Oncol Educ Book.* (2018):741–50. doi: 10.1200/EDBK_200819
23. Fabi A, Felici A, Metro G, Mirri A, Bria E, Telera S, et al. Brain metastases from solid tumors: disease outcome according to type of treatment and therapeutic resources of the treating center. *J Exp Clin Cancer Res.* (2011) 30:10. doi: 10.1186/1756-9966-30-10
24. Balch CM, Balch GC, Sharma RR. Identifying early melanomas at higher risk for metastases. *J Clin Oncol.* (2012) 30:1406–7. doi: 10.1200/JCO.2011.40.6983
25. Gramsch C, Göricke SL, Behrens F, Zimmer L, Schadendorf D, Krasny A, et al. Isolated cerebral susceptibility artefacts in patients with

malignant melanoma: metastasis or not? *Eur Radiol.* (2013) 23:2622–7. doi: 10.1007/s00330-013-2857-3
26. Miller D, Zappala V, El Hindy N, Livingstone E, Schadendorf D, Sure U, et al. Intracerebral metastases of malignant melanoma and their recurrences–a clinical analysis. *Clin Neurol Neurosurg.* (2013) 115:1721–8. doi: 10.1016/j.clineuro.2013.03.019
27. Gorantla V, Kirkwood JM, Tawbi HA. Melanoma brain metastases: an unmet challenge in the era of active therapy. *Curr Oncol Rep.* (2013) 15:483–91. doi: 10.1007/s11912-013-0335-3
28. Falchook GS, Long GV, Kurzrock R, Kim KB, Arkenau TH, Brown MP, et al. Dabrafenib in patients with melanoma, untreated brain metastases, and other solid tumours: a phase 1 dose-escalation trial. *Lancet.* (2012) 379:1893–901. doi: 10.1016/S0140-6736(12)60398-5
29. Long GV, Trefzer U, Davies MA, Kefford RF, Ascierto PA, Chapman PB, et al. Dabrafenib in patients with Val600Glu or Val600Lys BRAF-mutant melanoma metastatic to the brain (BREAK-MB): a multicentre, open-label, phase 2 trial. *Lancet Oncol.* (2012) 13:1087–95. doi: 10.1016/S1470-2045(12)70431-X
30. Gershenwald JE, Scolyer RA, Hess KR, Sondak VK, Long GV, Ross MI, et al. Melanoma staging: evidence-based changes in the American Joint Committee on Cancer eighth edition cancer staging manual. *CA Cancer J Clin.* (2017) 67:472–92. doi: 10.3322/caac.21409
31. Aspelund A, Antila S, Proulx ST, Karlsen TV, Karaman S, Detmar M, et al. A dural lymphatic vascular system that drains brain interstitial fluid and macromolecules. *J Exp Med.* (2015) 212:991–9. doi: 10.1084/jem.20142290
32. Louveau A, Smirnov I, Keyes TJ, Eccles JD, Rouhani SJ, Peske JD, et al. Structural and functional features of central nervous system lymphatic vessels. *Nature.* (2015) 523:337. doi: 10.1038/nature14432
33. Harris MG, Hulseberg P, Ling C, Karman J, Clarkson BD, Harding JS, et al. Immune privilege of the CNS is not the consequence of limited antigen sampling. *Sci Rep.* (2014) 4:4422. doi: 10.1038/srep04422
34. Anandasabapathy N, Victora GD, Meredith M, Feder R, Dong B, Kluger C, et al. Flt3L controls the development of radiosensitive dendritic cells in the meninges and choroid plexus of the steady-state mouse brain. *J Exp Med.* (2011) 208:1695–705. doi: 10.1084/jem.20102657
35. Hodi FS, Oble DA, Drappatz J, Velazquez EF, Ramaiya N, Ramakrishna N, et al. CTLA-4 blockade with ipilimumab induces significant clinical benefit in a female with melanoma metastases to the CNS. *Nat Clin Pract Oncol.* (2008) 5:557–61. doi: 10.1038/ncponc1183
36. Berghoff AS, Preusser M. The inflammatory microenvironment in brain metastases: potential treatment target? *Chin Clin Oncol.* (2015) 4:21. doi: 10.3978/j.issn.2304-3865.2015.06.03
37. Harter PN, Bernatz S, Scholz A, Zeiner PS, Zinke J, Kiyose M, et al. Distribution and prognostic relevance of tumor-infiltrating lymphocytes (TILs) and PD-1/PD-L1 immune checkpoints in human brain metastases. *Oncotarget.* (2015) 6:40836–49. doi: 10.18632/oncotarget.5696
38. Berghoff AS, Ricken G, Widhalm G, Rajky O, Dieckmann K, Birner P, et al. Tumour-infiltrating lymphocytes and expression of programmed death ligand 1 (PD-L1) in melanoma brain metastases. *Histopathology.* (2015) 66:289–99. doi: 10.1111/his.12537
39. Margolin K, Ernstoff MS, Hamid O, Lawrence D, McDermott D, Puzanov I, et al. Ipilimumab in patients with melanoma and brain metastases: an open-label, phase 2 trial. *Lancet Oncol.* (2012) 13:459–65. doi: 10.1016/S1470-2045(12)70090-6
40. Goldberg SB, Gettinger SN, Mahajan A, Chiang AC, Herbst RS, Sznol M, et al. Pembrolizumab for patients with melanoma or non-small-cell lung cancer and untreated brain metastases: early analysis of a non-randomised, open-label, phase 2 trial. *Lancet Oncol.* (2016) 17:976–83. doi: 10.1016/S1470-2045(16)30053-5
41. Nishino M, Giobbie-Hurder A, Manos MP, Bailey N, Buchbinder EI, Ott PA, et al. Immune-related tumor response dynamics in melanoma patients treated with pembrolizumab: identifying markers for clinical outcome and treatment decisions. *Clin Cancer Res.* (2017) 23:4671–9. doi: 10.1158/1078-0432.CCR-17-0114
42. Long GV, Atkinson V, Lo S, Sandhu S, Guminski AD, Brown MP, et al. Combination nivolumab and ipilimumab or nivolumab alone in melanoma brain metastases: a multicentre randomised phase 2 study. *Lancet Oncol.* (2018) 19:672–81. doi: 10.1016/S1470-2045(18)30139-6
43. Meireson A, Chevolet I, Hulstaert E, Ferdinande L, Ost P, Geboes K, et al. Peritumoral endothelial indoleamine 2, 3-dioxygenase expression is an early independent marker of disease relapse in colorectal cancer and is influenced by DNA mismatch repair profile. *Oncotarget.* (2018) 9:25216–24. doi: 10.18632/oncotarget.25393
44. Daud AI, Wolchok JD, Robert C, Hwu W-J, Weber JS, Ribas A, et al. Programmed death-ligand 1 expression and response to the anti–programmed death 1 antibody pembrolizumab in melanoma. *J Clin Oncol.* (2016) 34:4102–9. doi: 10.1200/JCO.2016.67.2477
45. Godin-Ethier J, Hanafi LA, Duvignaud JB, Leclerc D, Lapointe R. IDO expression by human B lymphocytes in response to T lymphocyte stimuli and TLR engagement is biologically inactive. *Mol Immunol.* (2011) 49:253–9. doi: 10.1016/j.molimm.2011.08.017
46. Mbongue JC, Nicholas DA, Torrez TW, Kim NS, Firek AF, Langridge WH. The role of indoleamine 2, 3-dioxygenase in immune suppression and autoimmunity. *Vaccines.* (2015) 3:703–29. doi: 10.3390/vaccines3030703
47. Terness P, Chuang JJ, Opelz G. The immunoregulatory role of IDO-producing human dendritic cells revisited. *Trends Immunol.* (2006) 27:68–73. doi: 10.1016/j.it.2005.12.006
48. Patel JK, Didolkar MS, Pickren JW, Moore RH. Metastatic pattern of malignant melanoma. A study of 216 autopsy cases. *Am J Surg.* (1978) 135:807–10. doi: 10.1016/0002-9610(78)90171-X
49. Davies MA, Liu P, McIntyre S, Kim KB, Papadopoulos N, Hwu WJ, et al. Prognostic factors for survival in melanoma patients with brain metastases. *Cancer.* (2011) 117:1687–96. doi: 10.1002/cncr.25634
50. Zimmer L, Apuri S, Eroglu Z, Kottschade LA, Forschner A, Gutzmer R, et al. Ipilimumab alone or in combination with nivolumab after progression on anti-PD-1 therapy in advanced melanoma. *Eur J Cancer.* (2017) 75:47–55. doi: 10.1016/j.ejca.2017.01.009
51. Larkin J, Chiarion-Sileni V, Gonzalez R, Grob JJ, Cowey CL, Lao CD, et al. Combined nivolumab and ipilimumab or monotherapy in untreated melanoma. *N Engl J Med.* (2015) 373:23–34. doi: 10.1056/NEJMoa1504030
52. Hodi FS, O'Day SJ, McDermott DF, Weber RW, Sosman JA, Haanen JB, et al. Improved survival with ipilimumab in patients with metastatic melanoma. *N Engl J Med.* (2010) 363:711–23. doi: 10.1056/NEJMoa1003466
53. Wolchok JD, Neyns B, Linette G, Negrier S, Lutzky J, Thomas L, et al. Ipilimumab monotherapy in patients with pretreated advanced melanoma: a randomised, double-blind, multicentre, phase 2, dose-ranging study. *Lancet Oncol.* (2010) 11:155–64. doi: 10.1016/S1470-2045(09)70334-1
54. Quail DF, Joyce JA. The microenvironmental landscape of brain tumors. *Cancer Cell.* (2017) 31:326–41. doi: 10.1016/j.ccell.2017.02.009
55. Doron H, Pukrop T, Erez N. A Blazing landscape: neuroinflammation shapes brain metastasis. *Cancer Res.* (2019) 79:423–36. doi: 10.1158/0008-5472.CAN-18-1805
56. Sleeman JP. The metastatic niche and stromal progression. *Cancer Metastasis Rev.* (2012) 31:429–40. doi: 10.1007/s10555-012-9373-9
57. Frenard C, Peuvrel L, Jean MS, Brocard A, Knol AC, Nguyen JM, et al. Development of brain metastases in patients with metastatic melanoma while receiving ipilimumab. *J Neurooncol.* (2016) 126:355–60. doi: 10.1007/s11060-015-1977-9
58. Robert C, Schadendorf D, Messina M, Hodi FS, O'Day S, investigators M-. Efficacy and safety of retreatment with ipilimumab in patients with pretreated advanced melanoma who progressed after initially achieving disease control. *Clin Cancer Res.* (2013) 19:2232–9. doi: 10.1158/1078-0432.CCR-12-3080
59. Tawbi HA-H, Forsyth PAJ, Hodi FS, Lao CD, Moschos SJ, Hamid O, et al. Efficacy and safety of the combination of nivolumab (NIVO) plus ipilimumab (IPI) in patients with symptomatic melanoma brain metastases (CheckMate 204). *J Clin Oncol.* (2019) 37:9501. doi: 10.1200/JCO.2019.37.15_suppl.9501
60. Long GV, Atkinson V, Menzies AM, Lo S, Guminski AD, Brown MP, et al. A randomized phase II study of nivolumab or nivolumab combined with ipilimumab in patients (pts) with melanoma brain metastases (mets): the Anti-PD1 Brain Collaboration (ABC). *J Clin Oncol.* (2017) 35:9508. doi: 10.1200/JCO.2017.35.15_suppl.9508
61. Helfrich I, Scheffrahn I, Bartling S, Weis J, von Felbert V, Middleton M, et al. Resistance to antiangiogenic therapy is directed by vascular phenotype, vessel stabilization, and maturation in malignant melanoma. *J Exp Med.* (2010) 207:491. doi: 10.1084/jem.20091846
62. Iwamoto T, Takahashi M, Ito M, Hamatani K, Ohbayashi M, Wajjwalku W, et al. Aberrant melanogenesis and melanocytic tumour development in transgenic mice that carry a metallothionein/ret fusion gene. *EMBO J.* (1991) 10:3167–75. doi: 10.1002/j.1460-2075.1991.tb04878.x
63. Jung KH, LoRusso PM, Burris HA, Gordon MS, Bang Y-J, Hellmann MD, et al. Phase I study of the indoleamine 2,3-dioxygenase 1 (IDO1)

inhibitor navoximod (GDC-0919) administered with PD-L1 inhibitor (Atezolizumab) in advanced solid tumors. *Clin Cancer Res.* (2019) 25:3220–8. doi: 10.1158/1078-0432.CCR-18-2740
64. Gibney GT, Hamid O, Lutzky J, Olszanski AJ, Mitchell TC, Gajewski TF, et al. Phase 1/2 study of epacadostat in combination with ipilimumab in patients with unresectable or metastatic melanoma. *J Immunother Cancer.* (2019) 7:80. doi: 10.1186/s40425-019-0562-8
65. Botticelli A, Cerbelli B, Lionetto L, Zizzari I, Salati M, Pisano A, et al. Can IDO activity predict primary resistance to anti-PD-1 treatment in NSCLC? *J Transl Med.* (2018) 16:219. doi: 10.1186/s12967-018-1595-3
66. Brown ZJ, Yu SJ, Heinrich B, Ma C, Fu Q, Sandhu M, et al. Indoleamine 2,3-dioxygenase provides adaptive resistance to immune checkpoint inhibitors in hepatocellular carcinoma. *Cancer Immunol Immunother.* (2018) 67:1305–15. doi: 10.1007/s00262-018-2190-4
67. Berghoff AS, Lassmann H, Preusser M, Höftberger RJC, Metastasis E. Characterization of the inflammatory response to solid cancer metastases in the human brain. *Clin Exp Metastasis.* (2013) 30:69–81. doi: 10.1007/s10585-012-9510-4
68. Berghoff AS, Fuchs E, Ricken G, Mlecnik B, Bindea G, Spanberger T, et al. Density of tumor-infiltrating lymphocytes correlates with extent of brain edema and overall survival time in patients with brain metastases. *Oncoimmunology.* (2016) 5:e1057388. doi: 10.1080/2162402X.2015.1057388
69. Zakaria R, Platt-Higgins A, Rathi N, Radon M, Das S, Das K, et al. T-cell densities in brain metastases are associated with patient survival times and diffusion tensor MRI changes. *Cancer Res.* (2018) 78:610–6. doi: 10.1158/0008-5472.CAN-17-1720
70. Sasiain MC, de la Barrera S, Fink S, Finiasz M, Alemán M, Fariña MH, et al. Interferon-gamma (IFN-gamma) and tumour necrosis factor-alpha (TNF-alpha) are necessary in the early stages of induction of CD4 and CD8 cytotoxic T cells by Mycobacterium leprae heat shock protein (hsp) 65 kD. *Clin Exp Immunol.* (1998) 114:196–203. doi: 10.1046/j.1365-2249.1998.00702.x
71. Brandacher G, Perathoner A, Ladurner R, Schneeberger S, Obrist P, Winkler C, et al. Prognostic value of indoleamine 2,3-dioxygenase expression in colorectal cancer: effect on tumor-infiltrating T cells. *Clin Cancer Res.* (2006) 12:1144–51. doi: 10.1158/1078-0432.CCR-05-1966
72. Ino K, Yamamoto E, Shibata K, Kajiyama H, Yoshida N, Terauchi M, et al. Inverse correlation between tumoral indoleamine 2,3-dioxygenase expression and tumor-infiltrating lymphocytes in endometrial cancer: its association with disease progression and survival. *Clin Cancer Res.* (2008) 14:2310–7. doi: 10.1158/1078-0432.CCR-07-4144
73. Schulz M, Salamero-Boix A, Niesel K, Alekseeva T, Sevenich L. Microenvironmental regulation of tumor progression and therapeutic response in brain metastasis. *Front Immunol.* (2019) 10:1713. doi: 10.3389/fimmu.2019.01713
74. Wischhusen J, Jung G, Radovanovic I, Beier C, Steinbach JP, Rimner A, et al. Identification of CD70-mediated apoptosis of immune effector cells as a novel immune escape pathway of human glioblastoma. *Cancer Res.* (2002) 62:2592–9.
75. Soffietti R, Abacioglu U, Baumert B, Combs SE, Kinhult S, Kros JM, et al. Diagnosis and treatment of brain metastases from solid tumors: guidelines from the European Association of Neuro-Oncology (EANO). *Neuro Oncol.* (2017) 19:162–74. doi: 10.1093/neuonc/now241
76. Ramakrishna N, Margolin KA. Multidisciplinary approach to brain metastasis from melanoma; local therapies for central nervous system metastases. *Am Soc Clin Oncol Educ Book.* (2013):399–403. doi: 10.1200/EdBook_AM.2013.33.399
77. Kowal J, Kornete M, Joyce JA. Re-education of macrophages as a therapeutic strategy in cancer. *Immunotherapy.* (2019) 11:677–89. doi: 10.2217/imt-2018-0156

Conflict of Interest: GR has received research grants from Roche and Merck, as well as honoraria for advisory boards from Abbvie. DS has received research grants from BMS and Novartis, as well as honoraria for being a member of advisory boards/consultant or as speaker from the following companies: Amgen, Array, Astra Zeneca, BMS, EMD-Serono, Incyte, Immunocore, Merck, Novartis, Philogen, Pierre Fabre, Pfizer, Regeneron, Roche, 4SC.

The remaining authors declare that the research was conducted in the absence of any commercial or financial relationships that could be construed as a potential conflict of interest.

frontiers in Immunology

ORIGINAL RESEARCH
published: 27 May 2020
doi: 10.3389/fimmu.2020.00839

Indoleamine 2,3-Dioxygenase 2 Immunohistochemical Expression in Resected Human Non-small Cell Lung Cancer: A Potential New Prognostic Tool

Martina Mandarano[1], Guido Bellezza[1], Maria Laura Belladonna[2], Jacopo Vannucci[3], Alessio Gili[4], Ivana Ferri[1], Chiara Lupi[5], Vienna Ludovini[6], Giulia Falabella[1], Giulio Metro[6], Giada Mondanelli[2], Rita Chiari[7], Lucio Cagini[3], Fabrizio Stracci[4,5], Fausto Roila[6], Francesco Puma[3], Claudia Volpi[2] and Angelo Sidoni[1]*

[1] Section of Anatomic Pathology and Histology, Department of Experimental Medicine, Medical School, University of Perugia, Perugia, Italy, [2] Section of Pharmacology, Department of Experimental Medicine, University of Perugia, Perugia, Italy, [3] Department of Thoracic Surgery, Medical School, University of Perugia, Perugia, Italy, [4] Section of Public Health, Department of Experimental Medicine, University of Perugia, Perugia, Italy, [5] Umbria Cancer Registry, Perugia, Italy, [6] Department of Medical Oncology, Santa Maria della Misericordia Hospital, Perugia, Italy, [7] Medical Oncology, Ospedali Riuniti Padova sud, Padova, Italy

OPEN ACCESS

Edited by:
Lieve Brochez, Cancer Research Institute, Ghent University, Belgium

Reviewed by:
Marie-Andree Forget, University of Texas MD Anderson Cancer Center, United States
Avinoam Nevler, Thomas Jefferson University, United States

***Correspondence:**
Martina Mandarano
mandaranomartina@gmail.com

Specialty section:
This article was submitted to Cancer Immunity and Immunotherapy, a section of the journal Frontiers in Immunology

Received: *09 January 2020*
Accepted: *14 April 2020*
Published: *27 May 2020*

Citation:
Mandarano M, Bellezza G, Belladonna ML, Vannucci J, Gili A, Ferri I, Lupi C, Ludovini V, Falabella G, Metro G, Mondanelli G, Chiari R, Cagini L, Stracci F, Roila F, Puma F, Volpi C and Sidoni A (2020) Indoleamine 2,3-Dioxygenase 2 Immunohistochemical Expression in Resected Human Non-small Cell Lung Cancer: A Potential New Prognostic Tool. Front. Immunol. 11:839. doi: 10.3389/fimmu.2020.00839

Indoleamine 2,3-dioxygenase 2 (IDO2) is an analog of the tryptophan degrading and immunomodulating enzyme indoleamine 2,3-dioxygenase 1 (IDO1). Although the role of IDO1 is largely understood, the function of IDO2 is not yet well-elucidated. IDO2 overexpression was documented in some human tumors, but the linkage between IDO2 expression and cancer progression is still unclear, in particular in non-small cell lung cancer (NSCLC). Immunohistochemical expression and cellular localization of IDO2 was evaluated on 191 formalin-fixed and paraffin-embedded resected NSCLC. Correlations between IDO2 expression, clinical-pathological data, tumor-infiltrating lymphocytes (TILs), immunosuppressive tumor molecules (IDO1 and programmed cell death ligand-1 – PD-L1 –) and patients' prognosis were evaluated. IDO2 high expression is strictly related to high PD-L1 level among squamous cell carcinomas group ($p = 0.012$), to either intratumoral or mixed localization of TILs ($p < 0.001$) and to adenocarcinoma histotype ($p < 0.001$). Furthermore, a significant correlation between IDO2 high expression and poor non-small cell lung cancer prognosis was detected ($p = 0.011$). The current study reaches interesting knowledge about IDO2 in non-small cell lung cancer. The close relationship between IDO2 expression, PD-L1 increased levels, TILs localization and NSCLC poor prognosis, assumed IDO2 as a potential prognostic biomarker to be exploited for optimizing innovative combined therapies with immune checkpoint inhibitors.

Keywords: indoleamine 2,3-dioxygenase 2, non-small cell lung cancer, immunohistochemistry, biomarker, immunomodulator

INTRODUCTION

Lung cancer is one of the major cause of cancer-related morbidity and mortality across the globe, and non–small cell lung cancer (NSCLC) represents the majority of lung malignancies (1). In recent years, the treatment of NSCLC has been partly improved by the introduction of immunotherapies and, in particular, employing the FDA approved immune checkpoint inhibitors (2). However, only about 20% of these patients can benefit from this therapy, resulting in the need for new biomarkers both to amplify the effect of immune checkpoint inhibitors and to identify new and more efficient therapeutic targets (3).

A large body of evidence indicates that tryptophan (Trp) metabolism is of paramount importance in cancer progression and for the increase of malignant properties of cancer cells (4–6). The immunoregulatory molecule indoleamine 2,3-dioxygenase 1 (IDO1)—which catalyzes the first, rate-limiting step of Trp degradation through the kynurenine (Kyn) pathway—is highly expressed in many types of human cancers (6, 7) and is generally associated with poor prognosis (8). Similarly, tryptophan 2,3-dioxygenase (TDO), which catalyzes the same reaction of IDO1, is expressed in a wide range of malignancies and has been shown to promote tumor progression and metastasis (9). Less is known about the third member of the Trp-degrading enzyme family, indoleamine 2,3-dioxygenase 2 (IDO2) (6). IDO1 and IDO2 are closely linked on chromosome 8 in humans, probably originating from an ancient gene duplication which occurred prior to the evolution of vertebrates (10, 11). Although characterized by a high level of sequence identity (11), IDO1 and IDO2 exhibit important functional differences, such as IDO2 being endowed with a very weak catalytic activity *in vitro* (12). Moreover, plasmatic levels of Trp and Kyn are similar in wild-type and *Ido2* $^{-/-}$ mice, suggesting that IDO2 is not as efficient as IDO1 or TDO in converting Trp to Kyn *in vivo* (13). In tumors, IDO2 seems to be less frequently overexpressed than IDO1. Human gastric, colorectal, and renal carcinomas constitutively express both IDO1 and IDO2 (6, 14), as well as brain tumors, such as gliomas and meningiomas (15), and pancreatic ductal adenocarcinomas, in which IDO2 appears to be overexpressed (16).

However, despite the evidence of IDO2 expression in several types of malignancies, there are a limited number of studies about it in human tissues and its supposed functional role in the development and/or progression of cancer is still to be corroborated, in particular in NSCLC (6).

Recent studies showed that IDO1 is commonly expressed by NSCLC (17, 18) while there is still no evidence about its paralogue IDO2.

Our purpose is to evaluate the level of IDO2 through its immunohistochemical expression in a series of resected NSCLCs, in order to assess its presence and localization in the tumor cells of this specific type of cancer. Moreover, we aim to unveil potential correlations between IDO2 expression, clinical-pathological parameters, immunosuppressive molecules of the tumor microenvironment and patients' prognosis, in order to outline IDO2 as both a potential new biomarker for better patient risk stratification and as a possible target for the pharmacological treatment of NSCLC.

MATERIALS AND METHODS

Patient Selection

The study has been prepared according to ethical guidlines regarding the informed consent of the involved human participants (Number of Local Ethic Committee Decision: 2216/13 of CEAS Umbria).

Patients were recruited from the computer archive of the Institute of Anatomic Pathology and Histology, S. M. Misericordia Hospital, Perugia, Italy, involving all the NSCLC cases which underwent a surgical resection in the period from 2009 to 2015. Moreover, only the cases with both known clinical parameters (summarized in **Table 1**) and with a complete clinical follow-up until 31st December 2017 were considered. The cases in pathological stage IV, according to the 8th edition for cancer staging by the American Joint Committee on Cancer (AJCC), were not taken into account. Regarding the other stages of disease, we arranged the NSCLCs into two groups: a Stage I group, encompassing the stages from IA1 to IB, and a Stage II-III one, enclosing the stages from IIA to IIIB.

Histology and Immunohistochemistry

Surgical specimens were formalin-fixed (10% buffered formalin) and paraffin-embedded (FFPE). Sections of 4 μm were taken and placed on slides with a permanent positive charged surface, both to obtain the Hematoxylin and Eosin (H&E) stain and the Immunohistochemical (IHC) stains. The H&E stain was carried out using a Leica ST5020 Multistainer (Leica Microsystems), employing the kit ST Infinity H&E Staining System (Leica Biosystems). All the IHC stains (peroxidase immunoenzymatic reaction with development in diaminobenzinidine) were obtained by employing the BOND-III fully automated immunohistochemistry stainer (Leica Biosystems). In particular, IDO2 immunohistochemical slides were carried out using a heat-induced antigen retrieval with the ready to use Bond™ Epitope Retrieval Solution 1 (Leica Biosystems, Catalog No: AR9961) for 20 min, primary antibody incubation for 15 min (IDO2, Thermofisher Scientific, Cat# PA5-71696, RRID: AB_2717550, dilution 1:500) and the ready to use Bond™ Polymer Refine Detection System (Leica Biosystems, Catalog No: DS9800). Proper positive and negative controls were included.

Histological subtype was assigned based on H&E slides, according to 2015 World Health Organization (WHO) classification for lung tumors. Moreover, in line with the immunohistochemical expression both of TTF-1 (Agilent, Cat#M357501-2, RRID: AB_2801260; dilution 1:100; BOND-III fully automated immunohistochemistry stainer, Leica Biosystems) and p40 (ScyTek Laboratories, Cat#A00112-C, RRID: AB_2800554, dilution 1:50; BOND-III fully automated immunohistochemistry stainer, Leica Biosystems) poorly differentiated NSCLCs were classified as adenocarcinomas or as squamous cell carcinomas.

TABLE 1 | Expression of IDO2, clinical-pathological parameters and other microenvironmental molecule associations.

Parameter	IDO2 low		IDO2 high			Total	
	N	%	*N*	%	*p*	*N*	%
	31	**16**	**160**	**84**		**191**	**100**
GENDER							
M	23	17	114	83	0.739	137	72
F	8	15	46	85		54	28
AGE							
<68 years	13	15	74	85	0.659	87	46
≥68 years	18	17	86	83		104	54
SMOKING							
Current smokers	13	17	64	83	0.910	77	40
Former smokers	16	16	82	84		98	51
Never smokers	2	12	14	88		16	9
RELAPSE							
Yes	12	16	61	84	0.951	73	38
No	19	16	99	84		118	62
EXITUS							
Yes	6	9	58	91	0.068	64	34
No	25	20	102	80		127	66
STAGE							
Adc[a] stage						***122***	***64***
I	6	8	68	92	0.964	74	61
II - III	4	8	44	92		48	39
Sqcc[b] stage						***69***	***36***
I	7	26	20	74	0.513	27	39
II - III	14	33	28	67		42	61
HISTOTYPE							
Adc[a]	10	8	112	92	**<0.001**	122	64
Sqcc[b]	21	30	48	70		69	36
Adc[a] pattern						***122***	***64***
Other than solid	6	6	89	94	0.155	95	78
Solid	4	15	23	85		27	22
TILs DENSITY							
Adc[a]						***122***	***64***
Low	5	8	57	92	0.956	62	51
High	5	8	55	92		60	49
Sqcc[b]						***69***	***36***
Low	12	34	23	66	0.480	35	51
High	9	26	25	74		34	49
TILs LOCALIZATION							
Adc[a]						***122***	***64***
Intratumoral	4	6	61	94	**<0.001**	65	53
Peritumoral	5	71	2	29		7	6
Mixed	4	9	42	91		46	38
Absent	0	0	4	100		4	3
Sqcc[b]						***69***	***36***
Intratumoral	8	33	16	67	0.905	24	35
Peritumoral	2	29	5	71		7	10
Mixed	11	30	26	70		37	54
Absent	0	0	1	100		1	1
IDO1							
Adc[a]						***122***	***64***
Low	4	7	52	93	0.695	56	46
High	6	9	60	91		66	54
Sqcc[b]						***69***	***36***
Low	10	32	21	68	0.766	31	45
High	11	29	27	71		38	55
PD-L1							
Adc[a]						***122***	***64***
Low	6	6	96	94	**0.035**	102	84
High	4	20	16	80		20	16
Sqcc[b]						***69***	***36***
Low	19	40	29	60	**0.012**	48	70
High	2	10	19	90		21	30

[a]***Adc:*** *adenocarcinoma.* [b]***Sqcc:*** *squamous cell carcinoma.*

The H&E slides were also employed to determine both the localization of tumor-infiltrating lymphocytes (TILs) (absent; intratumoral= among tumor cells; peritumoral= at the interface between the neoplasia and healthy lung parenchyma; mixed= mixture of the last two localizations) and the density of TILs, according to the percentage of lymphocytes observed in a given localization (Low < 20%; High ≥ 20%) (19).

The immunohistochemical stains for IDO2 were evaluated on neoplastic cells and were interpreted, as previously reported (19), using an H Score resulting from the sum of the intensity of the stain (evaluated as 0: absent; 1+: mild; 2+: moderate; 3+: intense) and the percentage of the tumor cells labeled (0: 0%; 1: 1–25%; 2: 26–50%; 3: 51–75%; 4: 76–100%). Thereafter, two groups of staining were obtained: a low expression one—scores from 0 to 2—and a high expression one—scores from 3 to 7.

In addition, the results concerning the expression of both indoleamine 2,3-dioxygenase (IDO1) [courtesy of professor Benoit J Van den Eynde, Ludwing Institute for Cancer Research, clone 4.16H1 (7); dilution 1:1000; BOND-III fully automated immunohistochemistry stainer, Leica Biosystems] and programmed cell death Ligand-1 (PD-L1) (Cell Signaling Technology, Cat# 13684S, RRID: AB_2687655, dilution 1:200; BOND-III fully automated immunohistochemistry stainer, Leica Biosystems) were obtained from a previous study (19), in which they were divided into the same classes of expression as abovementioned for IDO2.

Moreover, the localization of the label of IDO2 in the peritumoral lung tissue was noted, according to histomorphological parameters to identify the various cellular types present.

Statistical Analysis

Categorical variables were presented as frequencies with row and column percentages. Patients were divided into a young and an elderly group, according to the cut-off age (68 years, corresponding to patients' median age) for analysis. Categorical variables were compared between the groups (IDO2 low or IDO2 high) using Chi-square test or Fisher's exact test as appropriate. Odds Ratio (OR) was estimated when association was statistically significant.

Other causes of death were regarded as competing risk events in the patients' end-point. The cumulative incidence function (CIF) was compared between groups using Gray's method and was shown on a plot (20). Analysis of disease free survival (DFS) and overall survival (OS) were evaluated using a Fine and Gray model (competing risks regression in **Supplementary Material 1**) (21).

Continuous variables were categorized and the proportional hazards assumption of categorical variables was verified using a log-minus-log plot.

A p-value (p) < 0.05 was considered as statistically significant.

Statistical analyses were performed by STATA 15.1 (StataCorpLP, Collage Station TX, USA) (22).

RESULTS

Patients Series

Data about patients' series were shown in **Table 1**.

One hundred and ninety-one patients were eligible for the study. Patients were all Caucasian, the median age was 68 years (range 38–84), with a median follow-up period of 50 months (range 1–107 months). One hundred and thirty-seven (72%) patients were males; 175 (91%) were either current smokers or former smokers. Regarding the pathological staging classification, 101 cases (53%) belonged to stage I, whereas 90 (47%) patients were in stage II-III. Fifty-six (29%), 16 (8%) and 1 (0.5%) patients relapsed after surgery, presenting 1, 2, or 3 localizations, respectively. Moreover, 12 patients presented nodal metastasis, 10 of which with one or more that were synchronous and hematogenous. Sixty-four (34%) died from NSCLC (**Table 1**).

Pathological Findings

Data about pathological findings were summarized in **Table 1**.

Regarding histological characterization, the series was composed of 122 (64%) adenocarcinomas and 69 (36%) squamous cell carcinomas.

The most frequent predominant pattern of adenocarcinomas was the acinar (78; 64%).

Just over half of the adenocarcinomas (74; 61%) belonged to stage I, whereas the majority of squamous cell carcinomas (42; 61%) were in stage II-III.

IDO2 Immunohistochemical Analysis

Concerning IDO2 evaluation, the majority of the tumors (160 cases, 84%) belonged to the high expression group of this molecule, both among adenocarcinomas (112; 92%) and among squamous cell carcinomas (48; 70%, **Table 1**).

Most of the tumors (158; 83%) presented a membrane reinforcement of the stain (**Figure 1A**), with only 19 (12%) of those cases presenting a focal IDO2 labeling. In addition, 17 (11%) cases presented simultaneous cytoplasmic stains (**Figure 1B**) and, among these, only one had diffuse IDO2 expression. Eighty (51%) of the cases with only membranous immunostaining (which were 77–96% adenocarcinomas and 3–4% squamous cell carcinomas) presented IDO2 expression on the basolateral side of the tumor cellular membrane, with a reinforcement of the stain at the interface between tumor and stromal tissue and without an apical immunolabel (**Figure 1C**). Similarly, the immunostains presented a reinforcement at the interface between the tumor nest and healthy lung parenchima in 4 (6%) squamous cell carcinomas. Twenty cases (10%) also presented a nuclear pattern of staining (**Figure 1D**), most of which were in adenocarcinomas (19; 95%) seemed to highlight the nucleoli of the cells.

As for the peritumoral lung tissues, there was a constant IDO2 expression in bronchial epithelial cells, localized in their cytoplasm, with membrane reinforcement (**Figure 1D**); due to this aspect, we used this expression as an internal control for the labeling. We also found IDO2 in subepithelial bronchial glands with a diffuse pattern of staining.

In the lung parenchyma, IDO2 marked reactive pneumocytes close to tumor tissue and also intralveolar macrophages. In both cases there was a granular intracytoplasmatic staining.

Clinical-Pathological Associations

The IDO2 associations with clinical-pathological parameters were reported in **Table 1**.

IDO2 showed a high expression when associated with a specific NSCLC histotype: in fact, in our series its high expression was found especially in adenocarcinomas ($p < 0.001$; OR = 4.9).

There were no correlations between IDO2 expression and the other clinical-pathological parameters examined, although there was almost a statistically significant association ($p = 0.068$) with patients who died from NSCLC: 91% presented a high IDO2 expression.

Microenvironmental Associations

Data about associations between IDO2 and microenvironment molecules were shown in **Table 1**.

Interestingly, a high IDO2 expression correlated with high PD-L1 among the squamous cell carcinomas group ($p = 0.012$; OR = 6.2). On the other hand, among the adenocarcinomas group it was seen that the higher the expression of IDO2, the lower the expression of PD-L1 ($p = 0.035$; OR = 4.0).

There was no association between IDO1 and IDO2 expression, both in the adenocarcinomas and the squamous cell carcinomas groups.

It is worthy of note that among the adenocarcinoma subgroup, high IDO2 expression was associated with an intratumoral or mixed localization of the TILs (94 and 91% of the cases, respectively), in a statistically significant manner ($p < 0.001$; OR = 11.4). On the other hand, there was no association with IDO2 expression and TIL density, in either of the histotype groups.

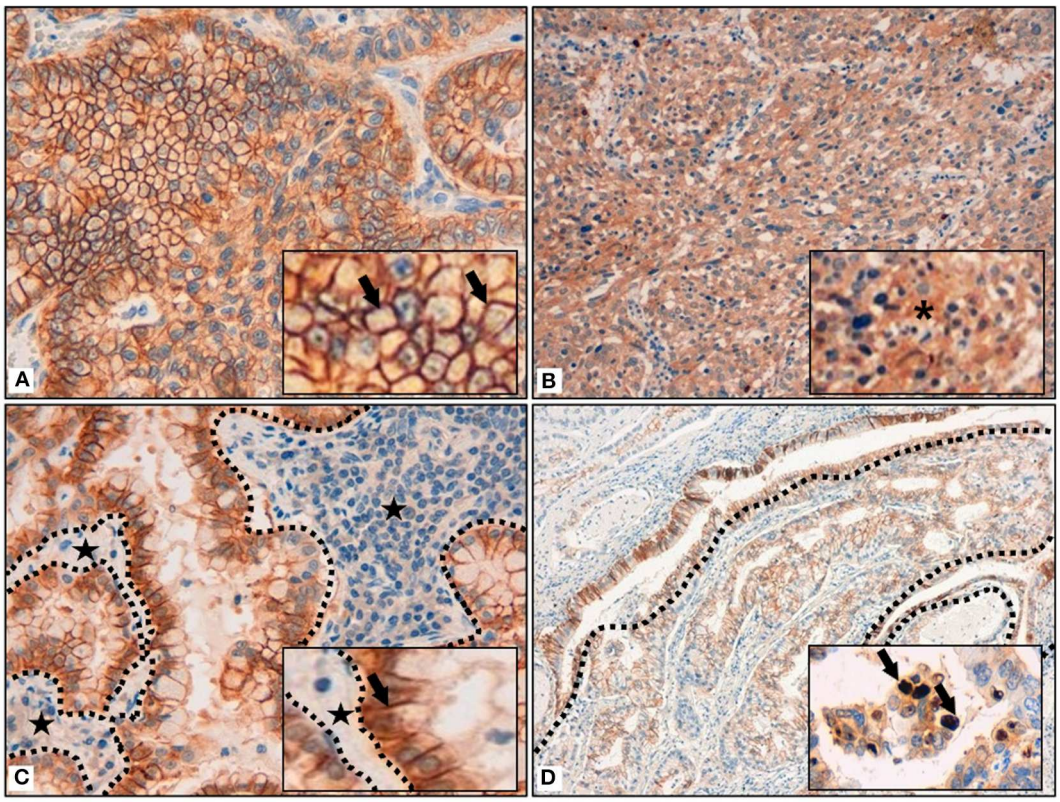

FIGURE 1 | (A) Membrane reinforcement of IDO2, as black arrows shown in the inset. (**B**) Cytoplasmic expression of IDO2, as indicated in the inset by an asterisk. **(C)** IDO2 staining reinforcement at tumor-stroma interface. Dotted lines circumscribe the stroma and the black stars highlight it; IDO2 staining reinforcement is shown by the black arrow in the inset. **(D)** IDO2 bronchial epithelium staining (top left of the longer dotted line and circumscribed by the shorter dotted lines) and membranous tumoral staining (bottom right of the longer dotted line). Arrows in the inset highlight the nuclear staining of IDO2. Original magnification 400× **(A,C)**, 200× **(B)**, 100× **(D)**; insets: 600× **(A,C)**, 400× **(B,D)**.

Survival Analysis

The results concerning the survival analysis were displayed in **Tables 2**, **3**.

Regarding the univariate analysis, the most relevant statistically significant associations were between the increased probability of death from NSCLC and high expression of both IDO2 (SHR 2.64, 95% Confidence Interval—CI−1.11–6.31, $p = 0.028$) and IDO1 (SHR 1.71, 95% CI 1.02–2.85, $p = 0.041$); these relationships persisted also in the multivariate analysis, which highlighted a greater probability of death for the patients with a tumor high expression of either IDO2 or IDO1 than the NSCLC with a low expression level of these molecules (SHR 2.94, 95% CI 1.28–6.77, $p = 0.011$ and SHR 1.64, 95% CI 1.12–2.76, $p = 0.041$, respectively; **Table 2**). In addition, regarding patients with a high tumor expression of IDO2, the probability of death within 36 months was roughly 18% compared to almost 7% for the group with a low expression of IDO2 ($p < 0.001$). This difference increased within 60 months (28 vs. 12%, respectively, $p<0.001$; **Figure 2**).

Similarly, both in the univariate and in the multivariate analysis, either being a male patient or presenting a stage II-III of disease increased the probability of death from NSCLC (**Table 2**).

The histotype, age of the patient, smoking habits, expression of PD-L1, TILs density and TILs localization had no statistically significant correlations with the probability of death from NSCLC (**Table 2**).

Belonging to either the stage II-III group or the adenocarcinoma group increased the risk of recurrence in the present NSCLC series, both regarding the univariate (SHR 1.60 and 1.96; 95% CI 1.01–2.54 and 1.16–3.32; $p = 0.044$ and 0.012, respectively) and the multivariate analysis (SHR 1.92 and 2.31; 95% CI 1.20–3.09 and 1.35–3.96; $p= 0.006$ and 0.002, respectively), as reported in **Table 3**.

IDO2 and the other parameters considered showed no association with the DFS.

DISCUSSION

Little is known about the role of indoleamine 2,3-dioxygenase 2 (IDO2) and its implications both in normal lung tissue and in NSCLC. In this scenario, we examined IDO2 immunolabeling in 191 resected NSCLC cases, in order to better understand its expression in this cancer type and to determine its correlations

TABLE 2 | Fine and Gray model on overall survival (OS).

Parameter	Univariate analysis			Multivariate analysis		
	SHR[a]	*p-value*	*95% CI*[b]	*SHR*[a]	*p-value*	*95% CI*[b]
IDO2						
Low	ref	–	–	ref	–	–
High	2.64	**0.028**	(1.11–6.31)	2.94	**0.011**	(1.28–6.77)
IDO1						
Low	ref	–	–	ref	–	–
High	1.71	**0.041**	(1.02–2.85)	1.64	**0.041**	(1.12–2.76)
SEX						
Female	ref	–	–	ref	–	–
Male	2.03	**0.029**	(1.08–3.85)	2.22	**0.019**	(1.14–4.31)
STAGE						
I	ref	–	–	ref	–	–
II–III	1.88	**0.011**	(1.16–3.07)	1.99	**0.005**	(1.23–3.24)
HISTOTYPE						
Adc[c]	1.41	0.189	(0.84–2.37)	–		
Sqcc[d]	ref	–	–			
AGE						
<68 years	ref	–	–	–		
≥68 years	1.04	0.887	(0.64–1.69)			
SMOKING						
Current smoker	1.86	0.219	(0.69–5.04)	–		
Former smoker	1.60	0.350	(0.60–4.29)			
Never smoker	ref	–	–			
PD–L1						
Low	1.04	0.904	(0.57–1.87)	–		
High	ref	–	–			
TILs DENSITY						
Low	ref	–	–	–		
High	1.05	0.841	(0.65–1.71)			
TILs LOCALIZATION						
Intratumoral	1.04	0.972	(0.12–9.19)	–		
Peritumoral	1.45	0.752	(0.14–10.81)			
Mixed	1.24	0.848	(0.14–10.81)			
Absent	ref	–	–			

[a]*SHR: Subdistribution Hazard Ratio.* [b]*CI: Confidence Interval.* [c]*Adc: adenocarcinoma.* [d]*Sqcc: squamous cell carcinoma.*

TABLE 3 | Fine and Gray model on disease free survival (DFS).

Parameter	Univariate analysis			Multivariate analysis		
	SHR[a]	*p-value*	*95% CI*[b]	*SHR*[a]	*p-value*	*95% CI*[b]
IDO2						
Low	ref	–	–	–		
High	1.03	0.937	(0.55–1.91)			
IDO1						
Low	ref	–	–	–		
High	1.44	0.133	(0.89–2.31)			
SEX						
Female	ref	–	–	–		
Male	1.22	0.461	(0.72–2.05)			
STAGE						
I	ref	–	–	ref	–	–
II–III	1.60	**0.044**	(1.01–2.54)	1.92	**0.006**	(1.20–3.09)
HISTOTYPE						
Adc[c]	1.96	**0.012**	(1.16–3.32)	2.31	**0.002**	(1.35–3.96)
Sqcc[d]	ref	–	–	ref	–	–
AGE						
<68 years	ref	–	–	–		
≥68 years	0.72	0.163	(0.45–1.14)			
SMOKING						
Current smoker	1.91	0.173	(0.75–4.87)	–		
Former smoker	1.23	0.663	(0.47–3.17)			
Never smoker	ref	–	–			
PD–L1						
Low	1.06	0.834	(0.60–1.88)	–		
High	ref	–	–			
TILs DENSITY						
Low	ref	–	–	–		
High	1.00	0.986	(0.63–1.58)			
TILs LOCALIZATION						
Intratumoral	1.80	0.563	(0.25–13.15)	–		
Peritumoral	2.54	0.380	(0.31–20.34)			
Mixed	1.50	0.691	(0.20–11.01)			
Absent	ref	–	–			

[a]*SHR: Subdistribution Hazard Ratio.* [b]*CI: Confidence Interval.* [c]*Adc: adenocarcinoma.* [d]*Sqcc: squamous cell carcinoma.*

with clinical-pathological parameters, other immunomodulatory molecules and patients' prognosis.

Unlike IDO1, the real IDO2 cellular function is poorly understood even today, in both normal and tumor cells. As a matter of fact, it seems to have no—or just low—enzymatic activity on tryptophan, so some other mechanisms could be involved to explain its putative role in the tumoral immunoescape (6, 11, 13, 14, 23–26).

Previous studies demonstrated a constitutive expression of only IDO2 mRNAs in human liver, small intestine, spleen, brain, thyroid, placenta, thymus, lung, kidney, colon, endometrium and testis, with a full length and functional transcript highlighted only for the placenta and brain (6, 27–29). Surprisingly we found, as an incidental observation, an almost constant immunohistochemical IDO2 staining of both the bronchial epithelium and peribronchial sub-epithelial glands. The continuous exposure of the airways, particularly the upper ones, to external stimuli could explain the induction of a putatively tolerogenic IDO2 in the abovementioned tissues, as happens in antigen presenting cells (APCs) or in B cells during either inflammatory or reactive states (25–28).

Furthermore, the IDO2 labeling of both reactive pneumocytes and alveolar macrophages, observed in the current study, seems to confirm the existence of an adjunctive mechanism triggering IDO2 expression under specific microenvironmental conditions, such as stress. Nevertheless, if the immunohistochemical expression corresponds to a functionally active IDO2 protein (6, 16, 29) in human lung tissues it would need further studies.

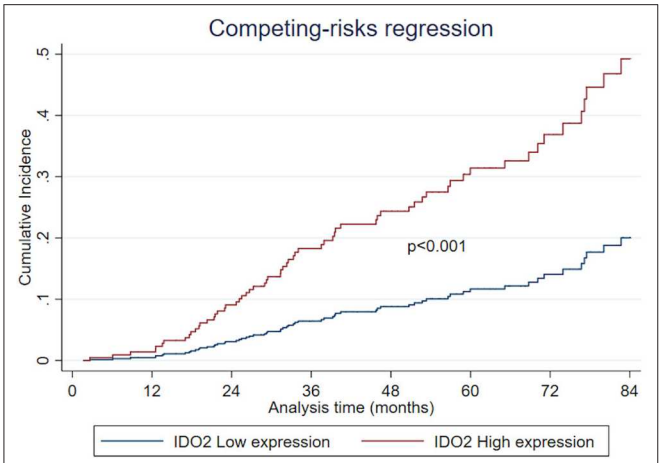

FIGURE 2 | The cumulative incidence of IDO2 expression after competing-risks regression.

Another interesting and incidental finding is that 10% of NSCLCs presented a nuclear pattern of IDO2 staining in tumor cells. This was already observed in murine series regarding hepatocytes (13). Moreover, in a previous study (19) we reported a nuclear labeling for IDO1 in NSCLC. However, it is generally not known how these two molecules would act at nuclear level, but the observation that some tumors present a nuclear localization of both IDO1 and IDO2 may suggest a signal-transducing function (13, 30), something already noted about IDO1 (31).

Furthermore, the consistent percentage (83%) of NSCLC in our series with an intense membranous IDO2 immunolabeling might open the way to further studies about its correlation with adhesion molecules, such as those from the cadherin family. It is known how the latter are involved in epithelial-mesenchymal transition in an Aryl hydrocarbon Receptor (AhR)-kynurenine dependent manner (32, 33), and that the kynurenines are in turn the product of IDO1 enzymatic activity. On the other hand, it is also known that IDO2 is not expressed as a functional tryptophan-degrading enzyme (6), at least not in human cancer cells lines (14). As an alternative, other authors (29) have correlated the IDO2-dependent/tryptophan-independent activation of an inhibitory isoform of immunoregulatory transcription factor NF-IL6 (LIP) to a potential IDO2 role in metastatization. Consequently, a difference between IDO1 and IDO2 activity may really exist. These findings could support either a direct role of IDO2 in cellular adhesion (13) or an indirect role in modulating other adhesion molecules, promoting tumor invasiveness and transition toward a mesenchymal and more aggressive phenotype. Regarding the correlation between this IDO2 localization and the patients' prognosis, we did not find any statistically significant results. Furthermore, the majority of the NSCLCs with such an immunolabeling pattern were, interestingly, adenocarcinomas. Moreover, this histotype often (64%) has a basolateral staining of the tumor cells, possibly related to the presence of intracytoplasmic mucus, which is a characteristic of the adenocarcinoma, in particular of the most differentiated ones. In addition, a high IDO2 level was more frequently present in adenocarcinomas than in the squamous cell carcinoma subgroup, a finding that corroborates the strict relationship between this molecule and the specific microenvironment of this NSCLC histotype. Despite the fact that IDO2 action in adenocarcinomas and in adenocarcinoma patterns may differ from that of IDO1 (6, 11, 14, 17–19, 24–26), we could speculate about the existence of other immunosuppressive mechanisms induced by IDO2 in this NSCLC subgroup. An alternative splicing of IDO2 (6, 13) could explain the different localizations found and suggest the occurrence of a distinctive splicing induction under certain conditions, such as inflammatory states, or according to particular tumor histotype—adenocarcinomas—as above reported. Some authors suggest that IDO2 activation is related to specific microenvironmental conditions (13, 26, 34) in specific cell types (11, 25), such as the neoplastic ones in our study, which is consistent with its possible immunomodulatory role in either stress conditions or disease response (13, 25).

Interestingly, we found a high co-expression of both PD-L1 and IDO2 in the squamous cell carcinomas subgroup, further evidence that IDO2 expression occurs in cells displaying tolerance markers. Based on this finding, a dual combination NSCLC therapy, such as inhibitors of both PD-1/PD-L1 immune checkpoints and IDO2, might be hypothesized. Currently, the combination of immunocheckpoint inhibitors and IDO1 hinderers has already been tested in ongoing clinical trials, with encouraging results in NSCLC patients (35, 36). This approach could be easily transposed into further researches targeting combination therapies including IDO2 inhibitors.

Moreover, the fact that high IDO2 expression is associated, among adenocarcinomas, with intratumoral and mixed localization of TILs could suggest a possible role for IDO2 as an immunomodulatory molecule. As a matter of fact, it is partly already known how IDO2 could be involved in B cell-mediated autoimmunity (23, 37) and may also influence Treg activation (37). Although in some murine models IDO2 has been associated with a potential pro-inflammatory role, particularly in autoimmune diseases (38), other authors showed that IDO2 contributions to inflammation, both in the context of cancer and autoimmune disorders, remains to be elucidated (38, 39). Moreover, Metz et al. (26) demonstrated an immune modulation role of IDO2, and distinguished its non-redundant contributions to inflammation. Consequently, the increased IDO2 expression in NSCLC could likely occur when the tumor cells are closely in contact with the inflammatory infiltrate, and could be interpreted as a tumor attempt to evade the immune system attack (40–43).

Furthermore, there is a strict correlation, never described before, between high IDO2 expression and a worse NSCLC outcome. Moreover, from the long follow-up period we highlighted an increasing difference in the probability of death between the patients belonging to the group with a high tumor expression of IDO2 and those belonging to the low

expression group (28% compared to near 12% within 60 months). This finding could suggest a delayed role for IDO2 in both NSCLC progression and aggressiveness, which deserves further investigation.

Although many efforts have been made in order to identify prognostic molecules for NSCLC, nowadays the results are still conflicting (17, 18, 44–50). In this regard, the lack of a statistically significant correlation between DFS and the high tumor expression of both IDO2 and IDO1 could appear to be a confounding result, in particular when compared to the OS analysis of the current series. Despite the fact that some studies have found an association between IDO1 expression and disease progression (7, 51–55), some other authors have claimed that there was no impact on survival, regarding both DFS and OS (17, 56–59). Nevertheless, a focus on the highly versatile nature of IDO1 might explain this contradiction, because IDO1 has not only an enzymatic activity, but also a signaling function (31). Therefore, IDO1 is reported to be related to both immunoescape and inflammatory responses, strictly depending on the surrounding microenvironment (31, 60), and its expression could relate to a wide spectrum of patients' outcomes (61). Regarding IDO2, we could assume a similar role, resulting both in the induction of and in the resistance to the host's immune system (13, 23, 26, 34, 37, 38, 60); consequently, IDO2 could be implicated either in delaying or promoting tumor aggressiveness, based on the highly fluctuating interactions with all of the other activated molecules of the tumor microenvironment (11, 13, 25, 26, 34). However, additional studies are needed to demonstrate this, since IDO1 and IDO2 seem to be functionally different (12, 13, 31, 60) and the biological relevance of IDO2 is not fully understood yet (60, 62).

On the other hand, encouraging evidence about the prognostic role of both IDO1 and PD-L1 in NSCLC has been found (19), as confirmed in the current study by the correlation between the IDO1 overexpression and the high probability of death from cancer. At the moment, we could suggest the immunohistochemical assessment of IDO2 together with the abovementioned molecules, in order to better stratify the risk of patients with NSCLC, assuming that more than one biomarker influences, in an independent manner, the outcome of these tumors.

The present study supports the idea that there is the need to combine multiple biomarker assays, due to the multifactorial and complex nature of cancer-immune interactions (63, 64).

To the best of our knowledge, this is the first study about IDO2 immunohistochemical expression in NSCLC. The close relationships found between IDO2 and other molecules in the NSCLC microenvironment, together with its potential prognostic implications, could open the way for the assessment of possible combined therapeutic strategies with IDO2 selective inhibitors, both by figuring new mechanisms out and by exploring new pharmacological tools for NSCLC. The objectives are both to overcome the existing drug resistances and to increase the number of patients who could benefit from immunotherapy in this cancer type. Due to the so far limited knowledge of IDO2 expression and cellular functions, further studies at a molecular level are required to make this promising molecule become a new biomarker for NSCLC.

DATA AVAILABILITY STATEMENT

The datasets analyzed in this article are not publicly available in order to respect the confidentiality and protection of patients' data, in compliance with the processing of data covered and protected by the Italian Privacy Law and by the GDPR (General Data Protection Regulation, EU regulation no. 2016/679). However, requests for access to a properly anonymized dataset of the present article could be directed to MM, mandaranomartina@gmail.com.

ETHICS STATEMENT

The studies involving human participants were reviewed and approved by Comitato Etico delle Aziende Sanitarie della Regione Umbria (CEAS Umbria), Regione Umbria Palazzo Broletto Floor 3, Via Mario Angeloni 61, 06124 Perugia, Italy. The patients/participants provided their written informed consent to participate in this study.

AUTHOR CONTRIBUTIONS

MM, GB, MB, CV, and AS conceived and designed the study. JV, LC, and FP provided the resected surgical specimens. IF and GF performed both the histological slides and the immunohistochemical stains. MM, GB, and AS performed the histopathological analysis. MM, GB, MB, CV, GMo, JV, RC, VL, GMe, and FR filed and analyzed data. AG, CL, and FS provided the follow up data and performed the statistical analysis. MM, GB, MB, and CV wrote the paper. All the authors edited and contributed to manuscript revision, giving the final approval for publication.

FUNDING

MM, GB, MB, and CV received a research grant from Fondazione Cassa Risparmio Perugia for the project entitled *Validazione del catabolismo del triptofano come biomarker nei carcinomi polmonari non a piccole cellule*, number of the project 2018.0413.021 RICERCA SCIENTIFICA E TECNOLOGICA. CV is, also, the P.I. of the PRIN 20155C2PP7 entitled *IDO2, much more than a clone of IDO1: unveiling a new biological role for an ancient enzyme* and of the PRIN 20173EAZ2Z entitled *Linking tryptophan catabolism to amyotrophic lateral sclerosis: from the pathogenesis to the pharmacological treatment*.

SUPPLEMENTARY MATERIAL

The Supplementary Material for this article can be found online at: https://www.frontiersin.org/articles/10.3389/fimmu.2020.00839/full#supplementary-material

REFERENCES

1. Travis WD, Brambilla E, Noguchi M, Nicholson AG, Geisinger KR, Yatabe Y, et al. International association for the study of lung cancer/american thoracic society/european respiratory society international multidisciplinary classification of lung adenocarcinoma. *J Thorac Oncol*. (2011) 6:244–85. doi: 10.1097/JTO.0b013e318206a221
2. Zimmermann S, Peters S, Owinokoko T, Gadgeel SM. Immune checkpoint inhibitors in the management of lung cancer. *Am Soc Clin Oncol Educ Book*. (2018) 38:682–95. doi: 10.1200/EDBK_201319
3. Pu X, Wu L, Su D, Mao W, Fang B. Immunotherapy for non-small cell lung cancers: biomarkers for predicting responses and strategies to overcome resistance. *BMC Cancer*. (2018) 18:1082. doi: 10.1186/s12885-018-4990-5
4. Munn DH, Mellor AL. IDO in the tumor microenvironment: inflammation, counter-regulation, and tolerance. *Trends Immunol*. (2016) 37:193–207. doi: 10.1016/j.it.2016.01.002
5. Uyttenhove C, Pilotte L, Theate I, Stroobant V, Colau D, Parmentier N, et al. Evidence for a tumoral immune resistance mechanism based on tryptophan degradation by indoleamine 2,3-dioxygenase. *Nat Med*. (2003) 9:1269–74. doi: 10.1038/nm934
6. van Baren N, van den Eynde BJ. Tryptophan-degrading enzymes in tumoral immune resistance. *Front Immunol*. (2015) 6:34. doi: 10.3389/fimmu.2015.00034
7. Theate I, van Baren N, Pilotte L, Moulin P, Larrieu P, Renauld JC, et al. Extensive profiling of the expression of the indoleamine 2,3-dioxygenase 1 protein in normal and tumoral human tissues. *Cancer Immunol Res*. (2015) 3:161–72. doi: 10.1158/2326-6066.CIR-14-0137
8. Platten M, von Knebel Doeberitz N, Oezen I, Wick W, Ochs K. Cancer immunotherapy by targeting IDO1/TDO and their downstream effectors. *Front Immunol*. (2014) 5:673. doi: 10.3389/fimmu.2014.00673
9. D'Amato NC, Rogers TJ, Gordon MA, Greene LI, Cochrane DR, Spoelstra NS, et al. A TDO2-AhR signaling axis facilitates anoikis resistance and metastasis in triple-negative breast cancer. *Cancer Res*. (2015) 75:4651–64. doi: 10.1158/0008-5472.CAN-15-2011
10. Yuasa HJ, Mizuno K, Ball HJ. Low efficiency IDO2 enzymes are conserved in lower vertebrates, whereas higher efficiency IDO1 enzymes are dispensable. *FEBS J*. (2015) 282:2735–45. doi: 10.1111/febs.13316
11. Fatokun AA, Hunt NH, Ball HJ. Indoleamine 2,3-dioxygenase 2 (IDO2) and the kynurenine pathway: characteristics and potential roles in health and disease. *Amino acids*. (2013) 45:1319–29. doi: 10.1007/s00726-013-1602-1
12. Yuasa HJ, Ball HJ, Ho YF, Austin CJ, Whittington CM, Belov K, et al. Characterization and evolution of vertebrate indoleamine 2, 3-dioxygenases IDOs from monotremes and marsupials. *Comp Biochem Physiol B Biochem Mol Biol*. (2009) 153:137–44. doi: 10.1016/j.cbpb.2009.02.002
13. Jusof FF, Bakmiwewa SM, Weiser S, Too LK, Metz R, Prendergast GC, et al. Investigation of the tissue distribution and physiological roles of indoleamine 2,3-dioxygenase-2. *Int J Tryptophan Res*. (2017) 10:1178646917735098. doi: 10.1177/1178646917735098
14. Lob S, Konigsrainer A, Zieker D, Brucher BL, Rammensee HG, Opelz G, et al. IDO1 and IDO2 are expressed in human tumors: levo- but not dextro-1-methyl tryptophan inhibits tryptophan catabolism. *Cancer Immunol Immunother*. (2009) 58:153–57. doi: 10.1007/s00262-008-0513-6
15. Guastella AR, Michelhaugh SK, Klinger NV, Fadel HA, Kiousis S, Ali-Fehmi R, et al. Investigation of the aryl hydrocarbon receptor and the intrinsic tumoral component of the kynurenine pathway of tryptophan metabolism in primary brain tumors. *J Neurooncol*. (2018) 139:239–49. doi: 10.1007/s11060-018-2869-6
16. Witkiewicz AK, Costantino CL, Metz R, Muller AJ, Prendergast GC, Yeo CJ, et al. Genotyping and expression analysis of IDO2 in human pancreatic cancer: a novel, active target. *J Am Coll Surg*. (2009) 208:781–87. doi: 10.1016/j.jamcollsurg.2008.12.018
17. Volaric A, Gentzler R, Hall R, Mehaffey JH, Stelow EB, Bullock TN, et al. Indoleamine-2,3-dioxygenase in non-small cell lung cancer: a targetable mechanism of immune resistance frequently coexpressed with PD-L1. *Am J Surg Pathol*. (2018) 42:1216–23. doi: 10.1097/PAS.0000000000001099
18. Parra ER, Villalobos P, Zhang J, Behrens C, Mino B, Swisher S, et al. Immunohistochemical and image analysis-based study shows that several immune checkpoints are co-expressed in non-small cell lung carcinoma tumors. *J Thorac Oncol*. (2018) 13:779–91. doi: 10.1016/j.jtho.2018.03.002
19. Mandarano M, Bellezza G, Belladonna ML, Van den Eynde BJ, Chiari R, Vannucci J, et al. Assessment of TILs, IDO-1, and PD-L1 in resected non-small cell lung cancer: an immunohistochemical study with clinicopathological and prognostic implications. *Virchows Arch*. (2019) 474:159–68. doi: 10.1007/s00428-018-2483-1
20. Gray RJ. A class of k-sample tests for comparing the cumulative incidence of a competing risk. *Ann Stat*. (1988) 16:1141–54. doi: 10.1214/aos/1176350951
21. Fine JP, Gray RJ. A proportional hazards model for the subdistribution of a competing risk. *J Am Stat Assoc*. (1999) 94:496–509. doi: 10.1080/01621459.1999.10474144
22. Stata Statistical Software: Relase 14. *StataCorp*. (2015) (accessed August 31, 2017).
23. Merlo LM, DuHadaway JB, Grabler S, Prendergast GC, Muller AJ, Mandik-Nayak L. IDO2 modulates T cell-dependent autoimmune responses through a B cell-intrinsic mechanism. *J Immunol*. (2016) 196:4487–97. doi: 10.4049/jimmunol.1600141
24. Ball HJ, Yuasa HJ, Austin CJ, Weiser S, Hunt NH. Indoleamine 2,3-dioxygenase-2; a new enzyme in the kynurenine pathway. *Int J Biochem Cell Biol*. (2009) 41:467–71. doi: 10.1016/j.biocel.2008.01.005
25. Pantouris G, Serys M, Yuasa HJ, Ball HJ, Mowat CG. Human indoleamine 2,3-dioxygenase-2 has substrate specificity and inhibition characteristics distinct from those of indoleamine 2,3-dioxygenase-1. *Amino Acids*. (2014) 46:2155–63. doi: 10.1007/s00726-014-1766-3
26. Metz R, Smith C, DuHadaway JB, Chandler P, Baban B, Merlo LM, et al. IDO2 is critical for IDO1-mediated T-cell regulation and exerts a non-redundant function in inflammation. *Int Immunol*. (2014) 26:357–67. doi: 10.1093/intimm/dxt073
27. Prendergast GC, Malachowski WJ, Mondal A, Scherle P, Muller AJ. Indoleamine 2,3-dioxygenase and its therapeutic inhibition in cancer. *Int Rev Cell Biol*. (2018) 336:175–203. doi: 10.1016/bs.ircmb.2017.07.004
28. Platten M, Nollen EAA, Rohrig UF, Fallarino F, Opitz CA. Tryptophan metabolism as a common therapeutic target in cancer, neurodegeneration and beyond. *Nat Rev Drug Discov*. (2019) 18:379–401. doi: 10.1038/s41573-019-0016-5
29. Metz R, Duhadaway JB, Kamasani U, Laury-Kleintop L, Muller AJ, Prendergast GC. Novel tryptophan catabolic enzyme IDO2 is the preferred biochemical target of the antitumor indoleamine 2,3-dioxygenase inhibitory compound D-1-methyl-tryptophan. *Cancer Res*. (2007) 67:7082–87. doi: 10.1158/0008-5472.CAN-07-1872
30. Yamamoto Y, Yamasuge W, Imai S, Kunisawa K, Hoshi M, Fujigaki H, et al. Lipopolysaccharide shock reveals the immune function of indoleamine 2,3-dioxygenase 2 through the regulation of IL-6/stat3 signalling. *Sci Rep*. (2018) 8:15917. doi: 10.1038/s41598-018-34166-4
31. Mondanelli G, Ugel S, Grohmann U, Bronte V. The immune regulation in cancer by the amino acid metabolizing enzymes ARG and IDO. *Curr Opin Pharmacol*. (2017) 35:30–9. doi: 10.1016/j.coph.2017.05.002
32. Chen JY, Li CF, Kuo CC, Tsai KK, Hou MF, Hung WC. Cancer/stroma interplay via cyclooxygenase-2 and indoleamine 2,3-dioxygenase promotes breast cancer progression. *Breast Cancer Res*. (2014) 16:410. doi: 10.1186/s13058-014-0410-1
33. Duan Z, Li Y, Li L. Promoting epithelial-to-mesenchymal transition by D-kynurenine via activating aryl hydrocarbon receptor. *Mol Cell Biochem*. (2018) 448:165–73. doi: 10.1007/s11010-018-3323-y
34. Ball HJ, Sanchez-Perez A, Weiser S, Austin CJ, Astelbauer F, Miu J, et al. Characterization of an indoleamine 2,3-dioxygenase-like protein found in humans and mice. *Gene*. (2007) 396:203–13. doi: 10.1016/j.gene.2007.04.010
35. Zhu MMT, Dancsok AR, Nielsen TO. Indoleamine dioxygenase inhibitors: clinical rationale and current development. *Curr Oncol Rep*. (2019) 21:2. doi: 10.1007/s11912-019-0750-1
36. Mitchell TC, Hamid O, Smith DC, Bauer TM, Wasser JS, Olszanski AJ, et al. Epacadostat plus pembrolizumab in patients with advanced solid tumors: phase i results from a multicenter, open-label phase I/II trial (ECHO-202/KEYNOTE-037). *J Clin Oncol*. (2018) 36:3223–30. doi: 10.1200/JCO.2018.78.9602
37. Nevler A, Muller AJ, Sutanto-Ward E, DuHadaway JB, Nagatomo K, Londin E, et al. Host IDO2 gene status influences tumor progression and radiotherapy

response in KRAS-driven sporadic pancreatic cancers. *Clinical Cancer Res*. (2019) 25:724–34. doi: 10.1158/1078-0432.CCR-18-0814
38. Merlo LMF Mandik-Nayak L. IDO2: a pathogenic mediator of inflammatory autoimmunity. *Clin Med Insights Pathol*. (2016) 9 (Suppl. 1):21–8. doi: 10.4137/CPath.S39930
39. Prendergast GC, Metz R, Muller AJ, Merlo Lauren MF, Mandik-Nayak L. IDO2 in immunomodulation and autoimmune disease. *Front Immunol*. (2014) 5:585. doi: 10.3389/fimmu.2014.00585
40. Dunn GP, Old LJ, Schreiber RD. The three Es of cancer immunoediting. *Annu Rev Immunol*. (2004) 22:329–60. doi: 10.1146/annurev.immunol.22.012703.104803
41. Brambilla E, Le Teuff G, Marguet S, Lantuejoul S, Dunant A, Graziano S, et al. Prognostic effect of tumor lymphocytic infiltration in resectable non-small-cell lung cancer. *J Clin Oncol*. (2016) 34:1223–30. doi: 10.1200/JCO.2015.63.0970
42. Hendry S, Salgado R, Gevaert T, Russell PA, John T, Thapa B, et al. Assessing tumor-infiltrating lymphocytes in solid tumors: a practical review for pathologists and proposal for a standardized method from the international immunooncology biomarkers working group: part 1: assessing the host immune response, TILs in invasive breast carcinoma and ductal carcinoma *in situ*, metastatic tumor deposits and areas for further research. *Adv Anat Pathol*. (2017) 24:235–51. doi: 10.1097/PAP.0000000000000162
43. Hiraoka K, Miyamoto M, Cho Y, Suzuoki M, Oshikiri T, Nakakubo Y, et al. Concurrent infiltration by CD8+ T cells and CD4+ T cells is a favourable prognostic factor in non-small-cell lung carcinoma. *Br J Cancer*. (2006) 94:275–80. doi: 10.1038/sj.bjc.6602934
44. Gridelli C, Ardizzoni A, Barberis M, Cappuzzo F, Casaluce F, Danesi R, et al. Predictive biomarkers of immunotherapy for non-small cell lung cancer: results from an experts panel meeting of the italian association of thoracic oncology. *Transl Lung Cancer Res*. (2017) 6:373–86. doi: 10.21037/tlcr.2017.05.09
45. Thunnissen E, Allen TC, Adam J, Aisner DL, Beasley MB, Borczuk AC, et al. Immunohistochemistry of pulmonary biomarkers: a perspective from members of the pulmonary pathology society. *Arch Pathol Lab Med*. (2018) 142:408–19. doi: 10.5858/arpa.2017-0106-SA
46. Schalper KA, Carvajal-Hausdorf D, McLaughlin J, Altan M, Velcheti V, Gaule P, et al. Differential expression and significance of PD-L1, IDO-1, and B7-H4 in human lung cancer. *Clin Cancer Res*. (2017) 23:370–78. doi: 10.1158/1078-0432.CCR-16-0150
47. Tsao MS, Le Teuff G, Shepherd FA, Landais C, Hainaut P, Filipits M, et al. PD-L1 protein expression assessed by immunohistochemistry is neither prognostic nor predictive of benefit from adjuvant chemotherapy in resected non-small cell lung cancer. *Ann Oncol*. (2017) 28:882–9. doi: 10.1093/annonc/mdx003
48. Yang CY, Lin MW, Chang YL, Wu CT, Yang PC. Programmed cell death-ligand 1 expression is associated with a favourable immune microenvironment and better overall survival in stage I pulmonary squamous cell carcinoma. *Eur J Cancer*. (2016) 57:91–103. doi: 10.1016/j.ejca.2015.12.033
49. Wang A, Wang HY, Liu Y, Zhao MC, Zhang HJ, Lu ZY, et al. The prognostic value of PD-L1 expression for non-small cell lung cancer patients: a meta-analysis. *Eur J Surg Oncol*. (2015) 41:450–6. doi: 10.1016/j.ejso.2015.01.020
50. Driver BR, Miller RA, Miller T, Deavers M, Gorman B, Mody D, et al. Programmed death ligand-1 (PD-L1) expression in either tumor cells or tumor-infiltrating immune cells correlates with solid and high-grade lung adenocarcinomas. *Arch Pathol Lab Med*. (2017) 141:1529–32. doi: 10.5858/arpa.2017-0028-OA
51. Kozuma Y, Takada K, Toyokawa G, Kohashi K, Shimokawa M, Hirai, et al. Indoleamine 2,3-dioxygenase 1 and programmed cell death-ligand 1 co-expression correlates with aggressive features in lung adenocarcinoma. *Eur J Cancer*. (2018) 101:20–9 doi: 10.1016/j.ejca.2018.06.020
52. Tang D, Yue L, Yao R, Zhou L, Yang Y, Lu L, et al. P53 prevent tumor invasion and metastasis by down-regulating IDO in lung cancer. *Oncotarget*. (2017) 8:54548–57. doi: 10.18632/oncotarget.17408
53. Brochez L, Chevolet, Kruse V. The rationale of indoleamine 2, 3-dioxygenase inhibition for cancer therapy (2017) 76:167–82. doi: 10.1016/j.ejca.2017.01.011
54. Ferdinande L, Decaestecker C, Verset L, Mathieu A, Moles Lopez X, Negulescu AM, et al. Clinicopathological significance of indoleamine 2,3-dioxygenase 1 expression in colorectal cancer. *Br J Cancer*. (2012) 106:141–7. doi: 10.1038/bjc.2011.513
55. Banzola I, Mengus C, Wyler S, Hudolin T, Manzella G, Chiarugi A, et al. Expression of indoleamine 2,3-dioxygenase induced by IFN-γ and TNF-α as potential biomarker of prostate cancer progression. *Front Immunol*. (2018) 9:1051. doi: 10.3389/fimmu.2018.01051
56. Zhang ML, Kem M, Mooradian MJ, Eliane JP, Huynh TG, Iafrate AJ, et al. Differential expression of PD-L1 and IDO1 in association with the immune microenvironment in resected lung adenocarcinomas. *Mod Pathol*. (2019) 32:511–23. doi: 10.1038/s41379-018-0160-1
57. Kim JW, Nam KH, Ahn SH, Park DJ, Kim HH, Kim SH, et al. Prognostic implications of immunosuppressive protein expression in tumors as well as immune cell infiltration within the tumor microenvironment in gastric cancer. *Gastric Cancer*. (2016) 19:42–52. doi: 10.1007/s10120-014-0440-5
58. Karanikas V, Zamanakou M, Kerenidi T, Dahabreh J, Hevas A, Nakou M, et al. Indoleamine 2,3-dioxygenase (IDO) expression in lung cancer. *Cancer Biol Ther*. (2007) 6:1258–62. doi: 10.4161/cbt.6.8.4446
59. de Jong RA, Toppen NL, Ten Hoor KA, Boezen HM, Kema IP, Hollema H, et al. Status of cellular immunity lacks prognostic significance in vulvar squamous carcinoma. *Gynecol Oncol*. (2012) 125:186–93. doi: 10.1016/j.ygyno.2011.12.416
60. Ricciuti B, Leonardi GC, Puccetti P, Fallarino F, Bianconi V, Sahebkar A, et al. Targeting indoleamine-2,3-dioxygenase in cancer: Scientific rationale and clinical evidence. *Pharmacol Ther*. (2019) 196:105–16. doi: 10.1016/j.pharmthera.2018.12.004
61. Schollbach J, Kircher S, Wiegering A, Anger F, Rosenwald A, Germer CT, et al. The local immune phenotype influences prognosis in patients with nodal-positive rectal cancer after neoadjuvant chemoradiation. *Int J Colorectal Dis*. (2020) 35:365–70. doi: 10.1007/s00384-019-03466-0
62. Lee YK, Lee HB, Shin DM, Kang MJ, Yi EC, Noh S, et al. Heme-binding-mediated negative regulation of the tryptophan metabolic enzyme indoleamine 2,3-dioxygenase 1 (IDO1) by IDO2. *Exp Mol Med*. (2014) 46:e121. doi: 10.1038/emm.2014.69
63. Blank CU, Haanen JB, Ribas A, Schumacher TN. Cancer immunology. the "cancer immunogram." *Science*. (2016) 352:658–60. doi: 10.1126/science.aaf2834
64. Nadal E, Massuti B, Domine M, Garcia-Campelo R, Cobo M, Felip E. Immunotherapy with checkpoint inhibitors in non-small cell lung cancer: insights from long-term survivors. *Cancer Immunol Immunother*. (2019) 68:341–52. doi: 10.1007/s00262-019-02310-2

Conflict of Interest: The authors declare that the research was conducted in the absence of any commercial or financial relationships that could be construed as a potential conflict of interest.

frontiers in Immunology

ORIGINAL RESEARCH
published: 09 June 2020
doi: 10.3389/fimmu.2020.00968

Tumor-Targeted Gene Silencing IDO Synergizes PTT-Induced Apoptosis and Enhances Anti-tumor Immunity

Yujuan Zhang[1†], Yuanyuan Feng[1,2†], Yanqing Huang[1,3], Yifan Wang[1,3], Li Qiu[4], Yanling Liu[1,3], Shanshan Peng[1,3], Rong Li[1], Nanzhen Kuang[1], Qiaofa Shi[1], Yanmei Shi[5], Yiguo Chen[6], Rakesh Joshi[7], Zhigang Wang[1,3], Keng Yuan[1,3] and Weiping Min[1,3,5,7*]*

[1] Institute of Immunotherapy and College of Basic Medicine of Nanchang University, and Jiangxi Academy of Medical Sciences, Nanchang, China, [2] Medical Science Laboratory, Children's Hospital, Maternal and Child Health Hospital of Guangxi Zhuang Autonomous Region, Nanning, China, [3] Jiangxi Provincial Key Laboratory of Immunotherapy, Nanchang, China, [4] Department of Endocrinology and Metabolism, Peking University People's Hospital, Beijing, China, [5] Department of Oncology, The First Affiliated Hospital of Nanchang University, Nanchang, China, [6] Medical Laboratory, Jiangxi Provincial People's Hospital, Nanchang, China, [7] Department of Surgery, Pathology and Oncology, University of Western Ontario, London, ON, Canada

OPEN ACCESS

Edited by:
Alexander Muller, Lankenau Institute for Medical Research, United States

Reviewed by:
Zong Sheng Guo, University of Pittsburgh, United States
Amir Sharabi, Harvard Medical School, United States

***Correspondence:**
Keng Yuan
kengyuan@ncu.edu.cn
Weiping Min
weiping.min@uwo.ca

[†]These authors have contributed equally to this work

Specialty section:
This article was submitted to Cancer Immunity and Immunotherapy, a section of the journal Frontiers in Immunology

Received: *26 October 2019*
Accepted: *24 April 2020*
Published: *09 June 2020*

Citation:
Zhang Y, Feng Y, Huang Y, Wang Y, Qiu L, Liu Y, Peng S, Li R, Kuang N, Shi Q, Shi Y, Chen Y, Joshi R, Wang Z, Yuan K and Min W (2020) Tumor-Targeted Gene Silencing IDO Synergizes PTT-Induced Apoptosis and Enhances Anti-tumor Immunity. Front. Immunol. 11:968. doi: 10.3389/fimmu.2020.00968

Background: Photothermal therapy (PTT) has been demonstrated to be a promising cancer treatment approach because it can be modulated to induce apoptosis instead of necrosis *via* adjusting irradiation conditions. Recently, an abscopal anti-tumor immunity has been highlighted, in which PTT on the primary tumor also induced repression of distant tumors. In PTT cancer treatments, the mechanism and the role of immune checkpoints to enhance anti-tumor immunity needs to be investigated.

Methods: We prepared a multi-functional gold nanorod reagent, GMPF-siIDO, that is composed of gold nanorods (GNRs) that act as the nano-platform and photothermal sensitizer; folic acid (FA) as the tumor-targeting moiety; and IDO-specific RNA (siIDO) as an immune-stimulator functionality for inducing anti-tumor immunity. For this study, we adjusted the irradiation condition of PTT to induce apoptosis and to silence the immune checkpoint indoleamine 2,3 dioxygeonase (IDO), simultaneously.

Results: Our studies provide evidence that photothermal effects kill tumor cells mainly *via* inducing apoptosis, which can significantly improve antitumor immunity when IDO was down-regulated in TME through significant increases of localized $CD8^+$ and $CD4^+$ lymphocytes in tumor tissue, the downregulation of $CD8^+$ and $CD4^+$ lymphocyte apoptosis, and the upregulation of antitumor cytokines, TNF-α and IFN-γ.

Conclusion: In this study, we, for the first time, validated the role of IDO as a negative regulator for both PTT-induced tumor cell apoptosis and anti-tumor immunity; IDO is a critical immune checkpoint that impedes PTT while combination of gene knockdown of IDO in TME enhances anti-tumor efficacy of PTT.

Keywords: GNR (gold nanorods), LLC (lewis lung cancer), PTT (photothermal therapy), LSPR (localized surface plasmon resonance), IDO (Indoleamine 2,3-dioxygenase)

INTRODUCTION

Cancer, especially solid tumors, has become a major global health threat in the twenty-first century. Lung cancer ranks first in incidence and mortality rates in cancer patients (1). Many studies have shown that various malignant tumors highly express Indoleamine 2,3-dioxygenase-1 (IDO) (2–4). IDO is a critical endogenous immune suppressive factor, which exhausts tryptophan levels of T cells to produce kynurenic acid. This results in suppression of the activation of T cells in a cancer milieu (5). IDO is also known to facilitate the generation of regulatory T cells, which further attenuates anti-tumor immune action (6, 7). IDO, as an immune checkpoint, is a major hurdle for anti-tumor immunity and immunotherapy for cancers. Our previous studies have shown that gene silencing of IDO, through RNA interference, can stimulate anti-tumor immunity and inhibit tumor angiogenesis, thereby resulting in the killing of tumor cells and suppressing tumor invasion, metastasis, and growth (8, 9). These results make IDO a promising targeting molecular cancer immunotherapy.

In recent years, near-infrared (NIR) light-mediated photothermal therapy (PTT) has become attractive for cancer therapy because of low invasiveness and high specificity of the treatment (10–12). PTT can induce tumor cell apoptosis or necrosis, thus inhibiting tumor growth through localized hyperthermia (13, 14). Among various light absorbers in photothermal therapy, gold nanorod (GNR) is capable of variable longitudinal surface plasmon resonance (LSPR) and shows high efficiency in converting the photothermal effect of the near-infrared spectrum. It is widely used in PPT-based cancer treatments under study *in vivo* (12, 14). More recently, combination treatment of PTT with other therapeutic strategies such as chemotherapy has demonstrated enhanced clinical efficacy by upregulating the systemic immune anti-tumor system (15). However, PTT-treatment also elevated the expression of IDO, which suppresses tumor cell apoptosis as well as impairs anti-tumor immunity, resulting in impediment of PTT therapy efficacy (16). Therefore, a new strategy of PTT which can simultaneously knockdown negative immune regulator IDO to suppress tumor-derived immune suppression while increase tumor cell apoptosis would be beneficial.

In this study, we attempted to deliver IDO siRNA (siIDO) to lung tumor cells for immuno-photothermal therapy using a novel gold nanorod reagent, GMPF-siIDO. Our results indicate that GMPF-siIDO could effectively deliver siRNA for the IDO gene into LLC tumor cells with high specificity *in vitro* and *in vivo*. We demonstrated that silencing IDO not only increased LLC cell apoptosis under PTT, but also enhanced the anti-tumor immune response. Treatment with GMPF-siIDO synergized PPT in suppressing tumor growth *in vivo* with high efficacy, minimal invasiveness, and minimal normal tissue side-effects, providing evidence for a novel combined targeted strategy as a fundamental principle for personalized medicine in the treatment of lung cancer.

Abbreviations: GNR, Gold nanorods; LLC, Lewis lung cancer; FA, Folic acid; IDO, Indoleamine 2,3-dioxygenase; PTT, Photothermal therapy; NIR, near infrared radiation; TEM, Transmission electron microscope; NMR, Nuclear magnetic resonance; CTAB, Cetyltrimethylammonium bromide; MUA, Mercaptoundecanoic acid; PEI, Poly ethylene imine; GMPF, GNR-MUA-PEI-FA construct; siRNA, small interfering RNA; LSPR, Localized surface plasmon resonance.

MATERIALS AND METHODS

Animal Usage

Female C57BL/6 mice, 6–8 weeks of age and weighing 18–20 g, were purchased from Changsha Animal Laboratory (Changsha, China). All mice were housed in a specific pathogen free (SPF) grade animal center. The use of the mice complied with the Regulations for the Administration of Affairs Concerning Experimental Animals of China. All animal experiments received the ethical approval of Animal Care and Use Committee of Nanchang University, China.

Synthesis of GNRs

Soluble gold nanorods were synthesized using a previously published seed-mediated growth protocol (17). Briefly, a seed solution was first prepared by mixing 1 mL of cetyltrimethylammonium bromide (CTAB) solution (0.2 M) with 1 mL of $HAuCl_4$ (0.5 mM), followed by the addition of 0.12 mL of ice-cold 0.01 M $NaBH_4$ until the resulting seed solution turned in to brownish yellow color. Secondly, 2.5 mL of $AgNO_3$ (4 mM) was added to the mixture containing 50 mL of $HAuCl_4$ (1 mM) and 50 mL of CTAB (0.2 M). Then, 670 mL of ascorbic acid (0.079 M) was added, making the solution colorless. Finally, 120 mL of the seed solution was added to the growth solution for 24 h, followed by a centrifuge (14,000 g for 15 min) to remove the excess of CTAB. The nanorod was characterized by UV-vis-NIR spectrometer and transmission electron microscope (TEM).

Synthesis of GNR-MUA-PEI (GMP) and GNR-MUA-PEI-FA (GMPF)

Synthesis of MUA-PEI and MUA-PEI-FA is in accordance with the protocol as we described previously (18). In brief, the synthesis steps included (1) carboxyl groups of MUA reacting with amino groups of polyethyleneimine (PEI), by ethyl (dimethylaminopropyl) carbodiimide (EDC)-mediated amidation of N-hydroxysuccinimide (NHS), in the presence of $HCCl_3$, (2) carboxyl groups of folic acid (FA), reacting with the remaining free amino groups of PEI by the similar steps of EDC-mediated amidation with NHS, but in presence of DMSO instead of $HCCl_3$. The MUA-PEI moiety replaced CTAB on GNRs to produce the GNR-MUA-PEI species, and 1:1 ratio of MUA-PEI to MUA-PEI-FA replaced CTAB on GNRs to form the GNRs-MUA-PEI-FA species of nanocarriers. The products were characterized by Hydrogen Nuclear Magnetic Resonance (HNMR), UV-vis-NIR spectrometer and TEM.

siRNA Synthesis

The siRNAs specific for IDO or GAPDH mRNA were designed and synthesized based on previously published methods (19, 20). siRNAs were synthesized commercially (Sigma, St. Louis, MO). Luciferase GL2 siRNA) was synthesized (Sigma) and used as a silencing negative control.

Gel Shift Assay

The GMPF-siRNA nano-complexes with different ratios of GMPF to siRNA were prepared by mixing 0.6 μg IDO siRNA and varying amounts of GMPF. The weight ratios of siRNA to GMPF used were 1:0, 1:0.5, 1:1, 1:1.5, 1:2, 1:2.5, 1:3, 1:3.5, 1:4, 1:4.5, and 1:5. The components were mixed and incubated for 30 min, followed by electrophoresis at 80 V in 1.5% agarose gels in TAE (Tris-acetate-EDTA) buffer, supplemented with ethidium bromide. The gels were visualized under UV illumination and imaged using an Olympus C8080 camera system.

Release of siRNA From GMPF

An established gel-shift method was applied to evaluate the release of siRNA from GMPF-siRNA (21). All the above prepared GMPF samples, with various ratios of GMPF-siRNA, were incubated with 4 μL of 2% sodium dodecyl sulfate (SDS) for 10 min. The siRNA release of from GMPF was determined by band-shifts in 1.5% agarose gel after electrophoresis.

GMPF-siRNA Stability in Serum

GMPF-siIDO aliquots were incubated in 50% FBS at 37°C for 0, 4, 8, 24, 48, and 72 h, then immediately mixed with 2% SDS-containing gel loading buffer. Samples underwent 1.5% agarose gel electrophoresis to assess disconjugation of the nano-complex moieties as indicated by band-shifts.

Photothermal Conversion Measurement

The photothermal efficiency was measured on a customized in-house laser equipment. 24-well microplate with 2 mL of the nano-carrier samples were prepared. A fiber-coupled continuous semiconductor laser (808 nm) with a power density of 2 W/cm^2 was applied. The temperatures of the solutions were measured. Each sample was irradiated for 10 min and the temperature was recorded at 0, 1, 2, 3, 4, 5, and 10 min.

Cell Culture

The Lewis lung cancer (LLC) cells were obtained from the American Type Culture Collection (ATCC). The cells were cultured in DMEM medium (Invitrogen Life Technologies, Carlsbad, CA, USA) with 10% FBS and standard amounts of L-glutamine, penicillin, and streptomycin at 37°C in 5% CO_2, using a routine method (22).

Cell Uptake of GMPF-siRNA

The uptake efficiency of siRNA delivered by the GMPF construct was determined by flow cytometry and fluorescence microscopy as described previously (18). Briefly, the same amounts (1 μg) of Cy3-siGAPDH siRNA were mixed with various concentrations of GMPF at 10, 20, 40, and 80 μg/mL. These GMPF-siRNA mixtures were added to LLC cells (5×10^4 cells) in 24-well microplates. After 24 h, the internalization of siRNA in the cells was confirmed by fluorescent microscopy. The cells were trypsinized, harvested, washed (PBS), and analyzed by flow cytometry (BD FACS Calibur, BD Biosciences, Mountain View, CA).

Gene Silencing and Quantitative Real-Time Quantitative PCR (qRT-PCR)

LLC cells were seeded in a 12-well plate (10^5 cells/well) and transfected with a final concentration of 40 μg/mL of GMPF-siRNA [wt(FA-GNR):wt(siRNA) = 30:1, wt(siRNA) = 0.6 μg] for 24 h. The total RNA was prepared and used to synthesize cDNA using reverse transcriptase (MMLV-RT, Invitrogen Life Technologies). The following primer sets were used for q-PCR amplifications: β-Actin, 5'-AGGGAAATCGTG CGTGACAT-3' (sense) and 5'-AACCGCTCGTTGCCA ATAGT-3' (antisense); IDO, 5'-GTACATCACCATGGCGTATG-3' (sense) and 5'-CGAGGAAGAAGCCCTTGT C-3' (antisense). The qRT-PCR was conducted using SYBR green PCR reagents (Invitrogen Life Technologies). The reactions of qRT-PCR were amplified, in accordance to the manufacturer's protocol, in Stratagene Mx3000P QPCR System (Agilent Technologies, Santa Clara, CA, USA). The difference in gene expressions in treatment groups were calculated using the ΔCt method.

Western Blot Analysis

Cells (1×10^5/well) were seeded into a 12-well plate and were transfected with a final concentration of 40 μg/mL of GMPF-siRNA [wt(FA-GNR):wt(siRNA) = 30:1, wt(siRNA) = 0.6 μg] for 48 h. Cells were harvested and lysed after transfection of GMPF-siRNA. The cell lysates were separated on a 10% SDS-PAGE, and then transferred to nitrocellulose membrane. The membranes were probed with a mouse anti-human IDO mAb (Santa Cruz Biotechnology, Santa Cruz, CA, USA) and anti-β-actin mAb (Santa Cruz Biotechnology) according to the manufacturer's instructions. The membranes were finally visualized by an ECL assay kit (Pierce, Rockford, lL, USA).

Bio-Distribution of GMPF-siRNA *in vivo*

Mice bearing established tumors were hydro-dynamically injected with 200 μL GMP-Cy3-siGAPDH (containing 200 μg GMP and 30 μg Cy3-siGAPDH) or GMPF-Cy3-siGAPDH (containing 200 μg GMPF and 30 μg Cy3-siGAPDH). 24 h post-administration, all mice were sacrificed and the tumors, heart, liver, spleen, lung, and kidney were isolated and frozen using an optimal cutting temperature (OCT) compound (Triangle Biomedical Sciences, USA); it was then sliced into 7 μm horizontal sections. Images were captured using a fluorescence microscope (Olympus, Model BX 51, Japan).

Treatment of Lung Cancer Using Photothermal-Immunotherapy

The cancer-bearing mice were generated by inoculating 5×10^5 LLC cell suspensions at subcutaneous tissues of the mice's back. When the diameter of tumor was ∼3 mm, the mice were randomized into five groups. The mice were hydro-dynamically injected with 400 μL PBS (control), GMPF-siGL2 or GMPF-siIDO (containing 400 μg GMPF and 50 μg siRNA) at day 4, 9, 14, 19. 24 h after each injection, the treated mice were irradiated by the 808 nm near-infrared laser irradiation (1 W/cm^2, 5 min). The length (L) and width (W) of tumor diameters were measured every other day using a digital caliper. The tumor volumes were calculated using a formula: V =1/2 (L × W^2). At day 22 after

tumor inoculation, the mice were sacrificed and tumors, blood, and spleens were collected. The tumor weights were measured, and images were taken with a camera.

Immunohistochemistry

The tumor tissues were collected, fixed in 10% formalin and sectioned into 5-μm slices. After blocking endogenous peroxidase using in 3% H2O2-methanol,block the slides were incubated with 5% normal goat serum 60 min and stained with rat anti-IDO, anti-CD8, or anti-CD4 polyclonal antibody (1:50, Santa Cruz Biotechnology) overnight at 4°C. The slides were then incubated with biotinylation secondary antibody at 37°C for 60 min, following an incubation with horseradish peroxidase (HRP)-labeled streptavidin at 37°C. After development, using diaminobenzene (DAB), the sample slides were observed and photographed under microscope. The integrated optical density (IOD) of IDO were measured in immunostained sections, following the instructions of the Image Pro Plus 6.0 software (Media CY Company, USA).

TUNEL Assay

The tumor tissues were frozen in liquid nitrogen and then sectioned into 5 mm segments. The *in-situ* cell death was detected by a TUNEL assay kit (7 Sea Pharmtech, Shanghai, China), following the manufacturer's instructions. The prepared specimens were examined using a light microscope.

ELISA Assay

Triplicate serum samples (100 μL/well) were collected from experimental mice and placed in mAb (against TNF-α or IFN-γ)-precoated microtiter plates overnight. The plates were blocked with 5% BSA for 1 h at 37°C, then with Biotin-labeled secondary mAb (against TNF-α or IFN-γ, respectively) for 1 h at 37°C, followed by four washes with PBS buffer. After incubation with Strepavidin-HRP 1 h at 37°C, the samples were washed and treated with ELISA solutions (Liankebio, Hangzhou, China). The plate signals were read at 450 nm using an ELISA Reader (SpectraMax, MD, USA). Concentrations of TNF-α and IFN-γ in samples were calculated after calibrating the standard curves that were plotted as absorbance vs. logarithm of the analyte concentration.

Flow Cytometry

Lymphocytes isolated from collected spleens were incubated with anti-CD4 and anti-CD8 antibodies at 4°C for 30 min. These anti-CD4 and anti-CD8 stained T cells were further stained with Annexin V (eBioscience, USA) at 4°C for 15 min. Cells were sorted by flow cytometry using FACS Calibur II (BD Biosciences).

Statistics

Data is presented as mean ± SD (Standard deviation). Student's *t*-test (2-tailed) was used to determine differences between two means. To compare multiple groups, a one-way ANOVA test was applied. A difference with a $p < 0.05$ was considered significant.

RESULTS

Photothermal Effects of Multi-Functionalized Gold Nanorod-MUA-PEI-Folate (GMPF)

CTAB-stabilized GNRs were synthesized as previously described using a seed-mediated growth method. Transmission electron microscopy (TEM) was used to analyze the morphology of GNRs. The GNRs were 10 × 40 nm (width x length) (**Figure 1A**). As shown in **Figure 1B**, the original GNRs exhibited two SPR peaks: a weak transverse SPR (TSPR) peak at ∼525 nm and a strong peak of longitudinal SPR (LSPR) at ∼770 nm. A peak with slight red-shifting to 785 nm was observed from the LSPR curve for GMP after the MUA-PEI modification process. This was followed with a further red-shift to 790 nm of the LSPR curve of GMPF, which suggests that GMP and GMPF were successfully synthesized. It has been reported that the shift of LSPR band peak from the GNRs result from the local refractive index around the GNRs, which is sensitive to the changes on the surface of the GNRs (23). Next, we detected GMPF using ^{1}H NMR spectra. As shown in **Figure 1C**, peaks at δ1.013, δ3.881, and δ8.387 suggest that folic acid (FA) was successfully conjugated on the surface of GMP. FA was used as a tumor-targeting moiety on GMPF, as most tumor cells such as those found in lung cancers, breast cancers, and melanomas highly express FA receptors (24–27).

Research has shown that gold nanorods are promising candidates for photothermal therapy under NIR irradiation (12, 14). Therefore, we determined the photothermal effects of the GMPF under the 808 nm laser irradiation. An increase of temperature to 74 and 71°C from room temperature, after 10 min of NIR laser irradiation of GNRs (120 μg/mL) and GMPF (120 μg/mL), respectively, was recorded (**Figure 1D**). The temperature increase gradients were associated with the GMPF concentrations. In contrast, the temperature in pure water after NIR irradiation only showed a marginal increase to 33°C. These results indicate that the GMPF possess excellent photothermal properties. We next used 40 μg/mL of GMPF and irradiation condition of 2 W/cm^2 for 5 min to treat the tumor cell *in vitro*. This treatment elicited temperature increases up to 50°C, which is optimal for apoptotic and necrotic killing of tumor cells (28, 29).

Gene Silencing of IDO Using GMPF-siIDO

We next evaluated the ability of GMPF carrying IDO siRNA based on the fact that the free siRNA migrates faster, while GMPF-bound siRNA is nearly immobile due to electrostatic interactions (30), and the gel shift visually represents the capacity of GMPF binding to siIDO. The results showed that when the ration of GMPF to siIDO reached 3.5:1 (w/w), unbound siIDO was not observed to be above this ratio (**Figure 2A**). These data suggested that the effective ratio required to saturate GMPF with siIDO is 3.5:1.

To test whether bound siRNA can be released from GMPF, the release profile of siRNA from GMPF-siRNA complexes was determined by a SDS replacement assay (21). **Figure 2B** shows that siRNA is effectively released from GMPF, with a more than 91.5% release.

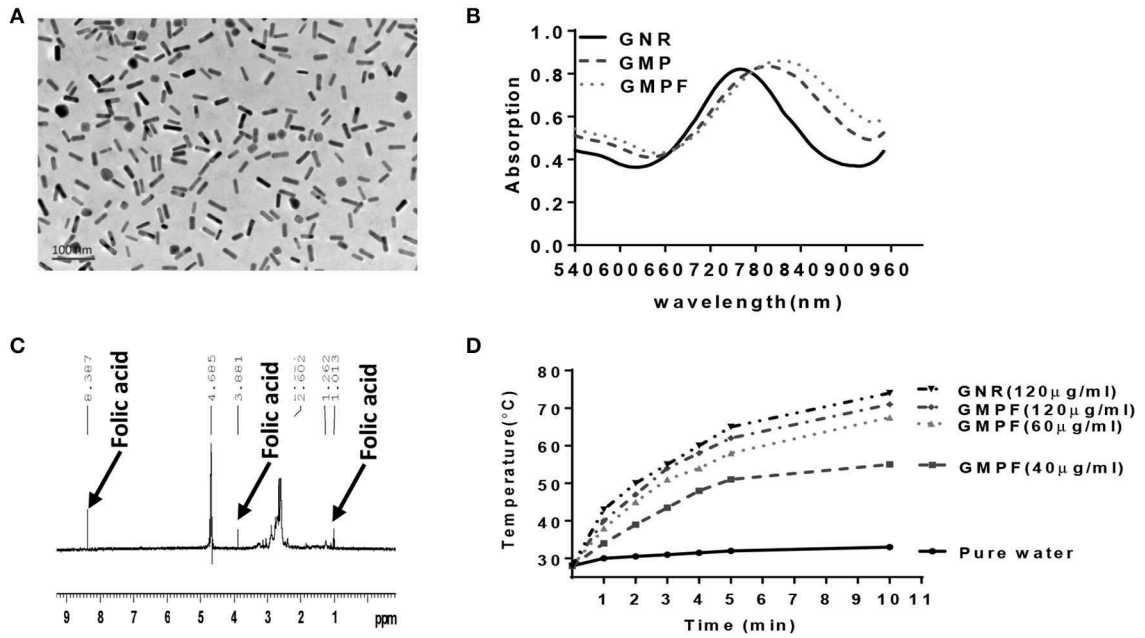

FIGURE 1 | Characterization of photo-thermal effects of a multi-functionalized gold nanorod GNR-MUA-PEI-FA, GMPF. **(A)** Transmission Electron Microscopy (TEM) image of modified GNRs, GMPF. **(B)** UV-Vis absorption spectra of GNR modified by CTAB (GNR), or MUA-PEI (GMP), or MUA-PEI-FA (GMPF). **(C)** The chemical signature of folic acid on the surface of GNR determined by NMR after GNR conjugation with folic acid. **(D)** Temperature increase induced by photothermal effects of GNR or GMPF *in vitro*. 2 mL of GNR (120 μg/mL) or GMPF (40, 60, 120 μg/mL), or deionized water was irradiated at 2 W/cm^2 with the laser wavelength at 808 nm for 10 min. The temperatures were measured and plotted at indicated time points.

Previous reports suggest that free siRNA is easily degraded in serum and stable for only 6 h (31, 32). We tested whether GMPF protected bound siRNA from degradation by enzymes in serum. The stability of GMPF-bound siRNA was evaluated after incubating GMPF-siRNA with 50% FBS at various time-points (i.e.., 0, 4, 8, 24, 48, 72 h), and was then examined by SDS replacement. As shown in **Figure 2C**, the GMPF-siRNA samples had visible bands, suggesting that about 93.0% siRNA were not degraded even after 72 h of incubation in serum. This result indicates that the GMPF construct can protect siRNA against enzymatic degradation *in sera* longer than previously reported.

Next, we assessed the cellular uptake of the GMPF-siRNA by LLC cells. The red fluorescence of Cy3 was observed in LLC cells incubated with the GMPF-Cy3-siGAPDH (**Figure 2D**). In contrast, the cells treated with Cy3-siGAPDH in PBS show no red fluorescent signals. We observed that an increase of red fluorescent signals correlate to the increase of the GMPF concentrations from 10 to 80 μg/mL (**Figure 2D**). Compared to the control cells, 92.3% of cells transfected with GMPF-cy3-siGAPDH (40 μg/mL) were red fluorescence positive, which is significantly higher than the cells transfected with the conventional transfection reagent Lipofectamine 2000 (75.9%; **Figure 2E**). This suggests that the GMPF is a tumor-targeted and effective nano-carrier for transfecting siRNA into LLC cancer cells.

Finally, we determined the gene silencing efficiency of GMPF-siIDO in tumor cells. The transfection with GMPF-siIDO significantly knocked down IDO expression in LLC cells by 60% after (**Figure 2F**), as compared to control transfection with GMPF-siGL2. The knocking down of IDO at the protein level was also obvious in LLC cells (**Figure 2G**).

Gene Silencing of IDO Using GMPF-siIDO Enhances Photothermal Effects of the Multifunctional Gold Nanorods

PTT can induce apoptosis instead of necrosis *via* adjusting the irradiation conditions to kill tumor cells (29). Our previous studies have demonstrated that gene silencing of IDO2 can induce B16-BL6 tumor cell apoptosis (18, 33). In this study, we evaluated whether GMPF-siIDO could enhance tumor apoptosis in the combined condition of silencing IDO along with the photothermal effect induced by gold nanorods. As shown in **Figure 3**, while treatment with control siRNA silencing (**Figure 3B**) alone did not alter the ratio of apoptosis as compared to the untreated control tumor cells (**Figure 3A**), however, knockdown of IDO significantly increased apoptosis of tumor cells (**Figure 3C**). On the other hand, laser irradiation alone, without GMPF nanoparticles, did not induce apoptosis (**Figure 3D**), and significant apoptosis was displayed in the tumor cells in the presence of GMPF after laser irradiation (**Figure 3E**). Most significantly, the combination of GMPF-siIDO and laser irradiation treatments achieved the highest ratio of apoptosis in tumor cells (**Figure 3F**). The statistical analysis showed that combination treatment induced significantly more apoptotic cells (36.8 ± 3.06%) than individual treatment witheither silencing

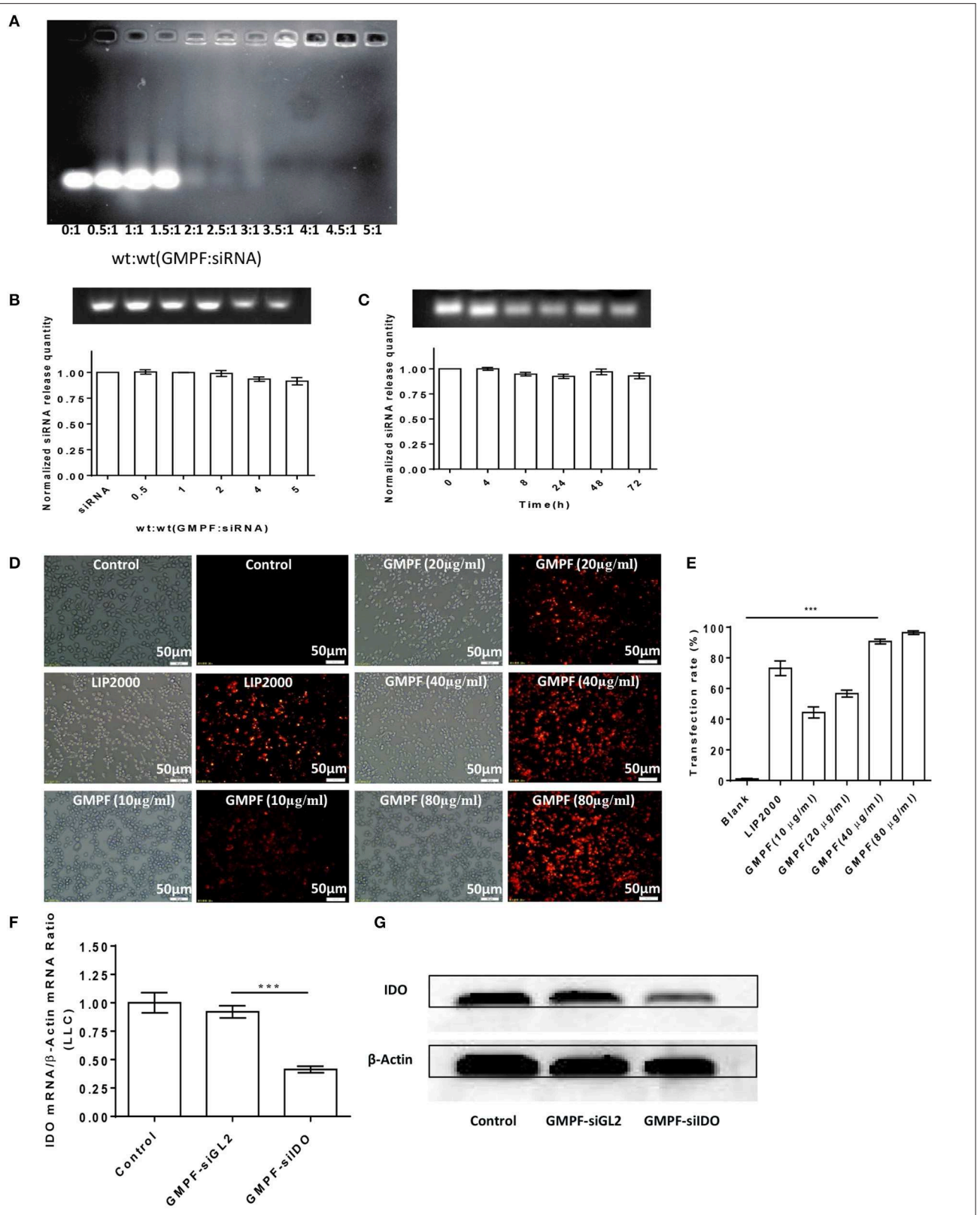

FIGURE 2 | Bio-characterization of GMPF-siIDO. **(A)** Gel shift assays were used to determine the siRNA-loading capacity of GMPF. Equal volumes containing 0.6 μg of siRNA and the desired amount of GMPF were incubated at the indicated weight ratios for 30 min, run on agarose gels, and visualized with ethidium bromide. **(B)** Determination of siRNA release from GMPF-siIDO using SDS analysis. Various ratios of GMPF to siRNA [wt(siRNA) = 0.6 μg] were prepared and all the samples were

(Continued)

FIGURE 2 | treated with 4 μL of 2% SDS and incubated for 10 min at room temperature. Release of siRNA from GMPF-siIDO was determined by electrophoresis (upper panel). The relative quantity of released siRNA was, respectively, calculated by released siRNA/total siRNA (lower panel). **(C)** Serum stability of GMPF-siIDO. GMPF-siIDO [wt(GMPF): wt(siRNA) = 4:1, wt(siRNA) = 0.6 μg] was incubated in 50% FBS at 37°C for 0, 4, 8, 24, 48, and 72 h, and then incubated with 2% SDS. The SDS-treated samples were subjected to gel electrophoresis. The quantity of stable siRNA was calculated by serum-incubated siRNA /non-serum incubated siRNA. **(D,E)** Targeted siRNA transfection efficiency by GMPF. Cy3-labeled siRNA (1 μg) were transfected into LLC by PBS as control, lipofectamine 2000 (LIP2000), GMPF with various concentrations 10, 20, 40, and 80 μg/ml. After 24 h incubation, the intracellular fluorescence intensity was observed under fluorescence microscope **(D)** (scale bar = 50 μm) and the transfection rates were measured using flow cytometry **(E)**. **(F,G)** *in vitro* gene silencing using GMPF-siIDO. LLC cells were incubated with a final concentration of 40 μg/mL of GMPF-siIDO or GMPF-siGL2 (non-specific control siRNA) [wt(FA-GNR): wt(siRNA) = 30:1, wt(siRNA) = 0.6 μg] or PBS as the null treatment control for 24 h. Transcript levels of IDO were quantified by qRT-PCR. Error bars represent the standard deviation of three experiments (**$P < 0.01$) **(F)**, or 48 h after transfection, the protein levels of IDO and β-actin was determined by western blot **(G)**. Error bars represent the standard deviation of three experiments (***$P < 0.001$).

of IDO (20.4 ± 0.35%) or laser irradiation (23.2 ± 2.52%) (**Figure 3G**).

In vivo Tumor-Targeted Photothermal-Immunotherapy for Lung Cancer Using GMPF-siIDO

To assess *in vivo* tumor-targeted siRNA delivery by GMPF, we injected Cy3-labeled GMPF-siRNA into LLC lung cancer-bearing mice for the *in vivo* observation of GMPF distribution. The results showed that red fluorescence was displayed in liver, lungs, kidneys, and spleen, suggesting that the siRNA carried by both targeted and non-targeted nanoparticles were distributed to the blood-rich organs. However, for the delivery of tumor tissues, only GMPF-siRNA was markedly accumulated in tumors compared to control or by non-targeted GMP-siRNA (**Figure 4A**).

To evaluate the anti-neoplastic therapeutic efficacy of immunostimulatory multi-functional gold nanorods, we treated the LLC cancer-bearing mice with GMPF-siIDO. The tumor grew aggressively in the mice sham-treated with PBS or PBS with irradiation (**Figure 4B**). The treatment with non-specific siRNA-conjugated gold nanorods (GMPF-siGL2) only achieved minor suppression of tumor growth, however, the treatment with GMPF-siIDO significantly delayed the tumor growth by day 22 post-inoculation of tumor cells (**Figure 4B**). The anti-tumor effect was enhanced when the lung cancer bearing mice received a combination treatment with GMPF-siIDO and laser irradiation, which further suppressed tumor growth (**Figure 4B**). The therapeutic efficacy of combination treatment of GMPF-siIDO and laser irradiation was further confirmed by the tumor weight (**Figure 4C**) and size (**Figure 4D**), which were remarkably smaller (0.09 ± 0.064 g) than that in the mice that received treatment with laser irradiation (0.97 ± 0.11 g) or gene silencing of IDO (0.38 ± 0.08 g).

Tumor-Targeted Gene Silencing of IDO Enhanced Apoptosis of Tumor Cells After Photothermal-Immunotherapy *in vivo*

To confirm the siIDO carried by GMPF-siIDO was functional *in vivo*, we determined the gene knockdown of IDO in the above treated mice. The IDO expression in tumors significantly declined after the treatment of GMPF-siIDO compared to the control or GMPF-siGL2 (**Figure 5A**). The repression of IDO expression was also confirmed at the protein level (**Figure 5B**) and immunochemistry (**Figure 5C**). These results highlight that GMPF-siIDO is effective in knocking down IDO gene *in vivo* as well.

The recently developed GMPF-siIDO possesses multiple advantages: tumor-specific targeting *via* the FA moiety, siRNA-based IDO gene knockdown, and GNR-induced photothermal tumor-killing effects. As gene silencing of IDO promotes tumor cell apoptosis, photothermal therapy (PTT) with GNRs also directly kill the tumor cells through inducing apoptosis. Therefore, we tested whether the GMPF-siIDO may synergize the gene silencing of IDO and photothermal effects in induction of apoptosis of tumor cells *in vivo*. As shown in **Figure 6**, the apoptosis rates in the untreated tumor (**Figure 6A**) and control laser irradiation (**Figure 6B**) were low. In contrast, combination treatment of GMPF-siIDO and laser irradiation induced the highest level of tumor cell apoptosis (49.11 ± 2.26%, **Figure 6E**), while laser irradiation (8.40 ± 1.52%, **Figure 6C**) or GMPF-siIDO treatment (22.06 ± 1.84%, **Figure 6D**) alone showed lower efficiency in inducing apoptosis off tumor cells. These data verified that knockdown of the checkpoint regulatory molecule IDO can synergize *in vivo* apoptosis of the tumor cell.

Increase of Tumor Infiltrating T Cells and Upregulation of Inflammatory Cytokines After GMPF-siIDO Photothermal-Immunotherapy Treatment

IDO is a primary endogenous immunosuppressive factor. It facilitates the tumor cell escape from immune privilege *via* exhausting the tryptophan in T cells used to produce kynurenic acid, thus inhibiting activation of T cells and inducing regulatory T cells. Therefore, we posited that the multi-functional gold nanorod-based reagent GMPF-siIDO could specifically silence IDO expression in tumor tissues leading to an increase of the number of tumor-infiltrating T cells and the secretion of anti-tumor inflammatory cytokines. We analyzed the infiltrated T cells (TILs) in the tumor tissues. As shown in **Figures 7A–D**, the $CD8^+$ and $CD4^+$ TILs were markedly increased after the combination treatment with GMPF-siIDO and laser irradiation. Untreated mice showed few CD8+ TILs inside the tumor (4.28 ± 1.83%). The TILs, after combination treatment, were notably increased (22.91 ± 4.28%), which were significantly higher than that in the tumors from the mice treated with laser irradiation

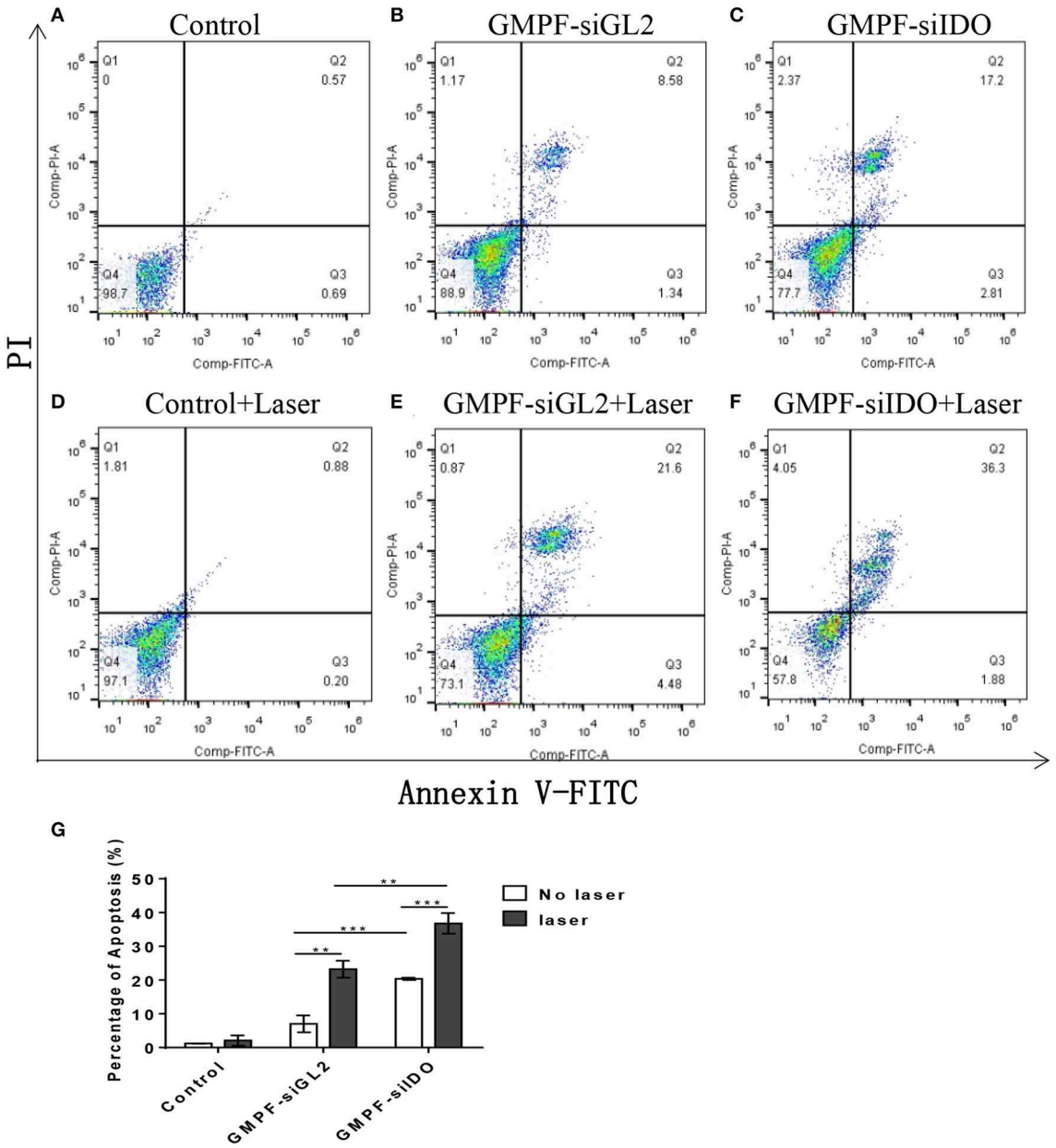

FIGURE 3 | Assessment of tumor cell apoptosis by photo-thermal effects of GMPF-siIDO *in vitro*. LLC cells were incubated with 40 μg/mL of GMPF-siGL2 or GMPF-siIDO overnight, and samples were then irradiated at 2 W/cm^2 for 5 min. The apoptotic cell distribution of all was determined at 24 h using the Annexin V-FITC/PI Apoptosis Detection Kit and analyzed by flow cytometry **(A–F)**, and the percentages of apoptosis are **(G)**. Error bars represent the standard divination of three experiments (**$p < 0.01$; ***$p < 0.001$).

alone (6.73 ± 1.32%) or with IDO silencing alone (17.30 ± 3.35%) (**Figure 7B**). Similarly, the CD4$^+$ TILs in the tumor mice after combination treatment with GMPF-siIDO and laser irradiation (20.85 ± 1.05%) were significantly higher than that in the tumors from the un-treated mice (3.72 ± 1.25%), mice treated with laser irradiation alone (5.87 ± 1.62%) or with IDO silencing alone (14.52 ± 1.46%) (**Figure 7D**). These results indicate that gene silencing IDO was capable of synergizing PTT-induced T cell infiltration, thus, enhancing anti-tumor immunity in the combination treatment of GMPF-siIDO in lung cancer.

Additionally, anti-tumor inflammatory cytokines TNF-α and IFN-γ in serum were increased by 2.1-fold (39.38% ± 2.41 pg/mL vs. 19.47 ± 0.92 pg/mL) and 2.8-fold (151.9 ± 5.66 pg/mL vs. 55.34% ± 3.01 pg/mL) after the treatment with GMPF-siIDO and laser irradiation, respectively, compared to the treatment of GMPF and laser irradiation without IDO silencing (**Figures 7E,F**).

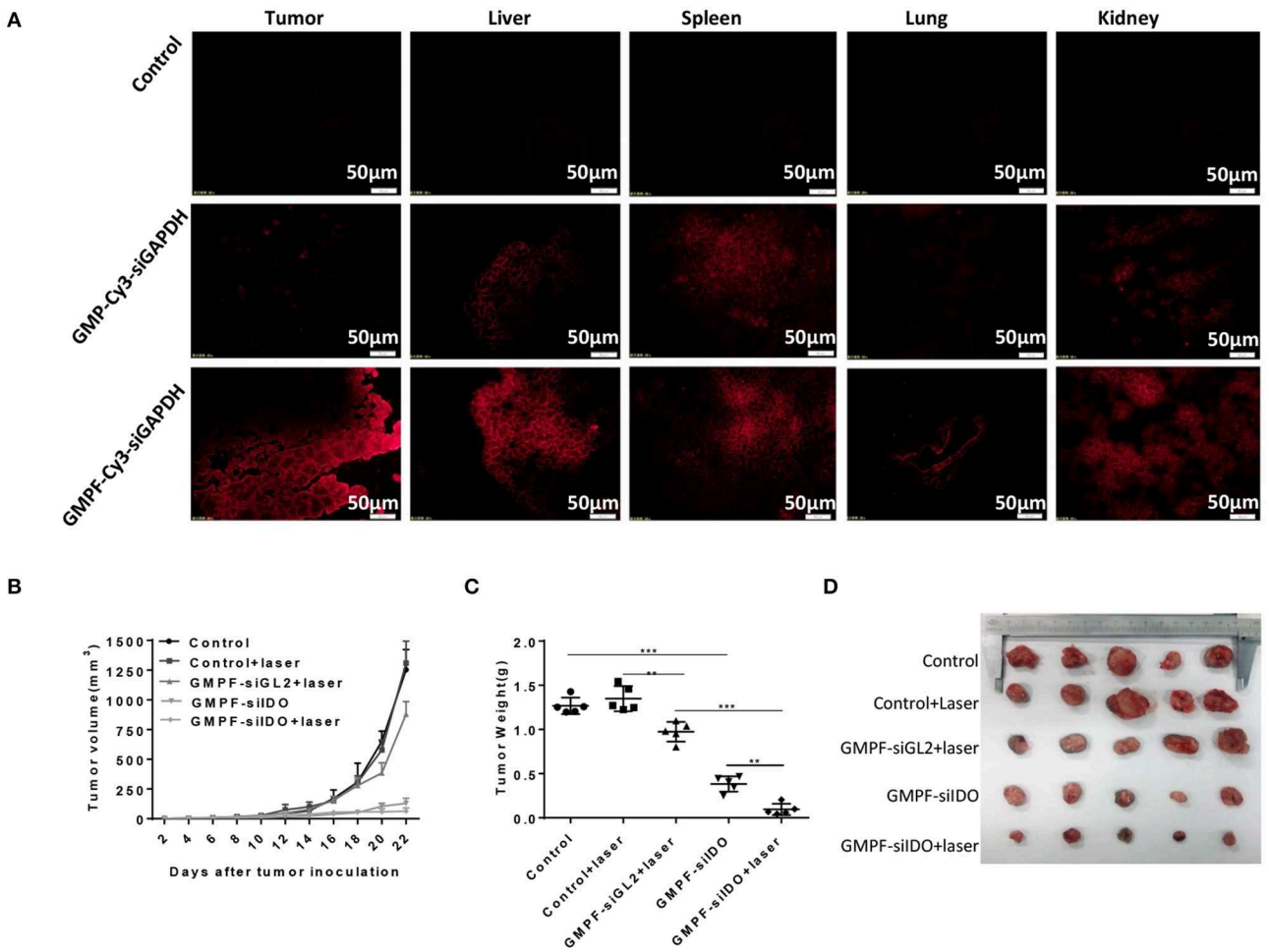

FIGURE 4 | Tumor-targeted photothermal-immunotherapy for lung cancer using multi-functionalized gold nanorods, GMPF-siIDO. **(A)** *in vivo* targeted delivery of GMFP-siGAPDH. LLC tumor bearing mice were intravenously injected with PBS (control), Cy3-labeled GMP-siGAPDH or GMFP-siGAPDH. 24 h post administration, mice were sacrificed and the tumors, livers, spleens, lungs, and kidneys were isolated for frozen tissue sectioning. The fluorescent intensity of tissue sections was visualized using fluorescence microscopy. The data represents one of three independent experiments (Scale bar = 50 μm). **(B–D)** Anti-tumor effects of GMPF-siIDO. LLC lung cancer bearing mice were intravenously injected with PBS (control), GMPF-siGL2 or GMPF-siIDO on day 4, 9, 14, and 19 after tumor inoculation. 24 h after each treatment, the mice were irradiated by the 808 nm near-infrared laser at 1 W/cm^2 for 5 min. The tumor sizes were measured for 22 days after tumor inoculation **(B)**. At the end point of observation, the mice were sacrificed, and tumors collected. The tumor weights were measured **(C)** and the images of tumors are displayed in **(D)**. Error bars represent the standard deviation of three experiments (**$P < 0.01$; ***$P < 0.001$).

Suppression of T-Cell Apoptosis by Photothermal-Immunotherapy Using GMPF-siIDO

IDO is a negative regulator that induces T cell apoptosis and suppresses anti-tumor immunity. To determine whether GMPF-siIDO could rescue T cells from apoptosis, we collected T cells from spleens of the LLC cancer mice after the treatment with photothermal-immunotherapy by GMPF-siIDO. As shown in **Figure 8**, the T cell apoptosis was significantly decreased after the photothermal-immunotherapy). The percentages of apoptotic $CD8^+$ T cells were significantly decreased (4.2 vs. 22.7%; **Figure 8B**); similar suppression of apoptotic $CD4^+$ T cells was also observed (13.0 vs. 39.9% in **Figure 8D**). These data suggest that treatment with photothermal-immunotherapy by GMPF-siIDO suppressed apoptosis of T cells in tumor bearing mice.

DISCUSSION

GNR has obvious localized surface plasmon resonance (LSPR). LSPR refers to the collective oscillation of conduction band electrons caused by the interaction between incident light and the electron cloud on the surface of noble metal nanoparticles, which leads to the absorption and scattering of incident light in the electromagnetic field and produces some unique optical and thermal properties (34, 35). The conversion of absorption

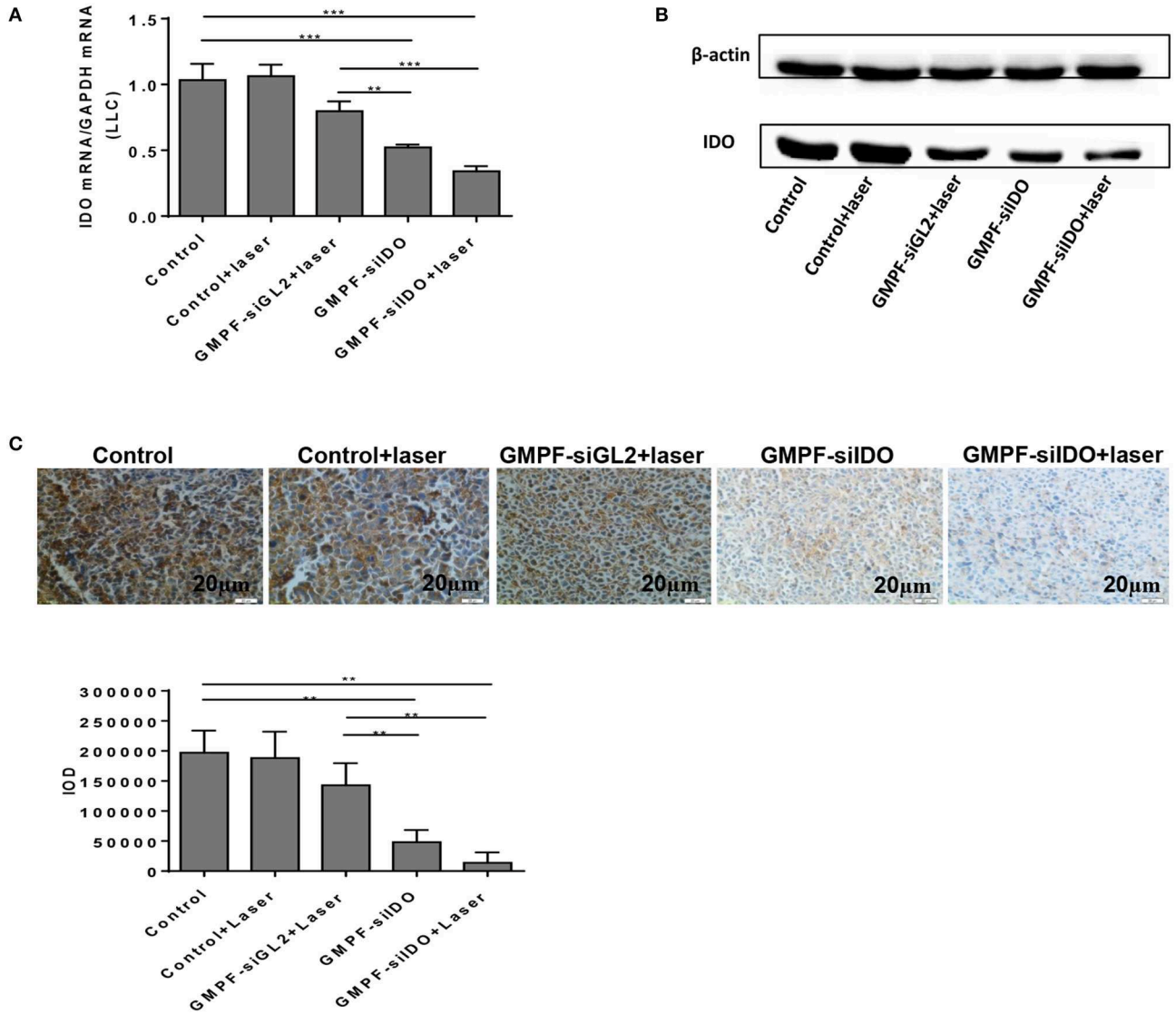

FIGURE 5 | Tumor-targeted gene silencing of IDO using GMPF-siIDO *in vivo*. Tumor-targeted gene silencing. Lung cancer-bearing mice were treated with PBS (control), GMPF-siGL2, or GMPF-siIDO, with or without laser irradiation. At the endpoint of the experiment, the mice were sacrificed, and tumor tissues were collected. The IDO expression was detected by RT-qPCR **(A)**, western blot **(B)**, and immunohistochemistry assays **(C)**. Error bars represent the standard deviation of three experiments. Error bars represent the standard deviation of three experiments (**$P < 0.01$; ***$P < 0.001$).

light of LSPR into heat is called plasmonic photothermal effects (34, 35). Photothermal therapy (PTT) or plasmonic photothermal therapy (PPTT) refers to the application of the plasma photothermal effects of nanoparticles in the treatment of diseases (10, 36). The plasmonic photothermal effects has achieved selective heating of the local temperature of the tumor to above 50–70°C, which is far igher than the threshold required for vascular injury and cell death (37, 38). The maximum wavelength of resonance absorption of GNR can be tuned to the region of 600–900 nm by changing the axial ratio of rods (12, 39). This near-infrared (NIR) wavelength range is a therapeutic window that can be used in biological applications, so it has been widely used (12, 39, 40). Our study showed that GNR can raise the surrounding temperature to about 74°C under 808 nm laser irradiation, which is far higher than the threshold temperature required to kill tumor cells (28). The main mechanisms of the photothermal effect of GNR to kill tumor cells are necrosis and apoptosis. When the temperature is higher than 50°C, the killing mechanism is mainly necrosis; when the temperature is lower than 50°C, the killing mechanism is mainly apoptosis (28, 29). However, due to the fact that there is no leakage of cell components and no induction of inflammation, apoptosis is considered to be a "clean" way to induce cell death (41). Therefore, we adjusted the concentration of GMPF and the irradiation condition to treat tumors to achieve highly apoptotic percentages *in vitro* and *in vivo* while inducing very low percentages of necrosis (**Figures 3**, **6**).

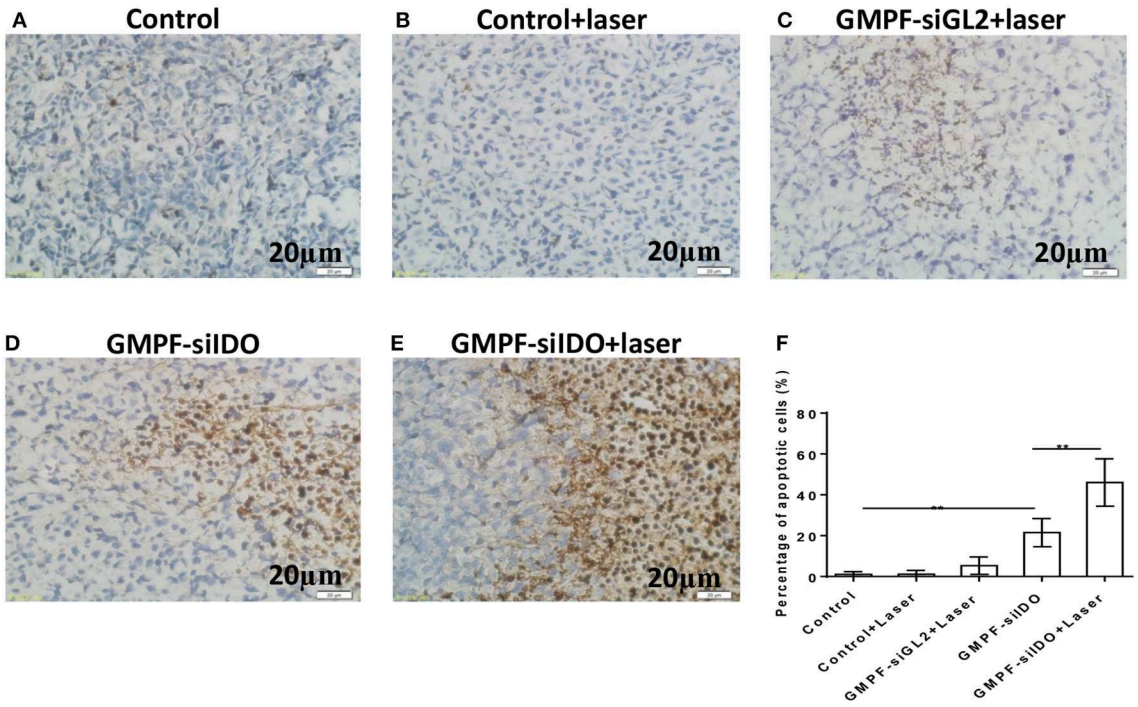

FIGURE 6 | Enhanced apoptosis of tumor cells by photothermal-immunotherapy. LLC lung cancer-bearing mice were treated with PBS (control), GMPF-siGL2, or GMPF-siIDO, with or without laser irradiation. Tumor tissues were collected, and apoptosis was detected by TUNEL assays **(A–E)** and percentages of apoptotic cells were calculated **(G)**. Error bars represent the standard deviation of three experiments. Error bars represent the standard deviation of three experiments (**$P < 0.01$).

In addition to its photothermal effects, GNRs possess excellent capacity for carrying siRNA and conjugating targeting adaptors to tumors. To load IDO siRNA and target LLC cells, we utilized a synthesized MUA-PEI-FA coating for the nano-construct GMPF where positively charged PEI absorbs negatively-charged siRNA, in addition, the folic acid (FA) targets FA- receptors that are highly expressed on tumor cells (24–27). Optimal capacities for loading and release of siRNA are essential for the therapy using nano-carriers. There is increasing evidence that the administration of siRNA, either in naked form or wrapped by nanoparticles, distribute mainly to blood-rich organs such as the liver, lungs, kidneys, and spleen, in comparison to tumor tissues where the delivery is lower due to the lack of blood supply (24–27). Therefore, a delivery method that can efficiently carry siRNA to tumor tissues is a highly clinical demand. In this study, we developed a tumor-targeted nanomaterial GMPF that showed high efficiency of delivering siRNA to tumor cells (**Figure 4A**). Although this method is not tumor specific, we were able to demonstrate that tumor-targeted delivery (e.g., by GMPF) can enhance siRNA delivery to tumor tissues. We note that GMPF is not perfect in its present format and the specific targeting needs to be improved in future studies. In addition, more than 91.5% siRNA can be released effectively from the GMPF-siRNA complex (**Figure 2**). siIDO was specifically delivered into tumor cells by the nano-construct (**Figure 2**), and this effectively silenced IDO *in vitro* and *in vivo* (**Figures 2**, **5**). Furthermore, serum is a primary inhibitor for delivering siRNA into cells due to degradation of the siRNA by enzymatic activity (31). In this study, GMPF-siIDO could significantly resist the degradation of siRNA by enzymes in serum for more than 72 h. Therefore, we conclude that GMPF can load, release, and protect siRNA effectively. Moreover, GMPF-siIDO can target LLC tumor tissues and cells and silence IDO molecules efficiently *in vitro* and *in vivo*.

PTT is a promising emerging anti-tumor strategy for not only primary local tumor, but also for distal metastatic tumors *via* "abscopal effects" (15, 16). The therapeutic mechanisms of PTT is mainly involved in hyperthermal killing of tumor cells and upregulating systemic or local immune responses, triggering immune killing by activated TILs. The efficacy of PTT varies depending on the irradiation power, time, and the distance of the irradiation source, in addition to the type of nanomaterials. Theoretically, upregulating the power and/or extending the time of irradiation can allow reaching higher efficiency of PTT, however, this may also damage the normal cells and tissues. Therefore, we optimized the irradiation condition with the power of 2 W/cm^2 for 5 min, which can maximally protect the normal tissues while killing tumor cells. Unfortunately, PTT-treatment also elevated the expression of IDO, which suppresses tumor cell apoptosis as well as impairs anti-tumor immunity, resulting in the impediment of PTT therapy efficacy (16). Studies have shown that IDO molecules are highly expressed in tumor cells such as LLC (42). Our previous studies have demonstrated that gene silencing of IDO can induce tumor cell apoptosis and sensitize

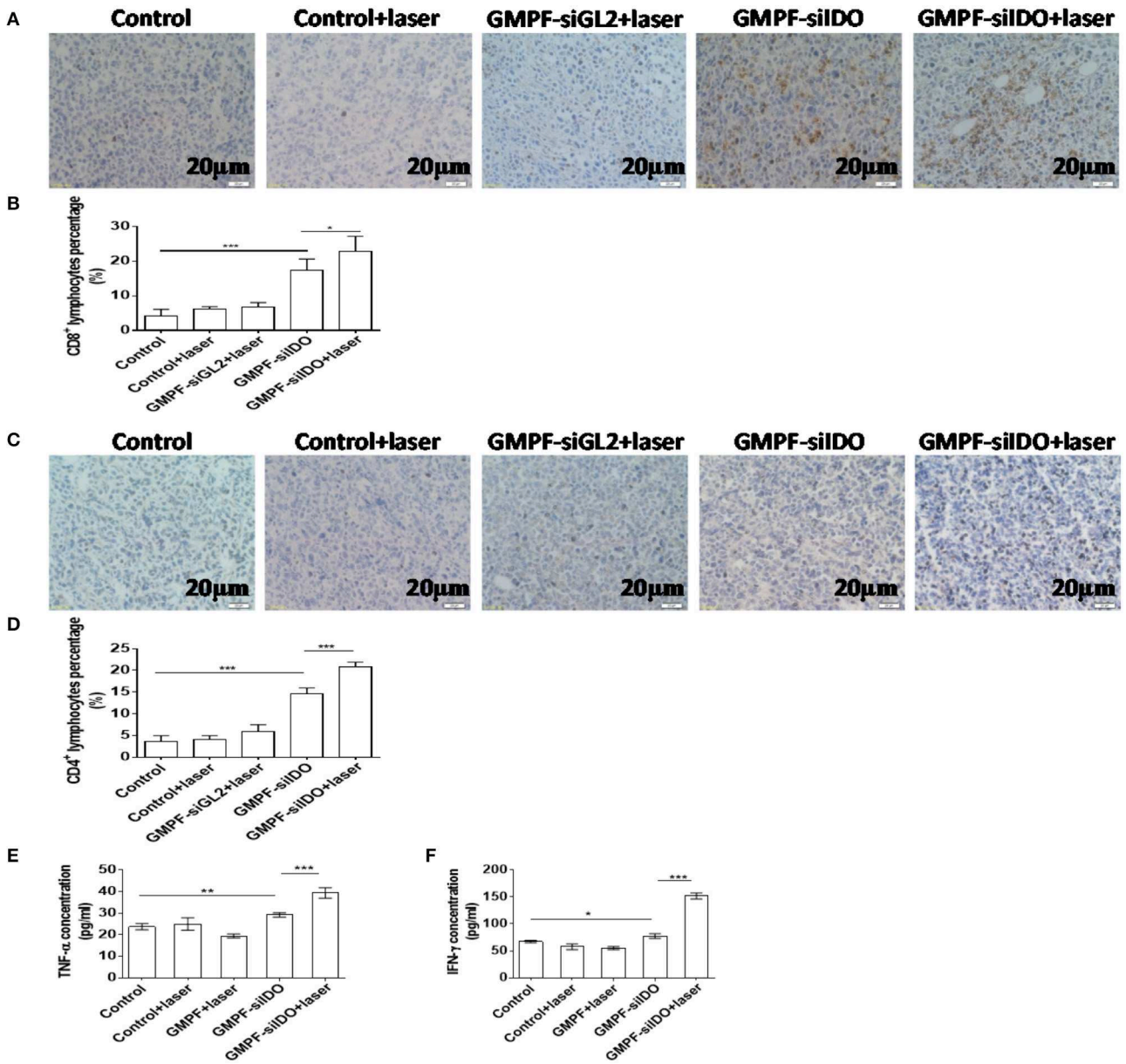

FIGURE 7 | Increased tumor-infiltrating T cells and up-regulated inflammatory cytokines after photothermal-immunotherapy. **(A–D)** Increased TILs in tumor tissue. Lung cancer-bearing mice were treated with PBS (control), GMPF-siGL2 or GMPF-siIDO, with or without laser irradiation. Tumor tissues were collected and subjected to immunohistochemistry assays and $CD8^+$ **(A,B)** and $CD4^+$ **(C,D)** lymphocytes in tumor tissue were counted. **(E,F)** Upregulated inflammatory cytokines. At the endpoint of experiment, the mice were sacrificed, and total blood was also collected. The TNF-α **(B)** and IFN-γ **(C)** in blood were analyzed by ELISA assay. Error bars represent the standard deviation of three experiments (*$P < 0.05$; **$P < 0.01$; ***$P < 0.001$).

tumor cells to PTT (18, 33), which was also observed in this study (**Figure 3**). We reported that knocking down IDO enhanced apoptosis of tumor cells through the suppression of NAD^+, highlighting a novel non-immune mechanism of IDO in tumor growth (33). In this study, the combination of gene silencing of IDO and PTT demonstrated the highest efficacy in anti-tumor therapy (**Figure 4**). Furthermore, IDO silencing greatly enhanced PTT-inducing apoptosis about 8 folds *in vivo* (**Figure 4**). Indeed, knockdown of IDO using GMPF-siIDO significantly induced apoptosis of LLC tumor cell *in vitro* and *in vivo* (**Figures 3**, **6**). On the other hand, the most significant feature of PTT treating cancers is inducing tumor cell apoptosis (28, 29). In support of this notion, we observed PTT-induced apoptosis *in vitro* in our previous studies. However, the efficiency of apoptosis is limited for the therapeutic purpose in terms of killing tumor cells *in vivo* (**Figures 4B–D**). Encouragingly, the use of GMPF-siIDO, which silences checkpoint regulatory molecule IDO in tumors, greatly synergized the tumor cell apoptosis in PTT *in vitro* and especially

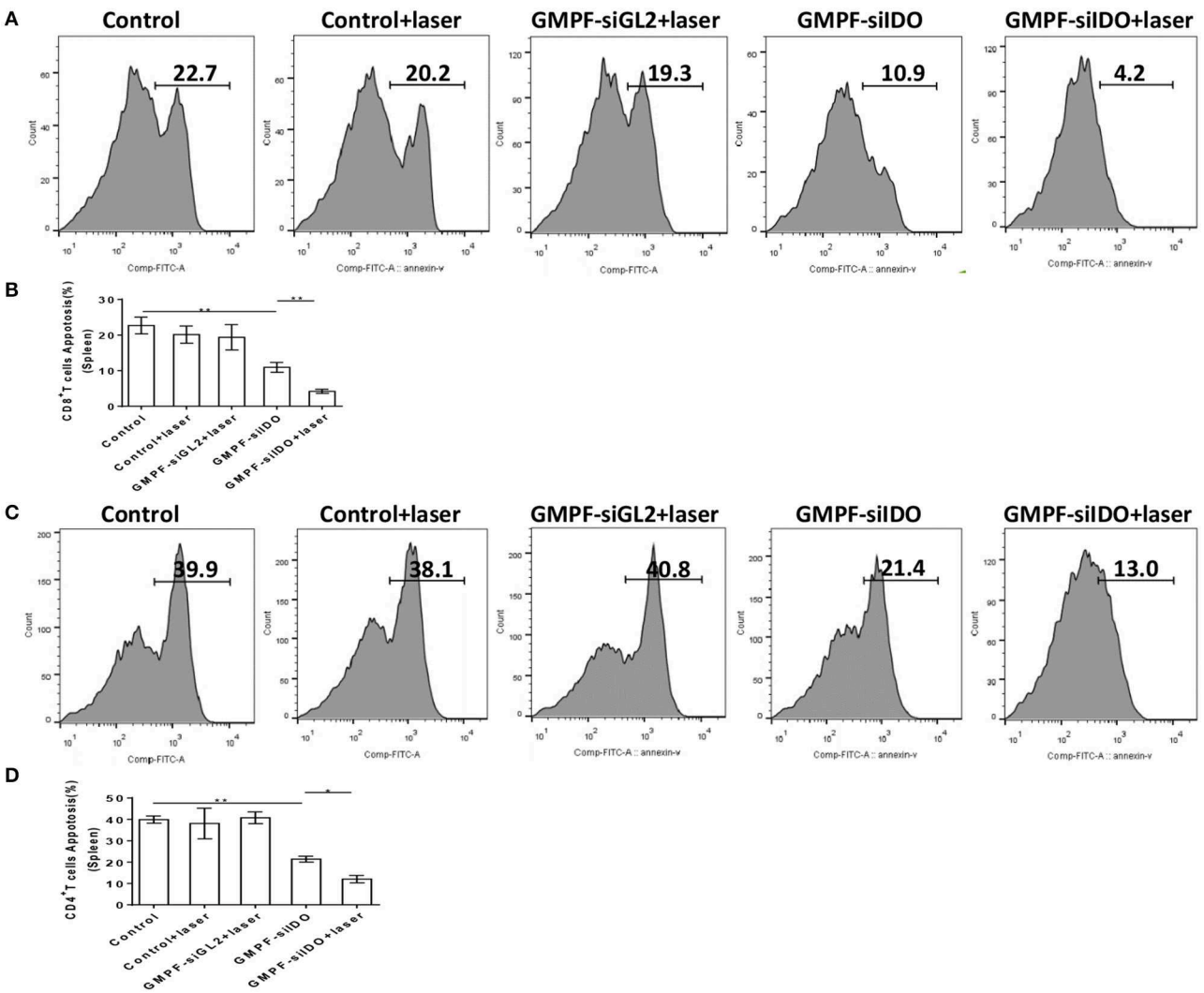

FIGURE 8 | Suppression of T cell apoptosis by photothermal-immunotherapy. Lung cancer-bearing mice were treated with PBS (control), GMPF-siGL2, or GMPF-siIDO, with or without laser irradiation. T cells were isolated and apoptosis of $CD4^+$ **(A)** and $CD8^+$ **(C)** T cells in spleens were analyzed by flow cytometry after Annexin V staining. The correspondent apoptotic percentages of $CD8^+$ T cells **(B)** and $CD4^+$ T cells **(D)** were calculated and results represent one of three experiments. Error bars represent the standard deviation of three experiments (*$P < 0.05$; **$P < 0.01$).

in vivo (**Figures 4B–D**). These data suggested that IDO is a negative regulator in PTT-induced tumor cell apoptosis; PTT treatment alone is not efficient to induce sufficient tumor cell apoptosis to kill tumor cells in the presence of IDO.

IDO is expressed in immune cells, including dendritic cells. We have previously examined the levels of IDO in DCs and silenced IDO in DCs using siRNA (8). We further demonstrated a therapeutic benefit of gene silencing IDO through a non-specific systemic delivery method using hydro-dynamic injection, which is effective in suppressing tumor growth *in vivo*. *In vivo* application for the treatment of melanoma mice using IDO siRNA showed promising therapeutic effects, including delayed tumor onset and decreased tumor size. Moreover, *in vivo* knockdown of IDO, using siRNA treatment, reinstalled T cell responses and enhanced tumor-specific killing. Therefore, IDO siRNA treatment displayed promising clinical potential through breaking IDO-mediated immune suppression, as well as reinstalling anticancer immunity (20). Additionally, IDO is an essential factor for generating Treg cells. On the other hand, Treg plays a vital role in immune suppression in most cancer patients. We have demonstrated that silencing IDO resulted in enhancing anti-tumor immunity which is associated with the decrease of Treg (8, 18, 43). In agreement with our previously findings, we observed a robust anti-tumor effect (**Figure 4**) and strong anti-immune response (**Figure 7**) in this study, when a combination treatment with PPT and siIDO is applied to the tumor-bearing mice. Moreover, IDO as a newly recognized checkpoint molecule exhausts T cells and inhibits proliferation and activation of T cells, and induces regulatory T cells to help tumor cells escape immune surveillance (8). PTT killing tumor

cells can activate a systemic immune response (15, 16). However, the presence of immune checkpoint IDO, which is upregulated by apoptotic tumor cells after PTT, may cause significant immune suppression. It has been reported that IDO can induce T cell apoptosis through depleting tryptophan, a critical amino acid for the survival of T cells (44, 45). Therefore, knockdown of IDO can rescue T cells from apoptosis induced by IDO, which has been demonstrated in our previous study (8). We have also demonstrated that tumor cells highly upregulate the expression of IDO which causes apoptosis of both CD4 and CD8 T cells (20). In this study, we observed the increase of infiltrated T cells in the tumors after treatment with siIDO, presumably due to knockdown of IDO, preventing T cells from apoptosis. Moreover, we observed that PTT treatment alone only induced marginal upregulation of anti-tumor immunity. In contrast, when IDO is knocked down, PTT induced robust anti-tumor immunity including enhanced TILs in tumors and increased secretion of anti-tumor inflammatory cytokines (**Figure 7**). Furthermore, we have previously demonstrated that IDO can suppress anti-tumor immunity through the induction of T cell apoptosis (20). In this study, we further verified that PTT-induced upregulation of IDO also induced T cell apoptosis, whereas knockdown of IDO prevented both $CD4^+$ and $CD8^+$ T cells from apoptosis (**Figure 8**). Altogether, these results indicate that gene silencing IDO is capable of synergizing PTT-induced T cell infiltration and cytokine release, suggesting a concert of related mechanisms involved in the anti-tumor immunity after the treatment of GMPF-siIDO. These results also agree with previous studies in which silencing IDO enhanced anti-tumor immunity with increased localization of lymphocytes in tumor tissue (8, 34).

In conclusion, we, for the first time validated the role of IDO as a negative regulator for both PTT-induced tumor cell apoptosis and anti-tumor immunity; IDO is a critical immune checkpoint that impedes the PTT efficiency while combination of gene knockdown of IDO enhances anti-tumor efficacy of PTT. We successfully constructed an immune-stimulatory nano-complex, GMPF-siIDO. GMPF-siIDO can specifically target LLC tumor cells and silence IDO *in vitro* and *in vivo*. Simultaneously, using a novel laser irradiation protocol, GMPF-siIDO exerted synergistic anti-neoplastic effects by inducing tumor cell apoptosis *via* PTT as well as enhancing anti-tumor immunity. Our study provides a novel pipeline design for developing a synergistic clinical treatment method for lung cancer. Therefore, our research developed a new strategy of anti-tumor photothermal-immunotherapy using GMPF-siIDO, which synergizes tumor cell apoptosis *in vivo* through the knockdown of IDO and photothermal mechanisms.

DATA AVAILABILITY STATEMENT

All datasets generated for this study are included in the article/supplementary material.

ETHICS STATEMENT

The animal study was reviewed and approved by Institutional Animal Care and Use Committee of Nanchang University, China.

AUTHOR CONTRIBUTIONS

YZ, KY, and WM planned experiments. YZ, YF, YH, YW, YL, SP, YS, ZW, and YC performed experiments. YZ, KY, WM, RL, QS, NK, and LQ analyzed data. YZ, YF, RJ, KY, and WM wrote the paper. All authors are assured that we met the criteria for authorship, and all reviewed the manuscript. All authors contributed this manuscript.

FUNDING

This current study was supported by grants from the National Natural Science Foundation of China (Grant Nos. 81673009, 81660274, 81803064), and the Natural Science Foundation of Jiangxi (Grant Nos. 20192ACBL20021, 20192ACB21027).

REFERENCES

1. Bray F, Ferlay J, Soerjomataram I, Siegel RL, Torre LA. Global cancer statistics 2018: GLOBOCAN estimates of incidence and mortality worldwide for 36 cancers in 185 countries. *CA Cancer J Clin.* (2018) 68:394–424. doi: 10.3322/caac.21492
2. Karanikas V, Zamanakou M, Kerenidi T, Dahabreh J, Hevas A, Nakou M, et al. Indoleamine 2,3-dioxygenase (IDO) expression in lung cancer. *Cancer Biol Ther.* (2007) 6:1258–62. doi: 10.4161/cbt.6.8.4446
3. Pan K, Wang H, Chen MS, Zhang HK, Weng DS, Zhou J, et al. Expression and prognosis role of indoleamine 2,3-dioxygenase in hepatocellular carcinoma. *J Cancer Res Clin Oncol.* (2008) 134:1247–53. doi: 10.1007/s00432-008-0395-1
4. Ristimaki A, Sivula A, Lundin J, Lundin M, Salminen T, Haglund C, et al. Prognostic significance of elevated cyclooxygenase-2 expression in breast cancer. *Cancer Res.* (2002) 62:632–5.
5. Brandacher G, Perathoner A, Ladurner R, Schneeberger S, Obrist P, Winkler C, et al. Prognostic value of indoleamine 2,3-dioxygenase expression in colorectal cancer: effect on tumor-infiltrating T cells. *Clin Cancer Res.* (2006) 12:1144–51. doi: 10.1158/1078-0432.CCR-05-1966
6. Prendergast GC, Smith C, Thomas S, Mandik-Nayak L, Laury-Kleintop L, Metz R, et al. Indoleamine 2,3-dioxygenase pathways of pathogenic inflammation and immune escape in cancer. *Cancer Immunol Immunother.* (2014) 63:721–35. doi: 10.1007/s00262-014-1549-4
7. Ninomiya S, Narala N, Huye L, Yagyu S, Savoldo B, Dotti G, et al. Tumor indoleamine 2,3-dioxygenase (IDO) inhibits CD19-CAR T cells and is downregulated by lymphodepleting drugs. *Blood.* (2015) 125:3905–16. doi: 10.1182/blood-2015-01-621474
8. Zheng X, Koropatnick J, Chen D, Velenosi T, Ling H, Zhang X, et al. Silencing IDO in dendritic cells: a novel approach to enhance cancer immunotherapy in a murine breast cancer model. *Int J Cancer.* (2013) 132:967–77. doi: 10.1002/ijc.27710
9. Pan J, Yuan K, Peng S, Huang Y, Zhang Y, Hu Y, et al. Gene silencing of indoleamine 2,3-dioxygenase hinders tumor growth through angiogenesis inhibition. *Int J Oncol.* (2017) 50:2136–2144. doi: 10.3892/ijo.2017.3975
10. Huang X, Jain PK, El-Sayed IH, El-Sayed MA. Plasmonic photothermal therapy (PPTT) using gold nanoparticles, Plasmonic photothermal therapy (PPTT) using gold nanoparticles. *Lasers in Med Sci.* (2007) 23:217. doi: 10.1007/s10103-007-0470-x

11. El-Sayed IH, Huang X, El-Sayed MA. Selective laser photo-thermal therapy of epithelial carcinoma using anti-EGFR antibody conjugated gold nanoparticles. *Cancer Lett.* (2006) 239:129–35. doi: 10.1016/j.canlet.2005.07.035
12. Huang X, El-Sayed IH, Qian W, El-Sayed MA. Cancer cell imaging and photothermal therapy in the near-infrared region by using gold nanorods. *J Am Chem Soc.* (2006) 128:2115–20. doi: 10.1021/ja057254a
13. Perez-Hernandez M, Del Pino P, Mitchell SG, Moros M, Stepien G, Pelaz B, et al. Dissecting the molecular mechanism of apoptosis during photothermal therapy using gold nanoprisms. *ACS Nano.* (2015) 9:52–61. doi: 10.1021/nn505468v
14. Ali MR, Rahman MA, Wu Y, Han T, Peng X, Mackey MA, et al. Efficacy, long-term toxicity, and mechanistic studies of gold nanorods photothermal therapy of cancer in xenograft mice. *Proc Natl Acad Sci USA.* (2017) 114:E3110–8. doi: 10.1073/pnas.1619302114
15. Nam J, Son S, Ochyl LJ, Kuai R, Schwendeman A, Moon JJ. Chemo-photothermal therapy combination elicits anti-tumor immunity against advanced metastatic cancer. *Nat Commun.* (2018) 9:1074. doi: 10.1038/s41467-018-03473-9
16. Peng J, Xiao Y, Li W, Yang Q, Tan L, Jia Y, et al. Combined photothermal therapy and immunotherapy: photosensitizer micelles together with IDO inhibitor enhance cancer photothermal therapy and immunotherapy. *Adv Sci.* (2018) 5:1700891. doi: 10.1002/advs.201700891
17. Nikoobakht B, El-Sayed MA. Preparation and growth mechanism of gold nanorods (NRs) using seed-mediated growth method. *Chem Mater.* (2003) 15:1957–62. doi: 10.1021/cm020732l
18. Zhang Y, Song N, Fu J, Liu Y, Zhan X, Peng S, et al. Synergic therapy of melanoma using GNRs-MUA-PEI/siIDO2-FA through targeted gene silencing and plasmonic photothermia. *Rsc Adv.* (2016) 6:79236–7. doi: 10.1039/C6RA90075E
19. Min WP, Zhou D, Ichim TE, Strejan GH, Xia X, Yang J, et al. Inhibitory feedback loop between tolerogenic dendritic cells and regulatory T cells in transplant tolerance. *J Immunol.* (2003) 170:1304–12. doi: 10.4049/jimmunol.170.3.1304
20. Zheng X, Koropatnick J, Li M, Zhang X, Ling F, Ren X, et al. Reinstalling antitumor immunity by inhibiting tumor-derived immunosuppressive molecule IDO through RNA interference. *J Immunol.* (2006) 177:5639–46. doi: 10.4049/jimmunol.177.8.5639
21. Yang Z, Liu T, Xie Y, Sun Z, Liu H, Lin J, et al. Chitosan layered gold nanorods as synergistic therapeutics for photothermal ablation and gene silencing in triple-negative breast cancer. *Acta Biomaterialia.* (2015) 25:S1742706115300246. doi: 10.1016/j.actbio.2015.07.026
22. Zhang Y, Wang Z, Huang Y, Ying M, Wang Y, Xiong J, et al. TdIF1: a putative oncogene in NSCLC tumor progression. *Signal Transduct Target Ther.* (2018) 3:28. doi: 10.1038/s41392-018-0030-9
23. Marinakos SM, Chen S, Chilkoti A. Plasmonic detection of a model analyte in serum by a gold nanorod sensor. *Anal Chem.* (2007) 79:5278–83. doi: 10.1021/ac0706527
24. O'Shannessy DJ, Yu G, Smale R, Fu YS, Singhal S, Thiel RP, et al. Folate receptor alpha expression in lung cancer: diagnostic and prognostic significance. *Oncotarget.* (2012) 3:414–25. doi: 10.18632/oncotarget.519
25. Iwakiri S, Sonobe M, Nagai S, Hirata T, Wada H, Miyahara R. Expression status of folate receptor α is significantly correlated with prognosis in non-small-cell lung cancers. *Ann Surg Oncol.* (2008) 15:889–99. doi: 10.1245/s10434-007-9755-3
26. Meier R, Henning TD, Boddington S, Tavri S, Arora S, Piontek G, et al. Breast cancers: MR imaging of folate-receptor expression with the folate-specific nanoparticle P1133. *Radiology.* (2010) 255:527–35. doi: 10.1148/radiol.10090050
27. Lu Y, Low PS. Folate-mediated delivery of macromolecular anticancer therapeutic agents. *Adv Drug Deliv Rev.* (2002) 54:675–93. doi: 10.1016/S0169-409X(02)00042-X
28. Chu KF, Dupuy DE. Thermal ablation of tumours: biological mechanisms and advances in therapy. *Nat Rev Cancer.* (2014) 14:199–208. doi: 10.1038/nrc3672
29. Pattani VP, Shah J, Atalis A, Sharma A, Tunnell JW. Role of apoptosis and necrosis in cell death induced by nanoparticle-mediated photothermal therapy. *J Nanopart Res.* (2015) 17:1–11. doi: 10.1007/s11051-014-2822-3
30. Siu KS, Chen D, Zheng X, Zhang X, Johnston N, Liu Y, et al. Non-covalently functionalized single-walled carbon nanotube for topical siRNA delivery into melanoma. *Biomaterials.* (2014) 35:3435–42. doi: 10.1016/j.biomaterials.2013.12.079
31. Borna H, Imani S, Iman M, Azimzadeh Jamalkandi S. Therapeutic face of RNAi: in vivo challenges. *Expert Opin Biol Ther.* (2015) 15:269–85. doi: 10.1517/14712598.2015.983070
32. Li JM, Zhao MX, Su H, Wang YY, Tan CP, Ji LN, et al. Multifunctional quantum-dot-based siRNA delivery for HPV18 E6 gene silence and intracellular imaging. *Biomaterials.* (2011) 32:7978–87. doi: 10.1016/j.biomaterials.2011.07.011
33. Liu Y, Zhang Y, Zheng X, Zhang X, Wang H, Li Q, et al. Gene silencing of indoleamine 2,3-dioxygenase 2 in melanoma cells induces apoptosis through the suppression of NAD+ and inhibits in vivo tumor growth. *Oncotarget.* (2016) 7:32329–40. doi: 10.18632/oncotarget.8617
34. Lob S, Konigsrainer A, Rammensee HG, Opelz G, Terness P. Inhibitors of indoleamine-2,3-dioxygenase for cancer therapy: can we see the wood for the trees? *Nat Rev Cancer.* (2009) 9:445–52. doi: 10.1038/nrc2639
35. Jain PK, Lee KS, El-Sayed IH, El-Sayed MA. Calculated absorption and scattering properties of gold nanoparticles of different size, shape, and composition: applications in biological imaging and biomedicine. *J Phys Chem B.* (2006) 110:7238–48. doi: 10.1021/jp057170o
36. Raghavan V, O'Flatharta C, Dwyer R, Breathnach A, Zafar H, Dockery P, et al. Dual plasmonic gold nanostars for photoacoustic imaging and photothermal therapy. *Nanomedicine.* (2017) 12:457–71. doi: 10.2217/nnm-2016-0318
37. Mackey MA, Ali MRK, Austin LA, Near RD, El-Sayed MA. The most effective gold nanorod size for plasmonic photothermal therapy: theory and *in vitro* experiments. *J Phys Chem B.* (2014) 118:1319–26. doi: 10.1021/jp409298f
38. Huang X, Jain PK, El-Sayed IH, El-Sayed MA. Determination of the minimum temperature required for selective photothermal destruction of cancer cells with the use of immunotargeted gold nanoparticles. *Photochem Photobiol.* (2007) 82:412–7. doi: 10.1562/2005-12-14-RA-754
39. Eustis S, El-Sayed MA. Why gold nanoparticles are more precious than pretty gold: noble metal surface plasmon resonance and its enhancement of the radiative and nonradiative properties of nanocrystals of different shapes. *Chem Soc Rev.* (2006) 35:209–17. doi: 10.1039/B514191E
40. Weissleder R. A clearer vision for *in vivo* imaging. *Nat Biotechnol.* (2001) 19:316–7. doi: 10.1038/86684
41. Danial NN, Korsmeyer SJ. Cell death: critical control points. *Cell.* (2004) 116:205–19. doi: 10.1016/S0092-8674(04)00046-7
42. Friberg M, Jennings R, Alsarraj M, Dessureault S, Cantor A, Extermann M, et al. Indoleamine 2,3-dioxygenase contributes to tumor cell evasion of T cell-mediated rejection. *Int J Cancer.* (2002) 101:151–5. doi: 10.1002/ijc.10645
43. Zhang Y, Fu J, Shi Y, Peng S, Cai Y, Zhan X, et al. A new cancer immunotherapy via simultaneous DC-mobilization and DC-targeted IDO gene silencing using an immune-stimulatory nanosystem. *Int J Cancer.* (2018) 143:2039–52. doi: 10.1002/ijc.31588
44. Munn DH, Sharma MD, Lee JR, Jhaver KG, Johnson TS, Keskin DB, et al. Potential regulatory function of human dendritic cells expressing indoleamine 2,3-dioxygenase. *Science.* (2002) 297:1867–70. doi: 10.1126/science.1073514
45. Munn DH, Mellor AL. Indoleamine 2,3-dioxygenase and tumor-induced tolerance. *J Clin Invest.* (2007) 117:1147–54. doi: 10.1172/JCI31178

Conflict of Interest: The authors declare that the research was conducted in the absence of any commercial or financial relationships that could be construed as a potential conflict of interest.

frontiers in Immunology

REVIEW
published: 16 June 2020
doi: 10.3389/fimmu.2020.01185

Immunosuppressive IDO in Cancer: Mechanisms of Action, Animal Models, and Targeting Strategies

*Lijie Zhai[1], April Bell[1], Erik Ladomersky[1], Kristen L. Lauing[1], Lakshmi Bollu[1], Jeffrey A. Sosman[2,3], Bin Zhang[2,3,4], Jennifer D. Wu[3,4,5], Stephen D. Miller[4,6], Joshua J. Meeks[3,5,7], Rimas V. Lukas[3,8], Eugene Wyatt[9,10], Lynn Doglio[9,10], Gary E. Schiltz[3,9,11], Robert H. McCusker[12] and Derek A. Wainwright[1,2,3,4]**

[1] Department of Neurological Surgery, Feinberg School of Medicine, Northwestern University, Chicago, IL, United States, [2] Division of Hematology and Oncology, Department of Medicine, Feinberg School of Medicine, Northwestern University, Chicago, IL, United States, [3] Robert H. Lurie Comprehensive Cancer Center of Northwestern University, Chicago, IL, United States, [4] Department of Microbiology-Immunology, Feinberg School of Medicine, Northwestern University, Chicago, IL, United States, [5] Department of Urology, Feinberg School of Medicine, Northwestern University, Chicago, IL, United States, [6] Department of Dermatology, Feinberg School of Medicine, Northwestern University, Chicago, IL, United States, [7] Department of Biochemistry and Molecular Genetics, Feinberg School of Medicine, Northwestern University, Chicago, IL, United States, [8] Division of Neuro-Oncology, Department of Neurology, Feinberg School of Medicine, Northwestern University, Chicago, IL, United States, [9] Department of Pharmacology, Feinberg School of Medicine, Northwestern University, Chicago, IL, United States, [10] Transgenic and Targeted Mutagenesis Laboratory, Feinberg School of Medicine, Northwestern University, Chicago, IL, United States, [11] Center for Molecular Innovation and Drug Discovery, Feinberg School of Medicine, Northwestern University, Chicago, IL, United States, [12] Department of Animal Sciences, University of Illinois at Urbana-Champaign, Urbana, IL, United States

OPEN ACCESS

Edited by:
Alexander Muller, Lankenau Institute for Medical Research, United States

Reviewed by:
Graham Robert Leggatt, The University of Queensland, Australia
Kawaljit Kaur, University of California, Los Angeles, United States

***Correspondence:**
Derek A. Wainwright
derekwainwright@northwestern.edu; derekwainwright@hotmail.com

Specialty section:
This article was submitted to Cancer Immunity and Immunotherapy, a section of the journal Frontiers in Immunology

Received: *01 February 2020*
Accepted: *13 May 2020*
Published: *16 June 2020*

Citation:
Zhai L, Bell A, Ladomersky E, Lauing KL, Bollu L, Sosman JA, Zhang B, Wu JD, Miller SD, Meeks JJ, Lukas RV, Wyatt E, Doglio L, Schiltz GE, McCusker RH and Wainwright DA (2020) Immunosuppressive IDO in Cancer: Mechanisms of Action, Animal Models, and Targeting Strategies. Front. Immunol. 11:1185. doi: 10.3389/fimmu.2020.01185

Indoleamine 2, 3-dioxygenase 1 (IDO; IDO1; INDO) is a rate-limiting enzyme that metabolizes the essential amino acid, tryptophan, into downstream kynurenines. Canonically, the metabolic depletion of tryptophan and/or the accumulation of kynurenine is the mechanism that defines how immunosuppressive IDO inhibits immune cell effector functions and/or facilitates T cell death. Non-canonically, IDO also suppresses immunity through non-enzymic effects. Since IDO targeting compounds predominantly aim to inhibit metabolic activity as evidenced across the numerous clinical trials currently evaluating safety/efficacy in patients with cancer, in addition to the recent disappointment of IDO enzyme inhibitor therapy during the phase III ECHO-301 trial, the issue of IDO non-enzyme effects have come to the forefront of mechanistic and therapeutic consideration(s). Here, we review enzyme-dependent and -independent IDO-mediated immunosuppression as it primarily relates to glioblastoma (GBM); the most common and aggressive primary brain tumor in adults. Our group's recent discovery that IDO levels increase in the brain parenchyma during advanced age and regardless of whether GBM is present, highlights an immunosuppressive synergy between aging-increased IDO activity in cells of the central nervous system that reside outside of the brain tumor but collaborate with GBM cell IDO activity inside of the tumor. Because of their potential value for the *in vivo* study of IDO, we also review current transgenic animal modeling systems while highlighting three new constructs recently created by our group. This work

converges on the central premise that maximal immunotherapeutic efficacy in subjects with advanced cancer requires both IDO enzyme- and non-enzyme-neutralization, which is not adequately addressed by available IDO-targeting pharmacologic approaches at this time.

Keywords: aging, immunotherapy, glioblastoma, tryptophan, immunosuppression, Treg, IDO1, kynurenine

INTRODUCTION

Tumors arise from cell-intrinsic pro-growth mutations, the catastrophic dysfunction of host immune defense, and/or the evolution of tumor cell-intrinsic mechanisms that facilitate host immune system evasion. Amino acid metabolism is a fundamental biological event intrinsic to all living organisms that has long been recognized to play a crucial regulatory checkpoint, resulting in the sculpting of cellular responses during pathophysiological conditions such as infectious disease, autoimmunity, neurodegeneration, psychiatric conditions, as well as cancer (1). Over the past two decades, the kynurenine (Kyn) pathway of tryptophan (Trp) metabolism (**Figure 1**) has been intensely studied throughout both preclinical and clinical therapeutic settings (2). The majority of this work has focused on the two primary rate-limiting enzymes that catalyze the first step of Trp metabolism: indoleamine 2, 3-dioxygenase 1 (IDO) and tryptophan dioxygenase (TDO). The central dogma underlying the immunosuppressive role for these enzymes is associated with their canonical Trp catabolic properties: IDO and/or TDO-mediated depletion of Trp and/or the accumulation of Kyn, which is associated with the suppression of immune effector cells and the upregulation, activation, and/or induction of tolerogenic immune cells (3, 4). Although a plethora of *in vitro*-motivated investigation has generated compelling evidence confirming IDO enzyme activity as a source of therapeutic value, data challenging the Trp depletion dogma as the only mechanism by which IDO suppresses the immune response began emerging almost a decade ago. Furthermore, the phase III Keynote-252/ECHO-301 clinical trial that evaluated combination treatment with the potent IDO enzyme inhibitor, epacadostat, and pembrolizumab [anti-programmed cell death 1 (PD-1)] in patients with unresectable or metastatic melanoma, failed to meet its primary end point as compared to individuals treated with pembrolizumab as a monotherapy (5). Despite certain variables that include objective *in vivo* efficacy and the underlying rationale for this combination of therapy which may have contributed to its clinical failure (6), a careful consideration for IDO-targeting approaches is warranted. Additional conflicting results that describe the role of IDO across different cancers and the cell types expressing the immunosuppressive mediator highlight the various underlying mechanisms that are context-dependent, multi-dimensional, and temporally-sensitive.

Here, we summarize current knowledge of IDO-mediated immunomodulation with a focus on how it affects the anti-cancer immune response. Potential mechanism(s) that reshape and/or revise current IDO dogma as it relates to the cancer immunity cycle are also explored. Recent advances in our understanding of IDO expression changes during aging and the potential contribution of these effects on suppressing immunosurveillance mechanisms during cancer cell initiation and/or tumor cell outgrowth are also discussed. Finally, the diametrically-opposed relationship between intratumoral IDO levels and overall survival among different types of cancer patients will provide a unique perspective on how cancer immunity dogma is not universally applicable.

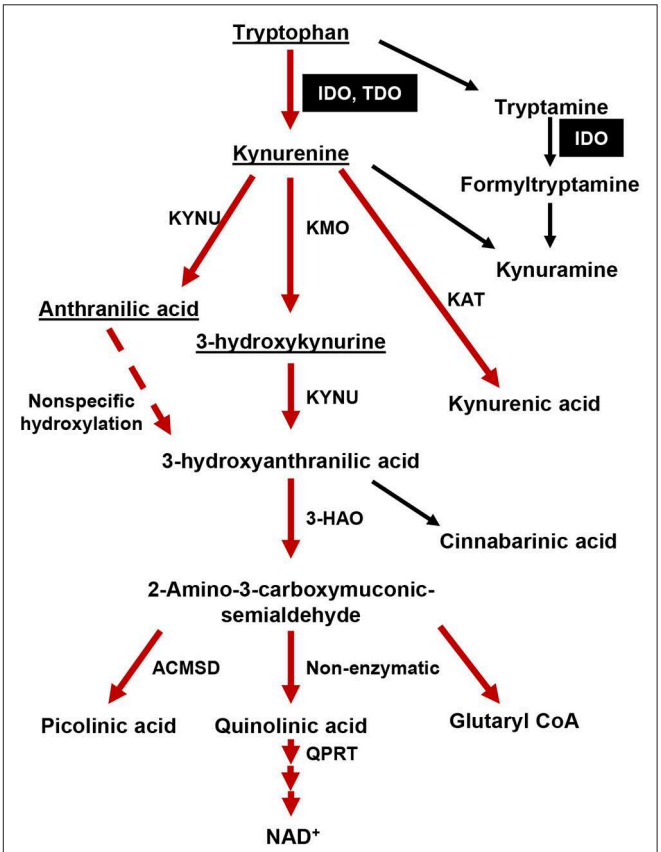

FIGURE 1 | The tryptophan (Trp)→ kynurenine (Kyn) metabolic pathway. The majority of dietary tryptophan (95%) is metabolized via the TrpKyn pathway (red arrows). A minor pathway that converts tryptamine into kynuramine is also included. Metabolites capable of crossing the blood brain barrier (BBB) are underlined. IDO and TDO are highlighted in black boxes. KMO, kynurenine 3-monooxygenase; KYNU, kynureninase; KAT, kynurenine aminotransferase (I, II, III); 3-HAO, 3-hydroxyanthranilate 3,4-dioxygenase; ACMSD: 2-amino-3-carboxymuconate semialdehyde carboxylase; QPRT, quinolinic-acid phosphoribosyl transferase.

IDO, Trp Metabolism and Its Association With Suppressing the Anti-cancer Immune Response

Less than 1% of dietary Trp is used for protein synthesis under physiological conditions while the remainder is degraded through decarboxylation, transamination, hydroxylation, or oxidation (7), which leads to the generation of physiologically active compounds including neuroactive tryptamine, neuroprotective melatonin, and/or immunomodulatory kynurenines. IDO and TDO catalyze the rate-limiting cleavage of the Trp indole ring 2, 3-double bond and incorporate molecular oxygen. The product of this reaction is *N*-formylkynurenine (NFK) that is rapidly converted into Kyn by formamidase. The latter catabolite is further transformed into downstream kynurenine-like intermediates, including 3-hydroxy-$_{L}$-kynurenine (3-HK), 3-hydroxyanthranilate (3-HAA) and quinolinic acid (Quin), which also affect the immune response (8). The ultimate product of Kyn pathway metabolism is nicotinamide adenine dinucleotide (NAD^+), a critical enzyme co-factor involved in a variety of fundamental biological events including acting as an electron transfer factor during glycolysis and oxidative phosphorylation, as well as being consumed by covalent modification of proteins and signaling enzymes. While IDO and TDO share similar functions as a mediator of Trp degradation, their biochemical properties are quite distinct. Monomeric IDO can act on a broad range of substrates that include $_{L}$-Trp, $_{D}$-Trp, tryptamine, 5-hydroxytryptophan and 5-hydroxytryptamine. In contrast, homotetrameric TDO is enantiomer specific and only metabolizes $_{L}$-Trp (9). The affinity of IDO for Trp and Trp-derivative substrates is highly variable such that binding to $_{D}$-Trp is low as compared to $_{L}$-Trp, with a K_m of human IDO for the $_{D}$-isomer that is 200-fold higher than that for the $_{L}$-isomer (10, 11). In contrast to IDO and TDO, the third Trp catabolic enzyme, IDO2, possesses a negligible level of intrinsic enzymic potential. The K_m of human IDO and IDO2 for $_{L}$-Trp is 20.90 ± 3.95 μmol/L and 6,809 ± 917 μmol/L, respectively (12) supporting the hypothesis that suggests IDO2 contributes a minimal role to overall Trp metabolism in humans. The lack of change in absolute Kyn among cell lines expressing high IDO2 cDNA levels, as well as the negligible change in systemic Kyn levels in mice with constitutional IDO2 deficiency (13–15), further support this hypothesis.

In addition to the distinct metabolic properties associated with Trp metabolism, the factors regulating IDO gene transcription and translation are different as compared to those that regulate TDO and IDO2 expression. Pro-inflammatory mediators tend to be the strongest agonists of IDO transcription that include the prototypical antitumor-associated T cell effector cytokine, interferon-gamma (IFN-γ), as well as the toll-like receptor 9 (TLR9) and TLR4 agonists, CpG DNA and lipopolysaccharide (LPS), respectively (16–19). Tumor necrosis factor-alpha (TNF-α), interleukin-6 (IL-6) and IL-1β also synergize with one another to facilitate the upregulation of IDO expression. Other modulators include soluble glucocorticoid-induced TNFR-related protein (GITR), prostaglandin E2, the oncogene c-Kit, as well as the tumor suppressor, Bin1 (20). The soluble fusion protein, cytotoxic T lymphocyte-associated protein 4-immunoglobulin (CTLA-4-Ig) induces IDO expression in dendritic cells (DCs) through the interaction of co-stimulatory receptors, CD80 (B7.1) and CD86 (B7.2) (21). Recent work further confirms that Wnt5α is another enhancer of IDO activity during β-catenin signaling in DCs (22).

Constitutive IDO expression can be found in healthy human subjects but is highly restricted to a select number of tissues and cells including mature DCs in secondary lymphoid organs, epithelial cells inside the female genital tract, as well as endothelial cells of term placenta and lung parenchyma (23). It should be noted that this superficial analysis does not capture the potential expression changes that occur across age groups as we previously found in the normal human brain parenchyma during advanced age (24). While some human tumor cell types constitutively express IDO, its presence is normal absent in human and mouse glioblastoma cells but is rapidly induced upon treatment with human and mouse IFNγ (25–29). Constitutive TDO expression is also expressed among different organs of healthy human subjects including bone marrow, muscle, gastrointestinal tract, kidney and urinary bladder, as well as inside the brain, with the highest levels in liver hepatocytes (30). TDO expression levels are regulated in-part by systemic levels of $_{L}$-Trp and corticosteroids (31, 32). Notably, common corticosteroid-like treatments such as dexamethasone rapidly increases TDO levels across multiple cell types. Similar to IDO, TDO is expressed by a bevy of different tumor types including glioblastoma, melanoma, ovarian carcinoma, hepatic carcinoma, breast cancer, non-small-cell lung cancer, lymphoid and myeloid cancers, renal cell carcinoma, and bladder cancer, with high expression levels associated with a more rapid rate of tumor progression and/or decreased patient survival (33–36). IDO2 mRNA is constitutively expressed in the human liver, brain, thyroid, placenta, endometrium, and testis, and is induced in antigen-presenting cells (APCs) and B cells (37). However, the role of IDO2 in affecting the anti-cancer immune response is less clear with the analysis of 129 human tumor samples and 25 human tumor cell lines showing no detectable full-length IDO2 mRNA transcript (36).

The primary dogma establishing a relationship between IDO, TDO, IDO2 and immunosuppression is associated with their individual and/or collective contribution toward the metabolism of Trp. The premise for this dogma is based on the Trp starvation theory that postulates the near absolute depletion of Trp, at or below <1 μM, facilitates the accumulation of uncharged tRNAs which then activate the general control non de-repressible 2 (GCN2) kinase pathway and the dysfunction of T cells (38). *In vitro* studies support the hypothesis that Trp depletion inhibits the master metabolic regulator mammalian target of rapamycin (mTOR) and protein kinase C (PKC-*Θ*) in cancer cells, which consequently enhances autophagy and T_{reg} development, respectively (39). Trp degradation may also suppress immune cell activities through the formation of Kyn and downstream derivative metabolites. *In vitro* and further requiring co-treatment with transforming growth factor-beta (TGF-β), Kyn facilitates the induction of FoxP3 in naïve $CD4^+$

T cells by activating the aryl hydrocarbon receptor (AhR) (40), a ligand-activated transcription factor that exerts potent effects on immune cells (41) and is involved in the differentiation of inducible Tregs (42, 43). The downstream pathway Kyn metabolites including kynurenic acid (KA) (44), xanthurenic acid (XA) (35), and cinnabarinic acid (CA) (45) interact with AhR and may also play a role in modulating the immune response. In striking contrast, Trp catabolites have been demonstrated to also induce $CD4^+$ T cell apoptosis. Terness et al. found that Kyn, 3-HK, and 3-HAA suppress T cell proliferation coincident with the induction of apoptosis (46). This finding was independently confirmed by Fallarino et al. (47) demonstrating *in vitro* that, Kyns induce the selective apoptosis of murine thymocytes and Th1-, but not Th2-cells. This immunoregulatory role of Kyns on different lymphocyte subsets may be important for maintaining peripheral lymphocyte homeostasis and for minimizing the accumulation of autoreactive and/or inflammatory lymphocytes. However, the exact molecular mechanism of Kyn-mediated selective apoptosis on T cell subsets remains unknown.

Despite a literature replete with previous work supporting the hypothesis that IDO-mediated Trp metabolism enhances suppression of the anti-cancer immune response, it's important to acknowledge that the predominant source for which these studies are based upon is derived from *in vitro* cell culture. Since Trp is an essential amino acid and not readily generated by mammalian cells, dietary consumption is critical for host survival and *in vivo* replenishment. It is therefore important to consider that the Trp concentrations required to inhibit T cell proliferation *in vitro* have been shown to be below 0.5–1 μM (38). Whether this cell culture condition can be transposed upon physiological conditions *in vivo* is controversial since human plasma Trp levels normally range between 50 and 100 μM. A number of conflicting results on this topic have recently arisen and was highlighted by Frumento et al. during their failure to observe an inhibition of T lymphocyte proliferation when the *in vitro* cell culture media was absent for Trp (48). Although it is arguable that high expression of IDO (or TDO) in tumor cells might lead to extremely low Trp levels within the tumor microenvironment, it's very difficult to fully validate this argument *in vivo*. Using the matrix-assisted laser desorption/ionization-time of flight mass spectrometry (MALDI-TOF MS) imaging technique, Sonner et al. (49) recently reported on TDO-mediated immunosuppression in experimental murine melanoma and demonstrated that, even in B16 melanoma highly expressing TDO by virtue of a cDNA-expressing plasmid, the intratumoral Trp levels were maintained at a similar level as compared to those inside unmodified B16 melanoma; thus suggesting that *in vivo* Trp levels are very stable even when Trp metabolism is maintained at an abnormally high rate.

Another hypothetical explanation regarding Trp depletion relies on the alteration of Trp transporter activity. This theory posits that even while there is no dramatic decrease of Trp in the peripheral blood circulation, alteration of the Trp transporter activity may cause intracellular Trp depletion which further triggers downstream immunosuppressive signals. In addition to the well-known non-specific low affinity Trp transporter (system L) (50), two Trp specific transporters with high affinity have been reported to be expressed on monocyte-derived macrophages and tumor cell lines (51, 52). Unfortunately, neither of these novel Trp transporters has been successfully cloned. Comprehensive functional analyses of the Trp transporters expressed by different immune cells and/or tumor cells *in vitro* and *in vivo* remain largely unexplored.

Intriguingly, T cell specific GCN2 knockout mice have similar anti-tumor effect against syngeneic B16 melanoma as compared to their wild type counterparts (49). Moreover, despite the elegant *in vitro* work by Mezrich et al. reporting that the 50 μM Kyn treatment activates AhR in naïve T cells and subsequently induces FoxP3 expression (40), human serological Kyn levels are normally within the range of 2–3 μM in both healthy individuals and in patients with inflammatory conditions (53–57). Theoretically, local tissue Kyn levels might transiently increase when IDO expression is highly expressed (58), but more precise *in vivo* detection and quantification techniques remain critically unavailable. Moreover, whether Kyn possesses an inducible or inhibitory effect on DC-mediated T_{reg} differentiation is also debatable. Somewhat conflicting with the report by Mezrich et al., Nguyen et al. reported that the addition of Kyn in a DC-T cell co-culture system led to the inhibition of naive T cell differentiation into $FoxP3^+$ Tregs (59). This latter observation supports the hypothesis that the Kyn-AhR mechanism is likely not responsible for the direct generation of Tregs in solid tumors; especially since the infiltrating component of tumors tend to primarily consist of thymus-derived natural T_{reg} (60, 61) that fail to express Ahr (62). It is also notable that other studies indicate the potential role of Kyn on T_{reg} activation as evidenced by the Munn and Mellor group who showed IDO-expressing plasmacytoid DCs in tumor draining lymph nodes preferentially activate pre-existing T_{reg} through the PD-1-PTEN pathway which was inhibited by the IDO pathway non-enzyme inhibitor, 1-methyl-$_D$-tryptophan (1-MT) (63, 64). In addition to the sometimes conflicting outcomes discussed above, results from studies suggesting that Kyns directly suppress the actions of effector T cells have also been revisited due to the high doses evaluated during those studies, which ranged from 100 to 1,000 μM (46, 47). The panoply of different observations across various modeling systems highlight the complexity of IDO immunobiology that, may be conveying artifactual effects during *in vitro* study and thereby supports the re-evaluation of previous interpretations with the use of new physiologically-relevant *in vivo* modeling systems.

Pleiotropic IDO Effects Reflect Multiple Functions, Diverse Cellular Origins, and Varying Kinetics

Beyond the restricted tissues that constitutively express IDO is the induction of its expression in a variety of cell types under normal and pathological conditions. This includes the changes of IDO expression during progressive aging (24), as well as in the setting of malignancy whereby levels change in response to T cell infiltration (65). Further complicating IDO functionality has been highlighted by immunohistochemical IDO detection across 15 different human cancer types that found

protein localization in myeloid cells, endothelial cells, tumor cells, or a combination of those origins (23). The select pattern of intratumoral IDO expression raises critical questions including: (i) does IDO perform the same role among different cell types; (ii) how do these cells coordinately contribute to tumor growth and/or suppression of anti-cancer immunity; (iii) what are the kinetics of endogenous IDO expression and its relationship to enzyme activity?

A peculiar trait of tumor cells expressing high IDO expression is the resultant effect on an overall slower rate of growth as compared to cells with lower intrinsic IDO levels (66). A derivative and competing hypothesis arising from this observation suggests that IDO functions as a tumor suppressor. This was corroborated with findings of higher intratumoral IDO expression positively associated with longer survival in renal cell carcinoma-, hepatocellular carcinoma-, and melanoma-patients (3, 67–69). It should also be considered, however, that higher levels of T cell infiltration are often associated with higher intratumoral IDO levels and this relationship has an established survival improvement in human subjects diagnosed with select malignancies (3, 70). Therefore, the higher intratumoral IDO levels are likely associative and may not have any effect on tumor growth itself. Regardless and in contrast to the alleged beneficial effects of slower growth, higher IDO expression was associated with an improved motility of lung cancer cells that enhanced their metastatic formation in the brain, liver, and bone (71), whereas IDO deficiency decreased metastasic burden and improved the survival of subjects with breast carcinoma-derived pulmonary metastases (72, 73). Intratumoral IDO expression also correlated with the frequency of liver metastases in colorectal cancer (74), distant metastases in hepatocellular cancer (69), and nodal metastases in endometrial carcinoma (75). Among human cancer cells, IDO activity has been implicated in improving DNA repair and mediating the resistance to treatments such as the poly-ADP-ribosyltransferase (PARP) inhibitor, olaparib, γ-radiation, and the chemotherapeutic agent, cisplatin, through generation of NAD^+ (76). It was reported that impaired Trp metabolism resulted in the inhibition of *de novo* NAD^+ synthesis, which led to hepatic tumorigenesis through DNA damage (77), further supporting the previous finding that NAD^+ serves as the only endogenous substrate of PARPs to facilitate the removal of oxidative DNA damage. However, it's important to note that IDO is not normally expressed in the liver, whereas, TDO is constitutively and highly expressed. Therefore, if either or both of these factors are associated with the impaired Trp metabolism, it may be associated with pathological injury and not necessarily the normal expression of those rate-limiting enzymes.

While IDO expression by tumor and immune cells receives the predominant attention, the immunosuppressive mediator is also expressed by endothelial cells (23). In healthy tissues, IDO is expressed by endothelial cells in a large proportion of placental and pulmonary blood vessels, as well as by a minority of blood vessels in select other organs. Intratumorally, vascular IDO expression is frequent among renal cell carcinoma, non-small lung carcinoma, endometrial carcinoma, and melanoma. Endothelial IDO appears to modulate vascular tone through several different signaling pathways including Kyn-mediated activation of soluble guanylate cyclase, adenylate cyclase, and voltage-dependent K^+ channels (78, 79). The Kyn metabolite, xanthurenic acid, has been shown to possess greater potency as compared to $_L$-Kyn in causing blood vessel relaxation that is dependent on nitric oxide (80). Stanley *et al.* found that in the presence of H_2O_2, IDO catalyzes Trp oxidation using singlet molecular oxygen ($^1O_2$), leading to the vasodilation product *cis*-WOOH (81). It's important to note that these experiments were conducted while utilizing high concentrations of the Trp catabolites between 300 μM to 1.5 mM *in vitro*. It's therefore unclear as to whether the vasodilating compounds attain a similar local level inside a solid tumor *in vivo*. However, other observations support the vaso-relaxing effects of endothelial IDO including a model of sepsis-induced hypotension (82). Intrinsic to the IDO expressed by endothelial cells there may also be a role for an effect on modulating tumor neovascularization (83), though the exact molecular mechanism explaining has yet to be elucidated (84).

Data suggesting that IDO possesses non-metabolic functions independent from those associated with its enzyme activity began emerging ∼10 years ago. Pallotta *et al.* was the first to report that the *in vitro* treatment of TGF-β in cultures of mouse plasmacytoid DCs (pDCs) leads to the phosphorylation of IDO immunoreceptor tyrosine-based inhibitory motifs (ITIMs), which subsequently recruits and activates the tyrosine phosphatases, SHP-1 and SHP-2, as well as inositol polyphosphatase (SHIP) (85). Activation of the pDC TGF-β-IDO-SHP axis enabled an autocrine loop through the induction of non-canonical NF-κB signaling, which further enhanced intra-pDC IDO expression levels. Treatment of the pDCs with 1-methyl-$_{D,L}$-tryptophan confirmed that the immunosuppressive IDO signaling mechanism was faithfully independent of its association with mediating Trp metabolism. However, it's notable that the 4 μM dose of 1-MT used in this study was lower than the EC_{50} of 1-MT (13). Future validation and replication of these results while utilizing a more potent IDO enzyme inhibitor will allow for confidence and verification of non-enzymic IDO functions. Our group found similar observations of IDO mediating both enzyme and non-enzyme effects that depend on context. Using a syngeneic brain tumor model, we previously demonstrated that the shRNA knockdown of GBM cell IDO leads to the suppression of intratumoral Treg accumulation and was associated with a significant improvement in long-term animal subject survival (86) independent of GBM cell IDO metabolism (29). We also showed that the forced expression of GBM cell IDO cDNA (IDO-O/E) enhances Treg recruitment even when animal subjects are treated with a potent blood brain barrier-penetrating pharmacologic IDO enzyme inhibitor (87). We further confirmed that while the IDO enzyme inhibitor significantly decreased intratumoral Kyn levels in GBM IDO-O/E *in vivo*, the reduction was not associated with decreased intratumoral Treg accumulation. Taken together, these observations support the hypothesis that new IDO-targeting approaches aimed at simultaneously reversing enzyme and non-enzymic activities will enhance the effectiveness of future cancer immunotherapy efforts.

IDO and Its Relationship to Host Age

Considering the suppressive role of the IDO/TDO axis in immunoregulation, as well as the changes in immunological status system during progressive aging, it's not surprising that several studies have investigated the relationship between the TrpKyn pathway as it relates to aging-dependent disease. The serological Kyn/Trp ratio is often used an indicator of IDO enzyme activity and progressively increases during normal aging in humans (88, 89). This increase has been associated with enhanced frailty in human subjects >65 years of age and predicts an increased mortality rate of individuals in their nineties (90). Additionally, meta-analysis of age-related gene expression changes in the peripheral blood of adult individuals identified the enzyme kynureninase (KYNU, **Figure 1**) as one of the most differentially expressed genes (91). In a large population screening analysis that included 7,074 human subjects that focused on studying bone mineralization, Apalset et al. reported that the serological Kyn/Trp ratio negatively correlated with bone mineral density in the 71–74 year old age group as compared to younger individuals that were 46–49 years of age (92). More recently, Ocampo et al. summarized the results from previous animal studies of brain diseases and the interaction with Kyns during aging that indicate a strong correlation between Kyn pathway metabolites across different rodent ages (93). They found an intriguing observation that while TDO and IDO expression decrease in the liver and kidney during progressive aging, TDO and IDO were dichotomized in the rat brain during advanced age such that TDO decreased and IDO increased in overall expression as compared to young animal subjects. Similarly, our group previously demonstrated that there is an ∼400 fold increase in IDO mRNA expression in the normal naïve brain of 72–74 week old C57BL/6 WT mice as compared to 6–8 week old subjects (94). Our most recent study evaluating the interactions between normal human aging and its relationship to brain cancer incidence and mortality also found a significant increase in IDO mRNA expression in the normal human brain of individuals aged 60–69 years of age as compared to younger human subjects (24). The increased human brain IDO expression was associated with a maximal $T_{reg}/CD8^+$ cytolytic T cell ratio in the peripheral blood of the 60–69 year old age group confirming a simultaneous increase of systemic- and local-immune suppression (24). To address these observations, we are currently in the process of determining as to whether the advanced age-dependent increase of central nervous system IDO expression directly increases the peripheral $T_{reg}/CD8^+$ cytolytic T cell ratio and how this relationship affects the incidence and mortality rate, as well as responsiveness to immunotherapy of GBM.

Understanding how aging-dependent molecular mechanisms affect IDO enzyme and non-enzymic activity is in its infancy. Refaey et al. reported that 22-month old mice have significantly higher serum N-formylkynurenine as compared to younger counterparts at 4 and 13 months of age, suggesting a potential role for Kyn pathway metabolism in aging-dependent bone loss (95). Strikingly, either the *in vitro* addition of Kyn to bone marrow-derived mesenchymal stromal cells (BMSCs), dietary supplementation of Kyn, or a direct administration of Kyn into the peritoneum suppressed the formation of new bone; possibly by decreasing osteoblast formation, failed recruitment capability and/or loss of effector functions. It should be noted, however, that neither age-matched IDOKO nor TDOKO mice were used in the study and it's therefore inconclusive as to the primary source of aging-dependent changes in Kyn levels. Independently, Minhas et al. demonstrated that the catabolic enzyme converting quinolinic acid into NAD^+, quinolate phosphoribosyltransferase (QPRT), significantly declines in aged human monocyte-derived macrophages (MDMs) from individuals ≥65 years old as compared to MDMs isolated from individuals ≤35 years of age (96). Loss of QPRT subsequently resulted in decreased *de novo* NAD^+ synthesis and was associated with an enhanced pro-inflammatory status and lower phagocytic ability of MDMs. It's worth noting that in addition to the enzymes and metabolites of the Kyn pathway, changes in AhR activity and/or expression have also been implicated during aging (97). However, the direct relationship between IDO, TDO, Kyn, and AhR has not been comprehensively established during a combined investigation of aging and in a specific pathophysiological setting.

Based on the relationship between increased incidence of patients with cancer and advanced age (98), it may be surprising that few studies have investigated IDO and/or TDO changes in subjects with cancer and across the health-/life-span. Adult glioblastoma is an age-related disease with a median age of diagnosis at 65 years old (99). To explore the mechanistic underpinnings between advanced age and its effects on the GBM immune response, we previously compared the survival rate of young 6–8 week- and adult 72–74 week-old mice intracranially-engrafted with the syngeneic GL261 glioma cell line. The young mice survived slightly longer than the older subjects with a median overall survival (mOS) of 27.5 days and 21.5 days, respectively ($p = 0.0292$) (94). Intriguingly, advanced age was associated with a large increase of IDO expression in the contralateral brain without tumor and as compared to young mice, whereas there was no such difference within the tumor itself. These data suggest that the majority of brain parenchymal cells expressing increased IDO during advanced age do not migrate into the GBM. Intriguingly, serological, and intra-GBM Trp and Kyn levels showed no differences between young and adult subjects despite the increased IDO expression in the older brain (94). We also studied the effects of advanced age on immunotherapeutic efficacy in adult mice at 72 weeks of age, which is closer to the analogous time frame of a human GBM patient diagnosis as compared to the standard 6–12 week old mouse. When the young and adult mice underwent therapy (87) with whole brain radiotherapy, anti-PD-1 mAb and pharmacological IDO enzyme inhibitor, older mice showed higher IDO mRNA in the non-tumor brain tissues as compared to younger subjects. Functionally, the triple combination therapy resulted in a median survival of 31.5 days in the older subjects, which was significantly decreased as compared to the younger 8-week-old mice with a survival of 40.5 days ($p < 0.001$), suggesting that the increased brain IDO expression during advanced age has a directly negative effect on immunotherapeutic efficacy in subjects with GBM.

Mouse Models for Studying IDO

Among preclinical studies, transgenic mouse models have demonstrated their substantial importance to understanding the function, effects and mechanism of IDO in a physiologically-relevant environment. The first IDO knockout (IDOKO) mouse strain originated from the Munn and Mellor group whereby exons 3–5 of IDO were replaced with a β-gal and neomycin cassette (100, 101). Surprisingly, the homozygous IDOKO mice are viable, fertile and possess a phenotypically normal immune system without any obvious graft vs. host-like symptoms, suggesting that IDO-mediated immune suppression is dispensable for the normal maintenance of central and peripheral tolerance to self-antigens. Given the functional similarity between TDO and IDO for mediating Trp catabolism, it's possible that TDO plays a compensatory role in the absence of IDO. However, it's notable that Kyn levels are significantly decreased in naïve IDOKO mice, so if TDO compensates, there appears to be a limit to those potential effects (29). The expression and function of TDO has yet to be investigated in IDOKO mice with cancer. Though IDO expression is not required for immune tolerance under homeostatic conditions, it plays a critical role during acquisition of tumor-immune tolerance as indicated by studies demonstrating that IDOKO mice have increased tumor infiltration of effector T lymphocytes, decreased immunosuppressive immune cells, as well as increased survival (102–105), implicating non-redundant functions between IDO and TDO in the various cancer settings.

Because of their normal growth and immune system development, constitutional IDOKO mice are widely used preclinically. However, this transgenic model does not reveal the role of IDO in different tissues or cell types. Recently, Bishnupuri et al. generated an intestinal epithelium specific IDO knockout mouse strain by breeding *Ido1*$^{tm1c(EUCOMM)Wtsi}$ mice with the villin promoter *Cre* mice (105). The mouse colon cancer model utilizing this conditional IDO knockout mouse strain discovered neoplastic colon epithelium cell IDO to be a critical

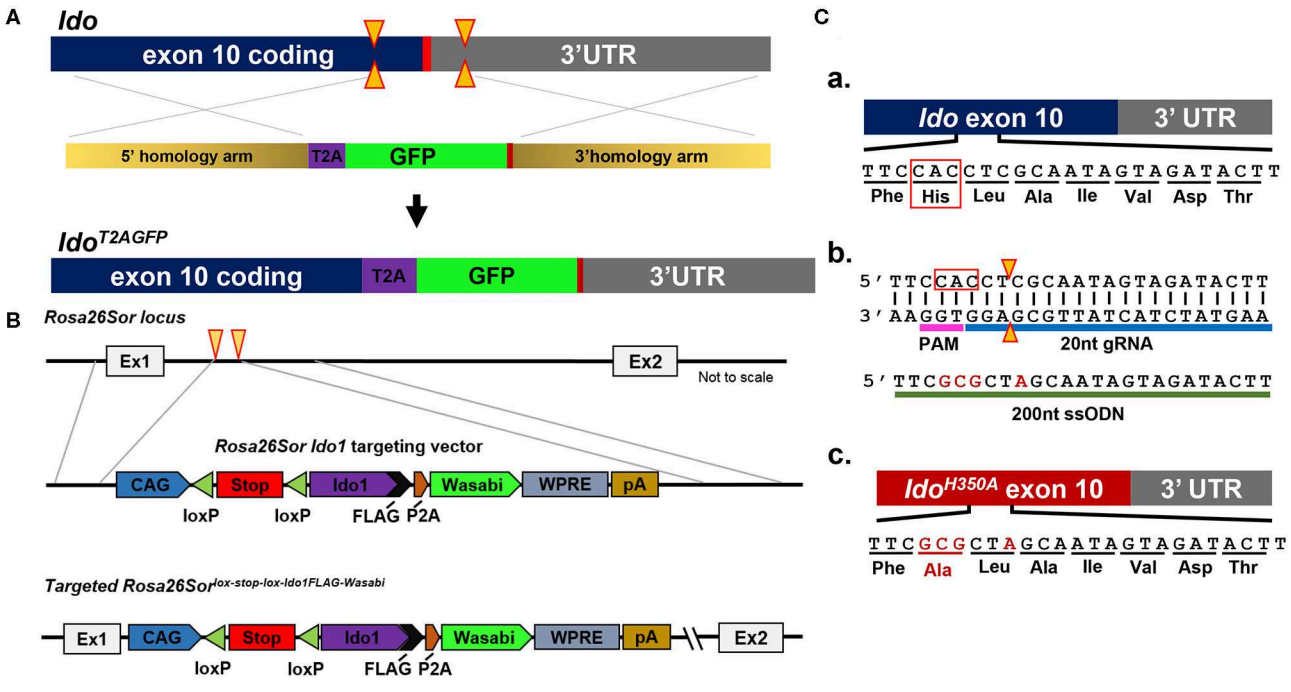

FIGURE 2 | Schema utilized to generate IDO-targeted transgenic mouse strains. **(A)** Generation of the *Ido1*^{T2AGFP} mouse line. CRISPR/Cas9 technology was employed in murine embryonic stem (ES) cells. Two separate guide RNAs directed Cas9 nuclease cleavage of the *Ido1* locus, creating double strand DNA breaks (yellow arrow) before and after the stop codon (red bar). The CRISPR ES cell reaction included a plasmid repair template, which encoded the T2A and GFP elements flanked by 5′ and 3′ homology arms of 700nt (tan bars). The T2A and GFP elements were introduced into the endogenous *Ido1* locus before the stop codon *via* homology directed repair (HDR). **(B)** Introduction of a *Cre*-dependent *Ido1* expression construct into the *Rosa26Sor* locus by CRISPR/Cas9 technology. Two separate guide RNAs directed Cas9 nuclease cleavage at the *Rosa26Sor* locus, creating double strand DNA breaks (yellow arrows). A plasmid repair temple (*Rosa26Sor Ido1* targeting vector) was included in the reaction and introduced *via* HDR. The edited locus encodes the CAG promoter driven, *Cre*-dependent conditional expression of a bi-cistronic *Ido1* construct. The *Ido1* transcript includes a C-terminal FLAG-tag, followed by a P2A element and expression of the Wasabi fluorophore. It also included a WPRE element and the bovine growth hormone polyadenylation (pA) signal. The construct is flanked by 800 bp 5′ and 750 bp 3′ homology arms (gray lines). **(C)** Generation of the *Ido1*^{H350A} mouse line. (a) Schematic showing the last coding exon of the *Ido1* gene, exon 10. The highlighted region encodes a histidine residue at position 350 (red box) that is essential for mouse IDO enzyme activity; (b) CRISPR/Cas9 technology generated a precise double strand DNA break in the *Ido1* exon 10 locus in fertilized mouse embryos (yellow triangle). A 200nt single stranded oligodeoxynucleotide repair template was included in the reaction (green bar). The ssODN introduced point mutations (red letters) into the endogenous *Ido1* locus via HDR. These point mutations altered the endogenous coding sequence from CAC→GCG, which changed the amino acid reside from histidine to alanine, H350A (red letters). An additional silent mutation (C→A) was included to add a restriction site for genotype analysis (red letter); (c) Schematic showing the mutated *Ido1* exon 10 locus encoding H350A in red.

constituent of colon tumorigenesis and that Kyn metabolites rapidly activated PI3K-Akt signaling in the neoplastic epithelium to promote cellular proliferation and resistance to apoptosis. In addition to the constitutional and conditional IDO knockout mice that have previously been reported, our group has created new constructs that will allow for addressing novel questions including an IDO reporter mouse that expresses a IDO-GFP (**Figure 2A**), an IDO knock-in mouse under tissue-specific Cre using Rosa26Sor-loxp-IDO-FLAG-GFP (**Figure 2B**), and an IDO enzyme nullified mouse whereby the histidine of the 350th amino acid is substituted to an alanine (**Figure 2C**). We are currently characterizing each of these recently created models and will publish data supporting their phenotypes in the near future.

The Expression, Immunosuppression, and Targetability of IDO in Subjects With GBM

Tumors arising from glia within the central nervous system (CNS) are considered to be potently immunosuppressive due to their surrounding immunospecialized neuroanatomical landscape (106). GBM is as an immunologically "cold" malignancy and associated with an immune system microenvironment that has resulted in the failure of all phase III clinical trials evaluating immunotherapy in patients with GBM to-date. Considering the work by our group and others in repeatedly demonstrating the remarkable pathogenic influence of IDO in subjects with GBM, the elucidation of its role and multi-variate functions may provide a path for enhancing the effectiveness of cancer immunotherapy against malignant glioma in the future.

IDO mRNA is highly expressed in ≥90% of GBM patients presenting with wild-type isocitrate dehydrogenase (wtIDH) and while not normally expressed, is inducible among a majority of human GBM cell lines after exposure to proinflammatory cytokines (23, 66, 107–110). While TDO expression is expressed at an even higher mRNA level than IDO in patient-resected GBM (33, 109–111), IDO2 levels are negligible or undetectable at the mRNA level (65), despite an IHC-focused study suggesting high IDO2 protein levels in GBM ($n = 52$) (109); the latter of which likely reflects conclusions based on non-specific antibody immunostaining. The cognate receptor for Kyn is AhR and is present throughout all grades of glioma, with the highest level reported in GBM. A recent study screening 75 glioma tissue samples by immunohistochemistry also confirmed higher IDO and TDO expression while low/no expression of IDO2 at protein levels (112). Studies from our group and others' have independently demonstrated that both Trp and Kyn are significantly decreased in GBM patient plasma as compared to human subjects without a tumor of the CNS (56, 57). Strikingly, in contrast to the absolute levels of metabolites, the Kyn/Trp ratio is significantly increased in GBM patient plasma

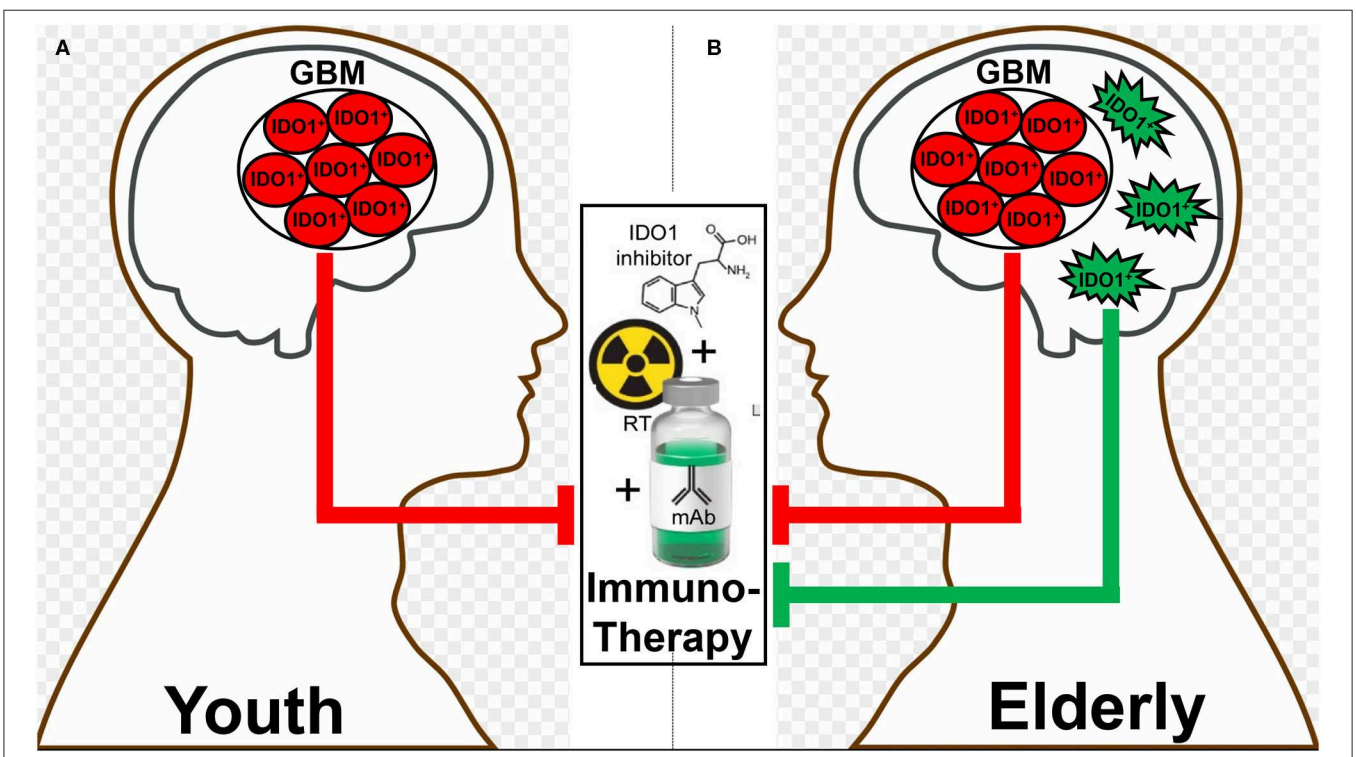

FIGURE 3 | A hypothetic schematic for how advanced aging decreases immunotherapeutic efficacy in subjects with glioblastoma (GBM). There is a basal level of IDO-mediated immunosuppression by GBM cells (red) that does not change between **(A)** young and **(B)** elderly (as defined by ≥65 years of age) individuals. In contrast, there is additional immunosuppression in the elderly brain due to the accumulation of brain-resident IDO-expressing dendritic cells (green), which synergize with the GBM cell IDO to suppress the anti-GBM immune response facilitated by combination radiation, anti-PD-1 mAb, and IDO enzyme inhibitor treatment (middle box).

TABLE 1 | Ongoing and historical clinical trials that target IDO in cancer.

Agent	Indication(s)	Phase	Status	Notes	NCT no.
Indoximod ($_D$-1-MT)	Metastatic solid tumor	I	Completed	Combined with docetaxel	NCT01191216
	Solid tumor	I	Completed	Single agent	NCT00567931
	Metastatic breast cancer	I/II	Active, not recruiting –> now completed	Combined with vaccine	NCT01042535
		II	Recruiting	Combined with fulvestrant or tamoxifen and palbociclib	NCT02913430
		II	Active, not recruiting –> now completed	Combined with docetaxel or paclitaxel	NCT01792050
	Melanoma	I/II	Recruiting –> now active, not recruiting	Combined with ipilimumab (CTLA-4 mAb), nivolumab, or. pembrolizumab	NCT02073123
	Metastatic Adenoma of Pancreas	I/II	Recruiting –> now completed	Combined with gemcitabine and nab-paclitaxel	NCT02077881
	Acute myeloid leukemia	I/II	Recruiting	Combined with cytarbine, idarubicin	NCT02835729
	GBM, glioma, gliosarcoma	I/II	Recruiting –> now active, not recruiting	Combined with temozolomide, bevacizumab (VEGF mAb) and radiation	NCT02052648
	GBM, glioma, ependymoma, medulloblastoma	I	Recruiting	Combined with temozolomide and radiation or cyclophosphamide and etoposide	NCT02502708
	Prostate carcinoma	II	Active, not recruiting–> now completed	Combined with sipuleucel-T	NCT01560923
	NSCLC	II	Recruiting –> now active, not recruiting	Combined with docetaxel and tergenpumatucel-L	NCT02460367
INCB024360	Advanced neoplasms	I	Completed	As single agent	NCT01195311
	Myelodysplastic Syndromes	II	Completed	As single agent	NCT01822691
	Melanoma	I/II	Recruiting –> now terminated	Combined with ipilimumab	NCT01604889
		II	Recruiting–> now completed	Combined with a multipeptide-based vaccine	NCT01961115
	Reproductive tract tumors	II	Completed –> now terminated	Compared to tamoxifen	NCT01685255
		I/II	Recruiting	Combined with vaccine and cyclophosphamide	NCT02785250
		I	Active, not recruiting	With therapeutic conventional surgery	NCT02042430
		I	Recruiting–> now completed	Combined with adoptive transfer of NK cells, IL-2, fludarabine, and cyclophosphamide	NCT02118285
		I/II	Recruiting–> now terminated	Combined with CRS-207 and Pembrolizumab (PD-1 mAb)	NCT02575807
		I/II	Recruiting	Combined with DC-targeted NY-ESO-1 and poly-ICLC	NCT02166905
		I/II	Withdrawn	As single agent	NCT01982487
		II	Suspended	Combined with pembrolizumab	NCT03602586
	Solid tumors	I/II	Recruiting–> now active, not recruiting	Combined with MK-3475	NCT02178722
		I	Recruiting–> now active, not recruiting	Alone or combined with combination of pembrolizumab, cisplatin, pemetrexed, carboplatin, or paclitaxel	NCT02862457
		I	Active, not recruiting	Combined with itacitinib (JAK inhibitor)	NCT02559492
		I/II	Recruiting–> now active, not recruiting	Combined with combination of pembrolizumab, ozaliplatin, leucovorin, 5-fluorouracil, gemcitabine, nab-paclitaxel, carboplatin, paclitaxel, pemetrexed, cyclophasphamide, or cisplatin	NCT03085914
		I/II	Recruiting –> now completed	Combined with MEDI4736 (PD-L1 mAb)	NCT02318277
		I/II	Active, not recruiting	Combined with azacitidine, pembrolizumab	NCT02959437
	Meta. colorectal cancer	I/II	Not yet recruiting	Combined with pembrolizumab and azacitidine	NCT03182894
	Gastric cancer	II	Not yet recruiting –> now recruiting	Combined with pembrolizumab	NCT03196232
	Meta. Pancreatic cancer	II	Not yet recruiting –> now recruiting	Combined with CRS-207, pembrolizumab, CY, CRS-207, GVAX	NCT03006302
		II	Withdrawn	Combined with pembrolizumab	NCT03432676

(Continued)

TABLE 1 | Continued

Agent	Indication(s)	Phase	Status	Notes	NCT no.
	*NSCLC, urothelial carcinoma	I	Active, not recruiting –> now terminated	Combined with atezolizumab (PD-L1 mAb)	NCT02298153
	SCCHN	II	Withdrawn	Combined with pembrolizumab	NCT03325465
	Head and neck cancer	III	Active, not recruiting	Combined with pembrolizumab vs. pembrolizumab alone or EXTREME regimen	NCT03358472
	Lung cancer	II	Active, not recruiting	Combined with pembrolizumab, platinum-based chemotherapy	NCT03322566
		II	Active, not recruiting	Combined with pembrolizumab	NCT03322540
	Renal cell carcinoma	III	Active, not recruiting	Combined with pembrolizumab vs. sunitinib and pazopanib	NCT03260894
	Muscle invasive bladder cancer	II	Not yet recruiting	Combined with pembrolizumab	NCT03832673
	Sarcoma	II	Recruiting	Combined with pembrolizumab	NCT03414229
GDC-0919 (formerly NLG-919)	Solid tumors	I	Completed	As single agent	NCT02048709
	Locally-advanced or metastatic solid tumors	I	Active, not recruiting	Combined with MPDL3280A (PD-L1 mAb)	NCT02471846
IDO1 peptide	NSCLC	I	Completed	As single agent	NCT01219348
	Melanoma	I	Recruiting –> now completed	Combined with ipilimumab or vemurafenib (BRAF inhibitor)	NCT02077114
		II	Recruiting –> now terminated	Combined with temozolomide, imiquimod, GM-CSF, and survivin peptide	NCT01543464
PF-06840003	GBM or grade III anaplastic glioma	I	Recruiting –> now completed	As single agent	NCT02764151
BMS986205	Advanced cancer, melanoma, NSCLC	I/II	Recruiting	Combined with nivolumab and ipilimumab	NCT02658890
	Hepatocellular Carcinoma	I/II	Recruiting	Combined with nivolumab	NCT03695250
	Lip, oral cavity squamous cell carcinoma, pharynx, larynx, squamous cell carcinoma	II	Recruiting	Combined with BMS-986205	NCT03854032
	Advanced cancer	I	Recruiting –> now completed	Combined with nivolumab	NCT03192943
DN1406131	Advanced Solid Tumors	I	Not yet recruiting	As single agent	NCT03641794
HTI-1090**	Advanced Solid Tumors	I	Active, not recruiting	As single agent	NCT03208959
NLG802	Solid tumor	I	Active, not recruiting	As single agent	NCT03164603
SHR9146+SHR-1210	Solid tumor, metastatic cancer, neoplasm malignant	I	Not yet recruiting	Combined with apatinib	NCT03491631
MK-7162	Solid Neoplasm	I	Recruiting	Combined with pembrolizumab	NCT03364049

NSCLC, non-small cell lung cancer; DLBCL, diffuse large B-cell lymphoma; SCCHN, squamous cell carcinoma of head/neck; UC, urothelial carcinoma.
***IDO1-TDO dual enzymatic inhibitor.*

long after surgical resection of the tumor which may reflect a treatment-related effect rather than due to the malignancy itself. A recent study by Kesarwani et al. provided additional insights into metabolomic profiling of newly diagnosed GBM ($n = 80$) and lower grade gliomas (LGG, $n = 28$) demonstrating that, GBM patients have increased intratumoral Trp and Kyn levels, but decreased KA as compared to LGG patients (110). Interestingly, Trp and Kyn accumulation was specific to classical and mesenchymal GBM subtypes, whereas KA accumulation was only evident in the proneural subtype. It's not clear why the systemic Kyn decreases while intratumoral Kyn increases in human subjects with GBM, which requires further investigation for both prognostic and therapeutic purposes.

Mechanistic studies investigating the full range of IDO-mediated immune modulation have primarily focused on the Kyn-AhR-Treg-MDSC (myeloid-derived suppressor cell) axis with data from several studies implying that alternative mechanisms of IDO behavior can occur. The inhibition of IDO enzyme activity in cultured human astroglioma cell lines decreases *de novo* synthesis of NAD^+, which is associated with decreased tumor growth (113). The triple combination of IDO pathway inhibitor with chemo-radiation achieved better overall survival as compared to the dual combination of chemo-radiation (55). Interestingly, the survival benefit was abrogated in mice deficient for complement C3, potentially suggesting that IDO activity conveys immune evasion properties to tumor cells

by suppressing complement activation (55). Finally, human GBM cell lines overexpress a translesion DNA polymerase, hpol κ, which helps to restore genome stability. Inhibition of AhR or the blockade of TDO enzyme activity decreases hpol κ expression, indicating that TDO contributes to tumor cell survival by supporting genome stability (114).

Different therapeutic interventions have profoundly different effects on both the systemic and local tumor-immune environment which include the alteration of IDO levels. In two recent glioma studies, both PCC0208009 (PCC), a potent IDO enzyme inhibitor with an IC_{50} of 4.52 nM, and RY103, an IDO-TDO dual inhibitor, have demonstrated suppression of tumor cell line- and intra-tumoral-IDO expression, respectively (112, 115). In contrary to the downregulation of IDO, a recent phase I clinical trial evaluating epidermal growth factor receptor variant III (EGFRvIII)-targeted chimeric antigen receptor (CAR) T cell therapy in GBM patients demonstrated a dramatic induction of intratumoral IDO expression after the adoptive transfer of CAR T cells (116). At almost the same time as when this clinical observation was reported, our group published a similar T cell-inducing IDO effect in humanized mice with intracranial human GBM and reconstituted with human immune cells (65). While the IDO-promoting effects of intratumoral T cell-infiltration appears to extend across human cancer types (3, 4), the association between IDO expression and overall survival depends on the type of tumor under investigation. This likely reflects the different composition of IDO expressing cells within tumors, the different function of intratumoral IDO that depends on the cell of origin, as well as for IDO expressing cells outside of the tumor microenvironment that also possess anti-cancer mechanisms depending on anatomical context. It remains notable that, to effectively target IDO with an enzyme inhibitor, the treatment must include an approach that yields robust inflammation such as irradiation. Accordingly, while studying the syngeneic GL261 in young C57BL/6 mice, we previously found that while neither radiation, anti-PD-1 mAb, nor IDO enzyme inhibitor treatment improved long-term survival as single- or dual-agent approaches, the simultaneous combination of all three modalities led to a remarkable synergistic durable survival improvement (87). Presumably, this was due to the induction of IDO by radiation, the neutralization of IDO enzyme activity by pharmacologic neutralization, and the enhancement of the anti-tumor immune response with PD-1 blockade. It's notable, however, that this triple combination was significantly less effective in older animal subjects when IDO expression is increased in the brain independent of tumor burden. As a means to explain this observation, we are currently investigating the working hypothesis that dendritic cells accumulate in the brain during advanced age (117, 118), express IDO and suppress immunotherapeutic efficacy (**Figures 3A,B**).

CONCLUDING REMARKS

It has been >20 years since the initial study by Munn et al. that uncovered the immunosuppressive role of IDO (119). Although extensive studies have been conducted to elucidate the underlying mechanisms of IDO-mediated immunosuppression, our knowledge remains incomplete. Notwithstanding, a growing list of clinical trials aimed at inhibiting the immunosuppressive effects of IDO have been undertaken as single agent and combinatorial regimens (**Table 1**)—without any remarkable success stories to-date. To this end, there are questions in the field including those that we previously addressed (3), as well as new considerations such as: (i) what are the immunosuppressive contributions of enzyme- and non-enzyme-IDO activity; (ii) will an IDO neutralizing pharmacologic that degrades protein, rather than only inhibiting enzyme activity, provide a superior therapeutic effect; (iii) given that IDO is expressed in tumor-draining lymph nodes (29), within the tumor itself, and inside the brain parenchyma during advanced age, are all anatomical sites required for mitigation to achieve optimal immunotherapeutic efficacy; (iv) among the growing compendium of possible immunological modifiers (i.e., radiation, anti-CTLA-4 mAb, anti-PD-(L)1 mAb, etc.), what is the optimal immunotherapeutic cocktail for combining with an IDO pharmacologic inhibitor? Also, the functional similarity between IDO and TDO requires further study and the use of an IDO-TDO double knockout mouse model might be helpful in validating their potency and half-life. Future investigations should also include the rigorous assessment of expression levels combined with an *in vivo* analysis of Trp and Kyn for better understanding how this immunosuppressive mediator functions among tissues, treatments, and across the lifespan. Understanding the full immunobiology of IDO and the generation of better neutralizing agents will allow for the potential future achievement of applying optimal therapeutic effects in human subjects with malignant cancer(s).

AUTHOR CONTRIBUTIONS

LZ and DW generated a draft of the manuscript. AB, EL, KL, LB, JS, BZ, JW, SM, JM, RL, EW, LD, GS, and RM provided feedback on the draft and/or data for inclusion. All authors contributed to the article and approved the submitted version.

FUNDING

This work was supported by NIH grants R01 NS097851-01 (DW), P50 CA221747 Project 2 (DW and RL), T32 CA070085 (EL), BrainUp grant 2136 (DW and RL), the Gail Boyter Magness (GBM) Foundation (DW), and the Grace Giving Foundation (DW).

REFERENCES

1. McGaha TL, Huang L, Lemos H, Metz R, Mautino M, Prendergast GC, et al. Amino acid catabolism: a pivotal regulator of innate and adaptive immunity. *Immunol Rev.* (2012) 249:135–57. doi: 10.1111/j.1600-065X.2012.01149.x

2. Platten M, Nollen EAA, Röhrig UF, Fallarino F, Opitz CA. Tryptophan metabolism as a common therapeutic target in cancer, neurodegeneration and beyond. *Nat Rev Drug Discov.* (2019) 18:379–401. doi: 10.1038/s41573-019-0016-5

3. Zhai L, Ladomersky E, Lenzen A, Nguyen B, Patel R, Lauing KL, et al. IDO1 in cancer: a Gemini of immune checkpoints. *Cell Mol Immunol.* (2018) 15:447–57. doi: 10.1038/cmi.2017.143
4. Zhai L, Spranger S, Binder DC, Gritsina G, Lauing KL, Giles FJ, et al. Molecular pathways: targeting IDO1 and other tryptophan dioxygenases for cancer immunotherapy. *Clin Cancer Res.* (2015) 21:5427–33. doi: 10.1158/1078-0432.CCR-15-0420
5. Long GV, Dummer R, Hamid O, Gajewski TF, Caglevic C, Dalle S, et al. Epacadostat plus pembrolizumab versus placebo plus pembrolizumab in patients with unresectable or metastatic melanoma (ECHO-301/KEYNOTE-252): a phase 3, randomised, double-blind study. *Lancet Oncol.* (2019) 20:1083–97. doi: 10.1016/S1470-2045(19)30274-8
6. Muller AJ, Manfredi MG, Zakharia Y, Prendergast GC. Inhibiting IDO pathways to treat cancer: lessons from the ECHO-301 trial and beyond. *Semin Immunopathol.* (2019) 41:41–8. doi: 10.1007/s00281-018-0702-0
7. Badawy AA-B, Guillemin G. The plasma [kynurenine]/[tryptophan] ratio and indoleamine 2,3-dioxygenase: time for appraisal. *Int J Tryptophan Res.* (2019) 12:1178646919868978. doi: 10.1177/1178646919868978
8. Grohmann U, Fallarino F, Puccetti Tolerance P. DCs tryptophan: much ado about IDO. *Trends Immunol.* (2003) 24:242–8. doi: 10.1016/S1471-4906(03)00072-3
9. Shimizu T, Nomiyama S, Hirata F, Hayaishi O. Indoleamine 2,3-dioxygenase. *Purification and some properties. J Biol Chem.* (1978) 253:4700–6.
10. Batabyal D, Yeh SR. Human tryptophan dioxygenase: a comparison to indoleamine 2,3-dioxygenase. *J Am Chem Soc.* (2007) 129:15690–701. doi: 10.1021/ja076186k
11. Basran J, Rafice SA, Chauhan N, Efimov I, Cheesman MR, Ghamsari L, et al. A kinetic, spectroscopic, and redox study of human tryptophan 2,3-dioxygenase. *Biochemistry.* (2008) 47:4752–60. doi: 10.1021/bi702393b
12. Pantouris G, Serys M, Yuasa HJ, Ball HJ, Mowat CG. Human indoleamine 2,3-dioxygenase-2 has substrate specificity and inhibition characteristics distinct from those of indoleamine 2,3-dioxygenase-1. *Amino Acids.* (2014) 46:2155–63. doi: 10.1007/s00726-014-1766-3
13. Liu X, Shin N, Koblish HK, Yang G, Wang Q, Wang K, et al. Selective inhibition of IDO1 effectively regulates mediators of antitumor immunity. *Blood.* (2010) 115:3520–30. doi: 10.1182/blood-2009-09-246124
14. Yuasa HJ, Ball HJ, Austin CJ, Hunt NH. 1-L-methyltryptophan is a more effective inhibitor of vertebrate IDO2 enzymes than 1-D-methyltryptophan. *Comp Biochem Physiol B Biochem Mol Biol.* (2010) 157:10–5. doi: 10.1016/j.cbpb.2010.04.006
15. Metz R, Smith C, DuHadaway JB, Chandler P, Baban B, Merlo LMF, et al. IDO2 is critical for IDO1-mediated T-cell regulation and exerts a non-redundant function in inflammation. *Int Immunol.* (2014) 26:357–67. doi: 10.1093/intimm/dxt073
16. Taylor MW, Feng GS. Relationship between interferon-gamma, indoleamine 2,3-dioxygenase, tryptophan catabolism. *FASEB J.* (1991) 5:2516–22. doi: 10.1096/fasebj.5.11.1907934
17. Mellor AL, Baban B, Chandler PR, Manlapat A, Kahler DJ, Munn DH. Cutting edge: CpG oligonucleotides induce splenic $CD19^+$ dendritic cells to acquire potent indoleamine 2,3-dioxygenase-dependent T cell regulatory functions via IFN Type 1 signaling. *J Immunol.* (2005) 175:5601–5. doi: 10.4049/jimmunol.175.9.5601
18. Fallarino F, Volpi C, Zelante T, Vacca C, Calvitti M, Fioretti MC, et al. IDO mediates TLR9-driven protection from experimental autoimmune diabetes. *J Immunol.* (2009) 183:6303–12. doi: 10.4049/jimmunol.0901577
19. Fujigaki H, Saito K, Fujigaki S, Takemura M, Sudo K, Ishiguro H, et al. The signal transducer and activator of transcription 1α and interferon regulatory factor 1 are not essential for the induction of indoleamine 2,3-dioxygenase by lipopolysaccharide: involvement of p38 mitogen-activated protein kinase and nuclear factor-κB pathways, and synergistic effect of several proinflammatory cytokines. *J Biochem.* (2006) 139:655–62. doi: 10.1093/jb/mvj072
20. Balachandran VP, Cavnar MJ, Zeng S, Bamboat ZM, Ocuin LM, Obaid H, et al. Imatinib potentiates antitumor T cell responses in gastrointestinal stromal tumor through the inhibition of Ido. *Nat Med.* (2011) 17:1094–100. doi: 10.1038/nm.2438
21. Grohmann U, Orabona C, Fallarino F, Vacca C, Calcinaro F, Falorni A, et al. CTLA-4-Ig regulates tryptophan catabolism *in vivo*. *Nat Immunol.* (2002) 3:1097–101. doi: 10.1038/ni846
22. Holtzhausen, Zhao F, Evans KS, Tsutsui M, Orabona C, Tyler DS, et al. Melanoma-derived Wnt5a promotes local dendritic-cell expression of IDO and immunotolerance: opportunities for pharmacologic enhancement of immunotherapy. *Cancer Immunol Res.* (2015) 3:1082–95. doi: 10.1158/2326-6066.CIR-14-0167
23. Theate A, van Baren N, Pilotte L, Moulin P, Larrieu P, Sempoux C, et al. Extensive profiling of the expression of the indoleamine 2,3-dioxygenase 1 protein in normal and tumoral human tissues. *Cancer Immunol Res.* (2015) 3:161–72. doi: 10.1158/2326-6066.CIR-14-0137
24. Ladomersky E, Scholtens DM, Kocherginsky M, Hibler EA, Bartom ET, Otto-Meyer S, et al. The coincidence between increasing age, immunosuppression, and the incidence of patients with glioblastoma. *Front Pharmacol.* (2019) 10:200. doi: 10.3389/fphar.2019.00200
25. Litzenburger UM, Opitz CA, Sahm F, Rauschenbach KJ, Trump S, Winter M, et al. Constitutive IDO expression in human cancer is sustained by an autocrine signaling loop involving IL-6, STAT3 and the AHR. *Oncotarget.* (2014) 5:1038–51. doi: 10.18632/oncotarget.1637
26. Li Q, Harden JL, Anderson CD, Egilmez NK. Tolerogenic phenotype of IFN-gamma-induced IDO^+ dendritic cells is maintained via an autocrine IDO-kynurenine/AhR-IDO loop. *J Immunol.* (2016) 197:962–70. doi: 10.4049/jimmunol.1502615
27. Hennequart M, Pilotte L, Cane S, Hoffmann D, Stroobant V, Plaen E, et al. Constitutive IDO1 expression in human tumors is driven by cyclooxygenase-2 and mediates intrinsic immune resistance. *Cancer Immunol Res.* (2017) 5:695–709. doi: 10.1158/2326-6066.CIR-16-0400
28. Miyazaki T, Moritake K, Yamada K, Hara N, Osago H, Shibata T, et al. Indoleamine 2,3-dioxygenase as a new target for malignant glioma therapy. Laboratory investigation. *J Neurosurg.* (2009) 111:230–7. doi: 10.3171/2008.10.JNS081141
29. Zhai L, Ladomersky E, Dostal CR, Lauing KL, Swoap K, Billingham LK, et al. Non-tumor cell IDO1 predominantly contributes to enzyme activity and response to CTLA-4/PD-L1 inhibition in mouse glioblastoma. *Brain Behav Immun.* (2017) 62:24–9. doi: 10.1016/j.bbi.2017.01.022
30. Uhlen M, Fagerberg L, Hallstrom BM, Lindskog C, Oksvold P, Mardinoglu A, et al. Proteomics. Tissue-based map of the human proteome. *Science.* (2015) 347:1260419. doi: 10.1126/science.1260419
31. Comings DE, Muhleman D, Dietz G, Sherman M, Forest GL. Sequence of human tryptophan 2,3-dioxygenase (TDO2): presence of a glucocorticoid response-like element composed of a GTT repeat and an intronic CCCCT repeat. *Genomics.* (1995) 29:390–6. doi: 10.1006/geno.1995.9990
32. Li DD, Gao YJ, Tian XC, Yang ZQ, Cao H, Zhang QL, et al. Differential expression and regulation of Tdo2 during mouse decidualization. *J Endocrinol.* (2014) 220:73–83. doi: 10.1530/JOE-13-0429
33. Opitz CA, Litzenburger UM, Sahm F, Ott M, Tritschler I, Trump S, et al. An endogenous tumour-promoting ligand of the human aryl hydrocarbon receptor. *Nature.* (2011) 478:197–203. doi: 10.1038/nature10491
34. Pilotte L, Larrieu P, Stroobant V, Colau D, Dolušić E, Frédérick R, et al. Reversal of tumoral immune resistance by inhibition of tryptophan 2,3-dioxygenase. *Proc Natl Acad Sci USA.* (2012) 109:2497–502. doi: 10.1073/pnas.1113873109
35. Novikov O, Wang Z, Stanford EA, Parks AJ, Ramirez-Cardenas A, Landesman E, et al. An aryl hydrocarbon receptor-mediated amplification loop that enforces cell migration in ER-/PR-/Her2-human breast cancer cells. *Mol Pharmacol.* (2016) 90:674–88. doi: 10.1124/mol.116.105361
36. van Baren N, Van den Eynde BJ. Tryptophan-degrading enzymes in tumoral immune resistance. *Front Immunol.* (2015) 6:34. doi: 10.3389/fimmu.2015.00034
37. Prendergast GC, Metz R, Muller AJ, Merlo LM, Mandik-Nayak L. IDO2 in immunomodulation and autoimmune disease. *Front Immunol.* (2014) 5:585. doi: 10.3389/fimmu.2014.00585
38. Munn DH, Sharma MD, Baban B, Harding HP, Zhang Y, Ron D, et al. GCN2 kinase in T cells mediates proliferative arrest and anergy induction in response to indoleamine 2,3-dioxygenase. *Immunity.* (2005) 22:633–42. doi: 10.1016/j.immuni.2005.03.013

39. Metz R, Rust S, Duhadaway JB, Mautino MR, Munn DH, Vahanian NN, et al. IDO inhibits a tryptophan sufficiency signal that stimulates mTOR: a novel IDO effector pathway targeted by D-1-methyl-tryptophan. *Oncoimmunology.* (2012) 1:1460–8. doi: 10.4161/onci.21716
40. Mezrich JD, Fechner JH, Zhang X, Johnson BP, Burlingham WJ, Bradfield CA. An interaction between kynurenine and the aryl hydrocarbon receptor can generate regulatory T cells. *J Immunol.* (2010) 185:3190–8. doi: 10.4049/jimmunol.0903670
41. Stockinger B, Di Meglio P, Gialitakis M, Duarte JH. The aryl hydrocarbon receptor: multitasking in the immune system. *Annu Rev Immunol.* (2014) 32:403–32. doi: 10.1146/annurev-immunol-032713-120245
42. Quintana FJ, Basso AS, Iglesias AH, Korn T, Farez MF, Bettelli E, et al. Control of Treg and TH17 cell differentiation by the aryl hydrocarbon receptor. *Nature.* (2008) 453:65–71. doi: 10.1038/nature06880
43. Marshall NB, Kerkvliet NI. Dioxin and immune regulation: emerging role of aryl hydrocarbon receptor in the generation of regulatory T cells. *Ann N Y Acad Sci.* (2010) 1183:25–37. doi: 10.1111/j.1749-6632.2009.05125.x
44. DiNatale BC, Murray IA, Schroeder JC, Flaveny CA, Lahoti TS, Laurenzana EM, et al. Kynurenic acid is a potent endogenous aryl hydrocarbon receptor ligand that synergistically induces interleukin-6 in the presence of inflammatory signaling. *Toxicol Sci.* (2010) 115:89–97. doi: 10.1093/toxsci/kfq024
45. Lowe MM, Mold JE, Kanwar B, Huang Y, Louie A, Pollastri MP, et al. Identification of cinnabarinic acid as a novel endogenous aryl hydrocarbon receptor ligand that drives IL-22 production. *PLoS ONE.* (2014) 9:e87877. doi: 10.1371/journal.pone.0087877
46. Terness P, Bauer TM, Röse L, Dufter C, Watzlik A, Simon H, et al. Inhibition of allogeneic T cell proliferation by indoleamine 2,3-dioxygenase–expressing dendritic cells: mediation of suppression by tryptophan metabolites. *J Exp Med.* (2002) 196:447–57. doi: 10.1084/jem.20020052
47. Fallarino F, Grohmann U, Vacca C, Bianchi R, Orabona C, Spreca A, et al. T cell apoptosis by tryptophan catabolism. *Cell Death Differ.* (2002) 9:1069–77. doi: 10.1038/sj.cdd.4401073
48. Frumento G, Rotondo R, Tonetti M, Damonte G, Benatti U, Ferrara GB. Tryptophan-derived catabolites are responsible for inhibition of T and natural killer cell proliferation induced by indoleamine 2,3-dioxygenase. *J Exp Med.* (2002) 196:459–68. doi: 10.1084/jem.20020121
49. Sonner JK, Deumelandt K, Ott M, Thome CM, Rauschenbach KJ, Schulz S, et al. The stress kinase GCN2 does not mediate suppression of antitumor T cell responses by tryptophan catabolism in experimental melanomas. *Oncoimmunology.* (2016) 5:e1240858. doi: 10.1080/2162402X.2016.1240858
50. Segawa H, Fukasawa Y, Miyamoto K, Takeda E, Endou H, Kanai Y. Identification and functional characterization of a Na^+-independent neutral amino acid transporter with broad substrate selectivity. *J Biol Chem.* (1999) 274:19745–51. doi: 10.1074/jbc.274.28.19745
51. Seymour RL, Ganapathy V, Mellor AL, Munn DH. A high-affinity, tryptophan-selective amino acid transport system in human macrophages. *J Leuk Biol.* (2006) 80:1320–7. doi: 10.1189/jlb.1205727
52. Silk JD, Lakhal S, Laynes R, Vallius L, Karydis I, Marcea C, et al. IDO induces expression of a novel tryptophan transporter in mouse and human tumor cells. *J Immunol.* (2011) 187:1617–25. doi: 10.4049/jimmunol.1000815
53. Schrocksnadel K, Wirleitner B, Winkler C, Fuchs D. Monitoring tryptophan metabolism in chronic immune activation. *Clin Chim Acta.* (2006) 364:82–90. doi: 10.1016/j.cca.2005.06.013
54. Huang, Fuchs D, Widner B, Glover C, Henderson DC, Allen-Mersh TG. Serum tryptophan decrease correlates with immune activation and impaired quality of life in colorectal cancer. *Br J Cancer.* (2002) 86:1691–6. doi: 10.1038/sj.bjc.6600336
55. Li M, Bolduc AR, Hoda MN, Gamble DN, Dolisca SB, Bolduc AK, et al. The indoleamine 2,3-dioxygenase pathway controls complement-dependent enhancement of chemo-radiation therapy against murine glioblastoma. *J Immunother Cancer.* (2014) 2:21. doi: 10.1186/2051-1426-2-21
56. Zhai L, Dey M, Lauing KL, Gritsina G, Kaur R, Lukas RV, et al. The kynurenine to tryptophan ratio as a prognostic tool for glioblastoma patients enrolling in immunotherapy. *J Clin Neurosci.* (2015) 22:5. doi: 10.1016/j.jocn.2015.06.018
57. Adams S, Teo C, McDonald KL, Zinger A, Bustamante S, Lim CK, et al. Involvement of the kynurenine pathway in human glioma pathophysiology. *PLoS ONE.* (2014) 9:e112945. doi: 10.1371/journal.pone.0112945
58. Takenaka MC, Gabriely G, Rothhammer V, Mascanfroni ID, Wheeler MA, Chao CC, et al. Control of tumor-associated macrophages and T cells in glioblastoma via AHR and CD39. *Nat Neurosci.* (2019) 22:729–40. doi: 10.1038/s41593-019-0370-y
59. Nguyen NT, Kimura A, Nakahama T, Chinen I, Masuda K, Nohara K, et al. Aryl hydrocarbon receptor negatively regulates dendritic cell immunogenicity via a kynurenine-dependent mechanism. *Proc Natl Acad Sci USA.* (2010) 107:19961–6. doi: 10.1073/pnas.1014465107
60. Wainwright DA, Sengupta S, Han Y, Lesniak MS. Thymus-derived rather than tumor-induced regulatory T cells predominate in brain tumors. *Neuro Oncol.* (2011) 13:1308–23. doi: 10.1093/neuonc/nor134
61. Malchow S, Leventhal DS, Nishi S, Fischer BI, Shen L, Paner GP, et al. Aire-dependent thymic development of tumor-associated regulatory T cells. *Science.* (2013) 339:1219–24. doi: 10.1126/science.1233913
62. Ye J, Qiu J, Bostick JW, Ueda A, Schjerven H, Li S, et al. The aryl hydrocarbon receptor preferentially marks and promotes gut regulatory T cells. *Cell Rep.* (2017) 21:2277–90. doi: 10.1016/j.celrep.2017.10.114
63. Sharma MD, Baban B, Chandler P, Hou DY, Singh N, Yagita H, et al. Plasmacytoid dendritic cells from mouse tumor-draining lymph nodes directly activate mature Tregs via indoleamine 2,3-dioxygenase. *J Clin Invest.* (2007) 117:2570–82. doi: 10.1172/JCI31911
64. Sharma MD, Shinde R, McGaha TL, Huang L, Holmgaard RB, Wolchok JD, et al. The PTEN pathway in Tregs is a critical driver of the suppressive tumor microenvironment. *Sci Adv.* (2015) 1:e1500845. doi: 10.1126/sciadv.1500845
65. Zhai L, Ladomersky E, Lauing KL, Wu M, Genet M, Gritsina G, et al. Infiltrating T cells increase IDO1 expression in glioblastoma and contribute to decreased patient survival. *Clin Cancer Res.* (2017) 23:6650–60. doi: 10.1158/1078-0432.CCR-17-0120
66. Uyttenhove C, Pilotte L, Theate I, Stroobant V, Colau D, Parmentier N, et al. Evidence for a tumoral immune resistance mechanism based on tryptophan degradation by indoleamine 2,3-dioxygenase. *Nat Med.* (2003) 9:1269–74. doi: 10.1038/nm934
67. Riesenberg R, Weiler C, Spring O, Eder M, Buchner A, Popp T, et al. Expression of indoleamine 2,3-dioxygenase in tumor endothelial cells correlates with long-term survival of patients with renal cell carcinoma. *Clin Cancer Res.* (2007) 13:6993–7002. doi: 10.1158/1078-0432.CCR-07-0942
68. Ishio T, Goto S, Tahara K, Tone S, Kawano K, Kitano S. Immunoactivative role of indoleamine 2,3-dioxygenase in human hepatocellular carcinoma. *J Gastroenterol Hepatol.* (2004) 19:319–26. doi: 10.1111/j.1440-1746.2003.03259.x
69. Pan K, Wang H, Chen MS, Zhang HK, Weng DS, Zhou J, et al. Expression and prognosis role of indoleamine 2,3-dioxygenase in hepatocellular carcinoma. *J Cancer Res Clin Oncol.* (2008) 134:1247–53. doi: 10.1007/s00432-008-0395-1
70. Piras F, Colombari R, Minerba L, Murtas D, Floris C, Maxia C, et al. The predictive value of CD8, CD4, CD68, and human leukocyte antigen-D-related cells in the prognosis of cutaneous malignant melanoma with vertical growth phase. *Cancer.* (2005) 104:1246–54. doi: 10.1002/cncr.21283
71. Tang D, Yue L, Yao R, Zhou L, Yang Y, Lu L, et al. P53 prevent tumor invasion and metastasis by down-regulating IDO in lung cancer. *Oncotarget.* (2017) 8:54548–57. doi: 10.18632/oncotarget.17408
72. Levina V, Su Y, Gorelik E. Immunological and nonimmunological effects of indoleamine 2,3-dioxygenase on breast tumor growth and spontaneous metastasis formation. *Clin Dev Immunol.* (2012) 2012:173029. doi: 10.1155/2012/173029
73. Smith C, Chang MY, Parker KH, Beury DW, DuHadaway JB, Flick HE, et al. IDO is a nodal pathogenic driver of lung cancer and metastasis development. *Cancer Discov.* (2012) 2:722–35. doi: 10.1158/2159-8290.CD-12-0014
74. Brandacher G, Perathoner A, Ladurner R, Schneeberger S, Obrist P, Winkler C, et al. Prognostic value of indoleamine 2,3-dioxygenase expression in colorectal cancer: effect on tumor-infiltrating T cells. *Clin Cancer Res.* (2006) 12:1144–51. doi: 10.1158/1078-0432.CCR-05-1966
75. Ino K, Yamamoto E, Shibata K, Kajiyama H, Yoshida N, Terauchi M, et al. Inverse correlation between tumoral indoleamine 2,3-dioxygenase expression and tumor-infiltrating lymphocytes in endometrial cancer: its

association with disease progression and survival. *Clin Cancer Res.* (2008) 14:2310–7. doi: 10.1158/1078-0432.CCR-07-4144
76. Vareki SM, Rytelewski M, Figueredo R, Chen D, Ferguson PJ, Vincent M, et al. Indoleamine 2,3-dioxygenase mediates immune-independent human tumor cell resistance to olaparib, gamma radiation, and cisplatin. *Oncotarget.* (2014) 5:2778–91. doi: 10.18632/oncotarget.1916
77. Tummala KS, Gomes AL, Yilmaz M, Grana O, Bakiri L, Ruppen I, et al. Inhibition of de novo NAD(+) synthesis by oncogenic URI causes liver tumorigenesis through DNA damage. *Cancer Cell.* (2014) 26:826–39. doi: 10.1016/j.ccell.2014.10.002
78. Wang Y, Liu H, McKenzie G, Witting PK, Stasch JP, Hahn M, et al. Kynurenine is an endothelium-derived relaxing factor produced during inflammation. *Nat Med.* (2010) 16:279–85. doi: 10.1038/nm.2092
79. Sakakibara K, Feng GG, Li J, Akahori T, Yasuda Y, Nakamura E, et al. Kynurenine causes vasodilation and hypotension induced by activation of KCNQ-encoded voltage-dependent K(+) channels. *J Pharmacol Sci.* (2015) 129:31–7. doi: 10.1016/j.jphs.2015.07.042
80. Fazio F, Carrizzo A, Lionetto L, Damato A, Capocci L, Ambrosio M, et al. Vasorelaxing action of the kynurenine metabolite, xanthurenic acid: the missing link in endotoxin-induced hypotension? *Front Pharmacol.* (2017) 8:214. doi: 10.3389/fphar.2017.00214
81. Stanley CP, Maghzal GJ, Ayer A, Talib J, Giltrap AM, Shengule S, et al. Singlet molecular oxygen regulates vascular tone and blood pressure in inflammation. *Nature.* (2019) 566:548–52. doi: 10.1038/s41586-019-0947-3
82. Changsirivathanathamrong D, Wang Y, Rajbhandari D, Maghzal GJ, Mak WM, Woolfe C, et al. Tryptophan metabolism to kynurenine is a potential novel contributor to hypotension in human sepsis. *Crit Care Med.* (2011) 39:2678–83. doi: 10.1097/CCM.0b013e31822827f2
83. Mondal, Smith C, DuHadaway JB, Sutanto-Ward E, Prendergast GC, Bravo-Nuevo A, et al. IDO1 is an integral mediator of inflammatory neovascularization. *EBioMedicine.* (2016) 14:74–82. doi: 10.1016/j.ebiom.2016.11.013
84. Prendergast GC, Mondal A, Dey S, Laury-Kleintop LD, Muller AJ. Inflammatory Reprogramming with IDO1 inhibitors: turning immunologically unresponsive 'cold' tumors 'hot'. *Trends Cancer.* (2018) 4:38–58. doi: 10.1016/j.trecan.2017.11.005
85. Pallotta MT, Orabona C, Volpi C, Vacca C, Belladonna ML, Bianchi R, et al. Indoleamine 2,3-dioxygenase is a signaling protein in long-term tolerance by dendritic cells. *Nat Immunol.* (2011) 12:870–8. doi: 10.1038/ni.2077
86. Wainwright DA, Balyasnikova IV, Chang AL, Ahmed AU, Moon KS, Auffinger B, et al. IDO expression in brain tumors increases the recruitment of regulatory T cells and negatively impacts survival. *Clin Cancer Res.* (2012) 18:6110–21. doi: 10.1158/1078-0432.CCR-12-2130
87. Ladomersky E, Zhai L, Lenzen A, Lauing KL, Qian J, Scholtens DM, et al. IDO1 Inhibition synergizes with radiation and PD-1 blockade to durably increase survival against advanced glioblastoma. *Clin Cancer Res.* (2018) 24:2559–73. doi: 10.1158/1078-0432.CCR-17-3573
88. Frick B, Schroecksnadel K, Neurauter G, Leblhuber F, Fuchs D. Increasing production of homocysteine and neopterin and degradation of tryptophan with older age. *Clin Biochem.* (2004) 37:684–7. doi: 10.1016/j.clinbiochem.2004.02.007
89. Pertovaara M, Raitala A, Lehtimaki T, Karhunen PJ, Oja SS, Jylha M, et al. Indoleamine 2,3-dioxygenase activity in nonagenarians is markedly increased and predicts mortality. *Mech Ageing Dev.* (2006) 127:497–9. doi: 10.1016/j.mad.2006.01.020
90. Marcos-Perez D, Sanchez-Flores M, Maseda A, Lorenzo-Lopez L, Millan-Calenti JC, Strasser B, et al. Frailty status in older adults is related to alterations in indoleamine 2,3-dioxygenase 1 and guanosine triphosphate cyclohydrolase I enzymatic pathways. *J Am Med Direc Assoc.* (2017) 18:1049–57. doi: 10.1016/j.jamda.2017.06.021
91. Sutphin GL, Backer G, Sheehan S, Bean S, Corban C, Liu T, et al. *Caenorhabditis elegans* orthologs of human genes differentially expressed with age are enriched for determinants of longevity. *Aging Cell.* (2017) 16:672–82. doi: 10.1111/acel.12595
92. Apalset EM, Gjesdal CG, Ueland PM, Midttun O, Ulvik A, Eide GE, et al. Interferon (IFN)-gamma-mediated inflammation and the kynurenine pathway in relation to bone mineral density: the Hordaland Health Study. *Clin Exp Immunol.* (2014) 176:452–60. doi: 10.1111/cei.12288
93. Reyes Ocampo J, Lugo Huitron R, Gonzalez-Esquivel D, Ugalde-Muniz P, Jimenez-Anguiano A, Pineda B, et al. Kynurenines with neuroactive and redox properties: relevance to aging and brain diseases. *Oxidat Med Cell Longev.* (2014) 2014:646909. doi: 10.1155/2014/646909
94. Ladomersky E, Zhai L, Gritsina G, Genet M, Lauing KL, Wu M, et al. Advanced age negatively impacts survival in an experimental brain tumor model. *Neurosci Lett.* (2016) 630:203–8. doi: 10.1016/j.neulet.2016.08.002
95. Refaey ME, McGee-Lawrence ME, Fulzele S, Kennedy EJ, Bollag WB, Elsalanty M, et al. Kynurenine, a tryptophan metabolite that accumulates with age, induces bone loss. *J Bone Miner Res.* (2017) 32:2182–93. doi: 10.1002/jbmr.3224
96. Minhas PS, Liu L, Moon PK, Joshi AU, Dove C, Mhatre S, et al. Macrophage *de novo* NAD(+) synthesis specifies immune function in aging and inflammation. *Nat Immunol.* (2019) 20:50–63. doi: 10.1038/s41590-018-0255-3
97. Eckers, Jakob S, Heiss C, Haarmann-Stemmann T, Goy C, Brinkmann V, et al. The aryl hydrocarbon receptor promotes aging phenotypes across species. *Sci Rep.* (2016) 6:19618. doi: 10.1038/srep19618
98. Sharpless N. *The Challenging Landscape of Cancer and Aging: Charting a Way Forward*. National Cancer Institute (2018).
99. Ostrom QT, Gittleman H, Liao P, Vecchione-Koval T, Wolinsky Y, Kruchko C, et al. CBTRUS statistical report: primary brain and other central nervous system tumors diagnosed in the United States in 2010–2014. *Neuro Oncol.* (2017) 19:v1–88. doi: 10.1093/neuonc/nox158
100. Mellor AL, Baban B, Chandler P, Marshall B, Jhaver K, Hansen A, et al. Cutting Edge: induced indoleamine 2,3 dioxygenase expression in dendritic cell subsets suppresses T cell clonal expansion. *J Immunol.* (2003) 171:1652–5. doi: 10.4049/jimmunol.171.4.1652
101. Baban B, Chandler P, McCool D, Marshall B, Munn DH, Mellor AL. Indoleamine 2,3-dioxygenase expression is restricted to fetal trophoblast giant cells during murine gestation and is maternal genome specific. *J Reprod Immunol.* (2004) 61:67–77. doi: 10.1016/j.jri.2003.11.003
102. Moreno ACR, Porchia B, Pagni RL, Souza PDC, Pegoraro R, Rodrigues KB, et al. The combined use of melatonin and an indoleamine 2,3-dioxygenase-1 inhibitor enhances vaccine-induced protective cellular immunity to HPV16-associated tumors. *Front Immunol.* (2018) 9:1914. doi: 10.3389/fimmu.2018.01914
103. Schafer CC, Wang Y, Hough KP, Sawant A, Grant SC, Thannickal VJ, et al. Indoleamine 2,3-dioxygenase regulates anti-tumor immunity in lung cancer by metabolic reprogramming of immune cells in the tumor microenvironment. *Oncotarget.* (2016) 7:75407–24. doi: 10.18632/oncotarget.12249
104. Takamatsu M, Hirata A, Ohtaki H, Hoshi M, Ando T, Ito H, et al. Inhibition of indoleamine 2,3-dioxygenase 1 expression alters immune response in colon tumor microenvironment in mice. *Cancer Sci.* (2015) 106:1008–15. doi: 10.1111/cas.12705
105. Bishnupuri KS, Alvarado DM, Khouri AN, Shabsovich M, Chen B, Dieckgraefe BK, et al. IDO1 and kynurenine pathway metabolites activate PI3K-Akt signaling in the neoplastic colon epithelium to promote cancer cell proliferation and inhibit apoptosis. *Cancer Res.* (2019) 79:1138–50. doi: 10.1158/0008-5472.CAN-18-0668
106. Reardon DA, Freeman G, Wu C, Chiocca EA, Wucherpfennig KW, Wen PY, et al. Immunotherapy advances for glioblastoma. *Neuro Oncol.* (2014) 16:1441–58. doi: 10.1093/neuonc/nou212
107. Avril T, Saikali S, Vauleon E, Jary A, Hamlat A, De Tayrac M, et al. Distinct effects of human glioblastoma immunoregulatory molecules programmed cell death ligand-1 (PDL-1) and indoleamine 2,3-dioxygenase (IDO) on tumour-specific T cell functions. *J Neuroimmunol.* (2010) 225:22–33. doi: 10.1016/j.jneuroim.2010.04.003
108. Mitsuka K, Kawataki T, Satoh E, Asahara T, Horikoshi T, Kinouchi H. Expression of indoleamine 2,3-dioxygenase and correlation with pathological malignancy in gliomas. *Neurosurgery.* (2013) 72:1031–9. doi: 10.1227/NEU.0b013e31828cf945
109. Guastella AR, Michelhaugh SK, Klinger NV, Fadel HA, Kiousis S, Ali-Fehmi R, et al. Investigation of the aryl hydrocarbon receptor and the intrinsic tumoral component of the kynurenine pathway of tryptophan metabolism in primary brain tumors. *J Neurooncol.* (2018) 139:239–9. doi: 10.1007/s11060-018-2869-6

110. Kesarwani P, Prabhu A, Kant S, Kumar P, Graham SF, Buelow KL, et al. Tryptophan metabolism contributes to radiation-induced immune checkpoint reactivation in glioblastoma. *Clin Cancer Res.* (2018) 24:3632–43. doi: 10.1158/1078-0432.CCR-18-0041
111. Ott M, Litzenburger UM, Rauschenbach KJ, Bunse L, Ochs K, Sahm F, et al. Suppression of TDO-mediated tryptophan catabolism in glioblastoma cells by a steroid-responsive FKBP52-dependent pathway. *Glia.* (2015) 63:78–90. doi: 10.1002/glia.22734
112. Du L, Xing Z, Tao B, Li T, Yang D, Li W, et al. Both IDO1 and TDO contribute to the malignancy of gliomas via the Kyn-AhR-AQP4 signaling pathway. *Signal Transduc Target Ther.* (2020) 5:10. doi: 10.1038/s41392-019-0103-4
113. Grant R, Kapoor V. Inhibition of indoleamine 2,3-dioxygenase activity in IFN-gamma stimulated astroglioma cells decreases intracellular NAD levels. *Biochem Pharmacol.* (2003) 66:1033–6. doi: 10.1016/S0006-2952(03)00464-7
114. Bostian AC, Maddukuri L, Reed MR, Savenka T, Hartman JH, Davis L, et al. Kynurenine signaling increases DNA polymerase kappa expression and promotes genomic instability in glioblastoma cells. *Chem Res Toxicol.* (2016) 29:101–8. doi: 10.1021/acs.chemrestox.5b00452
115. Sun S, Du G, Xue J, Ma J, Ge M, Wang H, et al. PCC0208009 enhances the anti-tumor effects of temozolomide through direct inhibition and transcriptional regulation of indoleamine 2,3-dioxygenase in glioma models. *Int J Immunopathol Pharmacol.* (2018) 32:2058738418787991. doi: 10.1177/2058738418787991
116. O'Rourke DM, Nasrallah MP, Desai A, Melenhorst JJ, Mansfield K, Morrissette JJD, et al. A single dose of peripherally infused EGFRvIII-directed CAR T cells mediates antigen loss and induces adaptive resistance in patients with recurrent glioblastoma. *Sci Transl Med.* (2017) 9:eaaa0984. doi: 10.1126/scitranslmed.aaa0984
117. Bulloch K, Miller MM, Gal-Toth J, Milner TA, Gottfried-Blackmore A, Waters EM, et al. CD11c/EYFP transgene illuminates a discrete network of dendritic cells within the embryonic, neonatal, adult, and injured mouse brain. *J Comp Neurol.* (2008) 508:687–710. doi: 10.1002/cne.21668
118. Kaunzner UW, Miller MM, Gottfried-Blackmore A, Gal-Toth J, Felger JC, McEwen BS, et al. Accumulation of resident and peripheral dendritic cells in the aging CNS. *Neurobiol Aging.* (2012) 33:681–93 e1. doi: 10.1016/j.neurobiolaging.2010.06.007
119. Munn DH, Zhou M, Attwood JT, Bondarev I, Conway SJ, Marshall B, et al. Prevention of allogeneic fetal rejection by tryptophan catabolism. *Science.* (1998) 281:1191–3. doi: 10.1126/science.281.5380.1191

Conflict of Interest: The authors declare that the research was conducted in the absence of any commercial or financial relationships that could be construed as a potential conflict of interest.

frontiers in Immunology

ORIGINAL RESEARCH
published: 07 July 2020
doi: 10.3389/fimmu.2020.01243

Tryptophan Catabolism as Immune Mechanism of Primary Resistance to Anti-PD-1

Andrea Botticelli[1], Silvia Mezi[2], Giulia Pomati[2], Bruna Cerbelli[2], Edoardo Cerbelli[2], Michela Roberto[1], Raffaele Giusti[3], Alessio Cortellini[4], Luana Lionetto[5], Simone Scagnoli[6], Ilaria Grazia Zizzari[7], Marianna Nuti[7], Maurizio Simmaco[8] and Paolo Marchetti[1]*

[1] Department of Clinical and Molecular Medicine, Sapienza University of Rome, Rome, Italy, [2] Department of Radiological, Oncological and Pathological Sciences, Faculty of Medicine and Dentistry, Sapienza University of Rome, Rome, Italy, [3] Medical Oncology Unit, Sant'Andrea Hospital of Rome, Rome, Italy, [4] Medical Oncology Unit, San Salvatore Hospital, L'Aquila, Italy, [5] Experimental Immunology Laboratory, Biochemistry Laboratory, IDI-IRCCS FLMM, Rome, Italy, [6] Department of Medical and Surgical Sciences and Translational Medicine, Sapienza University of Rome, Rome, Italy, [7] Department of Experimental Medicine, Faculty of Medicine and Dentistry, Sapienza University of Rome, Rome, Italy, [8] Advanced Molecular Diagnostics Unit, Sant'Andrea Hospital, Sapienza University of Rome, Rome, Italy

OPEN ACCESS

Edited by:
Lieve Brochez, Ghent University, Belgium

Reviewed by:
Luis De La Cruz-Merino, Hospital Universitario Virgen Macarena, Spain
Guilan Shi, University of South Florida, United States

***Correspondence:**
Giulia Pomati
giuliapomati@tiscali.it

Specialty section:
This article was submitted to Cancer Immunity and Immunotherapy, a section of the journal Frontiers in Immunology

Received: *12 December 2019*
Accepted: *18 May 2020*
Published: *07 July 2020*

Citation:
Botticelli A, Mezi S, Pomati G, Cerbelli B, Cerbelli E, Roberto M, Giusti R, Cortellini A, Lionetto L, Scagnoli S, Zizzari IG, Nuti M, Simmaco M and Marchetti P (2020) Tryptophan Catabolism as Immune Mechanism of Primary Resistance to Anti-PD-1. Front. Immunol. 11:1243. doi: 10.3389/fimmu.2020.01243

Background: Clinical trials showed that only a subset of patients benefits from immunotherapy, suggesting the need to identify new predictive biomarker of resistance. Indoleamine-2,3-dioxygenase (IDO) has been proposed as a mechanism of resistance to anti-PD-1 treatment, and serum kynurenine/tryptophan (kyn/trp) ratio represents a possible marker of IDO activity.

Methods: Metastatic non-small cell lung cancer (NSCLC), renal cell carcinoma (RCC), and head and neck squamous cell carcinoma (HNSCC) treated with nivolumab as second-line treatment were included in this prospective study. Baseline serum kyn and trp levels were measured by high-performance liquid chromatography to define the kyn/trp ratio. The χ^2-test and *t*-test were applied to compare frequencies and mean values of kyn/trp ratio between subgroups with distinct clinical/pathological features, respectively. Median baseline kyn/trp ratio was defined and used as cutoff in order to stratify the patients. The association between kyn/trp ratio, clinical/pathological characteristics, response, progression-free survival (PFS), and overall survival (OS) was analyzed.

Results: Fifty-five patients were included. Mean baseline serum kyn/trp ratio was significantly lower in female than in male patients (0.048 vs. 0.059, respectively, $p = 0.044$) and in patients with lung metastasis than in others (0.053 vs. 0.080, respectively, $p = 0.017$). Mean baseline serum kyn/trp ratio was significantly higher in early progressor patients with both squamous and non-squamous NSCLC ($p = 0.003$) and with a squamous histology cancer (19 squamous NSCLC and 14 HNSCC, $p = 0.029$). The median value of kyn/trp ratio was 0.06 in the overall population. With the use of median value as cutoff, patients with kyn/trp ratio > 0.06 had a higher risk to develop an early progression (within 3 months) to nivolumab with a trend toward significance ($p = 0.064$ at multivariate analysis). Patients presenting a baseline kyn/trp ratio ≤ 0.06 showed a longer PFS [median 8 vs. 3 months; hazard ratio (HR): 0.49; 95% confidence interval (CI) 0.24–1.02; $p = 0.058$] and a significantly better OS than did

those with a kyn/trp ratio > 0.06 (median 16 vs. 4 months; HR: 0.39; 95% CI 0.19–0.82; $p = 0.013$).

Conclusion: Serum kyn/trp ratio could have both prognostic and predictive values in patients with solid tumor treated with immunotherapy, probably reflecting a primary immune-resistant mechanism regardless of the primary tumor histology. Its relative weight is significantly related to gender, site of metastasis, NSCLC, and squamous histology, although these suggestive data need to be confirmed in larger studies.

Keywords: indoleamine-2,3-dioxygenase, tryptophan metabolism, tumor immunity, kynurenine, anti-PD-1

INTRODUCTION

Immune checkpoint inhibitors (ICIs), a class of drugs able to block immunosuppressive pathways in order to prime an anticancer immunity, revolutionized the standard of care in many solid tumors, including non-small cell lung cancer (NSCLC), recurrent/metastatic head and neck squamous cell carcinoma (R/M-HNSCC), and renal cell carcinoma (RCC) (1). In NSCLC, the programmed cell death protein 1 (PD-1) inhibitor, nivolumab showed long-term benefit in a significant proportion of pretreated patients with a 2-years overall survival (OS) of 23% and 29% in squamous and non-squamous histology, respectively, over-performing standard chemotherapy (1, 2). Nevertheless, emerging data from clinical trials showed that only 20–25% of pretreated patients with NSCLC really benefit from immunotherapy with ICI monotherapy (3–5). Recently, nivolumab and the anti-PD-1 pembrolizumab showed a significant activity in patients with HNSCC who progressed on or after platinum-based regimens (6, 7); consequently, both the drugs have been approved by Food and Drug Administration (FDA) for platinum-refractory R/M-HNSCC. However, CheckMate-141 (6) failed to demonstrate a significant association between PD-L1 expression, using different thresholds of expression in tumor cells, response rates to the anti-PD-1 nivolumab and OS not allowing any selection of patients eligible for treatment.

In RCC, nivolumab entered in clinical practice on the basis of the results of a phase III study that demonstrated an advantage in OS after first-line treatment with tyrosine-kinase inhibitors (TKIs) (8). Nivolumab was approved based on the CheckMate 025, demonstrating the superiority of nivolumab compared with everolimus in terms of OS but not progression-free survival (PFS). In the near future, immunotherapy will change the first-line standard of care of metastatic RCC on the basis of the results from a more recent phase III trial evaluating the combination of nivolumab and the anti-CTLA-4 monoclonal antibody ipilimumab (9). Actually, PD-L1 expression seems to have a prognostic value in RCC, but it is far from being considered as a marker of treatment benefit.

The emerging data from these clinical trials showed that only a relatively small subset of patients really benefit from ICIs, underlining the crucial role of patient selection in the choice of the best therapeutic strategy. Although PD-L1 expression in tumor microenvironment has been explored in several retrospective and prospective clinical trials, across many different tumor types, all the results suggest caution in considering PD-L1 as a reliable method for the selection of eligible patients for immunotherapy (4, 10–14). The expression of PD-L1 is dynamic and is the result of complex molecular crosstalk between different intracellular pathways, such as MAPK, PI3K, and Aky/PKB (15, 16). Although some other biomarkers of response to ICI have been proposed, such as tumor mutational burden and mismatch repair gene defect, biomarkers of primary resistance to immunotherapy are still lacking (17), and the mechanisms of immunoresistance in many types of cancer still remain largely unknown and poorly predictable before starting immunotherapy (18). The essential amino acid tryptophan (trp) catabolism is recognized as an important microenvironmental factor that suppresses antitumor immune responses in cancer. Depletion of trp, a fundamental factor for T-cell metabolism, is one of the main mechanisms involved in primary resistance to immunotherapy leading to T-cell anergy and apoptosis (19). Indoleamine-2,3-dioxygenase (IDO) is an enzyme able to catalyze the first and rate-limiting reaction of the essential amino acid L-tryptophan (trp) conversion into L-kynurenine (kyn), inducing an immunosuppressive microenvironment in cancers (20). IDO activity is involved in peripheral immune tolerance because it can promote the inhibition of T-cell proliferation induced by trp deprivation (19, 21–25). Moreover, IDO activity could represent the central and immunobiologically relevant enzyme of tumor immune escape, and it could be involved in the development of primary resistance to treatment with ICI (26).

In a previous study, a high level of kyn that cooperates with trp in suppression of antitumor immune-response by inducing regulatory T cells (Treg) (27) has been shown to correlate with advanced stage at diagnosis, worse prognosis, and response to chemotherapy (28–30). A crucial role in Treg expansion is determined by myeloid-derived suppressor cell (MDSC), which represents a myeloid cell population, at different grades of differentiation, involved in the inhibition of both the innate and adaptive immune response favored by the IDO activity. MDSCs are involved in the Treg expansion through an IDO-mediated mechanism. Indeed, the interaction between MDSC and activated T cell promotes the conversion of effector T cell in Treg (31, 32). Moreover, kyn promotes or suppresses neoplastic transformation and tumorigenesis and drives tumor growth in autocrine fashion, inducing survival and cell motility as described

in malignant glioma cells (27). In addition to IDO, alternative enzymatic pathways of trp catabolism involving tryptophan-2,3-dioxygenase (TDO) (33) and with lesser extent IDO2 (34–36) may also be involved in trp metabolism contributing to immune escape mechanism and tumor progression. IDO activity could represent one of the biomarkers of resistance to immunotherapy as universal and agnostic, not linked to individual neoplasms, easily assessable, and virtually useful in treatment planning and in the correct selection of cancer patients for immunotherapy.

The objective of this study was to investigate the possible association between the serum baseline kyn/trp ratio and the response to immunotherapy in patients affected by NSCLC, RCC, and R/M-HNSCC.

METHODS AND MATERIALS

Patient Population

Patients eligible for second-line treatment with nivolumab with metastatic RCC, who progressed after first line with the TKIs pazopanib or sunitinib, as well as patients with metastatic NSCLC non-oncogene addicted, progressed after first-line chemotherapy as well as recurrent/metastatic platinum refractory HNSCC, followed up at Policlinico Umberto I and at Policlinico Sant'Andrea, in Rome, from June 2016 to May 2019, were enrolled into this prospective study. Eligible patients were those aged >18 years with an Eastern Cooperative Oncology Group (ECOG) performance status ≤2 and adequate cardiac, pulmonary, renal, liver, and bone marrow function. Inclusion criteria were histologically confirmed diagnosis of RCC, NSCLC, and HNSCC; measurable disease according to RECIST version 1.1; and written informed consent. Exclusion criteria were autoimmune disease; symptomatic interstitial lung disease and any other significant comorbidity; systemic pharmacological immunosuppression; prior treatment with immune-stimulatory antitumor agents including checkpoint-targeted agents; patients who received checkpoint inhibitor in other setting; and patients with gastrointestinal malabsorption disorders that could modify the serum level of trp.

Nivolumab treatment was administered in NSCLC and in RCC at the dose of 3 mg/kg every 2 weeks i.v. until disease progression or development of unacceptable toxicity. Patients with HNSCC received 240 mg i.v. flat dose every 2 weeks until disease progression or unacceptable toxicity. Radiological response was assessed with i-RECIST Criteria and classified according to disease control (complete response, partial response, and stable disease) and progressive disease. Patients experiencing disease progression within 3 months from the beginning of nivolumab were defined as early progressors. All toxicity was graded according to the National Cancer Institute Common Terminology Criteria for Adverse Events (version 4.0), and toxicity assessments were performed at day 1 of every cycle until the end of treatment. PFS was defined as the time from patient registration on this prospective study until the first documented tumor progression or death from any cause. OS was defined as the time from patient registration to death from any cause. The association between kyn/trp ratio, clinical/pathological characteristics (including the analysis by tumor sites as well as by histology), response, PFS, and OS was analyzed. The study was conducted in accordance with good clinical practice guidelines and the Declaration of Helsinki. The study protocol and the final version of the protocol were approved by the Institutional Ethics Committee (CE 4421).

Tryptophan and Kynurenine Quantifying Analysis

We evaluated serum levels of trp and kyn by a modified liquid chromatography–tandem mass spectrometry (LC–MS/MS) method. Serum samples were collected and stored at −80°C until analysis. Fifty microliters of serum samples was deproteinized using 50 μl of internal standard (IS) solution [50 μM in tricarboxylic acid (TCA) 4%], vortex mixed, and centrifuged at 14,000 rpm for 15 min. Twenty microliters of clean upper layer was injected into a chromatographic system. Chromatographic separation of analytes was performed using an Agilent Liquid Chromatography System series 1100 (Agilent Technologies, USA), on a biphenyl column (100 × 2.1 mm, Kinetex 2.6 μm of biphenyl, 100 Å, Phenomenex, CA, USA) equipped with a security guard precolumn (Phenomenex, Torrance, CA, USA). The mobile phase consisted of a solution of 0.1% aqueous formic acid (A) and 100% methanol (B); elution was performed at flow rate of 400 μl/min, using an elution gradient. The MS method was performed on a 3200 triple quadrupole system (Applied Biosystems, Foster City, CA, USA) equipped with a Turbo Ion Spray source, as previous described (37). The detector was set in the positive ion mode. The instrument was set in the multiple reaction monitoring (MRM) mode. Data were acquired and processed by the Analyst 1.5.1 Software. A threshold to identify an unfavorable ratio was defined as >0.06, derived from the median kyn/trp ratio detected in the overall population, because a conventional cutoff has not yet been established.

Statistical Analysis

In the descriptive analysis, quantitative variables were described as mean and range, whereas qualitative variables as number and percentage. The χ^2-test and *t*-test for unpaired data were applied to compare frequencies and means, respectively. PFS and OS were estimated using the Kaplan–Meier method, comparisons between groups were made using the log-rank test, and the Mantel–Cox method was used to generate hazard ratios (HRs) and 95% confidence intervals (CIs). Comparison was evaluated using the non-parametric Mann–Whitney *U* test. To identify factors associated with early progressors, univariate and multivariate logistic regression models were used. According to the kyn/trp cutoff value of 0.06, we used kyn/trp ratio as a dichotomous variable for the analyses (kyn/trp ratio > 0.06 vs. kyn/trp ratio ≤ 0.06). The results of univariate and multivariate analyses were expressed in odds ratio and 95% CIs. Statistical significance was set at $p < 0.05$. Statistical analysis was performed using IBM SPSS Statistics Version 24.0 (Armonk, NY, USA).

TABLE 1 | Association between baseline clinicopathological characteristics of the study population and kyn/trp ratio.

Characteristics	*N* (%)	Median (range)	Serum kyn/trp ratio (mean ± SD)	*P*-value
AGE		65 (44–85)		
>65	31 (56.4)		0.056 ± 0.038	0.121
<65	24 (43.6)		0.048 ± 0.029	
BMI		22.4 (16.9–37.5)		
Normal	39 (70.9)		0.058 ± 0.031	0.839
Overweight/obese	13 (23.6)		0.054 ± 0.040	
Underweight	3 (5.5)		0.056 ± 0.025	
SEX				
Male	39 (70.9)		0.059 ± 0.037	**0.044***
Female	16 (29.1)		0.048 ± 0.020	
HISTOLOGY				
Clear cell carcinoma	15 (27.3)		0.036 ± 0.024	0.054
Squamous NSCLC	19 (34.5)		0.060 ± 0.04	
Adenocarcinoma	6 (10.9)		0.100 ± 0.04	
Undifferentiated NSCLC	1 (1.8)		0.040	
Squamous HNSCC	14 (25.5)		0.055 ± 0.034	
BASELINE (ECOG) PS				
PS 0	38 (69.1)		0.053 ± 0.025	0.054
PS 1	17 (30.9)		0.056 ± 0.047	
BRAIN METASTASIS				
Yes	6 (10.9)		0.064 ± 0.034	0.905
No	47 (89.1)		0.055 ± 0.035	
LUNG METASTASIS				
Yes	40 (72.7)		0.053 ± 0.029	**0.017***
No	15 (27.2)		0.080 ± 0.046	
PLEURAL EFFUSION				
Yes	6 (10.9)		0.062 ± 0.051	0.096
No	49 (89.1)		0.054 ± 0.032	
LIVER METASTASIS				
Yes	9 (16.4)		0.062 ± 0.050	0.076
No	46 (83.6)		0.054 ± 0.030	
EARLY PROGRESSOR				
Yes	29 (52.7)		0.056 ± 0.042	**0.047***
No	26 (47.3)		0.050 ± 0.021	

*kyn, kynurenine; trp, tryptophan; SD, standard deviation; BMI, body mass index; NSCLC, non-small cell lung cancer; HNSCC, head and neck squamous cell carcinoma; ECOG PS, Eastern Cooperative Oncology Group performance status; *Statistical significance was set at $p < 0.05$.*

RESULTS

Clinical Characteristics

Fifty-five metastatic patients treated with nivolumab were enrolled in this study: 26 patients in the NSCLC group, 15 patients in the RCC group, and 14 patients in the HNSCC group. Baseline clinical–pathological characteristics of patients are summarized in **Table 1**. Among lung cancer patients, 19 patients had squamous cell carcinoma, whereas the remaining had non-squamous histology (six adenocarcinoma and one undifferentiated tumor). All 15 patients in the RCC group had clear cell carcinoma histology. Thirty-nine patients were male (70.9%), 16 patients were female (29.1), and median age was 65 years (range 44–85). All patients were assessed at baseline for serum trp and kyn levels. The median value of kyn/trp in the overall population was 0.06 (range 0.018–0.180) (**Figure 1**).

Association Between Serum Kynurenine/Tryptophan Ratio, Clinicopathological Features, and Response to Immunotherapy

The association between mean baseline kyn/trp ratio and clinicopathological characteristics was analyzed as shown in **Table 1**.

Mean serum kyn/trp ratio was significantly lower in female than in male patients (0.048 vs. 0.059, respectively, $p = 0.044$).

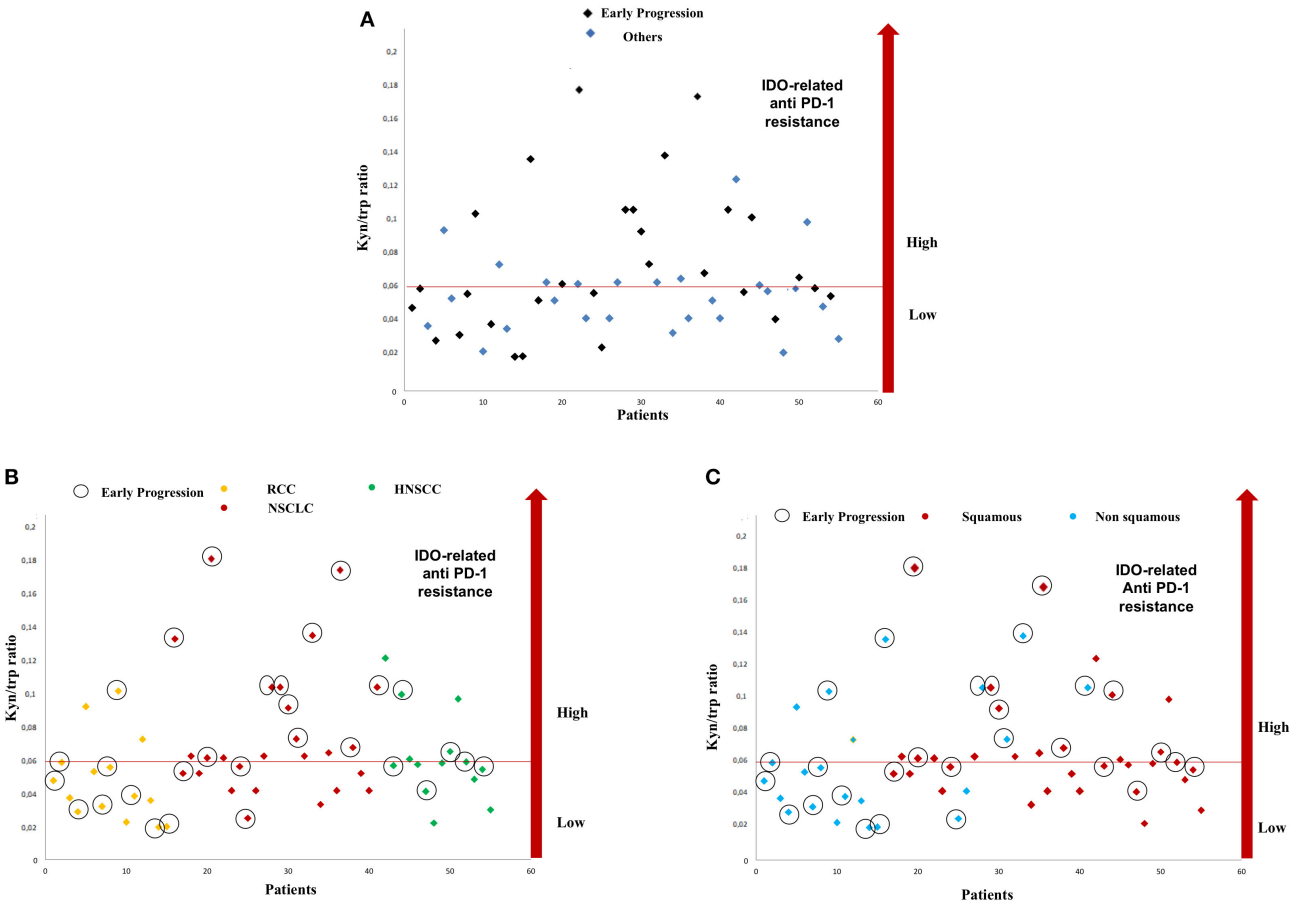

FIGURE 1 | Distribution of serum kyn/trp ratio and early progressions in study population **(A)**. Distribution of serum kyn/trp ratio and early progression according to primary tumor site **(B)** and on the basis of the squamous histology **(C)**. kyn, kynurenine; trp, tryptophan.

Moreover, in patients with lung metastasis, mean serum kyn/trp ratio was 0.053 vs. 0.080 in other patients ($p = 0.017$). No significant association was found between baseline serum kyn/trp ratio and age, body mass index (BMI), histology, baseline ECOG PS, or the presence of metastasis in the brain, liver, and pleura (**Table 1**).

With a median follow-up of 7.75 months, 11 (20%), 13 (23.6%), and 31 (56.3%) patients had a stable disease (SD), a partial response (PR), and a progressive disease (PD), respectively. An early progression (within 3 months from the start of immunotherapy) occurred in 29 patients (52.7%). The distribution of early progression in the study population is shown in **Figure 1**, according to the serum kyn/trp ratio (**Figure 1A**), primary tumor site (**Figure 1B**) and on the basis of the analysis by histology, the squamous one (**Figure 1C**). Overall, patients who showed an early progression had a slightly but significantly higher mean kyn/trp ratio than had others (0.056 vs. 0.050, respectively, $p = 0.047$) (**Table 1** and **Figure 2A**). In patients with NSCLC, regardless of the different histotypes, mean serum kyn/trp ratio was significantly higher in early progressors (0.094 vs. 0.050; p-value = 0.003), as shown in **Table 2** and **Figure 2B**, whereas no significant association was found between kyn/trp ratio and early progression in the RCC and HNSCC groups (**Table 2** and **Figures 2C,D**). Nevertheless, in the RCC group, there seems to be a tendency to an inverse correlation between kyn/trp ratio and early progression (**Figure 2C**). Considering all patients with squamous histology (both squamous NSCLC and HNSCC), mean kyn/trp ratio was higher in early progressors than in patients who experienced initial benefit from immunotherapy (0.072 vs. 0.055, respectively; p-value = 0.029, **Table 2**).

With the use of a univariate analysis (**Table 3**), age, PS ECOG 1, and a baseline kyn/trp ratio higher than the median value (>0.06) were significantly associated with an early progression of disease.

With the use of a multivariate analysis, including age, kyn/trp ratio, and PS, only PS was still significantly associated with early progression ($p = 0.015$, **Table 3**), whereas the association between a kyn/trp ratio > 0.06 and early progression was not confirmed in the overall population ($p = 0.064$).

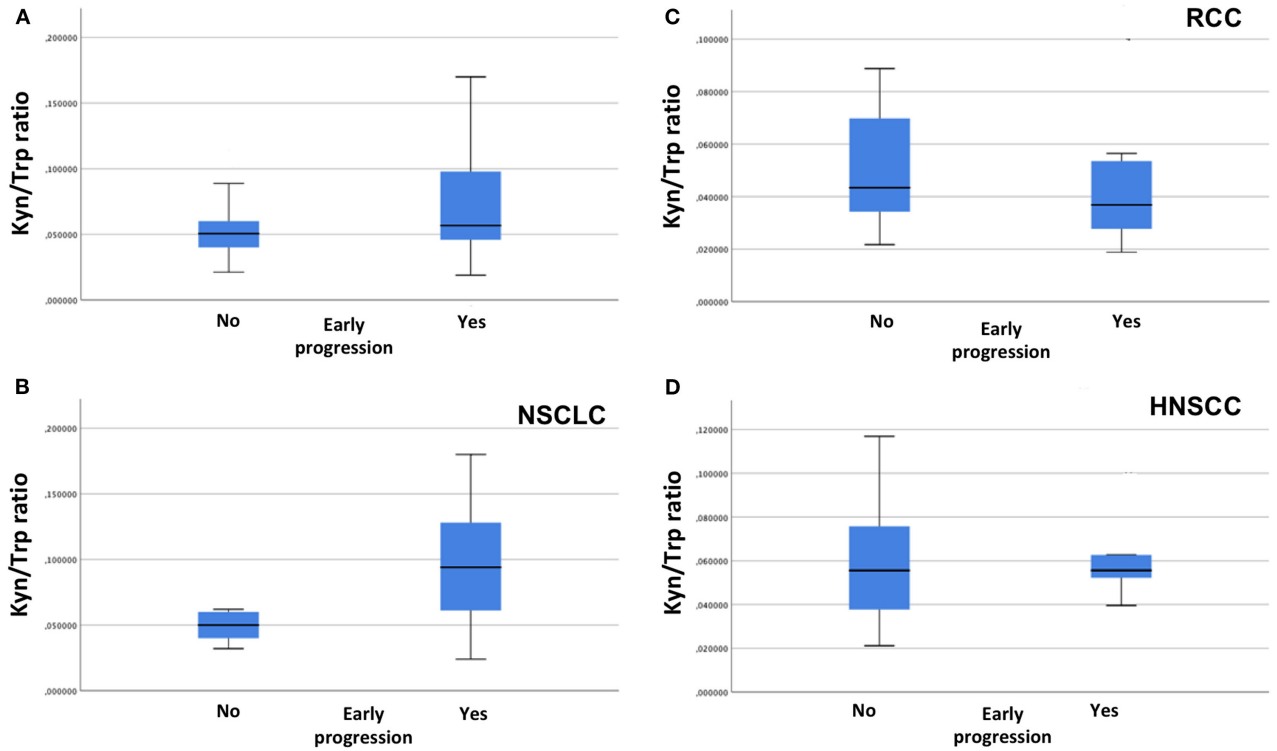

FIGURE 2 | Association between serum kyn/trp ratio and early progression in overall population **(A)**, in NSCLC group **(B)**, in RCC group **(C)**, and in HNSCC group **(D)** (Mann–Whitney *U* test). kyn, kynurenine; trp, tryptophan; NSCLC, non-small cell lung cancer; RCC, renal cell carcinoma; HNSCC, head and neck squamous cell carcinoma.

TABLE 2 | Association between kyn/trp ratio, early progression, and primary tumor.

	N (%)	Kyn/trp mean (±SD)	*P*-value
RCC	15	0.036 ± 0.024	
PD < 3 months (yes vs. no)	9 (60.0) vs. 6 (40.0)	0.036 vs. 0.043	0.590
NSCLC	26	0.06 ± 0.040	
PD < 3 months (yes vs. no)	14 (53.8) vs. 12 (46.2)	0.094 vs. 0.050	**0.003***
HNSCC	14	0.055 ± 0.026	
PD < 3 months (yes vs. no)	6 (42.8) vs. 8 (57.2)	0.055 vs. 0.055	0.961
Squamous histology (NSCLC and HNSCC)	33	0.057 ± 0.035	
PD < 3 months (yes vs. no)	14 (42.4) vs. 19 (57.6)	0.072 vs. 0.055	**0.029***

*kyn, kynurenine; trp, tryptophan; SD, standard deviation; RCC, renal cell carcinoma; PD, progressive disease; NSCLC, non-small cell lung cancer; HNSCC, head and neck squamous cell carcinoma; *Statistical significance was set at p < 0.05.*

The Serum Kynurenine/Tryptophan Ratio and Clinical Outcomes

Median PFS was 4 months (range 1–28 months) and median OS (range 1–28) was 5 months in the whole cohort.

Patients were stratified by median baseline value of serum kyn/trp (0.06) in patients with kyn/trp ratio >0.06 and ≤0.06. PFS was longer in patients presenting lower values of kyn/trp than in patients showing higher values (median PFS 8 vs. 3 months; HR: 0.49; 95% CI 0.24–1.02; $p = 0.058$). Patients with lower kyn/trp ratio showed even a significantly better OS than did patients with a higher kyn/trp ratio value (median OS 16 vs. median 4 months; HR: 0.39; 95% CI 0.19–0.82; $p = 0.013$) (**Figures 3A,B**). As it is shown in **Figure 4**, referring to the primary tumor, only in the NSCLC group (**Figures 4A,B**) PFS and OS were significantly longer in patients with kyn/trp ratio ≤ 0.06 vs. kyn/trp > 0.06 (median PFS not reached vs. 3 months; range 1.8–4.1; $p = 0.003$ and median OS not reached vs. 3 months, range 1.8–4.1; $p = 0.003$, respectively). Instead, in the RCC group (**Figures 4C,D**), median PFS was not reached vs. 8 months (range 4.6–11.3; $p = 0.406$), and OS was not reached vs. 16 months (range 11.0–23.6; $p = 0.567$) in patients with low and high kyn/trp ratios, respectively. Overall, in RCC, a lower kyn/trp

TABLE 3 | Univariate and multivariate analyses: association between patients characteristic and early progression.

	Univariate analysis		Multivariate analysis	
	OR (95% CI)	***P***	**OR (95% CI)**	***P***
Age (>65 vs. <65)	3.32 (104–10.58)	**0.042***	2.71 (0.74–9.97)	0.132
BMI (overweight vs. other)	1.33 (0.36–4.92)	0.666	–	
Sex (female vs. male)	0.85 (0.26–2.74)	0.795	–	
Histology (sq vs. non-sq)	0.34 (0.11–1.06)	0.065	–	
ECOG (PS 1 vs. PS 0)	7.15 (1.75–29.20)	**0.006***	6.80 (1.45–31.74)	**0.015***
Brain metastasis (yes vs. no)	1.76 (0.29–10.55)	0.536	–	
Lung metastasis (yes vs. no)	0.30 (0.07–1.28)	0.104	–	
Pleural effusion (yes vs. no)	0.80 (0.14–4.42)	0.806	–	
Liver metastasis (yes vs. no)	3.5 (0.65–18.75)	0.144	–	
Kyn/trp median (≤0.06 vs. >0.06)	0.25 (0.07–0.86)	**0.028***	0.24 (0.05–1.08)	**0.064***

*OR, odds ratio; BMI, body mass index; Sq, squamous; ECOG, Eastern Cooperative Oncology Group; PS, performance status; *Statistical significance was set at $p < 0.05$.*

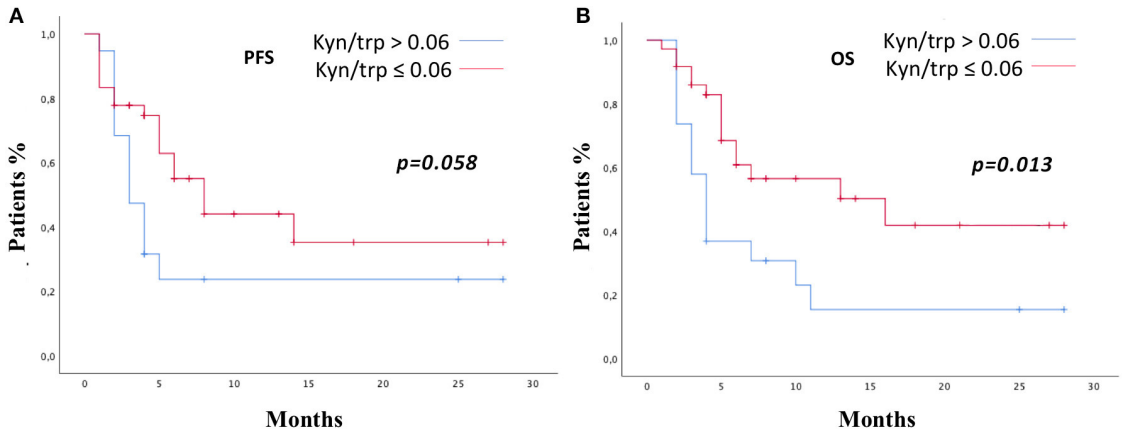

FIGURE 3 | PFS **(A)** and OS **(B)** in the study population according to kyn/trp ratio >0.06 or ≤0.06 were addressed by the Kaplan–Meier method and log-rank test. PFS, progression-free survival; OS, overall survival; kyn, kynurenine; trp, tryptophan.

ratio is inclined to be associated with a worse survival despite the lack of statistical significance.

In the HNSCC group (**Figures 4E,F**), median PFS was 3 months (range 1.0–4.9) vs. 5.0 months (range 3.2–6.2) in patients with kyn/trp > 0.06 and kyn/trp ratio ≤ 0.06, respectively ($p = 0.264$). Median OS was 4.0 months (range 0.0–9.8) in patients with kyn/trp ratio > 0.06 vs. 5.0 months (range 3.3–6.6) in patients with kyn/trp ratio ≤ 0.06 (p-value = 0.661).

DISCUSSION

In our study, including different solid tumors, baseline serum kyn/trp ratio is associated with early progression and survival, confirming its role as a possible predictive biomarker of primary resistance to immunotherapy. In particular, higher baseline kyn/trp value is associated with early progression and, consequently, poor prognosis. This study confirms the previous results in NSCLC cohort of patients (37). As a matter of fact, in our analysis, the statistical significance of the association between kyn/trp ratio and response to immunotherapy is strong when considered in the NSCLC population, whereas it is weak in the overall study population. Moreover, considering RCC and HNSCC separately, there is no correlation between kyn/trp ratio and response, suggesting that in these two types of tumors, the IDO activity could have a marginal role in the complex mechanism determining the primary resistance to immunotherapy or concurrent medications, able to induce TDO expression like the steroids, and nutritional state and infection may have a confounding effects on results. Indeed, the pathway is responsive to unspecific inflammation, and it is induced in chronic immune activation states because IDO is sensitive IFN gamma gene, and it is induced by inflammatory stimuli (27) that may be significant especially in locally relapsed HNSCC, which is generally an inflamed disease. Moreover, the extremely scarce sample size did not allow us to draw definitive conclusions.

In our analysis, kyn/trp ratio resulted to be significantly lower in patients with lung metastases than patients with

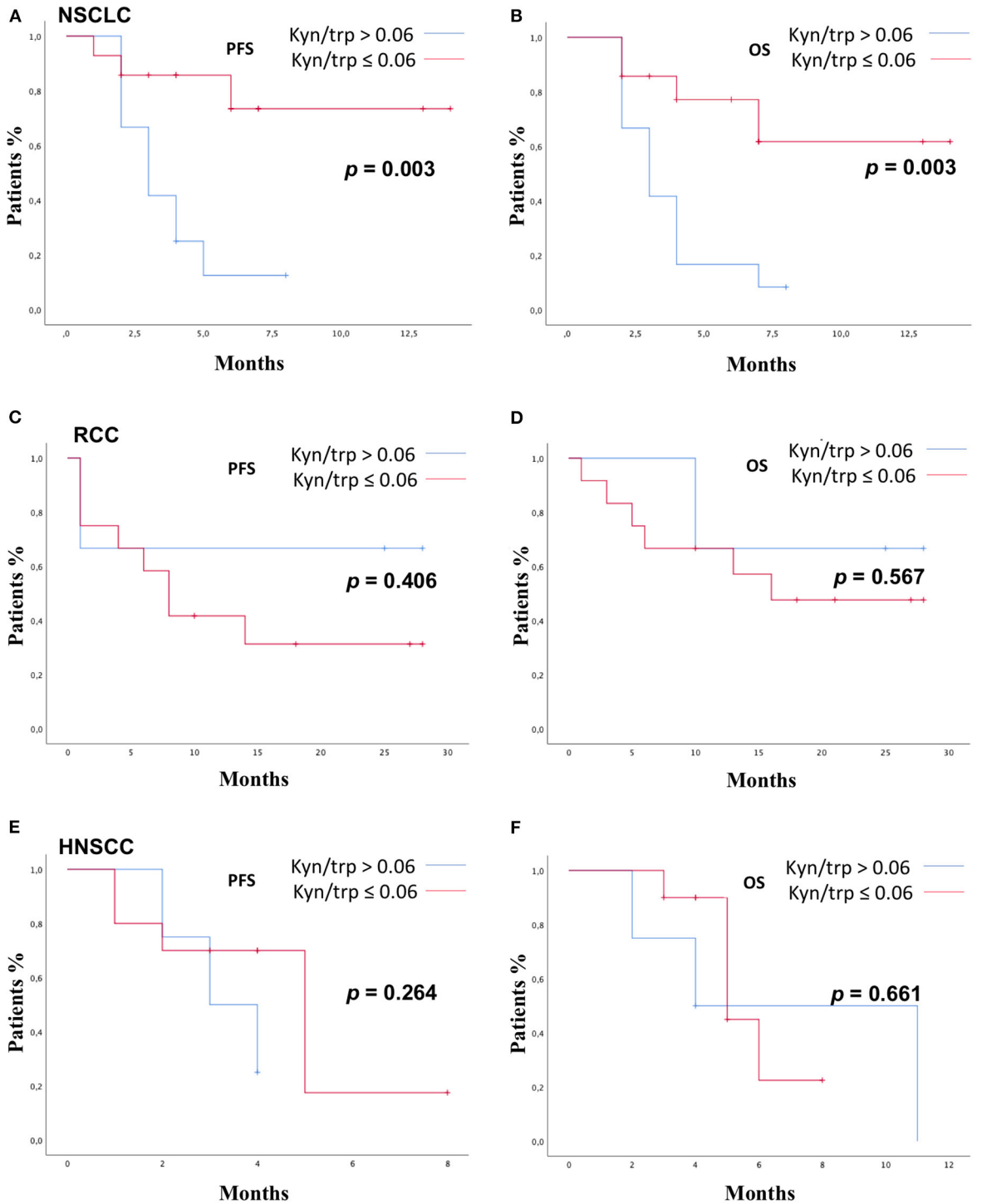

FIGURE 4 | PFS and OS according to kyn/trp in NSCLC group **(A,B)**, RCC group **(C,D)**, and HNSCC group **(E,F)** were addressed by the Kaplan–Meier method and log-rank test. PFS, progression-free survival; OS, overall survival; kyn, kynurenine; trp, tryptophan; NSCLC, non-small cell lung cancer; RCC, renal cell carcinoma; HNSCC, head and neck squamous cell carcinoma.

other metastatic sites. Indeed, immune response could be considered the result of a complex interplay between local tumor microenvironment and peripheral immunity. Moreover, the role of metastatic organ microenvironment in response or resistance to checkpoint inhibitor is still not completely understood. Recently, in a large retrospective study including NSCLC in

treatment with immunotherapy, lymph node metastases were associated with the best response, lung and pleura metastases were associated with an intermediate response, and liver, which expressed TDO at high levels, and bone metastases were associated with the least responses to immunotherapy (38). In a study including 102 patients with NSCLC in treatment with nivolumab, lung and liver metastases have been proven to be excellent parameters in predicting OS (39). Consequently, metastatic sites could have an impact on the development of primary resistance to immunotherapy (40), but the underlying biological mechanism should be further investigated, and our study must be considered as a hypothesis generator.

Looking at the baseline patients characteristics, kyn/trp ratio is slightly significantly lower in female compared with male patients. This result could be explained by the sexual dimorphism of the immune system able to influence the response to immunotherapy (41, 42). In a recent meta-analysis (43), the magnitude of benefit from immunotherapy was sex dependent with an improving effectiveness in male patients. However, in our study, there is no evidence that the early progression to immunotherapy is sex dependent, and the correlation between sex and IDO activity should be further evaluated in a large study population.

Considering the different subgroups on the basis of primary tumor site, the association between kyn/trp ratio and early progression was statistically significant in NSCLC, confirming the results from our previous report (37). Moreover, considering the different subgroups based on histology, the association between kyn/trp ratio and early progression was statistically significant in squamous histology group. IDO activity was recently investigated in different solid squamous tumors. In squamous cervical cancer, IDO activity expressed in terms of kyn/trp ratio was shown to be linked to poor survival (43). In squamous esophageal carcinoma, a high tissue IDO expression was associated with impaired OS and aggressive disease (44). Moreover, in a recent study including 88 squamous oral cavity carcinoma, high tissue IDO expression was associated with OS, acquiring the role of negative prognostic factor (45). These results support our data by suggesting that IDO could have a central role in the development of primary resistance to immunotherapy in tumor with squamous histology, regardless of the tumor site. In the RCC and HNSCC subgroups, we failed to demonstrate a significant association between serum kyn/trp ratio and early progression. In particular, in RCC, kyn/trp ratio seems to have a reverse trend because patients with low baseline ratio tend to often experience early progression, although the statistical significance was not reached. The prognostic and predictive values of kyn/trp ratio in the different disease could be influenced by the type of treatment administered in a first-line setting. In our study, all patients with RCC received TKI in the first line. In metastatic RCC, in the phase III study (8) comparing nivolumab with everolimus, a subgroup analysis found that patients previously treated with pazopanib showed statistically significant increase in OS with nivolumab, whereas patients previously treated with sunitinib did not show significant difference in OS between nivolumab and everolimus (8, 46). Thus, previous therapy with TKIs might enhance subsequent immunotherapy efficacy by different mechanisms. As a matter of fact, therapy with TKIs could induce a reduction in Treg levels and MDSCs, improving type 1 cytokine response (47, 48). Moreover, TKIs could also regulate the expression of NK cell ligands in tumor cells, conferring sensitivity to NK cell lysis, and normalize tumor vascularization, allowing helping CD8 T-cell influx into the tumor (49). Despite this immunomodulatory effect, it is still unknown whether and how TKIs could also influence IDO activity. Also, chemotherapy could have an immunomodulatory power. In our study population, patients with HNSCC and NSCLC received platinum-based chemotherapy in the first-line setting. Cisplatin-based regimen enhanced the T-cell activation and proliferation and their cytotoxic activity and inhibited the immunosuppressive pathways (50). Nevertheless, the effect of chemotherapy on IDO activity is unknown and should be further investigated.

In the multivariate analysis, probably the kyn/trp ratio loses statistical significance as a result of the heterogeneity of the resistance mechanisms to immunotherapy involved in the different tumor types. These mechanisms are not yet completely understood and deserved further investigation according to the primary tumor biology and previous treatment.

A possible limitation of the study is due to the presence of possible confounding factors that could interfere with a correct interpretation of serum kyn/trp ratio. First of all, malnutrition could modify the circulating trp levels representing a relevant issue in the management of HNSCC patients. In our study cohort population with HNSCC, nutritional support was provided to all patients with feeding difficulties. Secondly, serum kyn/trp ratio is the result of the activity of some different enzymes including mainly IDO and TDO2 (51). The enzyme TDO2 is expressed in the liver and is involved in the catabolism of trp. However, TDO2 was shown to be overexpressed in some tumor cells as a mean of immune escape (27, 52, 53). Thus, TDO seems to contribute to cancer-associated inflammation and tumor progression like IDO, and it is not possible to distinguish the activity of the two enzymes on the basis of serum ratio.

Nevertheless, measuring serum kyn/trp levels could be a reliable method to evaluate the overall impact of trp depletion in determining primary resistance to immunotherapy. To date, chromatography remains one of the most sensitive and accurate methods for quantifying both trp and kyn from biological matrices and measure trp catabolism.

One more limitation to be acknowledged is a relative small sample size of study population, with potential for inherent biases. Certainly, a prospective validation on a larger sample size is required to assess reproducibility and generalizability of our results.

Recently, the FDA-approved pembrolizumab in pediatric and adult solid tumors with microsatellite instability (MSI) or mismatch repair deficiency led to the first approval based on a specific biomarker rather than the organ-specific histology (54, 55). As well as MSI and tumor mutational burden (TMB), in the future, the enzyme pathways involved in trp catabolism could have the potential to become an additional agnostic biomarker of

TABLE 4 | Ongoing phase II/III trial evaluating IDO inhibitor or tryptophan mimetic agents in monotherapy or in combination strategy with others drugs.

Study title	Study number	Condition or disease	Treatments	Status—phase
A phase 2 study of the IDO inhibitor epacadostat vs. tamoxifen for subjects with biochemical-recurrent-only EOC, PPC or FTC following complete remission with first-line chemotherapy	NCT01685255	Ovarian cancer Genitourinary (GU) tumors	Epacadostat Tamoxifen	Terminated—phase 2
A phase II double-blinded, randomized, placebo-controlled study of indoximod in combination with a taxane chemotherapy in metastatic breast cancer	NCT01792050	Metastatic breast cancer	Docetaxel or paclitaxel Indoximod	Accrual completed—phase 2
A phase II trial of IDO-inhibitor, BMS-986205, and PD-1 inhibitor, nivolumab, in patients with recurrent or persistent endometrial cancer or endometrial carcinosarcomas (CA017-056)	NCT04106414	Endometrial adenocarcinoma Endometrial carcinosarcoma	Nivolumab BMS-986205	Recruiting—phase 2
A phase 1/2 study of the concomitant administration of indoximod plus immune checkpoint inhibitors for adult patients with advanced or metastatic melanoma	NCT02073123	Metastatic melanoma Stage III melanoma Stage IV melanoma	Indoximod Ipilimumab Nivolumab Pembrolizumab	Recruiting—phase 1/2
A phase I/II study of the combination of indoximod and temozolomide for adult patients with temozolomide-refractory primary malignant brain tumors	NCT02052648	Glioblastoma multiforme Glioma Gliosarcoma Malignant brain tumor	Indoximod + temozolomide Temozolomide Bevacizumab Stereotactic radiation	Completed—phase 1/2
A phase I/II study of indoximod in combination with gemcitabine and Nab-paclitaxel in patients with metastatic adenocarcinoma of the pancreas	NCT02077881	Metastatic pancreatic adenocarcinoma Metastatic pancreatic cancer	Nab-paclitaxel Gemcitabine Indoximod	Completed—phase 1–2
A phase II study of epacadostat and pembrolizumab in patients with imatinib refractory advanced gastrointestinal stromal tumors	NCT03291054	Gastrointestinal stromal tumors	Pembrolizumab Epacadostat	Recruiting—phase 2
A phase I/IIb study of DEC205mAb-NY-ESO-1 fusion protein (CDX-1401) given with adjuvant poly-ICLC in combination with INCB024360 for patients in remission with epithelial ovarian, fallopian tube, or primary peritoneal carcinoma whose tumors express NY-ESO-1 or LAGE-1 antigen	NCT02166905	Fallopian tube carcinoma Ovarian carcinoma Primary peritoneal carcinoma	Biological: DEC-205/NY-ESO-1 Fusion Protein CDX-1401 Epacadostat	Recruiting—phase 1/2
Phase I/II trial of BMS-986205 and nivolumab as first or second-line therapy in hepatocellular carcinoma	NCT03695250	Metastatic hepatocellular carcinoma Stage III hepatocellular carcinoma AJCC v8 Stage IIIA hepatocellular carcinoma AJCC v8	IDO1 inhibitor BMS-986205 Nivolumab	Recruiting—phase 1/2
A phase II study to determine the safety and efficacy of INCB024360 in patients with myelodysplastic syndromes	NCT01822691	Myelodysplastic syndromes	INCB024360	Terminated—phase 2
Influence of the celecoxib administration before surgery for endometrial cancer on indoleamine 2,3-dioxygenase 1 (IDO1) tumor expression and immune cells tumor's infiltration	NCT03896113	Endometrium cancer	Drug: celecoxib 200-mg capsule	Recruiting—phase 2
Window-of-opportunity trial of nivolumab and BMS986205 in patients with squamous cell carcinoma of the head and neck (CA017-087)	NCT03854032	Lip Oral cavity squamous cell carcinoma Pharynx Larynx squamous cell carcinoma	Nivolumab IDO1 inhibitor BMS-986205	Recruiting—phase 2
Phase II study of epacadostat (INCB024360) in combination with pembrolizumab in patients with locally advanced/metastatic sarcoma	NCT03414229	Locally advanced/Metastatic sarcoma	Epacadostat Pembrolizumab	Active not recruiting—phase 2
A phase II pilot trial of an indoleamine 2,3, dioxygenase-1 (IDO1) inhibitor (INCB024360) plus a multipeptide melanoma vaccine (MELITAC 12.1) in patients with advanced melanoma	NCT01961115	Advanced/metastatic melanoma (mucosal, uveal, skin)	Epacadostat MELITAC 12.1 peptide vaccine	Completed—phase 2

(Continued)

TABLE 4 | Continued

Study title	Study number	Condition or disease	Treatments	Status—phase
A phase 1/2, open-label, safety, tolerability, and efficacy study of epacadostat in combination with pembrolizumab and chemotherapy in subjects with advanced or metastatic solid tumors (ECHO-207/KEYNOTE-723)	NCT03085914	Solid tumors Colorectal cancer (CRC) Adenocarcinoma (PDAC) Lung cancer UC (urothelial cancer) Head and neck cancer	Epacadostat Pembrolizumab Oxaliplatin 5-Fluorouracil Gemcitabine Nab-paclitaxel Carboplatin Paclitaxel Pemetrexed Cyclophosphamide Cisplatin	Active not recruiting—phase 1–2
A phase 1/2, open-label, dose-escalation, safety, tolerability, and efficacy study of epacadostat and nivolumab in combination with immune therapies in subjects with advanced or metastatic malignancies (ECHO-208)	NCT03347123	Solid tumors	Epacadostat Nivolumab Ipilimumab Lirilumab	Active not recruiting—phase 1–2
A phase 1/2 study of relatlimab (anti-LAG-3 monoclonal antibody) administered in combination with both nivolumab (anti-PD-1 monoclonal antibody) and BMS-986205 (IDO1 inhibitor) or in combination with both nivolumab and ipilimumab (anti-CTLA-4 monoclonal antibody) in advanced malignant tumors	NCT03459222	Advanced cancer	Relatlimab Nivolumab BMS-986205 Ipilimumab	Recruiting—phase 1–2

primary resistance to immunotherapy beyond the histology and tumor site.

Actually, several clinical trials are investigating anti-IDO agents in several solid tumors in monotherapy or in combination strategy with other drugs (**Table 4**). The majority of IDO inhibitors are direct enzymatic inhibitors, such as epacadostat and navoximod, whereas the trp mimetic indoximod acts directly on immune cells, creating an artificially trp-mediated signal to reverse the IDO-related immunosuppressive mechanism (56).

The phase I/II KeyNote 037/ECHO 301 trial (57) evaluated epacadostat at different dose levels and pembrolizumab, an anti-PD-1 agent 200 mg every 3 weeks, in 62 patients with advanced solid tumors, showing promising results. High-grade toxicities occurred in 24% of patients, and no adverse events led to death. Objective response was achieved in 12 out of 22 patients with several types of solid tumors.

Moreover, the phase II trial (58), evaluating indoximod and pembrolizumab in naïve patients for immunotherapy with advanced melanoma, showed promising results with an objective response rate of 55.7% and a median PFS of 12.4 months.

Unfortunately, the phase III trial KeyNote/ECHO 301 (59), evaluating epacadostat 100 mg twice daily (BID) and pembrolizumab 200 mg every 3 weeks in naïve patients for immunotherapy with metastatic melanoma, failed to meet its primary endpoint of improving PFS.

To maximize the benefit of these combination strategies, it is important to improve the selection of clinical trial population through the detection of serum and/or tissue biomarkers.

Therefore, the role of serum kyn/trp should be evaluated and interpreted in the contest of other circulating and tissue immunological parameters: different T-cell subpopulations, MDSCs, circulating cytokines and chemokines, the immune cell death biomarkers, and other possible predictive biomarkers, such as T-cell immunoglobulin mucin-3 (TIM3), lymphocyte-activation gene-3 (LAG3), and T-cell immunoglobulin and ITIM domain (TIGIT) (60, 61). In our study, serum kyn/trp has been confirmed to be a possible prognostic and predictive biomarker of primary resistance to immunotherapy in patients with solid tumors in treatment with immunotherapy, regardless of the primary tumor histology, although its relative weight is significantly related to gender, site of metastasis, lung cancer, and squamous histology. However, the impact of serum kyn/trp levels on prognosis and resistance to immunotherapy should be further investigated and its role integrated together with other possible and dynamic mechanisms of resistance to immunotherapy treatment and definitively validated in further studies.

DATA AVAILABILITY STATEMENT

The datasets generated for this study are available on request to the corresponding author.

ETHICS STATEMENT

This study was approved by local ethics committee of Sapienza University of Rome, RIF. CE: 4421. The patients/participants provided their written informed consent to participate in this study.

AUTHOR CONTRIBUTIONS

AB and LL conceived the study. AB, MN, and PM designed the work. AB, SM, GP, and BC wrote the manuscript. LL, MR, RG, AC, EC, IZ, and SS acquired the samples, performed experiments, and acquired data. AB and MR analysed the data. AB, MN,

PM, SM, MS, and GP discussed the results and implications of findings. All authors contributed to the article and approved the submitted version.

FUNDING

This work was supported by Sapienza University of Rome.

REFERENCES

1. Postow MA, Callahan MK, Wolchok JD. Immune checkpoint blockade in cancer therapy. *J Clin Oncol.* (2015) 33:1974–82. doi: 10.1200/JCO.2014.59.4358
2. Horn L, Spigel DR, Vokes EE, Holgado E, Ready N, Steins M, et al. Nivolumab versus docetaxel in previously treated patients with advanced non-small-cell lung cancer: two-year outcomes from two randomized, open-label, phase III trials (checkmate 017 and checkmate 057). *J Clin Oncol.* (2017) 35:3924–33. doi: 10.1200/JCO.2017.74.3062
3. Borghaei H, Paz-Ares L, Horn L, Spigel DR, Steins M, Ready NE, et al. Nivolumab versus docetaxel in advanced nonsquamous non-small-cell lung cancer. *N Engl J Med.* (2015) 373:1627–39. doi: 10.1056/NEJMoa1507643
4. Garon EB1, Rizvi NA, Hui R, Leighl N, Balmanoukian AS, Eder JP, et al. Pembrolizumab for the treatment of non-small cell lung cancer. *N Engl J Med.* (2015) 372:2018–28. doi: 10.1056/NEJMoa1501824
5. Rittmeyer A, Barlesi F, Waterkamp D, Park K, Ciardiello F, von Pawel J, et al. Atezolizumab versus docetaxel in patients with previously treated non-small-cell lung cancer (OAK): a phase 3, open-label, multicentre randomised controlled trial. *Lancet.* (2017) 389:255–65. doi: 10.1016/S0140-6736(16)32517-X
6. Ferris RL, Blumenschein G Jr, Fayette J, Guigay J, Colevas AD, Licitra L, et al. Nivolumab vs investigator's choice in recurrent or metastatic squamous cell carcinoma of the head and neck: 2-year long-term survival update of CheckMate 141 with analyses by tumor PD-L1 expression. *Oral Oncol.* (2018) 81:45–51. doi: 10.1016/j.oraloncology.2018.04.008
7. Cohen EE, Soulières D, Le Tourneau C, Dinis J, Licitra L, Ahn MJ, et al. Pembrolizumab versus methotrexate, docetaxel, or cetuximab for recurrent or metastatic head-and-neck squamous cell carcinoma (KEYNOTE-040): a randomised, open-label, phase 3 study. *Lancet Oncol.* (2019) 393:156–67. doi: 10.1016/S0140-6736(18)31999-8
8. Motzer RJ, Escudier B, McDermott DF, George S, Hammers HJ, Srinivas S, et al. Nivolumab versus everolimus in advanced renal-cell carcinoma. *N Engl J Med.* (2015) 373:1803–13. doi: 10.1056/NEJMoa1510665
9. Motzer RJ, Tannir NM, McDermott DF, Arén Frontera O, Melichar B, Choueiri TK, et al. Nivolumab plus Ipilimumab versus Sunitinib in Advanced Renal-Cell Carcinoma. *N Engl J Med.* (2018) 378:1277–90. doi: 10.1056/NEJMoa1712126
10. Taube JM, Klein A, Brahmer JR, Xu H, Pan X, Kim JH, et al. Association of PD-1, PD-1 ligands, and other features of the tumor immune microenvironment with response to anti-PD-1 therapy. *Clin Cancer Res.* (2014) 20:5064–74. doi: 10.1158/1078-0432.CCR-13-3271
11. Darb-Esfahani S, Kunze CA, Kulbe H, Sehouli J, Wienert S, Lindner J, et al. Prognostic impact of programmed cell death-1 (PD-1) and PD-ligand 1 (PD-L1) expression in cancer cells and tumor infiltrating lymphocytes in ovarian high grade serous carcinoma. *Oncotarget.* (2016) 7:1486–99. doi: 10.18632/oncotarget.6429
12. Cimino-Mathews A, Thompson E, Taube JM, Ye X, Lu Y, Meeker A, et al. PD-L1 (B7-H1) expression and the immune tumor microenvironment in primary and metastatic breast carcinomas. *Hum Pathol.* (2016) 47:52–63. doi: 10.1016/j.humpath.2015.09.003
13. Mandal R, Senbabaoglu Y, Desrichard A, Havel JJ, Dalin MG, Riaz N, et al. The head and neck cancer immune landscape and its immunotherapeutic implications. *JCI Insight.* (2016) 1:e89829. doi: 10.1172/jci.insight.89829
14. Zandberg DP, Strome SE. The role of the PD-L1: PD-1 pathway in squamous cell carcinoma of the head and neck. *Oral Oncol.* (2014) 50:627–32. doi: 10.1016/j.oraloncology.2014.04.003
15. Lui VWY, Hedberg ML, Li H, Vangara BS, Pendleton K, Zeng Y, et al. Frequent mutation of the PI3K pathway in head and neck cancer defines predictive biomarkers. *Cancer Discov.* (2013) 3:761–9. doi: 10.1158/2159-8290.CD-13-0103
16. Network CGA. Comprehensive genomic characterization of head and neck squamous cell carcinomas. *Nature.* (2015) 517:576–82. doi: 10.1038/nature14129
17. Salati M, Baldessari C, Cerbelli B, Botticelli A. Nivolumab in pretreated non-small cell lung cancer: continuing the immunolution. *Transl Lung Cancer Res.* (2018) 7:S91–4. doi: 10.21037/tlcr.2018.01.14
18. Lee M, Samstein RM, Valero C, Chan TA, Morris LGT. Tumor mutational burden as a predictive biomarker for checkpoint inhibitor immunotherapy. *Hum Vaccin Immunother.* (2019) 30:1–4. doi: 10.1080/21645515.2019.1631136
19. Mellor AL, Munn DH. Tryptophan catabolism and T-cell tolerance: immunosuppression by starvation? *Immunol Today.* (1999) 20:469–73. doi: 10.1016/s0167-5699(99)01520-0
20. Badawy AA. Kynurenine pathway of tryptophan metabolism: regulatory and functional aspects. *Int J Tryptophan Res.* (2017) 15:1178646917691938. doi: 10.1177/1178646917691938
21. Munn DH, Shafzadeh E, Attwood JT, Bondarev I, Pashine A, Mellor AL., et al. Inhibition of T cell proliferation by macrophage tryptophan catabolism. *J Exp Med.* (1999) 189:1363–72. doi: 10.1084/jem.189.9.1363
22. Hwu P, Du MX, Lapointe R, Do M, Taylor MW, Young HA., et al. Indoleamine 2,3-dioxygenase production by human dendritic cells results in the inhibition of T cell proliferation. *J Immunol.* (2000) 164:3596–9. doi: 10.4049/jimmunol.164.7.3596
23. Curti A, Pandolf S, Valzasina B, Aluigi M, Isidori A, Ferri E, et al. Modulation of tryptophan catabolism by human leukemic cells results in the conversion of $CD25^-$ into $CD25^+$ T regulatory cells. *Blood.* (2007) 109:2871–7. doi: 10.1182/blood-2006-07-036863
24. Chen W, Liang X, Peterson AJ, Munn DH, Blazar BR. The indoleamine 2,3-dioxygenase pathway is essential for human plasmacytoid dendritic cell-induced adaptive T regulatory cell generation. *J Immunol.* (2008) 181:5396–404. doi: 10.4049/jimmunol.181.8.5396
25. Chung DJ, Rossi M, Romano E, Ghith J, Yuan J, Munn DH, et al. Indoleamine 2,3-dioxygenaseexpressing mature human monocyte-derived dendritic cells expand potent autologous regulatory T cells. *Blood.* (2009) 114:555–63. doi: 10.1182/blood-2008-11-191197
26. Holmgaard RB, Zamarin D, Munn DH, Wolchok JD, Allison JP. Indoleamine 2,3-dioxygenase is a critical resistance mechanism in antitumor T-cell immunotherapy targeting cTLA4. *J Exp Med.* (2013) 210:1389–402. doi: 10.1084/jem.20130066
27. Platten M1, Wick W, Van den Eynde BJ. Tryptophan catabolism in cancer: Beyond IDO and tryptophan depletion. *Cancer Res.* (2012) 72:5435–40. doi: 10.1158/0008-5472.CAN-12-0569
28. Uyttenhove C1, Pilotte L, Théate I, Stroobant V, Colau D, Parmentier N, et al. Evidence for a tumoral immune resistance mechanism based on tryptophan degradation by indoleamine 2,3-dioxygenase. *Nat Med.* (2003) 9:1269–74 doi: 10.1038/nm934
29. Zamanakou M, Germenis AE, Karanikas V. Tumor immune escape mediated by indoleamine 2,3-dioxygenase. *Immunol Lett.* (2007) 111:69–75. doi: 10.1016/j.imlet.2007.06.001
30. Wang Y, Hu GF, Wang ZH. The status of immunosuppression in patients with stage III B or IV non-small-cell lung cancer correlates with the clinical characteristics and response to chemotherapy. *OncoTargets Ther.* (2017) 10:3557–66. doi: 10.2147/OTT.S136259
31. Li F, Zhao Y, Wei L, Li S, Liu J. Tumor-infiltrating Treg, MDSC, and IDO expression associated with outcomes of neoadjuvant chemotherapy of breast cancer. *Cancer Biol Ther.* (2018) 19:695–705. doi: 10.1080/15384047.2018.1450116
32. Zoso A, Mazza EM, Bicciato S, Mandruzzato S, Bronte V, Serafini P, et al. Human fibrocytic myeloid-derived suppressor cells express IDO and promote tolerance via Treg-cell expansion. *Eur J Immunol.* (2014) 44:3307–19. doi: 10.1002/eji.201444522

33. Pilotte L, Larrieu P, Stroobant V, Colau D, Dolusic E, Frederick R, et al. Reversal of tumoral immune resistance by inhibition of tryptophan 2,3-dioxygenase. *Proc Natl Acad Sci USA*. (2012) 109:2497–502. doi: 10.1073/pnas.1113873109
34. Metz R, Duhadaway JB, Kamasani U, Laury-Kleintop L, Muller AJ, Prendergast GC., et al. Novel tryptophan catabolic enzyme IDO2 is the preferred biochemical target of the antitumor indoleamine 2,3-dioxygenase inhibitory compound D-1-methyl-tryptophan. *Cancer Res.* (2007) 67:7082–7. doi: 10.1158/0008-5472.CAN-07-1872
35. Lob S, Konigsrainer A, Schafer R, Rammensee HG, Opelz G, Terness P. Levo- but not dextro-1-methyl tryptophan abrogates the IDO activity of human dendritic cells. *Blood.* (2008) 111:2152–4. doi: 10.1182/blood-2007-10-116111
36. Meininger D, Zalameda L, Liu Y, Stepan LP, Borges L, McCarter JD, et al. Purification and kinetic characterization of human indoleamine 2,3-dioxygenases 1 and 2 (IDO1 and IDO2) and discovery of selective IDO1 inhibitors. *Biochim Biophys Acta.* (2011) 1814:1947–54. doi: 10.1016/j.bbapap.2011.07.023
37. Botticelli A, Cerbelli B, Lionetto L, Zizzari I, Salati M, Pisano A, et al. Can IDO activity predict primary resistance to anti-PD-1 treatment in NSCLC? *J Transl Med.* (2018) 16:219. doi: 10.1186/s12967-018-1595-3
38. Osorio JC, Arbour KC, Le DT, Durham JN3, Plodkowski AJ1, Halpenny DF, et al. Lesion-level response dynamics to programmed cell death protein (PD-1) blockade. *J Clin Oncol.* (2019) 37:3546–55. doi: 10.1200/JCO.19.00709
39. Botticelli A, Salati M, Di Pietro FR, Strigari L, Cerbelli B, Zizzari IG, et al. A nomogram to predict survival in non-small cell lung cancer patients treated with nivolumab. *J Transl Med.* (2019) 17:99. doi: 10.1186/s12967-019-1847-x
40. Botticelli A, Cirillo A, Scagnoli S, Cerbelli B, Strigari L, Cortellini A, et al. The agnostic role of site of metastasis in predicting outcomes in cancer patients treated with immunotherapy. *Vaccines (Basel).* (2020) 8:E203. doi: 10.3390/vaccines8020203
41. Capone I, Marchetti P, Ascierto PA, Malorni W, Gabriele L. Sexual dimorphism of immune responses: a new perspective in cancer immunotherapy. *Front Immunol.* (2018) 9:552. doi: 10.3389/fimmu.2018.00552
42. Conforti F, Pala L, Bagnardi V, De Pas T, Martinetti M, Viale G, et al. Cancer immunotherapy efficacy and patients' sex: a systematic review and meta-analysis. *Lancet Oncol.* (2018) 19:737–46. doi: 10.1016/S1470-2045(18)30261-4
43. Ferns DM, Kema IP, Buist MR, Nijman HW, Kenter GG, Jordanova ES., et al. Indoleamine-2,3-dioxygenase (IDO) metabolic activity is detrimental for cervical cancer patient survival. *Oncoimmunology.* (2015) 4:e981457. doi: 10.4161/2162402X.2014.981457
44. Zhang G, Liu WL, Zhang L, Wang JY, Kuang MH, Liu P, et al. Involvement of indoleamine 2,3-dioxygenase in impairing tumor-infiltrating CD8 T-cell functions in esophageal squamous cell carcinoma. *Clin Dev Immunol.* (2011) 2011:384726. doi: 10.1155/2011/384726
45. Laimer K, Troester B, Kloss F, Schafer G, Obrist P, Perathoner A, et al. Expression and prognostic impact of indoleamine 2,3-dioxygenase in oral squamous cell carcinomas. *Oral Oncol.* (2011) 47:352–7. doi: 10.1016/j.oraloncology.2011.03.007
46. Aparicio LMA, Fernandez IP, Cassinello J. Tyrosine kinase inhibitors reprogramming immunity in renal cell carcinoma: rethinking cancer immunotherapy. *Clin Transl Oncol.* (2017) 19:1175. doi: 10.1007/s12094-017-1657-7
47. Finke JH1, Rini B, Ireland J, Rayman P, Richmond A, Golshayan A, et al. Sunitinib reverses type-1 immune suppression and decreases T-regulatory cells in renal cell carcinoma patients. *Clin Cancer Res.* (2008) 15:6674–82. doi: 10.1158/1078-0432.CCR-07-5212
48. Ko JS1, Zea AH, Rini BI, Ireland JL, Elson P, Cohen P, et al. Sunitinib mediates reversal of myeloid-derived suppressor cell accumulation in renal cell carcinoma patients. *Clin Cancer Res.* (2009) 15:2148–57. doi: 10.1158/1078-0432.CCR-08-1332
49. Huang Y, Wang Y, Li Y, Guo K, He Y. Role of sorafenib and sunitinib in the induction of expressions of NKG2D ligands in nasopharyngeal carcinoma with high expression of ABCG2. *J Cancer Res Clin Oncol.* (2011) 137:829–37. doi: 10.1007/s00432-010-0944-2
50. de Biasi AR, Villena-Vargas J, Adusumilli PS. Cisplatin-induced antitumor immunomodulation: a review of preclinical and clinical evidence. *Clin Cancer Res.* (2014) 20:5384–91. doi: 10.1158/1078-0432.CCR-14-1298
51. Prendergast GC, Malachowski WJ, Mondal A, Scherle P, Muller AJ. Indoleamine 2,3-dioxygenase and its therapeutic inhibition in cancer. *Int Rev Cell Mol Biol.* (2018) 336:175–203. doi: 10.1016/bs.ircmb.2017.07.004
52. Platten M, von Knebel Doeberitz N, Oezen I, Wick W, Ochs K. Cancer immunotherapy by targeting IDO1/TDO and their downstream effectors. *Front Immunol.* (2014) 5:673. doi: 10.3389/fimmu.2014.00673
53. van Baren N, Van den Eynde BJ. Tumoral immune resistance mediated by enzymes that degrade tryptophan. *Cancer Immunol Res.* (2015) 3:978–85. doi: 10.1158/2326-6066.CIR-15-0095
54. Le DT, Durham JN, Smith KN, Wang H, Bartlett BR, Aulakh LK, et al. Mismatch repair deficiency predicts response of solid tumors to PD-1 blockade. *Science.* (2017) 357:409–13. doi: 10.1126/science.aan6733
55. Le DT, Uram JN, Wang H, Bartlett BR, Kemberling H, Eyring AD, et al. PD-1 blockade in tumors with mismatch-repair deficiency. *N Engl J Med.* (2015) 372:2509–20. doi: 10.1056/NEJMoa1500596
56. Prendergast GC, Malachowski WP, DuHadaway JB, Muller AJ. Discovery of IDO1 inhibitors: from bench to bedside. *Cancer Res.* (2017) 77:6795–811. doi: 10.1158/0008-5472.CAN-17-2285
57. Mitchell TC, Hamid O, Smith DC, Bauer TM, Wasser JS, Olszanski AJ, et al. Epacadostat plus pembrolizumab in patients with advanced solid tumors: phase I results from a multicenter, open-label phase I/II trial (ECHO-202/KEYNOTE-037). *J Clin Oncol.* (2018) 36:JCO2018789602. doi: 10.1200/JCO.2018.78.9602
58. Zakharia Y RO, Rixe O, Ward JH, Drabick JJ, Shaheen MF, Phase 2 trial of the IDO pathway inhibitor indoximod plus checkpoint inhibition for the treatment of patients with advanced melanoma. *J Clin Oncol.* (2018) 36:9512. doi: 10.1200/JCO.2018.36.15_suppl.9512
59. Long GV, Dummer R, Hamid O, Gajewski TF, Caglevic C, Dalle S, et al. Epacadostat plus pembrolizumab versus placebo plus pembrolizumab in patients with unresectable or metastatic melanoma (ECHO-301/KEYNOTE-252): a phase 3, randomised, double-blind study. *Lancet Oncol.* (2019) 20:1083–97. doi: 10.1016/S1470-2045(19)30274-8
60. Koyama S, Akbay EA, Li YY, Herter-Sprie GS, Buczkowski KA, Richards WG, et al. Adaptive resistance to therapeutic PD-1 blockade is associated with upregulation of alternative immune checkpoints. *Nat Commun.* (2016) 7:10501. doi: 10.1038/ncomms10501
61. Thommen DS, Schreiner J, Müller P, Herzig P, Roller A, Belousov A, et al. Progression of lung cancer is associated with increased dysfunction of T cells defined by coexpression of multiple inhibitory receptors. *Cancer Immunol Res.* (2015) 3: 1344–55. doi: 10.1158/2326-6066.CIR-15-0097

Conflict of Interest: PM has/had a consultant/advisory role for BMS, Roche, Genentech, MSD, Novartis, Amgen, Merck Serono, Pierre Fabre, and Incyte.

The remaining authors declare that the research was conducted in absence of any commercial or financial relationship that could be construed as a potential conflict of interest.

frontiers in Immunology

ORIGINAL RESEARCH
published: 14 August 2020
doi: 10.3389/fimmu.2020.01244

The Prognostic Value of Indoleamine-2,3-Dioxygenase Gene Expression in Urine of Prostate Cancer Patients Undergoing Radical Prostatectomy as First Treatment of Choice

Michael Thüring[1], *Robin Knuchel*[1], *Ludovica Picchetta*[1], *Daniel Keller*[1], *Tobias S. Schmidli*[1] *and Maurizio Provenzano*[1,2]*

[1] Oncology Research Unit, Department of Urology, University Hospital of Zurich, Zurich, Switzerland, [2] Department of Immunology, University Hospital of Zürich, Zurich, Switzerland

OPEN ACCESS

Edited by:
Lieve Brochez,
Ghent University, Belgium

Reviewed by:
Christopher Zahm,
University of Wisconsin-Madison, United States
Benjamin Bonavida,
University of California, Los Angeles, United States

***Correspondence:**
Maurizio Provenzano
maurizio.provenzano@usz.ch

Specialty section:
This article was submitted to Cancer Immunity and Immunotherapy, a section of the journal Frontiers in Immunology

Received: *18 September 2019*
Accepted: *18 May 2020*
Published: *14 August 2020*

Citation:
Thüring M, Knuchel R, Picchetta L, Keller D, Schmidli TS and Provenzano M (2020) The Prognostic Value of Indoleamine-2,3-Dioxygenase Gene Expression in Urine of Prostate Cancer Patients Undergoing Radical Prostatectomy as First Treatment of Choice. Front. Immunol. 11:1244. doi: 10.3389/fimmu.2020.01244

Prostate cancer (PCa) is a slow-growing tumor representing one of the major causes of all new cancer cases and cancer mortality in men worldwide. Although screening methods for PCa have substantially improved, the outcome for patients with advanced PCa remains poor. The elucidation of the molecular mechanism that drives the progression from a slow-growing, organ-confined tumor to a highly invasive and castration-resistant PCa (CRPC) is therefore important. We have already proved the diagnostic potential of indoleamine-2,3-dioxygenase (IDO) when detected in urine of individuals at risk of developing PCa. The aim of this study was to implement IDO as a prognostic marker for PCa patients undergoing surgical treatment. We have thus conducted an observational study by collecting 100 urine samples from patients undergoing radical prostatectomy as first treatment of choice. To test the integrity of our investigation, scale dilution cells of an established PC3 cell line were added to urine of healthy donors and used for gene expression analysis by a TaqMan assay on the catalytic part of IDO mRNA. Our data show that the quantification of IDO mRNA in urine of patients has a very promising ability to identify patients at high risk of cancer advancement, as defined by Gleason score. Our goal is to lay the groundwork to develop a superior test for PCa. The data generated are thus necessary (i) to strengthen the IDO-based diagnostic/prognostic test and (ii) to provide patients and clinicians with an affordable and easy screening test.

Keywords: prostate cancer, IDO—indoleamine 2,3-dioxygenase, prognostic marker, liquid biopsy, radical prostatectomy, immune regulation, inflammation

INTRODUCTION

Prostate cancer (PCa) represents the first leading cause of cancer morbidity and the third of cancer death in men in developed countries, with a worldwide incidence rate accounting for 14% of total newly diagnosed cases and a worldwide total cancer mortality rate of 6% (1). It is of relevance that prostate tissues appear to be characterized by features consistent with an

immunosuppressive microenvironment. Infiltrating $CD4^+$ and $CD8^+$ T lymphocytes (TILs) are predominantly characterized by regulatory (2, 3) and functionally exhausted (PD-1+, B7-H1+) phenotypes (4–6). Furthermore, enhanced suppressive function of adaptive $CD4^+$ Treg has been observed in the peripheral blood of patients with PCa and found to correlate with metastatic behavior (7).

The tumor microenvironment is the battlefield where not well-defined relationships between oncogenesis and immune surveillance to cancer take place. Tumor immune escape occurs through the secretion of different tumor-derived factors (TDFs) with immunosuppressive properties, such as indoleamine-2,3-dioxygenase (IDO). The specific IDO gene product plays a key role in tryptophan metabolism, and its enhanced activities might result in both the depletion of an amino acid essential for lymphocyte metabolism and in the generation of toxic metabolites (8).

The significant correlation between levels of expression of IDO and its activity (kynurenine/tryptophan ratio) in PCa specimens, the trend seen in relation to PCa patients' clinical features [Gleason score (GS)], and the finding that TGF-β expression was significantly correlated to IDO gene expression in PCa contributed to the identification of a peculiar subset of tumors (9). A high level of IDO has been reported to be correlated with poor clinical prognosis in cancers, such as ovarian cancer (10), endometrial cancer (11), colon carcinomas (12), malignant melanoma (13), and lung cancer (14). In renal cell carcinoma, levels of IDO mRNA in primary tumors or metastasis do not correlate with longer overall survival. In this specific setting, IDO was nearly exclusively expressed in endothelial cells of predominantly newly formed blood vessels, not in tumor cells, a condition that presumably inhibits tumor growth due to amino acid tryptophan depletion to cancer cells (15).

Currently, the selection of patients at risk of PCa and the indication for biopsy are based on the combination of prostate-specific antigen (PSA) blood test and the digital rectal examination (DRE) of the organ (16). Although PSA is the most commonly used screening parameter, it has a relatively poor specificity for PCa, which means that patients with benign prostate hyperplasia (BPH) or prostatitis might show higher PSA values and might therefore undergo unnecessary biopsies (17, 18).

To secure the diagnosis of PCa and to determine further therapeutic interventions, a fine-needle biopsy is necessary, although prostate sampling might be inconsistent at early stages (19, 20). In addition, complications like hematuria, hematospermia, and infection can occur during the procedure (21). Therefore, unnecessary costs and complications should be avoided for patients bearing no cancer lesions or an indolent form. A reliable biomarker that could identify without the use of biopsy patients with early aggressive or clinically significant tumors and rule them out while being easy to collect in a non-invasive procedure would be ideal (21, 22).

We have identified that the enzyme IDO could serve as a novel diagnostic biomarker for PCa in urine. We have developed a novel diagnostic approach based on the IDO mRNA and/or protein levels. Our current data show that the quantification of IDO mRNA in urine of patients has a very promising ability to identify patients harboring PCa (23). Because patients with higher expression of IDO in PCa at first diagnosis showed a significantly higher risk of tumor recurrence after prostatectomy, IDO may furthermore be used also as a recurrence marker.

Therefore, in this study, we evaluated the prognostic value of IDO gene expression in urine of PCa patients undergoing radical prostatectomy (RP) as first-line treatment. Urine was collected preoperatively, and results were correlated with clinicopathological characteristics.

MATERIALS AND METHODS

Patients' Accrual and Clinicopathological Characteristics

We evaluated a case series of 100 patients bearing PCa at first diagnosis and undergoing RP as first treatment of choice in our institution between June 2016 and June 2017. Relevant clinical data were collected by reviewing patients' files. Clinicopathological parameters (PSA levels, tumor stage, and GS were assigned according to European Association of Urology (EAU) guidelines for PCa; uroweb.org/guidelines/prostate-cancer/). Local ethics committee approval and written informed consent from patients were obtained in accordance with the requirements of the Ethical Committee of Zürich (BASEC_2018-02101).

Urine Processing

Urine of 20 to 50 ml was voided in DNA/RNA preservative cups (Sierra Diagnostic, USA) before RP. Depending on amount of urine collected, two-way processing was carried out: (i) for 20–50 cm^3 of urine, the extraction of RNA was performed by using urine pellet generated after urine centrifugation at 2,000 rpm for 10 min at 4°C. (ii) For limited amount of urine (<20 cm^3), the quantification of cell-free RNA was considered, and urine samples were aliquoted at 500 µl each test. Either pellet or cell-free RNA urine was treated with 700 µl of lysis solution (Ambion, USA), stored at −80°C or immediately used for RNA extraction (Ambion, USA). Total urine was used to test IDO enzymatic activity through the L-kynurenine/tryptophan ratio, as analyzed by ELISA (Immundiagnostik).

Established Prostate Cancer Cell Line Spiked in Patients' Urine

PC3 is an established cells line from bone metastasis and produces a high level of IDO constitutively (23). PC3 was cultured in Roswell Park Memorial Institute (RPMI) 1640 medium containing 2 mM of L-glutamine (Invitrogen, Carlsbad, CA) together with 10% fetal bovine serum (Atlanta Biologicals, Lawrenceville, GA), 100 U/ml of penicillin, and 100 µg/ml of streptomycin. Urine from healthy donors spiked with PC3 was used as control or to validate our system. Accordingly, IDO gene expression was tested by plating PC3 cell line in four different sized growing areas (150, 75, 25, and 6 cm^2) and cultured for 72 h, as previously described by us in Poyet et al. (24). Cells were harvested at about 90% confluence. Scale dilution of cells was added to urine of HD, and pellet was used for gene expression.

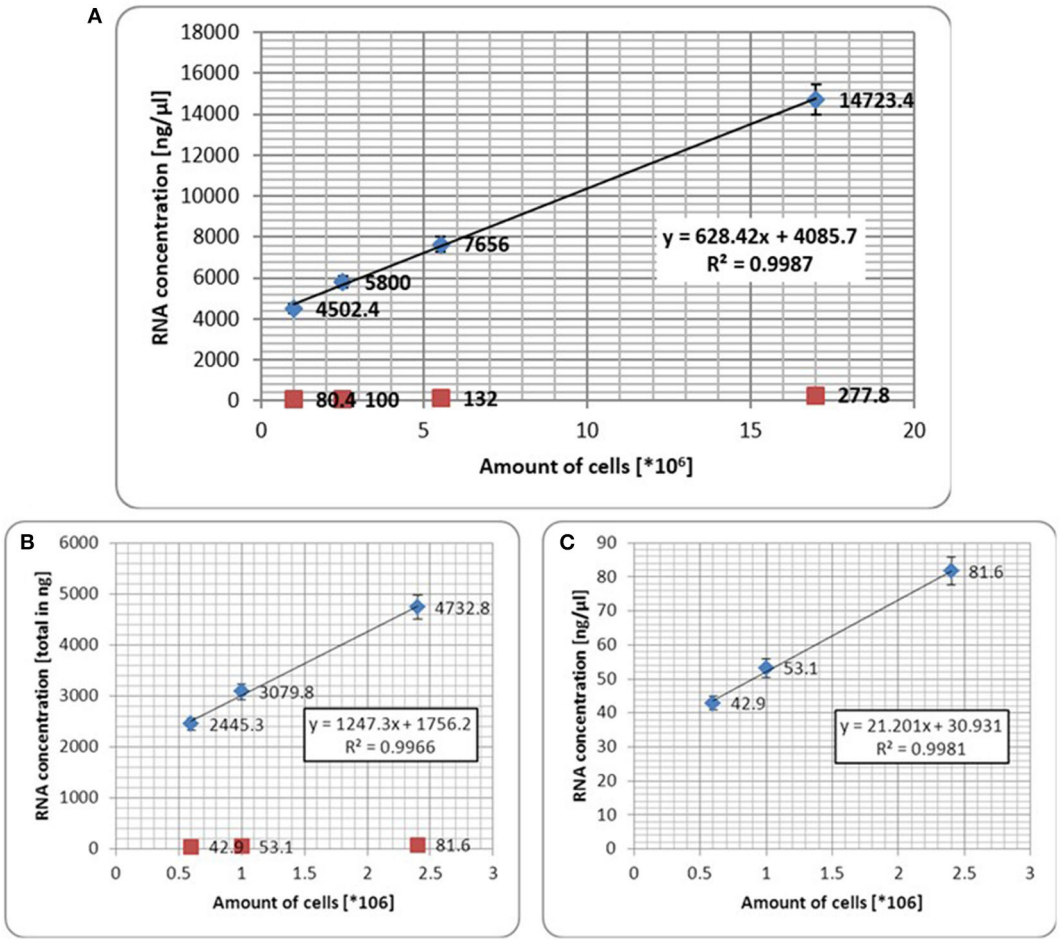

FIGURE 1 | (A) Correlation between scale dilution of established PC3 cells line and total RNA extraction. Red dots represent number of seeded cells *per* growing area (6, 25, 75, and 150 cm^2, respectively); blue dots represent amount of extracted total RNA from harvested cells *per* growing area (6, 25, 75, and 150 cm^2, respectively). The test shows that correlation between number of harvested cells $<1 \times 10^6$ and total RNA **(B)** or RNA in ng/µl **(C)** was markedly confirmed. Error bars represent the mean ± SD of three replicates.

Gene Expression Analysis

Total RNA extraction was performed by using the RNAqueous Kit according to the manufacturer's protocol (Applied Biosystems, USA). After extraction, RNA undertook DNase treatment and was subsequently retrotranscribed into cDNA (High Capacity cDNA Reverse Transcription Kit, Applied Biosystems). Quantitative gene amplification (qRT-PCR) was set up according to standard real-time PCR protocols using a Corbett Life Science Rotor-gene 3000 instrument (Corbett Life Science, Sydney, Australia) using TaqMan® Universal PCR Master Mix Reagents Kit (Labgene) and "on demand" sets of primers and probes for housekeeping genes (RNA ribosomal 18S and β-actin) (Thermo Fisher, Switzerland). The IDO assay (Custom TaqMan primers and probe design; Applied Biosystems) was designed to cover the exon–exon junction between exons 9 and 10. Primers were designed to allow a melting temperature of between 58 and 61°C, with an optimal length of 20 bp and CG content between 30 and 80%. The probe was designed not to start with G and in order to have a melting temperature 10°C higher than the one of the primers. A 3′ minor grove binder-probe [non-fluorescent quencher fitting the 5(6)-carboxyfluorescein (FAM) spectral qualities] was used. Primers and probe were used at a final concentration of 400 and 200 nM, respectively. TaqMan assay sequences are described in patent "INDOLEAMINE-2,3-DIOXYGENASE ASSAY FOR PROSTATE CANCER DIAGNOSIS AND PROGNOSIS" https://worldwide.espacenet.com/publicationDetails/biblio?II=0&ND=3&adjacent=true&locale=en_EP&FT=D&date=20180419&CC=WO&NR=2018069494A1&KC=A1#.

One microliter of cDNA was loaded into the TaqMan reaction mix, and reactions were run in a final volume of 20 µl. The reaction conditions were set accordingly to the manufacturer's instructions (TaqMan Gene Expression Master Mix, Applied Biosystems, USA). The absolute quantification of each gene's copies was calculated through the generation of a standard curve by serial dilution of synthetic oligonucleotides. Data were

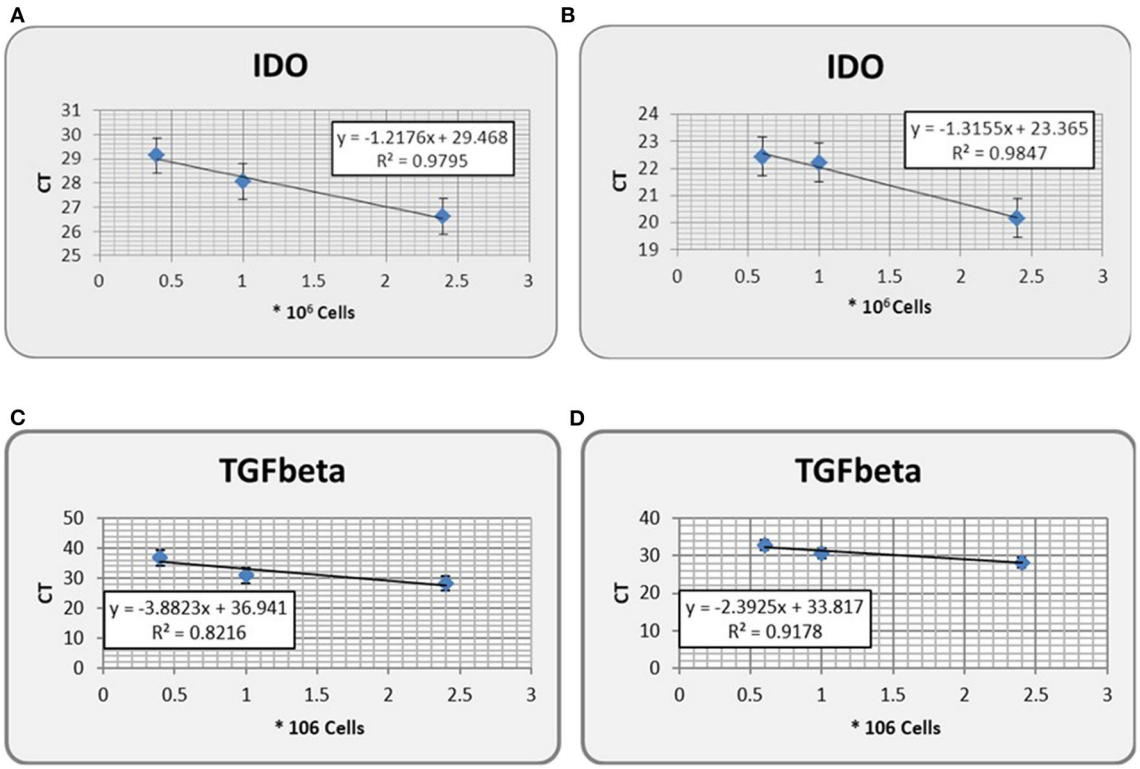

FIGURE 2 | IDO gene expression (in CT, threshold cycle) from non spiked PC3 urine of healthy donors **(A)**, as compared with its expression from PC3-spiked counterpart **(B)**. Gene expression of TGF-β, a tumor-derived soluble factor involved in PCa progression, in either non spiked PC3 **(C)** or PC3-spiked **(D)** urine, has been used as control. Error bars represent the mean ± SD of three replicates. IDO, indoleamine-2,3-dioxygenase.

then given in copies per milliliter of urine. Where appropriate, RNA ribosomal 18S and β-actin were used as endogenous reference genes, and normalized data were be analyzed by the $2^{-\Delta\Delta Ct}$ method.

Measurement of Tryptophan, Kynurenine, and Quinolinic Acid Concentration

IDO activity was measured in urine and performed as L-kynurenine vs. L-tryptophan (Kyn/Trp ratio) or quinolinic acid A vs. L-tryptophan (Q-A/Trp ratio) concentrations by ELISA according to manufacturer's instructions (Immundiagnostik, Bensheim, Germany). In addition, IDO protein release in urine of patients was analyzed as well by ELISA (Immundiagnostik, Bensheim, Germany).

Statistical Analysis

Statistical analysis was performed with GraphPad Prism (v5.1) and SPSS (v23). Non-parametric tests for gene expression levels (Mann–Whitney *U*-test and Kruskal–Wallis test) were run. Categorical variables were evaluated by contingency table analyses and Pearson chi-square test or Fisher exact test, as appropriate. Two-sided $p < 0.05$ (95% CI) were considered statistically significant. The performance of IDO as prognostic factor in PCa was evaluated by calculating the area under the receiver operating characteristic (ROC) curve (AUC). Previous cutoffs were confirmed by sensitivity, specificity, positive predictive value (PPV), and negative predictive value (NPV) of the test.

RESULTS

Indoleamine-2,3-Dioxygenase Gene Expression in Urine Represents a Valuable Test for Prostate Cancer Prognosis by Liquid Biopsy

To test the integrity of our investigation, which is the positive correlation between IDO gene expression in urine and number of cancer cells, PC3 cells were spiked in urine of healthy donors at various concentrations, as described in the *Materials and Methods*. To standardize IDO gene expression, the number of harvested cells was correlated with the amount of total RNA extracted after cell harvesting.

We first observed a positive correlation between number of cells harvested and total RNA extracted (**Figure 1A**). We additionally observed that the correlation between number of cells $<1 \times 10^6$ and RNA concentration, either total (**Figure 1B**) or in ng/μl (**Figure 1C**) was markedly confirmed ($R^2 < 0.9$). To mimic prostate massage yield, the same numbers of cells were spiked into urine. We observed that IDO gene expression was confirmed as equal as IDO gene expression from non-spiked

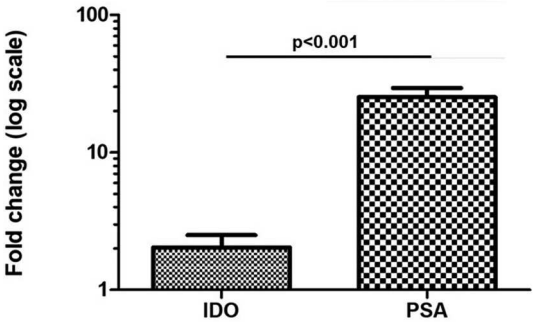

FIGURE 3 | Fold change in IDO and PSA gene expression in five PCa patients before/after DRE. Amount of IDO mRNA is significantly maintained in urine of PCa patients undergoing DRE (∼2-fold-increase), as compared with its expression in urine of same PCa patients before DRE. Differently, PSA value abundantly increased over 2-fold. Error bars represent the mean ± SD of three replicates. IDO, indoleamine-2,3-dioxygenase; PSA, prostate-specific antigen; PCa, prostate cancer; DRE, digital rectal examination.

cells (**Figures 2A,B**), although ΔCt between spiked and non-spiked urine was of about 2logs ($p > 0.5$). In addition, IDO gene expression showed a linear regression value higher than TGF-β gene expression, a cytokine constitutively expressed in PC3 cell lines (**Figures 2C,D**). Despite spiked urine showing higher IDO gene expression, the latter is not markedly strong to justify the use of prostate massage for IDO testing.

Detection of Indoleamine-2,3-Dioxygenase Gene in Urine Does Not Need Prostate Massage and Can Be Performed Either by Urine Pellet or by Cell-Free RNA

One of the major limitations in performing gene expression in urine is the amount of RNA. For PCa diagnosis, this hurdle can be overcome by squeezing the organ through a prostate massage and extracting RNA from urine pellet. However, prostate massage is not always feasible. We analyzed IDO gene expression in urine of five patients undergoing PCa standard diagnosis (PSA level + DRE) collected before and after DRE. PSA gene expression was used as control. We observed that change in IDO gene expression was abundantly lower (∼2-fold) than that of PSA (30-fold; $p < 0.001$; **Figure 3**). In addition, no significant differences for IDO gene expression were observed between pellet and cell-free RNA of urine collected before DRE (data not shown).

The Prognostic Potential of Indoleamine-2,3-Dioxygenase for Diagnosed Prostate Cancer Can Redirect Treatment Options

Out of 100 patients enrolled in this study, 20 were excluded owing to lack of complete clinicopathological parameters (TNM and GS after RP) and limited amount of material for IDO gene expression (rRNA 18S almost negligible; Ct > 30). By distributing patients on the basis of GS (GS ≤ 7; $n = 60$ and GS ≥ 8; $n = 20$), we found a significant variation for IDO gene expression in urine (GS ≤ 7 = mean 0.029 ± 0.046; median 0.012; GS ≥ 8 = 0.031 ± 0.075; median 0.033; $p < 0.01$; **Figure 4A**). To better determine the association between IDO gene expression in urine and cancer aggressiveness, we distributed patients on the basis of all GS patterns from GS = 7 to GS = 10 (no GS = 6 was reported, because indolent patients preferably undergo active surveillance). Therefore, we grouped our patients as follows: GS = 7 (3 + 4), $n = 32$; GS = 7 (4 + 3), $n = 28$; GS = 8, $n = 12$; and GS = 9 (4 + 5), $n = 8$. No PCa with GS = 9 (5 + 4) or GS = 10 was reported in our group of patients. A Kruskal–Wallis test was initially run to test mean variations among groups ($p < 0.01$). We found a significant difference of IDO gene expression in urine between patients with GS = 7 (3 + 4) and GS = 7 (4 + 3) ($p = 0.03$), GS = 8 ($p < 0.01$), and GS = 9 (4 + 5) ($p < 0.01$), whereas no significant differences were observed between GS = 7 (4 + 3) and higher scores [GS = 8 and GS = 9 (4 + 5)] (**Figure 4B**). Notably, no significant differences were observed for TNM distribution (data not shown).

To confirm the cutoff value previously defined (23), we run two ROC curves tests comparing PCa with GS = 7 (3 + 4) vs. GS = 7 (4 + 3)/higher score and GS ≤ 7 vs. GS ≥ 8. The AUC to dichotomize patients with indolent or aggressive PCa on the basis of on GSs either partially confirmed or ameliorated the sensitivity and specificity of the test calculated with the cutoff level defined previously (0.0096). Indeed, for GS = 7 (3 + 4) vs. GS = 7 (4 + 3)/higher score, the best cutoff level was 0.0123 (sensitivity 61% and specificity 60%), whereas at the cutoff level of 0.0096, the sensitivity was 70% and the specificity 53% (**Figure 4C**). Differently, for GS ≤ 7 vs. GS ≥ 8, the best cutoff level was 0.0288 (sensitivity 71% and specificity 78%), whereas at cutoff level of 0.0096, the sensitivity was 61% and the specificity was 60% (**Figure 4D**).

Indoleamine-2,3-Dioxygenase Enzymatic Activity Might Predict Prostate Cancer Clinical Outcome

To confirm previous finding, the IDO activity (Kyn/Trp ratio or Q-A/Trp ratio) and IDO protein release were analyzed in 15 selected PCa patients with different GS (7 to 9). In keeping with IDO mRNA expression in urine, IDO activity characterized by Q-A/Trp ratio correlated with GS (7–9) (R^2 0.88, $p < 0.001$; **Figure 5A**), whereas activity by Kyn/Trp ratio did not (data not shown). In addition, IDO protein release (ng/ml) showed a tendency with GS (7–9) ($p = 0.07$), although the correlation was inversed and not significant (R^2 0.24, $p = 0.3$; **Figure 5B**).

DISCUSSION

PCa is the most frequently diagnosed cancer among men in first-world countries and one of the leading causes of cancer-related death in men (22).

The management of PCa is still difficult, as indolent tumors often do not have any effect on the patient's life expectancy and therefore need a minimum or no treatment. In contrast, aggressive forms can grow and metastasize

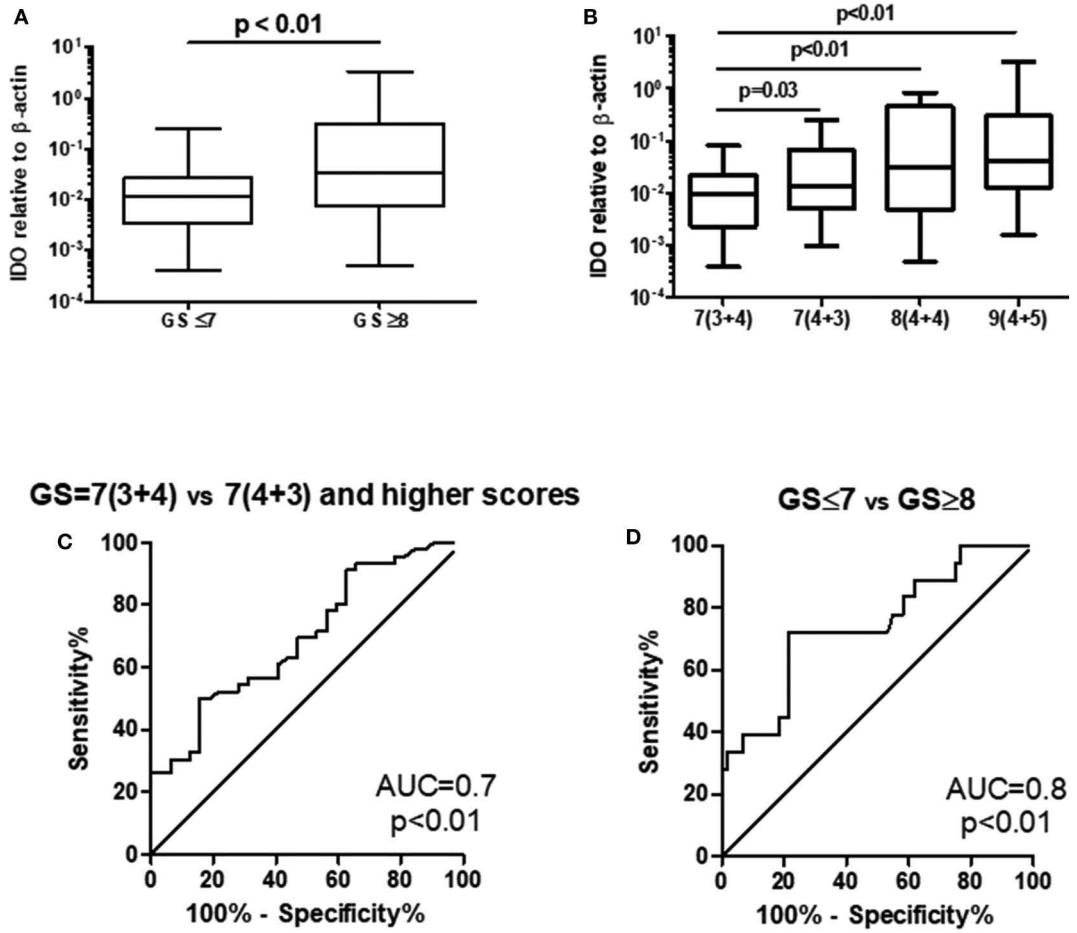

FIGURE 4 | IDO gene expression correlated with Gleason score either **(A)** when comparing GS ≤ 7 vs. GS ≥ 8 or **(B)** when expressing single GS patterns. A ROC (AUC 0.7) **(C)** that compared Gleason score 7 (3 + 4) vs. 7 (4 + 3)/higher failed to confirm a previously defined cutoff for discriminating indolent vs. aggressive PCa, while a ROC (AUC 0.8) **(D)** that compared GS ≤ 7 vs. GS ≥ 8 did confirm a previous cutoff for discriminating indolent vs. aggressive PCa. IDO, indoleamine-2,3-dioxygenase; GS, Gleason score; ROC, receiver operating characteristic; AUC, area under the ROC curve; PCa, prostate cancer.

quickly, which often leads to life-impairing consequences (25). For clinical stratification, the PSA, tumor size, and GS are being used.

Recently, urine-based biopsy has been considered the gold standard owing to the non-invasive procedure for their collection. Indeed, there are many new approaches that use urine as liquid biopsy for PCa diagnosis/prognosis, such as circulating tumor cells (26) and cell-free DNA (27) tests.

Recent studies showed the potential of IDO as such a novel marker (9, 23). The enzyme IDO is expressed in many tumor types including PCa and seems to contribute to the tumor's immunosuppressive abilities by converting tryptophan into kynurenine (28–30). It was shown that immunohistochemically measured IDO gene expression in prostate biopsies is highly specific for PCa (9). However, a clinically more viable way of measuring is required. A urine-based analysis of IDO RNA expression of men at risk of PCa development showed that it could reduce the number of unnecessary biopsies by 14.8–66.6% depending on the cutoff level (23).

Clinicians need a reliable, easy-to-handle, and affordable screening test. The IDO mRNA-based assay is possible in clinical/practitioner's routine. In our opinion, this IDO gene expression analysis in urine of PCa patients is stronger than a protein test in terms of sensitivity and affordability. Further investigation on larger cohort of patients is needed to confirm the results achieved at both studies with enough statistical power; to finalize the final procedures for a better detection of IDO; to rate with accurate estimation the sensitivity of this test; and to evaluate in more detail the significance of IDO localization in biopsies as a marker for the risk of biochemical recurrence.

The PSA blood test, despite being the gold standard for PCa active surveillance and recurrence, has several limitations for screening patients at risk of PCa. This is due to the following: (i) PSA is organ specific but not tumor specific. Elevated levels of PSA can be found in other pathologies (benign prostatic hyperplasia, and acute prostatitis) or in physiological conditions, such as age increase and sexual activity; (ii) PSA test lacks sensitivity because only 25% of patients with PSA of between 2.5

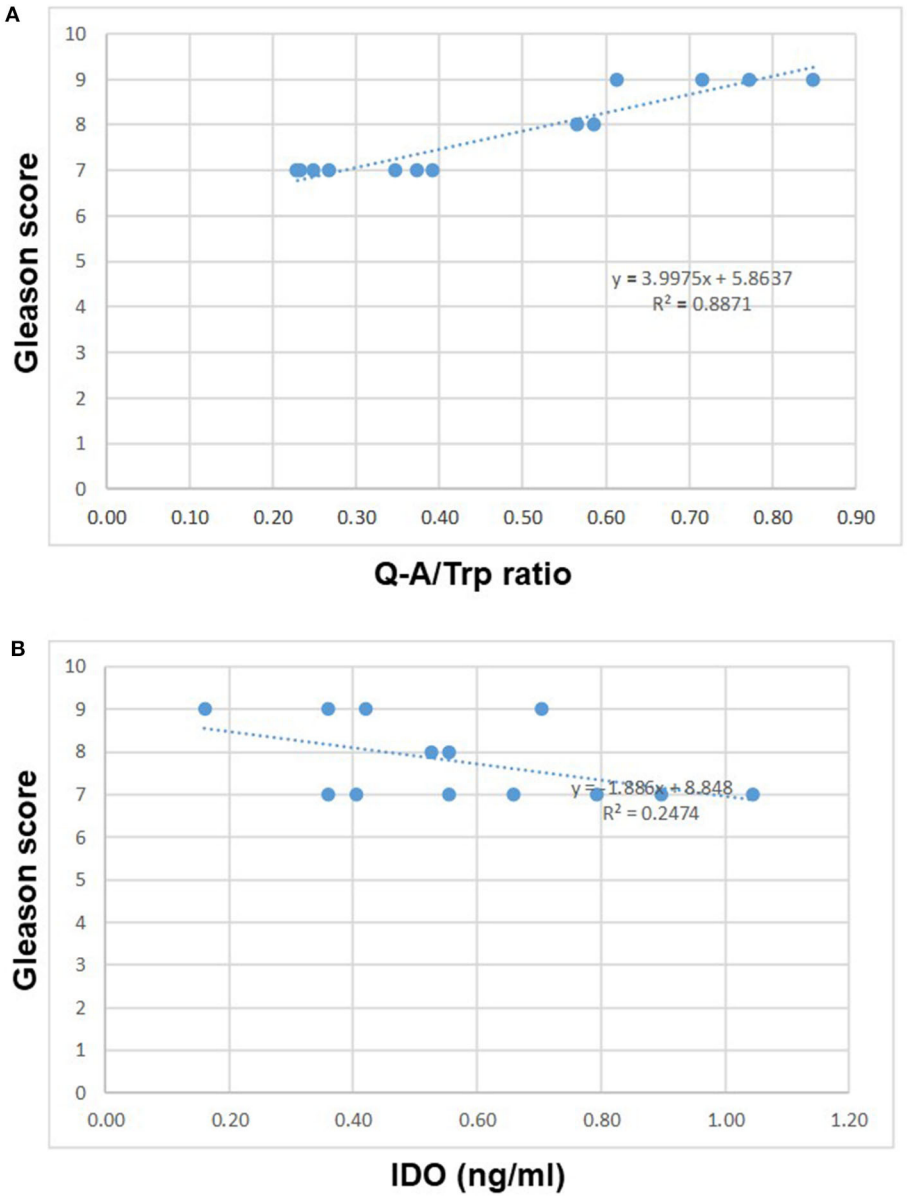

FIGURE 5 | IDO activity characterized by Q-A/Trp ratio in 15 selected PCa with different GS (7–9) correlated with GS (R^2 0.88, $p < 0.001$ **(A)**. Differently, IDO protein release (ng/ml) inversely correlated with GS **(B)**. IDO, indoleamine-2,3-dioxygenase; PCa, prostate cancer; GS, Gleason score.

and 10 ng/ml, *gray zone*, show positive biopsies; and (iii) PSA is not indicative of tumor staging and grading alone.

Improving current methods for screening of patients is therefore of great importance and will positively affect a significant part of the population. We have identified IDO as an important player in the mechanisms that regulate PCa progression and clarified its role and activity in these settings. Tumor cells expressing IDO have a higher chance of escaping the immune surveillance, and due to the presence of IFNγ and TNFα in the tumor microenvironment, they have a greater ability to migrate and invade. Furthermore, patients with higher expression of IDO in PCa at first diagnosis showed a significantly higher risk of tumor recurrence after prostatectomy.

Particularly in PCa, the expression of tumor-derived soluble factors (TDSFs) able to impair the functions of immune system in patients has been defined by us in Banzola et al. (23). In this context, we previously observed that cytokine possibly involved in PCa progression (such as IL-6) was found significantly higher expressed in PCa specimens, as compared with BPH (9). This information was confirmed by cytokine detection in sera of PCa patients (31).

In addition, arginase production by macrophages infiltrating prostatic tissues has been shown to favor the induction of anergy in resident lymphocytes (4). In this context, cytokines might play a relevant role in coordinating cancer immunoediting (32).

In conclusion, we proved that the quantification of IDO mRNA in the urine of PCa patients is a potential prognostic tool for this malignancy. This dataset is large enough to support the use of IDO as a recurrent marker in PCa patients undergoing RP as the first treatment of choice. However, in order to strengthen IDO as a robust prognostic marker for the identification of patients at higher risk of PCa recurrence, additional data on clinical samples from a larger cohort and the improvement of data acquisition for a more reliable IDO enzymatic activity are needed. Thus, the IDO detection in the urine of PCa patients could contribute, together with the standard parameters for the diagnosis/prognosis of this disease, to improve its outcome.

DATA AVAILABILITY STATEMENT

The datasets generated for this study are available on request to the corresponding author.

ETHICS STATEMENT

The studies involving human participants were reviewed and approved by Ethical Committee of Zürich (BASEC_2018-02101). The patients/participants provided their written informed consent to participate in this study.

AUTHOR CONTRIBUTIONS

MP conceived the study and supervised the project. MT, DK, RK, LP, and TS performed the experiments. MT, DK, RK, LP, and MP analyzed the data. MT, RK, and TS performed sample collection. MT, RK, TS, and MP arranged clinical aspect. TS and MP wrote informed consent. MT and MP wrote the paper. All authors contributed to the article and approved the submitted version.

FUNDING

This study was supported by Technologietransfer der Universitäten Basel, Bern und Zürich.

REFERENCES

1. Jemal A, Bray F, Center MM, Ferlay J, Ward E, Forman D. Global cancer statistics. *CA Cancer J Clin.* (2011) 61:69–90. doi: 10.3322/caac.20107
2. Kiniwa Y, Miyahara Y, Wang HY, Peng W, Peng G, Wheeler TM, et al. CD8+ Foxp3+ regulatory T cells mediate immunosuppression in prostate cancer. *Clin Cancer Res.* (2007) 13:6947–58. doi: 10.1158/1078-0432.CCR-07-0842
3. Miller AM, Lundberg K, Ozenci V, Banham AH, Hellstrom M, Egevad L, et al. CD4+CD25high T cells are enriched in the tumor and peripheral blood of prostate cancer patients. *J Immunol.* (2006) 177:7398–405. doi: 10.4049/jimmunol.177.10.7398
4. Bronte V, Kasic T, Gri G, Gallana K, Borsellino G, Marigo I, et al. Boosting antitumor responses of T lymphocytes infiltrating human prostate cancers. *J Exp Med.* (2005) 201:1257–68. doi: 10.1084/jem.20042028
5. Ebelt K, Babaryka G, Frankenberger B, Stief CG, Eisenmenger W, Kirchner T, et al. Prostate cancer lesions are surrounded by FOXP3+, PD-1+ and B7-H1+ lymphocyte clusters. *Eur J Cancer.* (2009) 45:1664–72. doi: 10.1016/j.ejca.2009.02.015
6. Sfanos KS, Bruno TC, Meeker AK, De Marzo AM, Isaacs WB, Drake CG. Human prostate-infiltrating CD8+ T lymphocytes are oligoclonal and PD-1+. *Prostate.* (2009) 69:1694–703. doi: 10.1002/pros.21020
7. Yokokawa J, Cereda V, Remondo C, Gulley JL, Arlen PM, Schlom J, et al. Enhanced functionality of CD4+CD25(high)FoxP3+ regulatory T cells in the peripheral blood of patients with prostate cancer. *Clin Cancer Res.* (2008) 14:1032–40. doi: 10.1158/1078-0432.CCR-07-2056
8. Weber WP, Feder-Mengus C, Chiarugi A, Rosenthal R, Reschner A, Schumacher R, et al. Differential effects of the tryptophan metabolite 3-hydroxyanthranilic acid on the proliferation of human CD8+ T cells induced by TCR triggering or homeostatic cytokines. *Eur J Immunol.* (2006) 36:296–304. doi: 10.1002/eji.200535616
9. Feder-Mengus C, Wyler S, Hudolin T, Ruszat R, Bubendorf L, Chiarugi A, et al. High expression of indoleamine 2,3-dioxygenase gene in prostate cancer. *Eur J Cancer.* (2008) 44:2266–75. doi: 10.1016/j.ejca.2008.05.023
10. Okamoto A, Nikaido T, Ochiai K, Takakura S, Saito M, Aoki Y, et al. Indoleamine 2,3-dioxygenase serves as a marker of poor prognosis in gene expression profiles of serous ovarian cancer cells. *Clin Cancer Res.* (2005) 11:6030–9. doi: 10.1158/1078-0432.CCR-04-2671
11. Ino K, Yoshida N, Kajiyama H, Shibata K, Yamamoto E, Kidokoro K, et al. Indoleamine 2,3-dioxygenase is a novel prognostic indicator for endometrial cancer. *Br J Cancer.* (2006) 95:1555–61. doi: 10.1038/sj.bjc.6603477
12. Brandacher G, Perathoner A, Ladurner R, Schneeberger S, Obrist P, Winkler C, et al. Prognostic value of indoleamine 2,3-dioxygenase expression in colorectal cancer: effect on tumor-infiltrating T cells. *Clin Cancer Res.* (2006) 12:1144–51. doi: 10.1158/1078-0432.CCR-05-1966
13. Speeckaert R, Vermaelen K, van Geel N, Autier P, Lambert J, Haspeslagh M, et al. Indoleamine 2,3-dioxygenase, a new prognostic marker in sentinel lymph nodes of melanoma patients. *Eur J Cancer.* (2012) 48:2004–11. doi: 10.1016/j.ejca.2011.09.007
14. Astigiano S, Morandi B, Costa R, Mastracci L, D'Agostino A, Ratto GB, et al. Eosinophil granulocytes account for indoleamine 2,3-dioxygenase-mediated immune escape in human non-small cell lung cancer. *Neoplasia.* (2005) 7:390–6. doi: 10.1593/neo.04658
15. Riesenberg R, Weiler C, Spring O, Eder M, Buchner A, Popp T, et al. Expression of indoleamine 2,3-dioxygenase in tumor endothelial cells correlates with long-term survival of patients with renal cell carcinoma. *Clin Cancer Res.* (2007) 13:6993–7002. doi: 10.1158/1078-0432.CCR-07-0942
16. Merriel SWD, Funston G, Hamilton W. Prostate cancer in primary care. *Adv Ther.* (2018) 35:1285–94. doi: 10.1007/s12325-018-0766-1
17. Zambon CF, Basso D, Prayer-Galetti T, Navaglia F, Fasolo M, Fogar P, et al. Quantitative PSA mRNA determination in blood: a biochemical tool for scoring localized prostate cancer. *Clin Biochem.* (2006) 39:333–8. doi: 10.1016/j.clinbiochem.2006.02.001
18. Catalona WJ, Southwick PC, Slawin KM, Partin AW, Brawer MK, Flanigan RC, et al. Comparison of percent free PSA, PSA density, and age-specific PSA cutoffs for prostate cancer detection and staging. *Urology.* (2000) 56:255–60. doi: 10.1016/S0090-4295(00)00637-3
19. Lee DH, Nam JK, Park SW, Lee SS, Han JY, Lee SD, et al. Visually estimated MRI targeted prostate biopsy could improve the detection of significant prostate cancer in patients with a PSA level <10 ng/mL. *Yonsei Med J.* (2016) 57:565–71. doi: 10.3349/ymj.2016.57.3.565
20. Klein EA, Cooperberg MR, Magi-Galluzzi C, Simko JP, Falzarano SM, Maddala T, et al. A 17-gene assay to predict prostate cancer aggressiveness in the context of Gleason grade heterogeneity, tumor multifocality, biopsy undersampling. *Eur Urol.* (2014) 66:550–60. doi: 10.1016/j.eururo.2014.08.001
21. Loeb S, Vellekoop A, Ahmed HU, Catto J, Emberton M, Nam R, et al. Systematic review of complications of prostate biopsy. *Eur Urol.* (2013) 64:876–92. doi: 10.1016/j.eururo.2013.05.049
22. Fitzmaurice C, Akinyemiju TF, Al Lami FH, Alam T, Alizadeh-Navaei R, Allen C, et al. Global, regional, and national cancer incidence, mortality, years of life

lost, years lived with disability, and disability-adjusted life-years for 29 cancer Groups, 1990 to 2016: a systematic analysis for the global burden of disease study. *JAMA Oncol.* (2018) 4:1553–68. doi: 10.1200/JCO.2018.36.15_suppl.1568

23. Banzola I, Mengus C, Wyler S, Hudolin T, Manzella G, Chiarugi A, et al. Expression of indoleamine 2,3-Dioxygenase induced by IFN-gamma and TNF-alpha as potential biomarker of prostate cancer progression. *Front Immunol.* (2018) 9:1051. doi: 10.3389/fimmu.2018.01051
24. Poyet C, Thomas L, Benoit TM, Delmo DA, Luberto L, Banzola I, et al. Implication of vascular endothelial growth factor A and C in revealing diagnostic lymphangiogenic markers in node-positive bladder cancer. *Oncotarget.* (2017) 8:21871–883. doi: 10.18632/oncotarget.15669
25. Lalonde E, Ishkanian AS, Sykes J, Fraser M, Ross-Adams H, Erho N, et al. Tumour genomic and microenvironmental heterogeneity for integrated prediction of 5-year biochemical recurrence of prostate cancer: a retrospective cohort study. *Lancet Oncol.* (2014) 15:1521–32. doi: 10.1016/S1470-2045(14)71021-6
26. Scher HI, Heller G, Molina A, Attard G, Danila DC, Jia X, et al. Circulating tumor cell biomarker panel as an individual-level surrogate for survival in metastatic castration-resistant prostate cancer. *J Clin Oncol.* (2015) 33:1348–55. doi: 10.1200/JCO.2014.55.3487
27. Cortese R, Kwan A, Lalonde E, Bryzgunova O, Bondar A, Wu Y, et al. Epigenetic markers of prostate cancer in plasma circulating DNA. *Hum Mol Genet.* (2012) 21:3619–31. doi: 10.1093/hmg/dds192
28. Liu M, Wang X, Wang L, Ma X, Gong Z, Zhang S, et al. Targeting the IDO1 pathway in cancer: from bench to bedside. *J Hematol Oncol.* (2018) 11:100. doi: 10.1186/s13045-018-0644-y
29. Stone TW, Darlington LG. Endogenous kynurenines as targets for drug discovery and development. *Nat Rev Drug Discov.* (2002) 1:609–20. doi: 10.1038/nrd870
30. Uyttenhove C, Pilotte L, Théate I, Stroobant V, Colau D, Parmentier N, et al. Evidence for a tumoral immune resistance mechanism based on tryptophan degradation by indoleamine 2,3-dioxygenase. *Nat Med.* (2003) 9:1269–74. doi: 10.1038/nm934
31. Mengus C, Le Magnen C, Trella E, Yousef K, Bubendorf L, Provenzano M, et al. Elevated levels of circulating IL-7 and IL-15 in patients with early stage prostate cancer. *J Transl Med.* (2011) 9:162. doi: 10.1186/1479-5876-9-162
32. Chow MT, Moller A, Smyth MJ. Inflammation and immune surveillance in cancer. *Semin Cancer Biol.* (2011) 22:23–32. doi: 10.1016/j.semcancer.2011.12.004

Conflict of Interest: The authors declare that the research was conducted in the absence of any commercial or financial relationships that could be construed as a potential conflict of interest.

frontiers in Oncology

ORIGINAL RESEARCH
published: 03 September 2020
doi: 10.3389/fonc.2020.01632

Correlation Patterns Among B7 Family Ligands and Tryptophan Degrading Enzymes in Hepatocellular Carcinoma

Raghavan Chinnadurai[1]*, *Rafaela Scandolara*[1], *Olatunji B. Alese*[2], *Dalia Arafat*[3], *Deepak Ravindranathan*[2], *Alton B. Farris*[4], *Bassel F. El-Rayes*[2] and *Greg Gibson*[3]

[1] Department of Biomedical Sciences, Mercer University School of Medicine, Savannah, GA, United States, [2] Department of Hematology and Oncology, Winship Cancer Institute, Emory University, Atlanta, GA, United States, [3] School of Biology, Georgia Institute of Technology, Atlanta, GA, United States, [4] Department of Pathology and Laboratory Medicine, Emory University, Atlanta, GA, United States

Mechanisms of dysfunctional T cell immunity in Hepatocellular Carcinoma (HCC) need to be well defined. B7 family molecules provide both co-stimulatory and co-inhibitory signals to T cells while tryptophan degrading enzymes like Indoleamine 2,3 dioxygenase (IDO) and Tryptophan 2,3 Dioxygenase (TDO) mediate tumor immune tolerance. It is necessary to identify their *in situ* correlative expression, which informs targets for combined immunotherapy approaches. We investigated B7 family molecules, IDO, TDO and immune responsive effectors in the tumor tissues of patients with HCC ($n = 28$) using a pathway-focused quantitative nanoscale chip real-time PCR. Four best correlative expressions, namely (1) B7-1 & PD-L2, (2) B7-H2 & B7-H3, (3) B7-2 & PD-L1, (4) PD-L1 & PD-L2, were identified among B7 family ligands, albeit they express at different levels. Although TDO expression is higher than IDO, PD-L1 correlates only with IDO but not TDO. Immune effector (Granzyme B) and suppressive (PD-1 and TGF-β) genes correlate with IDO and B7-1, B7-H5, PD-L2. Identification of the *in situ* correlation of PD-L1, PD-L2 and IDO suggest their cumulative immuno suppressive role in HCC. The distinct correlations among B7-1, B7-2, B7-H2, and B7-H3, correlation of PD-1 with non-cognate ligands such as B7-1 and B7-H5, and correlation of tumor lytic enzyme Granzyme B with IDO and PD-L2 suggest that HCC microenvironment is complexly orchestrated with both stimulatory and inhibitory molecules which together neutralize and blunt anti-HCC immunity. Functional assays demonstrate that both PDL-1 and IDO synergistically inhibit T cell responses. Altogether, the present data suggest the usage of combined immune checkpoint blocking strategies targeting co-inhibitory B7 molecules and IDO for HCC management.

Keywords: B7 family molecules, indoleamine 2,3 dioxygenase, hepatocellular carcinoma, T cell immunity, co-stimulation, co-inhibition, PD-L1

OPEN ACCESS

Edited by:
Lieve Brochez,
Cancer Research Institute,
Ghent University, Belgium

Reviewed by:
William J. Magner,
University at Buffalo, United States
Binfeng Lu,
University at Buffalo, United States

***Correspondence:**
Raghavan Chinnadurai
chinnadurai_r@mercer.edu

Specialty section:
This article was submitted to Cancer Immunity and Immunotherapy, a section of the journal Frontiers in Oncology

Received: *25 November 2019*
Accepted: *27 July 2020*
Published: *03 September 2020*

Citation:
Chinnadurai R, Scandolara R, Alese OB, Arafat D, Ravindranathan D, Farris AB, El-Rayes BF and Gibson G (2020) Correlation Patterns Among B7 Family Ligands and Tryptophan Degrading Enzymes in Hepatocellular Carcinoma. Front. Oncol. 10:1632. doi: 10.3389/fonc.2020.01632

INTRODUCTION

Hepatocellular carcinoma (HCC) is one of the leading causes of cancer-related mortalities (1). Defining the immunological mechanisms contributing to HCC pathogenesis in the intrahepatic tumor microenvironment is of translational interest (2). Co-stimulatory, co-inhibitory (B7 family) pathways and enzymes of tryptophan degradation predominantly attenuate anti-tumor T-cell

TABLE 1 | B7 Family ligand and receptors.

Ligand	Receptor	T Cell Fate
B7-1	CD28	+
B7-1	CTLA4	−
B7-2	CD28	+
B7-2	CTLA4	−
PD-L1 (B7-H1)	PD-1	−
PD-L2 (B7-DC)	PD-1	−
B7-H2	ICOS	+
B7-H3	?	−
B7-H4	?	−
B7-H5	CD28H	±
B7-H6	NKp30	+*
B7-H7	?	−

**NK cell fate.*

immunity. FDA-approved inhibitors of PD-L1 (B7-H1) & PD-L2 (B7-DC)-PD-1 interaction to revive exhausted anti-tumor T-cell immunity have shown benefit to cancer patients (3, 4). In addition, clinical trials are ongoing to test the efficacy of inhibitors of tryptophan degrading enzymes for cancer treatment (NCT03695250) (5–7). Early phase clinical trials are ongoing to test the effect of immunotherapy agents targeting B7 family and tryptophan degradation pathways on HCC (8–10). Importantly, inhibitors of PD-L1 (B7-H1) & PD-L2 (B7-DC)-PD-1 pathways are promising for anti-HCC management (11, 12). Defining the complex interaction among B7 family ligands and enzymes of tryptophan degradation pathways in the HCC microenvironment will inform additional checkpoint immune blocking strategies.

B7 family ligands are the dominant family of molecules providing co-stimulation and co-inhibition to T-cells. Accumulated evidence demonstrates that there are many members present in the B7 family, namely, B7-1, B7-2, PD-L1 (B7-H1), PD-L2 (B7-DC), B7-H2, B7-H3, B7-H4, B7-H5, B7-H6 and B7-H7 (13, 14). Receptors of the majority of the B7 family ligands have been defined on T-cells while some ambiguity exists in identifying definitive receptors of new members B7-H3, B7-H4, B7-H5, and B7-H7 (**Table 1**). Nevertheless, dysfunctional and exhausted T-cells co-express receptors of B7-family ligands, which suggest that a complex co-receptor and ligand interaction occur in a tumor microenvironment and confer dysfunctional immune response (15–18). The interaction of PD-L1/PD-L2 with PD-1 on T cells plays an important role in modulating tumor immunity (19). B7-H2 has been characterized as a co-stimulatory ligand for Inducible Costimulator (ICOS) and skews T-cell differentiation toward Th2 responses (20, 21). In contrast, B7-H3 is a negative regulator by preferentially affecting Th1 responses (22, 23). B7-H4 has been shown to play a major role in the negative regulation of T cell immunity (24, 25). B7-H5 or V-domain Ig Suppressor of T cell Activation (VISTA) is identified as both co-stimulatory (26) and co-inhibitory molecule (27). B7-H6 is highly expressed on many cancer conditions and interacts with NK-cell receptor NKP30 to induce activation while its significance on tumor immunity is yet to be defined (28). B7-H7 is a co-inhibitory molecule and inhibits CD4+ and CD8+ T cell functions (29). The pattern of correlative expressions of B7 family molecules and their interaction with the immune effectors of HCC microenvironment is currently unknown.

Indoleamine 2,3-dioxygenase (IDO) and tryptophan 2,3-dioxygenase (TDO) deplete tryptophan by converting it into the immunosuppressive catabolite, kynurenine (30–32). Although inconsistent results emerge in clinical trials targeting IDO (33), it needs to be further clarified on how IDO and/or TDO operate with B7 family ligands in modulating T-cell responses in the liver of patients with HCC. Important questions are: How are B7 family ligands expressed relative to each other in controlling T cell fate? How do B7 family ligands correlate among themselves in the tumor microenvironment of HCC? Do B7 family ligands co-express with IDO and TDO in an intricate intrahepatic tumor microenvironment? How do B7 family ligands, IDO and TDO correlate with immune responsive effector molecules in HCC? Better understanding of the underlying *in situ* associations of IDO/TDO and B7 family members will inform the rationale of translational development of specific checkpoint inhibitors for primary liver cancer management.

METHODS

Patient Characteristics

The Emory University Institutional Review Board (IRB) approved the study. All consecutive cases of patients with HCC who were older than 18 years of age and treated between 2013 and 2015 at Winship Cancer Institute/Emory University Hospital system were identified and enrolled. All the patients ($n = 28$) who were included in the study had active HCC (**Table 2**).

RNA Extraction and cDNA Preparation

Paraffin embedded tissue blocks from HCC patients were subjected to hematoxylin and eosin (H&E) staining to ensure that the tissue slices subjected to RNA analysis have adequate (minimum 30–40%) tumor volume. % Tumor volume and % leukocytes in tissue sections are given in **Table 2**. High Pure FFPE (formalin-fixed, paraffin-embedded) RNA Micro Kit was used to isolate RNA from the dissected paraffin slices according to the manufacturer instructions (Roche GmbH, Germany). Hundred to five-hundred nanogram of isolated RNA was used for total cDNA preparation (QuantiTect Reverse Transcription Kit, Qiagen, USA).

Fluidigm Nanoscale PCR

Quantitative RT-PCR was performed using Fluidigm 48 × 48 nanofluidic arrays. Briefly, cDNA samples were pre amplified with 14-cycle PCR reaction for each sample with the combination of 100 ng cDNA and pooled primers as described by TaqMan Pre-Amp Mastermix (Fluidigm BioMark™) manufacturer's protocols. Two thousand three hundred four parallel qRT-PCR reactions were performed for each primer pair on each sample on a 48 × 48 chip array. Human cDNA library was used as a positive control. Amplification was detected in Eva Green detection assay on a Biomark I machine based on standard Fluidigm protocols

TABLE 2 | HCC patient characteristics.

	Gender	Age	Race - A, AA, C, O	Diagnosis	AJCC stage	T	Serum AFP at diagnosis (ng/mL)	Tumor Grade	% Tumor	% Leukocytes
1	Male	65	O-Hispanic	HCC and Cholangio		pT2	93.1	G2: Moderately differentiated	50	10
2	Male	45	O-African	HCC		pT1	4.9	G2: Moderately differentiated	40	5
3	Female	71	Caucasian	HCC	IIIA	pT3a	1.6	G2: Moderately differentiated	80	3
4	Male	57	Caucasian	HCC	I	pT1	2.2	G1: Well-differentiated	70	2
5	Female	67	Caucasian	HCC	I	pT1	1.4	G1: Well-differentiated	80	2
6	Male	62	Caucasian	HCC		pT2	7	G2: Moderately differentiated	60	2
7	Male	69	Caucasian	HCC		pT2	15.2	G2: Moderately differentiated	30	N/A
8	Male	60	Caucasian	HCC	I	pT1	20.1	G2: Moderately differentiated	70	2
9	Male	60	AA	HCC	I	pT1	354	G2: Moderately differentiated	60	5
10	Female	59	AA	HCC	II	pT2	17.7	G2: Moderately differentiated	80	2
11	Male	66	Caucasian	HCC		pT2	4.7	G2: Moderately differentiated	70	10
12	Male	75	Caucasian	HCC	I	pT1	4.9	G2: Moderately differentiated	90	3
13	Female	61	AA	HCC		pT1	>2,000	G2: Moderately differentiated	90	0.5
14	Male	68	AA	HCC	II	pT2	21.7	G1: Well differentiated	30	2
15	Male	55	Caucasian	HCC		pT2	17.4	G2: Moderately differentiated	70	5
16	Female	35	AA	HCC		pT1	3,969	G3: poorly differentiated	60	2
17	Male	67	Caucasian	HCC	II	pT2	64.6	G1: Well differentiated	60	5
18	Male	65	Caucasian	HCC	I	pT1	2.9	G2: Moderately differentiated	40	2
19	Female	44	Caucasian	HCC		pT1	5.3	G1: Well differentiated	50	2
20	Male	47	Caucasian	HCC		pT2	4.6	G2: Moderately differentiated	30	1
21	Male	65	Caucasian	HCC		pT1	6.3	G2: Moderately differentiated	N/A	3
22	Male	71	AA	HCC	II	pT2	23	G2: Moderately differentiated	50	N/A
23	Male	53	Caucasian	HCC		pT2	18.4	Other: Well to moderately differentiated	60	5
24	Male	53	Caucasian	HCC		pT1	18.8	G3: poorly differentiated	50	3
25	Male	64	Caucasian	HCC	II	pT2	214.9	G2: Moderately differentiated	70	3
26	Male	51	Caucasian	HCC		pT2	1,750.6	Other: moderately to poor differentiated	60	5
27	Male	67	AA	HCC		pT1	20.4	G2: Moderately differentiated	80	1
28	Male	59	Caucasian	HCC		pT2	10.1	G2: Moderately differentiated	90	2

as described previously (34, 35). Two independent primer pairs were used for each target (**Table 3**). Cycle of Threshold (CT) values were normalized based on the endogenous GAPDH & beta actin controls. CT value of each target was subtracted with the CT value of endogenous GAPDH & beta actin (Control CT values) of the respective samples to get delta CT values. The delta CT values were subjected to a second standardization by adding all the delta CT values with a constant CT value, which was derived from the total average of control CT values from all the samples. In the case of Osteopontin or Glypican normalization, GAPDH & beta actin normalized CT values were further normalized with Osteopontin or Glypican-3. The normalized CT values are expressed as an inverse (CT^{-1}) to better graphically represent the increase or decrease in expression as described previously (36). Inverse CT values were obtained by dividing 1 with the appropriate normalized CT value. High or low inverse CT values represent high or low expression of target genes, respectively.

T Cell Proliferation and Cytokine Secretion

Peripheral Blood Mononuclear Cells (PBMCs) were isolated from heparin-anticoagulated whole blood using a Ficoll-Paque PLUS density gradient (GE Healthcare Biosciences, Sweden), and cryopreserved in medium containing 90% fetal calf serum (HyClone) and 10% dimethyl sulfoxide (Corning, USA). Prior to the experiment, cells were thawed and rested overnight in a 37°C CO_2 incubator. For proliferation assays, Carboxyfluorescein succinimidyl ester (CFSE) (Biolegend USA) labeled PBMC were stimulated for 4 days with plate bound 1 μg/ml anti-CD3 and anti-CD28 (Biolegend, USA) antibodies and 10ug/ml of PD-L1 Ig or Control Ig protein (Biolegend, USA) with varying concentrations of Kynurenine (Tocris, USA). Four days later, cells were stained with CD3-APCCy7 antibody (Biolegend, USA) and acquired in BD FACSAria instrument. Results were analyzed in Flow Jo software. Supernatants were analyzed for IFNγ using the kit, Human IFN gamma ELISA Ready-SET-Go according to the manufacture's instruction.

Statistics

Data were analyzed with GraphPad Prism 5.0 software for statistics. An unpaired two-sided *t*-test was used to determine significance between the means of two groups, and a one-way ANOVA with Tukey's multiple comparison tests was used to compare multiple groups simultaneously. P-value < 0.05 was considered statistically significant. Linear regression analysis

was performed using normalized CT values to obtain R^2 and P-values. R^2 = Goodness of Fit; P = Significance of the slope deviation from Zero. Correlations with R^2 values above 0.5 with the P-value of <0.05 were considered as the best correlation. Correlation with R^2 values between 0.3 and 0.5 with the P-value of <0.05 were considered as moderate correlations/statistical trend toward a correlation. Correlations with R^2 values below 0.3 were considered relatively less significant.

RESULTS

Differential Expression of B7 Family Ligands and Enzymes of Tryptophan Degradation in Patients With HCC

B7 family molecules are either co-stimulatory or co-inhibitory in stimulating and negating T-cell responses (**Table 1**). We have evaluated their relative expression in the hepatic tumor microenvironment in patients with HCC. Surgically resected liver tumor tissues of the patients with HCC (n = 28) were fixed with formalin and embedded in paraffin. Hematoxylin and Eosin (H&E) staining was performed for the inclusion criteria that the tissue slices subjected to RNA analysis have at least 30–40% tumor volume (**Table 2**). % Tumor volume and % leukocytes in tissue sections are given in **Table 2**. Patient #1 had a minute focus of cholangiocarcinoma on morphology which was excluded on histologic analysis. Total RNA was extracted from tissue sections, which was then converted into cDNA. cDNA samples were then used to perform Fluidigm nanoscale quantitative real-time chip PCR with two independent primer pairs for each target. Human cDNA library was used as a positive control to ensure the effectiveness of the primer pairs. The cycle of threshold (CT) values were normalized based on endogenous GAPDH & beta actin controls. Hierarchical organization of the cumulative median CT^{-1} values (inverse CT values were used to depict the expression) identified the ranking of expression as values identified the ranking of expression from high to low as B7-H5, B7-H3, B7-H2, B7-1, PD-L1, B7-2, PD-L2, B7-H6, B7-H4, and B7-H7 (**Figure 1A**). B7-H5 and B7-H3 showed statistically significant enhanced expression compared to all other B7 family molecules. B7-H2, PD-L1, PD-L2, B7-1, and B7-2 showed comparable expression among themselves while B7-H4, B7-H6, and B7-H7 are expressed at low levels (**Figures 1A,B**). The immunosuppressive tryptophan degradation pathway (IDO, TDO) is an immunotherapy target to revive anti-tumor immunity (30–32). We set out to identify the mRNA expression levels of IDO and TDO in HCC and our results show that TDO expression is higher than IDO (**Figure 1C**).

Dominant Correlative Pattern Among B7 Family Ligands in HCC

To identify the correlation among B7 family ligands, we subjected the CT values of each B7 family ligands in combinations through linear regression analysis. The degree of R^2 correlation values (Example: R^2 = 1 and R^2 = 0 represent the best and no correlation between two molecules, respectively) determines the correlation between two B7 family molecules. Fifty-five combinations tested among the B7 family members and the R^2 values were subjected to hierarchical ranking analysis ranging from best to no correlation. B7-1 expression showed the highest correlation with PD-L2 (R^2 = 0.7174; P < 0.0001) (**Figures 2A,B**). We also identified moderate correlations among three B7 combinations such as (1) B7-2 and PD-L1 (R^2 = 0.4244; P = 0.0002) (**Figures 2A,C**), (2) B7-H2 and B7-H3 (R^2 = 0.4090; P = 0.0002) (**Figures 2A,D**), (3) PD-L1 and PD-L2 (R^2 = 0.3863; P = 0.0004) (**Figures 2A,E**). All other combinations did not show a significant correlation. Altogether, the present analysis identified that B7-1, B7-2, PD-L1, PD-L2, and B7-H3 are correlated in a distinct combinatorial expression pattern.

TABLE 3 | Primer sequences of the targets used in nanoscale chip PCR.

Target	Primer Pair	Forward	Reverse
B7-1	1	GCTGTCCTGTGGTCACAATG	TGCCAGTAGATGCGAGTTTG
	2	CACCTCTCCTGGTTGGAAAA	TAAGGTAATGGCCCAGGATG
B7-2	1	GTATTTTGGCAGGACCAGGA	CTTGTGCGGCCCATATACTT
	2	GTATTTTGGCAGGACCAGGA	CGGCCCATATACTTGGAATG
PD-L1	1	TATGGTGGTGCCGACTACAA	TGACTGGATCCACAACCAAA
	2	CGAAGTCATCTGGACAAGCA	CTCTTGGAATTGGTGGTGGT
PD-L2	1	GGAACTTACTTTGGCCAGCA	GATGCAGAAGGGGATGAAAA
	2	AAGTCCAAGTGAGGGACGAA	GGCGACCCCATAGATGATTA
B7-H2	1	GTCCTGGACTGCTCTTCCTG	CCATCGCTCTGACTTCCTTC
	2	GTCCTGGACTGCTCTTCCTG	TCGCTCTGACTTCCTTCTCC
B7-H3	1	GTGGGGCTGTCTGTCTGTCT	TGATCTTTCTCCAGCACACG
	2	GTCTCATTGCACTGCTGGTG	TGATCTTTCTCCAGCACACG
B7-H4	1	GTCGGAGCAGGATGAAATGT	TGAGTTGCACGTTTTTCAGC
	2	GCTGAAAAACGTGCAACTCA	TAGCATTCCCCTTGCCTTTA
B7-H5	1	GGCAACTTCTCCATCACCAT	CAGTAGAGGCCGCTATCCAG
	2	GCATCGTAGGAATCCTCTGC	CCTGCCTTTGCTTGTAGACC
B7-H6	1	CACACCCCTGAATGACAATG	TGTTGAGGGGTTGGGAATAA
	2	CTGAAGGCACAGGGAACAGT	TTGATCCAGCAACAATCTGC
B7-H7	1	GACCATTTGGAAAGCCAAGA	CGCATTCCCATTTTGAATCT
	2	TAGAAGCCAGGAGGAGCAGA	CCAGGAGGGACACAACATCT
IFNγ	1	TTCAGCTCTGCATCGTTTTG	ATGGGTCCTGGCAGTAACAG
	2	TCATCCAAGTGATGGCTGAA	CTTCGACCTCGAAACAGCAT
TNFα	1	AACCTCCTCTCTGCCATCAA	GGAAGACCCCTCCCAGATAG
	2	GAGAAGGGTGACCGACTCAG	CCAAAGTAGACCTGCCCAGA
TGFβ	1	GTACCTGAACCCGTGTTGCT	CACGTGCTGCTCCACTTTTA
	2	AGCTCCACGGAGAAGAACTG	GTCCTTGCGGAAGTCAATGT
IL-10	1	GAGAACAGCTGCACCCACTT	TCTCGGAGATCTCGAAGCAT
	2	TTACCTGGAGGAGGTGATGC	GCCTTGATGTCTGGGTCTTG
IL-2	1	TCACCAGGATGCTCACATTT	GCACTTCCTCCAGAGGTTTG
	2	CCCAGGGACTTAATCAGCAA	ATGGTTGCTGTCTCATCAGC
IDO	1	GCCCTTCAAGTGTTTCACCAA	CCAGCCAGACAAATATATGCGA
	2	CCTGAGGAGCTACCATCTGC	GCTTGCAGGAATCAGGATGT
TDO	1	CAAATCCTCTGGGAGTTGGA	GTGCATCCGAGAAACAACCT
	2	GACGGCTGTCATACAGAGCA	CCTGGAACCTAGGCTCTTCC
Perforin	1	ACTCACAGGCAGCCAACTTT	GGGTGCCGTAGTTGGAGATA
	2	CCCTCTGTGAAAATGCCCTA	GGCTTAGGAGTCACGTCCAG
Granzyme B	1	ACTGCAGCTGGAGAGAAAGG	CTGGGCCTTGTTGCTAGGTA
	2	GGAGGCCCTCTTGTGTGTAA	TGCCATTGTTTCGTCCATAG
PD-1	1	TGCAGCTTCTCCAACACATC	CATGCGGTACCAGTTTAGCA
	2	GTGCCTGTGTTCTCTGTGGA	TTCTCTCGCCACTGGAAATC
Osteopontin	1	CATCACCTGTGCCATACCAG	GCCACAGCATCTGGGTATTT
	2	TGAAACGAGTCAGCTGGATG	GCTCTCATCATTGGCTTTCC
Glypican-3	1	CCAACATGCTGCTCAAGAAA	TCCATGTTCAATCGTGCTGT
	2	CTGGATGAGGAAGGGTTTGA	AGCCTCCAATGCACTCATCT

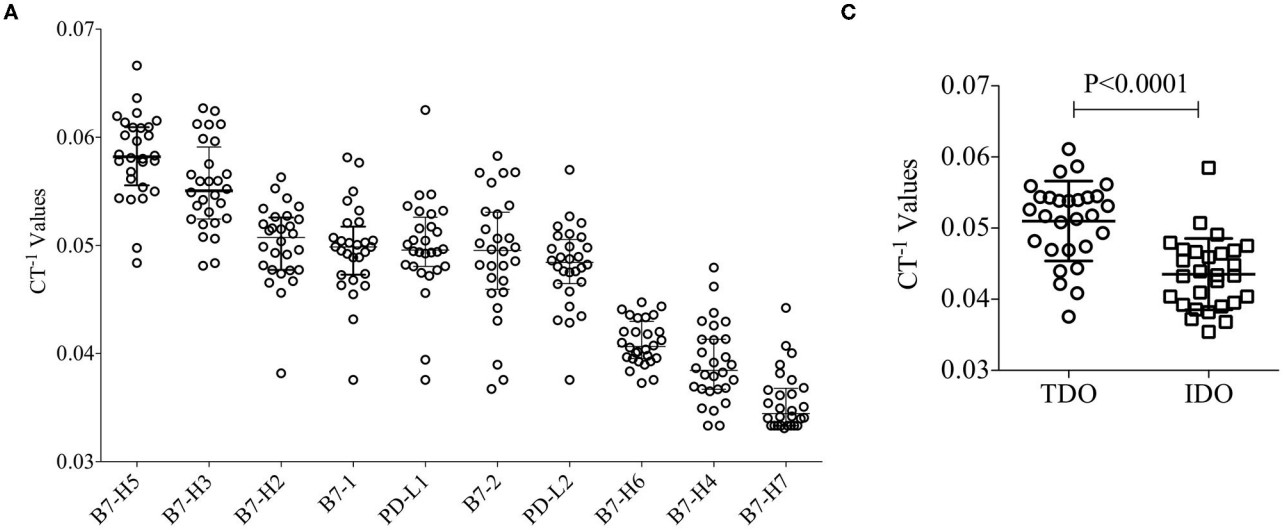

B

	B7-H5	B7-H3	B7-H2	B7-1	PD-L1	B7-2	PD-L2	B7-H6	B7-H4	B7-H7
B7-H5		NS	★★★	★★★	★★★	★★★	★★★	★★★	★★★	★★★
B7-H3			★★★	★★★	★★★	★★★	★★★	★★★	★★★	★★★
B7-H2				NS	NS	NS	NS	★★★	★★★	★★★
B7-1					NS	NS	NS	★★★	★★★	★★★
PD-L1						NS	NS	★★★	★★★	★★★
B7-2							NS	★★★	★★★	★★★
PD-L2								★★★	★★★	★★★
B7-H6									NS	★★★
B7-H4										★
B7-H7										

NS = Non Significant, ★★★ P≤0.001,★★ P≤0.01, ★ P≤0.05

FIGURE 1 | Relative expression of B7 familiy ligands and enzymes of Tryptophan degradation in HCC. Paraffin embedded liver tissue (10 micron) sections were collected in tubes and Hematoxylin and Eosin stained sections were reviewed to ensure tumor content. RNA was extracted and converted into cDNA which was used for the B7 Family ligand amplification in Fluidigm™ nanoscale quantitative RT PCR. Each target is validated with two independent primer sets with the amplicon length of <100 base pairs. **(A)** Inverse CT values (CT^{-1}) of B7 Family ligands derived from each patient were plotted with median and range. Median values were organized in hierarchical order of high to low expression. **(B)** One-way ANOVA and Tukey's multiple comparison test was performed to obtain *P*-values. Table shows the statistical significance of the median of CT^{-1} values of each B7 family ligand in comparison to others. **(C)** Inverse CT values (CT^{-1}) of TDO and IDO derived from each patient were plotted with the median and range. CT values were normalized based on GAPDH & beta actin controls.

Association of IDO and PD-L1 in HCC

To investigate the effect of the expression of IDO and TDO on B7 family ligands, we performed a linear regression analysis between the CT values of IDO, TDO and B7 family ligands. Twenty combinations were investigated to identify R^2 values. Although TDO expression is superior to IDO, it does not correlate with any of the B7 family ligands (**Figure 2F**). However, IDO shows a trend toward a correlation with PD-L1 ($R^2 = 0.3417$; $P = 0.001$) (**Figures 2F,G**). We did not observe any associations between IDO and other B7 family molecules. Altogether, these results demonstrate the correlation between IDO and PD-L1.

High Expression of TGF-β, IL-10, and PD-1 in HCC

Tumor microenvironment is not only occupied with the co-stimulatory and co-inhibitory ligands but also the immune responsive effector molecules that actually facilitate immune suppression or stimulation. We analyzed the expression of TGF-β, IL-10 (immune suppression), IFNγ, TNFα, IL-2, Perforin, Granzyme B (immune stimulation), and PD-1 (immune exhaustion). We categorized the expression levels of these effector molecules relative to each other by descending hierarchical organization of median CT^{-1} values. Our results demonstrate that TGF-β, PD-1, and IL-10 are expressed at high levels, TNFα and Granzyme B expressed at moderate levels, while IFNγ, IL-2, and Perforin are expressed at very low levels (**Figure 3A**). Descending hierarchical organization of median CT^{-1} values identified the ranking as TGF-β, PD-1, IL-10, GranzymeB, TNFα, IFNγ, IL-2 and Perforin (**Figures 3A,B**). Altogether these results demonstrate the dominant expression of immunosuppressive molecules (TGF-β, PD-1, IL-10) in HCC microenvironment.

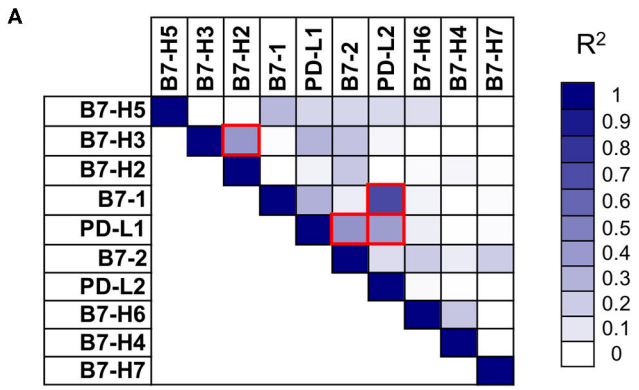

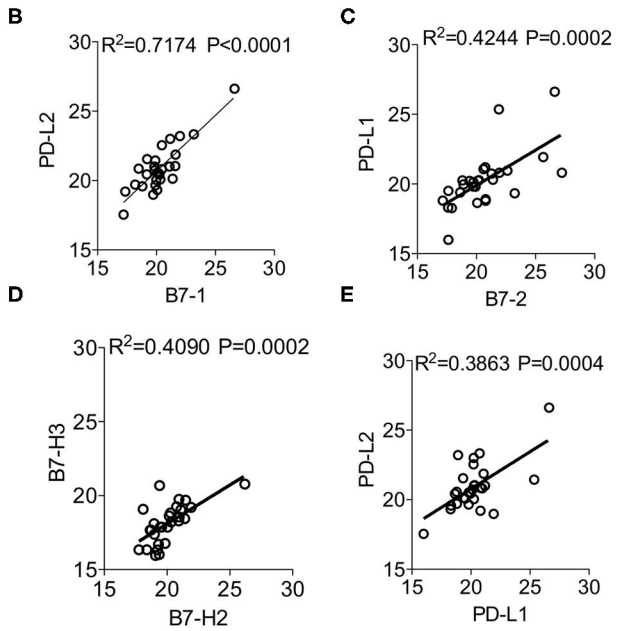

F

	TDO		IDO	
	R^2	P	R^2	P
B7-1	0.0532	NS	0.0707	NS
B7-2	0.0739	NS	0.1339	NS
PD-L1	0.0392	NS	**0.3417**	**0.001**
PD-L2	0.0583	NS	0.1204	NS
B7-H2	0.0907	NS	0.0628	NS
B7-H3	0.0002	NS	0.1485	0.043
B7-H4	0.0266	NS	0.0012	NS
B7-H5	0.0336	NS	0.1175	NS
B7-H6	0.0252	NS	0.0019	NS
B7-H7	0.2058	0.0153	0.0453	NS

G

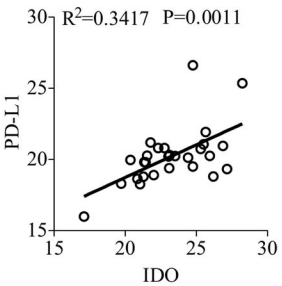

FIGURE 2 | Correlation patterns among B7-Familiy ligands and IDO in the liver of HCC patients. **(A)** CT Values of B7 Family ligands from HCC patients ($n = 28$) were subjected to linear regression analysis among each other. R^2 values were color-coded and red boxes indicate the best correlations based on the hierarchical ranking. Correlative plot with R^2 values above 0.3 are shown for the combination **(B)** B7-1&PD-L2, **(C)** B7-2&PD-L1, **(D)** B7-H2&B7-H3, and **(E)** PD-L2&PD-L1. **(F)** CT values of IDO and TDO were subjected to linear regression analysis with B7 family ligands. Correlative plot with the R^2 values above 0.3 is shown for the combination **(G)** IDO & PD-L1. Linear regression analysis was performed in GraphPad Prism to get R^2 and *P*-values. R^2, Goodness of Fit; P, Significance of the slope deviation from Zero.

Correlation Patterns of Immune Response Genes With B7 Family Ligands

Next we aim to determine the effect of the expression of individual B7 family ligands on the expression of immune responsive effector molecules within HCC microenvironment. CT values of the immune responsive effector molecules were subjected to linear regression analysis with the CT values of B7 family ligands. Eighty combinations were tested to identify R^2 values, which determine the correlation of immune responsive effector molecules with B7 family ligands. Our results identified the best correlation between TGF-β and B7-H5 ($R^2 = 0.6765$; $P < 0.0001$) (**Figures 4A,B**). In addition, a statistical trend toward the best correlation was identified with four other combinations. (1) PD-1 and B7-H5 ($R^2 = 0.48$; $P < 0.0001$), (**Figures 4A,C**), (2) PD-L2 and Granzyme B ($R^2 = 0.46$; $P < 0.0001$) (**Figures 4A,D**), (3) PD-1 and B7-1 ($R^2 = 0.4224$; $P = 0.0002$) (**Figures 4A,E**). (4) IFNγ and PD-L2 ($R^2 = 0.3174$; $P = 0.0018$) (**Figures 4A,F**).

None of the other combinations of B7 family ligands and immune responsive molecules showed a significant correlation values above 0.3 (**Figure 4A**). Correlations such as B7-H7 and IL-2, B7-H7 and Perforin were disregarded due to their very low expression levels (**Figures 1A**, **3A**). Altogether, these results demonstrate that although PD-1 is the cognate receptor for the ligands PD-L1 and PD-L2, its expression correlates with other B7 family ligands B7-1 and B7-H5. In addition, the immunosuppressive cytokine TGF-β correlates with B7-H5

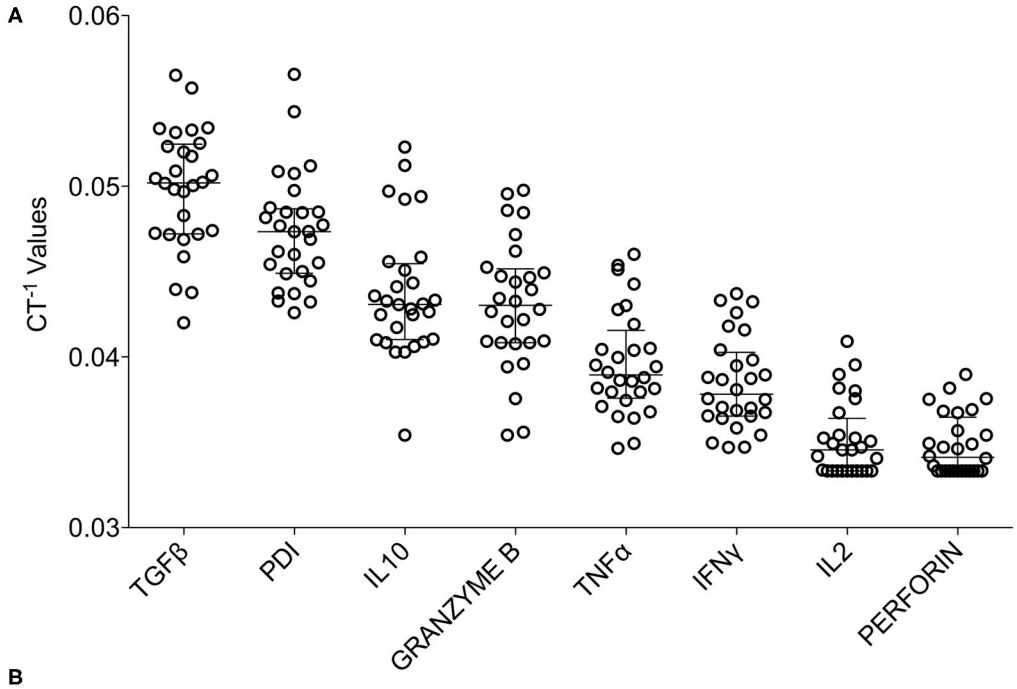

B

	TGFβ	PD1	IL10	GRZ-B	TNFα	IFNγ	IL2	PERF
TGFβ		★	★★	★★★	★★★	★★★	★★★	★★★
PD1			NS	NS	NS	★★★	★★★	★★★
IL10				NS	NS	★★★	★★★	★★★
GRANZYME B					NS	NS	★★★	★★★
TNFα						NS	★★★	★★★
IFNγ							★★★	★★★
IL2								NS
PERFORIN								

NS = Non Significant, ★★★ P≤0.001,★★ P≤0.01, ★ P≤0.05

FIGURE 3 | Expression pattern of immune responsive effector molecules in HCC. RNA transcripts of immune responsive effector molecules TGFβ, PD-1, IL-10, IFNγ, TNFα, IL-2, Granzyme B and Perforin were analyzed in Fluidigm™ nanoscale quantitative RT-PCR. **(A)** Inverse CT values (CT^{-1}) of immune responsive effector molecules derived from each patient were plotted with the median and range. Median values were organized in hierarchical order of high to low expression. **(B)** One-way ANOVA and Tukey's multiple comparison test was performed to obtain *P*-values. Table shows the statistical significance of the median of CT^{-1} values of each effector molecule in comparison to others. CT values were normalized based on GAPDH & beta actin controls.

while IFNγ and tumorlytic enzyme Granzyme B correlates with PD-L2.

IDO but Not TDO Correlate With Granzyme B

Next we investigated the correlation of IDO and TDO with immune responsive effector molecules. Linear regression analysis was performed between these two families of molecules with 16 combinations (**Figure 4G**). Identification of R^2 values demonstrates that TDO expression does not show any correlation with immune responsive effector molecules (**Figure 4G**). However, IDO expression shows a trend toward correlation with Granzyme B but not with any other immune responsive effector molecules ($R^2 = 0.3128$; $P = 0.002$) (**Figures 4G,H**). Altogether these results demonstrate that although TDO is dominant, it does not correlate with immune responsive effector molecules. In contrast, IDO expression correlates with Granzyme B.

Validation of Correlations Among B7 Family Ligands, Immune Response Genes and IDO After Glypican-3 and Osteopontin Normalization

Glypican-3 and Osteopontin are over expressed in HCC and studies have demonstrated that both of these molecules

A

	B7-1		B7-2		PD-L1		PD-L2		B7-H2		B7-H3		B7-H4		B7-H5		B7-H6		B7-H7	
	R^2	P	R^2	P	R^2	P	R^2	P	R^2	P	R^2	P	R^2	P	R^2	P	R^2	P	R^2	P
TGFβ	0.14	0.0462	0.21	0.0155	0.12	NS	0.09	NS	0.04	NS	0.01	NS	0.07	NS	**0.68**	**< 0.0001**	0.24	0.0075	0.00	NS
PD1	**0.42**	**0.0002**	0.01	NS	0.02	NS	0.23	0.01	0.13	NS	0.07	NS	0.02	NS	**0.48**	**< 0.0001**	0.02	NS	0.10	NS
IL-10	0.13	NS	0.01	NS	0.20	0.0166	0.27	0.0042	0.01	NS	0.12	NS	0.00	NS	0.01	NS	0.00	NS	0.08	NS
GZY-B	0.29	0.0032	0.05	NS	0.29	0.0034	**0.46**	**<0.0001**	0.04	NS	0.02	NS	0.06	NS	0.08	NS	0.07	NS	0.00	NS
TNFa	0.10	NS	0.03	NS	0.00	NS	0.14	0.0488	0.15	0.0396	0.10	NS	0.00	NS	0.02	NS	0.01	NS	0.09	NS
IFNγ	0.18	0.0247	0.01	NS	0.18	0.0227	**0.32**	**0.0018**	0.02	NS	0.04	NS	0.05	NS	0.07	NS	0.03	NS	0.28	0.0038
IL-2	0.01	NS	0.06	NS	0.01	NS	0.00	NS	0.01	NS	0.09	NS	0.06	NS	0.01	NS	0.03	NS	0.31	0.0021
Perforin	0.00	NS	0.18	0.0234	0.09	NS	0.04	NS	0.00	NS	0.06	NS	0.00	NS	0.01	NS	0.00	NS	0.32	0.0017

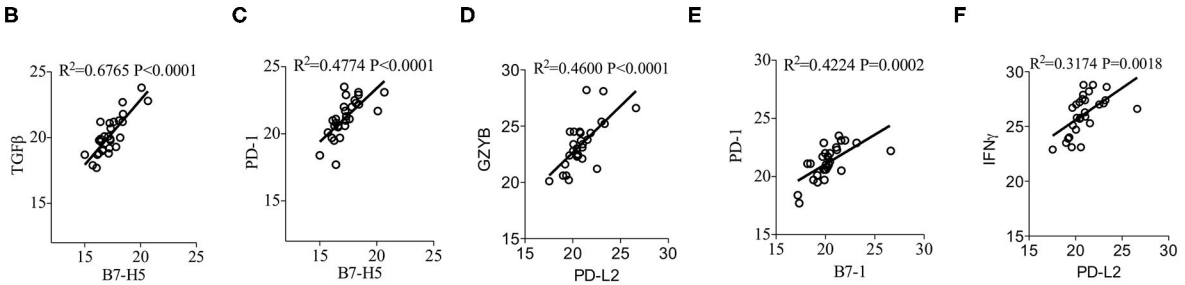

G

	TDO		IDO	
	R^2	P	R^2	P
TGFβ	0.02433	NS	0.08997	NS
PD1	0.06385	NS	0.04157	NS
IL-10	0.08595	NS	0.1081	NS
GZY-B	0.006192	NS	**0.3128**	**0.002**
TNFa	0.02746	NS	0.03625	NS
IFNγ	0.07859	NS	0.1589	0.0356
IL-2	0.04064	NS	0.02908	NS
Perforin	0.05312	NS	0.1172	NS

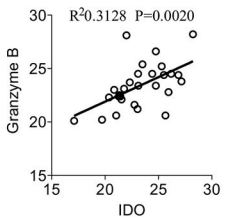

FIGURE 4 | Correlation of B7 family ligands and IDO with immune responsive effector molecules. CT values of each immune responsive effector molecules were subjected to linear regression analysis with the B7 family. **(A)** Correlation B7 family ligands with immune responsive effector molecules is shown in table format. Correlative plots with R^2 values above 0.3 are shown as **(B)** B7-H5&TGFβ, **(C)** PD-1&B7-H5, **(D)** PD-L2&GranzymeB, **(E)** B7-1&PD-1 and **(F)** PDL2&IFNγ. **(G)** IDO and TDO were subjected to linear regression analysis with immune responsive effector molecules to get R^2 and *p*-values. Correlative plots with the R^2 values above 0.3 is shown for the combination **(H)** IDO & Granzyme B. Linear regression analysis was performed in GraphPad Prism to get R^2 and *P*-values. R^2, Goodness of Fit; *P*, Significance of the slope deviation from Zero; NS, Non-significant.

could serve as the biomarker of HCC progression and could be targeted (37–39). Hence, we determined the mRNA expression levels of Glypican-3 and Osteopontin in HCC samples. Our results show that Glypican-3 and Osteopontin expressions are not significantly different from each other (**Figure 5A**). In addition, Glypican-3 and Osteopontin did not show significant levels of correlation with B7 family ligands, immune response genes and IDO, except Osteopontin showing a moderate correlation with B7-2 (**Figures 5B,C**). Next, we normalized CT values based on Osteopontin and Glypican-3 expression and validated the key identified correlation (as identified in **Figures 2**, **4**) that were determined based on GAPDH and beta-actin normalization. We recapitulated and confirmed the identified correlations among B7 family ligands, immune response genes and IDO based on the normalization with HCC associated biomarkers Glypican-3 and Osteopontin (**Figures 5D,E**).

IDO Metabolite Kynurenine and PD-L1 Synergistically Inhibit T Cell Responses

IDO correlates only with PD-L1 but not with other B family ligands, which suggests that this correlation is significant. Hence, to investigate the synergistic functional effect of IDO and PD-L1, we tested the effect of PD-L1 Ig/Control Ig and Kynurenine (IDO metabolite) on human peripheral blood mononuclear cells (PBMCs). We stimulated CFSE labeled human PBMCs with plate-bound anti-CD3 & anti-CD28 in the presence of PD-L1 Ig or Control Ig along with the dose escalating concentrations of Kynurenine. Four days later, T cell proliferation was determined by analyzing the percentage of CFSE dilution using flow cytometry. In addition, we also determined the concentrations of secreted Interferon γ (IFNg) in the supernatants of the cultures by Enzyme Linked Immunosorbent Assay (ELISA). Our results demonstrate that PD-L1 Ig inhibits T cell proliferation in the absence of Kynurenine. Similarly, Kynurenine inhibits T cell

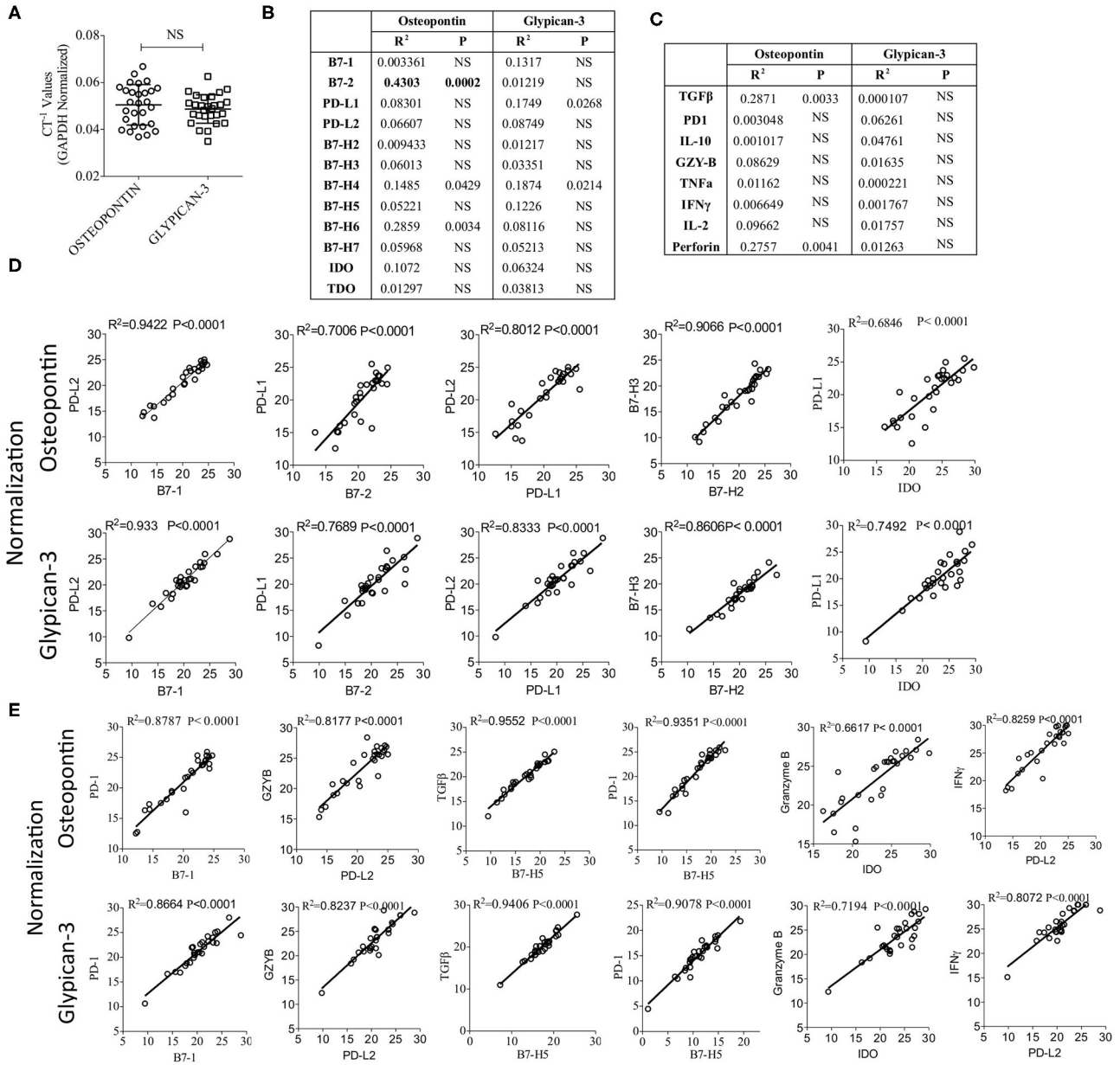

	Osteopontin		Glypican-3	
	R^2	P	R^2	P
B7-1	0.003361	NS	0.1317	NS
B7-2	**0.4303**	**0.0002**	0.01219	NS
PD-L1	0.08301	NS	0.1749	0.0268
PD-L2	0.06607	NS	0.08749	NS
B7-H2	0.009433	NS	0.01217	NS
B7-H3	0.06013	NS	0.03351	NS
B7-H4	0.1485	0.0429	0.1874	0.0214
B7-H5	0.05221	NS	0.1226	NS
B7-H6	0.2859	0.0034	0.08116	NS
B7-H7	0.05968	NS	0.05213	NS
IDO	0.1072	NS	0.06324	NS
TDO	0.01297	NS	0.03813	NS

	Osteopontin		Glypican-3	
	R^2	P	R^2	P
TGFβ	0.2871	0.0033	0.000107	NS
PD1	0.003048	NS	0.06261	NS
IL-10	0.001017	NS	0.04761	NS
GZY-B	0.08629	NS	0.01635	NS
TNFa	0.01162	NS	0.000221	NS
IFNγ	0.006649	NS	0.001767	NS
IL-2	0.09662	NS	0.01757	NS
Perforin	0.2757	0.0041	0.01263	NS

FIGURE 5 | Validation of the identified correlations using HCC biomarkers Osteopontin and Glypican-3. **(A)** Inverse CT values (CT^{-1}) of Osteopontin and Glypican-3 derived from each patient, after GAPDH & beta actin normalization, were plotted with median and range. CT values of Osteopontin and Glypican-3 were subjected to linear regression analysis with **(B)** B7 Family ligands, Tryptophan Degrading enzymes and **(C)** immune response genes. Correlation R^2 values and statistical significance are shown in a table format. **(D,E)** GAPDH & beta actin normalized CT values were further normalized based on the expression of Osteopontin or Glypican-3. Correlations that are identified in **Figures 2**, **4** were further confirmed using Osteopontin and Glypican-3 normalization. **(D)** Correlations between B7 family ligands and IDO. **(E)** Correlations between B7 family ligands, IDO and immune response genes. Linear regression analysis was performed in GraphPad Prism to get R^2 and *P*-values. R^2, Goodness of Fit; *P*, Significance of the slope deviation from Zero; NS, Non-significant.

proliferation in the absence of PD-L1 Ig (**Figures 6A,B**). In the cultures with both PD-L1 and Kynurenine, the inhibitory effect on T cell proliferation is superior over their individual counterparts (**Figures 6A,B**). Similarly, both PD-L1 Ig and Kynurenine synergistically inhibit Interferon γ (IFNg) secretion (**Figure 6C**). Altogether these results demonstrate the synergistic inhibition of PD-L1 and IDO on T cell responses.

DISCUSSION

Reviving the immune system with immunotherapy is becoming an attractive strategy to treat HCC (40, 41). Immunotherapy agents such as immune checkpoint blocking agents targeting single co-inhibitory molecule show some benefits to patients with HCC (11). These prompted to use second-generation combined

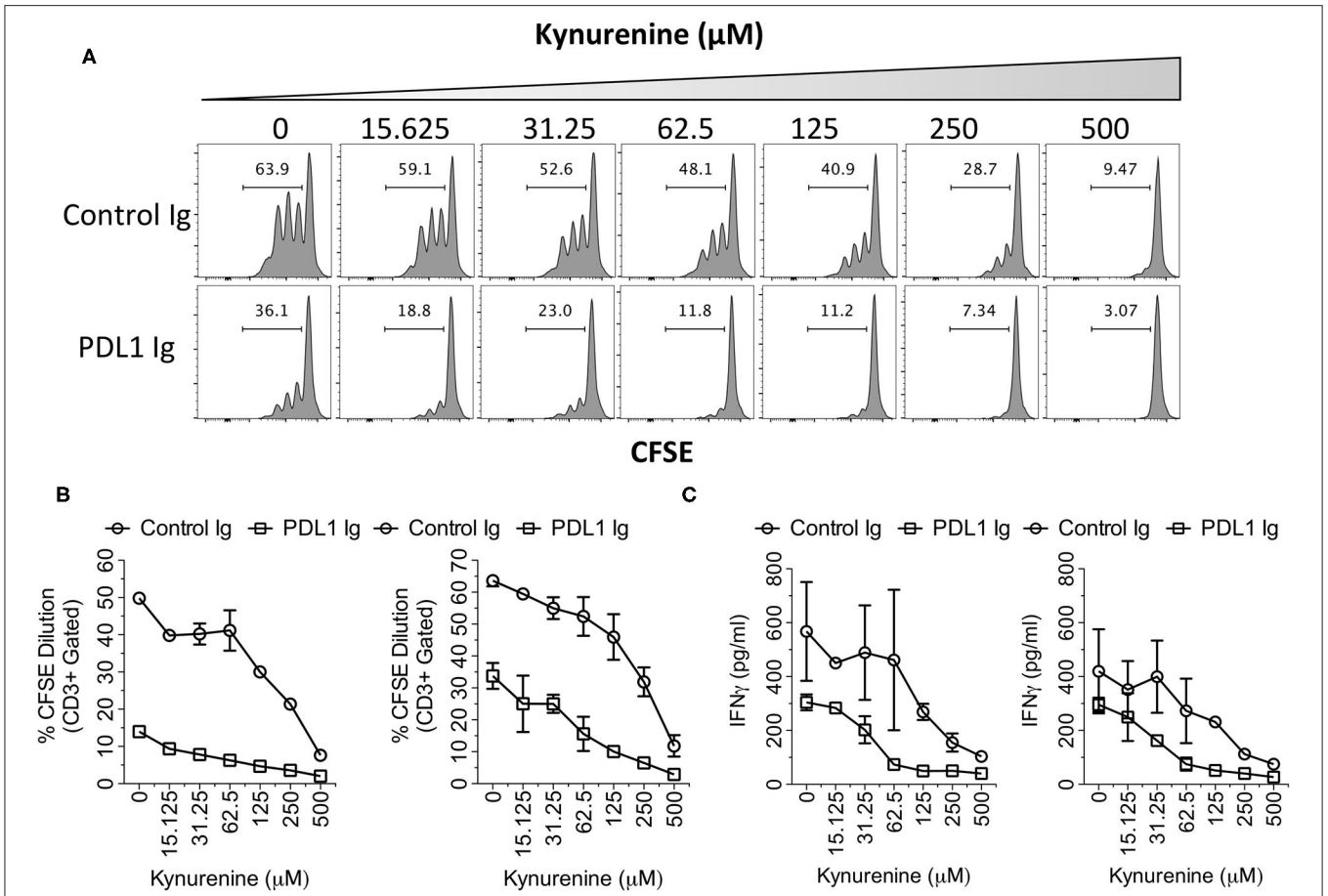

FIGURE 6 | Synergistic inhibitory effects of PD-L1 and Kynurenine on T cell responses. CFSE labeled PBMCs were stimulated on the plates coated with anti-CD3 and anti-CD28 (1 μg/ml) alone or in combination with PD-L1 Ig or Control Ig (10 μg/ml). Subsequently, Kynurenine was added to the culture at a final concentration as indicated. 4 days later, T cell proliferation analysis was performed using flow cytometry. **(A)** Representative CFSE dilution plot is shown. CFSE plots were derived from Forward Scatter, Side Scatter, CD3+ parental gates. **(B)** % CD3+ CFSE dilution is plotted with two independent donors. **(C)** Supernatants of the cultures were analyzed for human IFNγ using ELISA. Concentrations of the IFNγ are shown from two independent experiments using independent donor PBMCs.

immune blocking strategies targeting additional co-inhibitory molecules of the tumor microenvironment. However, practically it is not feasible to test combined immune blocking strategies targeting an array of immunomodulatory molecules with all the combinations in clinical trials or immunotherapy animal model studies. Hence, it is necessary to identify the *in situ* correlation and interaction of immunomodulatory molecules in the tumor microenvironment. We hypothesized that immunomodulatory molecules express in a specific combinatorial pattern in the HCC microenvironment and identification of such *in situ* combinations not only inform the targets for combined immunotherapy approaches but also unveil the immuno physiology of the tumor microenvironment.

Herein, we analyzed the correlative expressions of B7 family molecules and enzymes of tryptophan degradation in the tumor microenvironment of HCC. Consistent with other tumor types (42), we identified the differential expressions of B7 family molecules within the hepatic tumor microenvironment. Using a correlative hierarchical ranking analysis, we identified four best correlations out of 55 combinations tested among B7 family molecules. They are (1) B7-1 and PD-L2, (2) B7-2 and PD-L1 (3) PD-L1 and PD-L2, (4) B7-H2 and B7-H3. Identification of the correlative expression of PD-L1 and PD-L2 suggests that both of these ligands may function together in dampening T cell responses through its receptor PD-1. Clinical trials targeting PD-1 or PD-L1 with monoclonal antibodies showed encouraging results. FDA approved this immunotherapy for the patients who show advanced stage HCC and sorafenib resistance. Although FDA approved this therapy with the contingency that advanced phase clinical trials should demonstrate efficacy, the results are both positive and negative (40, 41). Thus, combined immunotherapy approach may be necessary to demonstrate consistent clinical efficacy. In addition, it has also been demonstrated that the binding structure, kinetics and affinity of PD-L1 and PD-L2 with PD1 are different (43, 44). These structural insights and our observation of the correlation of PD-L1 and PD-L2 suggest that the combined immunotherapy approaches targeting PD-L1, PD-L2 and PD-1 are warranted for advanced HCC management.

We also observed correlations such as (1) B7-1 and PD-L2, (2) B7-2 and PD-L1, (3) PD-1 and B7-1 which are intriguing since PD-L1, PD-L2, PD-1 are co-inhibitory ligands/receptor while B7-1 and B7-2 are dimorphic ligands since they can interact with CD28 or CTLA4 to promote co-stimulation or co-inhibition, respectively. It has been recently demonstrated that B7-1, B7-2 and CD28 co-stimulation is necessary to revive exhausted T cells using anti-PD-1 therapy in animal models and lung cancer patients (45). Thus, both of these two co-stimulatory and co-inhibitory pathways, (1) B7-1, B7-2-CD28 and (2) PD-L1, PD-L2-PD1 may function together in promoting T-cell exhaustion. Our results further support this hypothesis that in the liver tumor microenvironment, B7-1, B7-2, PD-L1, PD-L2 and PD-1 interactions occur extensively, which cumulatively confer dysfunctional anti-tumor immunity. In addition, our data shows the correlation of PD-1 with its non-cognate ligands B7-1 and B7-H5 which further suggests that PD-1 should be targeted in conjunction with other B7 family molecules.

B7-H2 and B7-H3 are co-stimulatory and co-inhibitory molecules, respectively (20, 22). The identification of their correlation suggests that neutralization/dampening of immune activation ensue as a result of the interaction of these molecules. In addition, it is also entirely possible that in the liver tumor microenvironment both of these pathways cumulatively promote T-cell exhaustion/tolerance similar to CD28 and PD-1 (45). Hence, these observations propose that blocking of the inhibitory pathways in HCC microenvironment will not only negate the immunosuppressive signals but also boost the functions of endogenous co-stimulatory molecules, which collectively revive exhausted/tolerized T cells.

B7-H5 plays an important role in the generation of inducible FoxP3+ regulatory T cells through TGF-β (46). Similarly, PD-1 and B7-H5 cumulatively attenuate T cell responses (47). Recent evidences suggest that HCC tumor microenvironment is enriched with Foxp3+CD4+ and PD-1+CD8+ T cells which together provide an extensive immunosuppressive microenvironment (48, 49). In addition, reduction in PD-1 and Foxp3 has been shown to be a predictor of the survival of HCC patients (50). Our observation of the correlation of B7-H5 with TGF-β and PD-1 add to these previous findings that B7-H5 plays an important role in the origin of intrahepatic regulatory T cells and in association with PD1+ T cells, it dampens anti-HCC T cell immunity.

IDO upregulation and its role in immunosuppression have been well established in generic and intrahepatic tumor immunity (51–53). TDO has a predominant homeostatic housekeeping role specific to liver (54), and the observation that TDO overexpression above IDO is due to the indigenous nature of the liver microenvironment. However, none of the B7 family molecules correlate with TDO expression in the liver while IDO shows a correlation with PD-L1 stronger than any other B7 family molecules. Correlation of IDO and PD-L1 has been shown in other tumors (55–57). Preclinical animal model studies also demonstrated that immune checkpoint blocking strategies with IDO targeting show an enhanced anti-tumor responses (58, 59). Our functional investigation on the effect of PD-L1 and IDO metabolite Kynurenine on T cell responses has demonstrated that both Kynurenine and PD-L1 exhibit synergistic inhibitory effect on T cells. Thus, co-blocking of IDO and PD-L1 is a promising strategy to promote anti-HCC T-cell immunity within the liver. However, although several clinical trials are aiming to test combined immune checkpoint blockade agents to revive anti-tumor immunity, some did not show efficacy. For example, a large phase III clinical trial investigating the combined checkpoint blockade of IDO and PD-L1 did not show efficacy in melanoma patients (60). This suggests that additional immune suppression persists beyond IDO and PD-L1 which neutralizes anti-tumor immunity. We have identified additional immunomodulatory pathways that coexist beyond IDO and PD-L1 suggesting that HCC tumor microenvironment is complex. Further mechanistic and functional studies are warranted to identify which pathways are dominant and superior over others in reviving anti-HCC immunity.

Granzyme B is a tumorlytic effector enzyme, which is predominantly used by cytotoxic lymphocytes and natural killer cells to lyse tumor cells (61, 62). In addition, Granzyme B+ lymphocytes were shown to be significantly associated with improved survival of HCC patients (63). We observed a correlation of Granzyme B with PD-L2 and IDO. IDO plays an important role in conferring adaptive tumor resistance to immune lysis since animal model studies have demonstrated that sole blocking of PD-1 or CTLA4 pathway enhances the IDO mediated tumor resistance. However, co-blocking of IDO and PD-1/CTLA4 significantly abolish tumor progression (58, 59). Similarly HCC patients treated with single immune checkpoint blocking antibodies to PD-1 or PDL-1 are always not responsive to therapy (40, 41). Thus, we speculate that although Granzyme B is tumorlytic, both PD-L2 and IDO may override and neutralize Granzyme B+ lymphocyte activity. This also proposes that both PDL1 and IDO may need to be targeted to enhance Granzyme B tumorlytic activity. Altogether, our data suggest that co-blocking of IDO and B7 family is a promising strategy to promote anti-HCC T-cell immunity without adaptive tumor resistance.

A limitation of our present study is the investigation of the correlation of B7 family molecules, Tryptophan degrading enzymes and immune effectors only at RNA but not protein expression levels. Although significance of our approach is the identification of correlation pattern by combination analysis, such an approach at protein levels is laborious and often limited with the sensitivity to demonstrate correlation. Nevertheless, our results were supported by previous studies which demonstrated that some B7 family molecules such as PD-L1 (64, 65), PD-L2 (66), PD-1 (67), B7-H2 (68), B7-H3 (69) and IDO (70) play a significant functional role in modulating anti-HCC immunity. Although we have demonstrated the synergistic functions of IDO and PD-L1, future studies are necessary to determine if the other identified correlation of costimulatory and coinhibitory molecules play a functional synergistic role in modulating anti-HCC immunity.

Liver is a tolerogenic organ rich in parenchymal and non-parenchymal cell types such as Hepatocytes, Kupffer Cells, Liver Sinusoidal Endothelial Cells, Hepatic Dendritic Cells, Hepatic Stellate Cells, Mesenchymal Stromal Cells and Hepatic B cells that constantly interact with T cells in order to execute immune tolerance. Upon injury, the resting status of these intrahepatic antigen presenting cells gets compromised leading to

inflammation followed by fibrosis/cirrhosis. Eventually, immune suppression prevails that leads to HCC and significance of these cell types in HCC progression is important. Our earlier study has demonstrated that Hepatic Stellate Cells upregulate PD-L1 and IDO by IFNγ while blocking of IDO activity completely abolishes their immunosuppressive potential (71). Similarly, Kupffer cells in HCC were shown to execute immune suppression through PD-L1-PD-1 pathways (72). In the present study, we observed a correlation between PD-L2 and IFNγ. Future studies are warranted to define the coexpression, regulation and functions of B7 family molecules and Tryptophan degrading enzymes in intrahepatic APCs derived from HCC microenvironment. In conclusion, our study provided evidence that co-stimulatory and co-inhibitory molecules exhibit specific correlation pattern among themselves, with IDO and immune responsive effector molecules. This information is important to inform second-generation immunotherapy approaches for liver cancer management.

DATA AVAILABILITY STATEMENT

All datasets generated for this study are included in the article/supplementary material.

ETHICS STATEMENT

The studies involving human participants were reviewed and approved by Emory University IRB. The ethics committee waived the requirement of written informed consent for participation.

AUTHOR CONTRIBUTIONS

RC conceived, designed the research plan, performed most experiments, analyzed results, and wrote the manuscript. RS performed experiments related to flow cytometer and ELISA. OA, DR, AF, and BE provided patient materials. DA and GG helped with qPCR array. All authors contributed to the article and approved the submitted version.

FUNDING

This study was supported by the Winship Cancer Institute's Gala Scholar Award to RC. RC was partly supported by the WES Leukemia Research Foundation. This research was also supported by Mercer University School of Medicine's research funds (RC) and generous support from the Landings Women's Golf Association (Savannah, GA).

ACKNOWLEDGMENTS

We thank Dr. Suresh Ramalingam (Professor, Emory University) for advice in this project. We also thank Dr. Jacques Galipeau (Professor, University of Wisconsin-Madison) and Dr. Devi Rajan (Instructor, Mercer University School of Medicine, Georgia) for critically reading the manuscript.

REFERENCES

1. Llovet JM, Zucman-Rossi J, Pikarsky E, Sangro B, Schwartz M, Sherman M, et al. Hepatocellular carcinoma. *Nat Rev Dis Primers*. (2016) 2:16018. doi: 10.1038/nrdp.2016.18
2. Kudo M. Immuno-oncology in hepatocellular carcinoma: 2017 update. *Oncology*. (2017) 93 (Suppl. 1):147–59. doi: 10.1159/000481245
3. Brahmer JR, Tykodi SS, Chow LQ, Hwu WJ, Topalian SL, Hwu P, et al. Safety and activity of anti-PD-L1 antibody in patients with advanced cancer. *N Engl J Med*. (2012) 366:2455–65. doi: 10.1056/NEJMoa1200694
4. Topalian SL, Drake CG, Pardoll DM. Immune checkpoint blockade: a common denominator approach to cancer therapy. *Cancer Cell*. (2015) 27:450–61. doi: 10.1016/j.ccell.2015.03.001
5. Komiya T, Huang CH. Updates in the clinical development of epacadostat and other indoleamine 2,3-dioxygenase 1 inhibitors (IDO1) for human cancers. *Front Oncol*. (2018) 8:423. doi: 10.3389/fonc.2018.00423
6. Gunther J, Dabritz J, Wirthgen E. Limitations and off-target effects of tryptophan-related IDO inhibitors in cancer treatment. *Front Immunol*. (2019) 10:1801. doi: 10.3389/fimmu.2019.01801
7. Labadie BW, Bao R, Luke JJ. Reimagining IDO pathway inhibition in cancer immunotherapy via downstream focus on the tryptophan-kynurenine-aryl hydrocarbon axis. *Clin Cancer Res*. (2019) 25:1462–71. doi: 10.1158/1078-0432.CCR-18-2882
8. Vacchelli E, Aranda F, Eggermont A, Sautes-Fridman C, Tartour E, Kennedy EP, et al. Trial watch: IDO inhibitors in cancer therapy. *Oncoimmunology*. (2014) 3:e957994. doi: 10.4161/21624011.2014.957994
9. El Dika I, Khalil DN, Abou-Alfa GK. Immune checkpoint inhibitors for hepatocellular carcinoma. *Cancer*. (2019) 125:3312–9. doi: 10.1002/cncr.32076
10. Keenan BP, Fong L, Kelley RK. Immunotherapy in hepatocellular carcinoma: the complex interface between inflammation, fibrosis, and the immune response. *J Immunother Cancer*. (2019) 7:267. doi: 10.1186/s40425-019-0749-z
11. El-Khoueiry AB, Sangro B, Yau T, Crocenzi TS, Kudo M, Hsu C, et al. Nivolumab in patients with advanced hepatocellular carcinoma (CheckMate 040): an open-label, non-comparative, phase 1/2 dose escalation and expansion trial. *Lancet*. (2017) 389:2492–502. doi: 10.1016/S0140-6736(17)31046-2
12. Zhu AX, Finn RS, Edeline J, Cattan S, Ogasawara S, Palmer D, et al. Pembrolizumab in patients with advanced hepatocellular carcinoma previously treated with sorafenib (KEYNOTE-224): a non-randomised, open-label phase 2 trial. *Lancet Oncol*. (2018) 19:940–52. doi: 10.1016/S1470-2045(18)30351-6
13. Schildberg FA, Klein SR, Freeman GJ, Sharpe AH. Coinhibitory pathways in the B7-CD28 ligand-receptor family. *Immunity*. (2016) 44:955–72. doi: 10.1016/j.immuni.2016.05.002
14. Ni L, Dong C. New B7 family checkpoints in human cancers. *Mol Cancer Ther*. (2017) 16:1203–11. doi: 10.1158/1535-7163.MCT-16-0761
15. Blackburn SD, Shin H, Haining WN, Zou T, Workman CJ, Polley A, et al. Coregulation of CD8+ T cell exhaustion by multiple inhibitory receptors during chronic viral infection. *Nat Immunol*. (2009) 10:29–37. doi: 10.1038/ni.1679
16. Popovic A, Jaffee EM, Zaidi N. Emerging strategies for combination checkpoint modulators in cancer immunotherapy. *J Clin Invest*. (2018) 128:3209–18. doi: 10.1172/JCI120775
17. Blank CU, Haining WN, Held W, Hogan PG, Kallies A, Lugli E, et al. Defining 'T cell exhaustion'. *Nat Rev Immunol*. (2019) 19:665–74. doi: 10.1038/s41577-019-0221-9
18. Kurachi M. CD8(+) T cell exhaustion. *Semin Immunopathol*. (2019) 41:327–37. doi: 10.1007/s00281-019-00744-5

19. Boussiotis VA. Molecular and biochemical aspects of the PD-1 checkpoint pathway. *N Engl J Med*. (2016) 375:1767–78. doi: 10.1056/NEJMra1514296
20. Mak TW, Shahinian A, Yoshinaga SK, Wakeham A, Boucher LM, Pintilie M, et al. Costimulation through the inducible costimulator ligand is essential for both T helper and B cell functions in T cell-dependent B cell responses. *Nat Immunol*. (2003) 4:765–72. doi: 10.1038/ni947
21. Marin-Acevedo JA, Dholaria B, Soyano AE, Knutson KL, Chumsri S, Lou Y. Next generation of immune checkpoint therapy in cancer: new developments and challenges. *J Hematol Oncol*. (2018) 11:39. doi: 10.1186/s13045-018-0582-8
22. Prasad DV, Richards S, Mai XM, Dong C. B7S1, a novel B7 family member that negatively regulates T cell activation. *Immunity*. (2003) 18:863–73. doi: 10.1016/S1074-7613(03)00147-X
23. Flem-Karlsen K, Fodstad O, Tan M, Nunes-Xavier CE. B7-H3 in cancer - beyond immune regulation. *Trends Cancer*. (2018) 4:401–4. doi: 10.1016/j.trecan.2018.03.010
24. Sica GL, Choi IH, Zhu G, Tamada K, Wang SD, Tamura H, et al. B7-H4, a molecule of the B7 family, negatively regulates T cell immunity. *Immunity*. (2003) 18:849–61. doi: 10.1016/S1074-7613(03)00152-3
25. Macgregor HL, Ohashi PS. Molecular pathways: evaluating the potential for B7-H4 as an immunoregulatory target. *Clin Cancer Res*. (2017) 23:2934–41. doi: 10.1158/1078-0432.CCR-15-2440
26. Zhu Y, Yao S, Iliopoulou BP, Han X, Augustine MM, Xu H, et al. B7-H5 costimulates human T cells via CD28H. *Nat Commun*. (2013) 4:2043. doi: 10.1038/ncomms3043
27. Lines JL, Pantazi E, Mak J, Sempere LF, Wang L, O'connell S, et al. VISTA is an immune checkpoint molecule for human T cells. *Cancer Res.* (2014) 74:1924–32. doi: 10.1158/0008-5472.CAN-13-1504
28. Schlecker E, Fiegler N, Arnold A, Altevogt P, Rose-John S, Moldenhauer G, et al. Metalloprotease-mediated tumor cell shedding of B7-H6, the ligand of the natural killer cell-activating receptor NKp30. *Cancer Res*. (2014) 74:3429–40. doi: 10.1158/0008-5472.CAN-13-3017
29. Janakiram M, Chinai JM, Fineberg S, Fiser A, Montagna C, Medavarapu R, et al. Expression, clinical significance, and receptor identification of the newest B7 family member HHLA2 protein. *Clin Cancer Res*. (2015) 21:2359–66. doi: 10.1158/1078-0432.CCR-14-1495
30. Munn DH, Mellor AL. Indoleamine 2,3 dioxygenase and metabolic control of immune responses. *Trends Immunol*. (2013) 34:137–43. doi: 10.1016/j.it.2012.10.001
31. Prendergast GC, Mondal A, Dey S, Laury-Kleintop LD, Muller AJ. Inflammatory reprogramming with IDO1 inhibitors: turning immunologically unresponsive 'cold' tumors 'hot'. *Trends Cancer*. (2018) 4:38–58. doi: 10.1016/j.trecan.2017.11.005
32. Lemos H, Huang L, Prendergast GC, Mellor AL. Immune control by amino acid catabolism during tumorigenesis and therapy. *Nat Rev Cancer*. (2019) 19:162–75. doi: 10.1038/s41568-019-0106-z
33. Garber K. A new cancer immunotherapy suffers a setback. *Science*. (2018) 360:588. doi: 10.1126/science.360.6389.588
34. Chinnadurai R, Copland IB, Ng S, Garcia M, Prasad M, Arafat D, et al. Mesenchymal stromal cells derived from Crohn's patients deploy indoleamine 2,3-dioxygenase-mediated immune suppression, independent of autophagy. *Mol Ther*. (2015) 23:1248–61. doi: 10.1038/mt.2015.67
35. Chinnadurai R, Rajan D, Qayed M, Arafat D, Garcia M, Liu Y, et al. Potency analysis of mesenchymal stromal cells using a combinatorial assay matrix approach. *Cell Rep*. (2018) 22:2504–17. doi: 10.1016/j.celrep.2018.02.013
36. Chinnadurai R, Garcia MA, Sakurai Y, Lam WA, Kirk AD, Galipeau J, et al. Actin cytoskeletal disruption following cryopreservation alters the biodistribution of human mesenchymal stromal cells *in vivo*. *Stem Cell Reports*. (2014) 3:60–72. doi: 10.1016/j.stemcr.2014.05.003
37. Sun T, Li P, Sun D, Bu Q, Li G. Prognostic value of osteopontin in patients with hepatocellular carcinoma: A systematic review and meta-analysis. *Medicine*. (2018) 97:e12954. doi: 10.1097/MD.0000000000012954
38. Nishida T, Kataoka H. Glypican 3-targeted therapy in hepatocellular carcinoma. *Cancers*. (2019) 11:1339. doi: 10.3390/cancers11091339
39. Guo M, Zhang H, Zheng J, Liu Y. Glypican-3: a new target for diagnosis and treatment of hepatocellular carcinoma. *J Cancer*. (2020) 11:2008–21. doi: 10.7150/jca.39972
40. Giannini EG, Aglitti A, Borzio M, Gambato M, Guarino M, Iavarone M, et al.). Overview of immune checkpoint inhibitors therapy for hepatocellular carcinoma, and the ITA.LI.CA cohort derived estimate of amenability rate to immune checkpoint inhibitors in clinical practice. *Cancers*. (2019) 11:1689. doi: 10.3390/cancers11111689
41. Mahipal A, Tella SH, Kommalapati A, Lim A, Kim R. Immunotherapy in hepatocellular carcinoma: is there a light at the end of the tunnel? *Cancers*. (2019) 11:1078. doi: 10.3390/cancers11081078
42. Xu Z, Shen J, Wang MH, Yi T, Yu Y, Zhu Y, et al. Comprehensive molecular profiling of the B7 family of immune-regulatory ligands in breast cancer. *Oncoimmunology*. (2016) 5:e1207841. doi: 10.1080/2162402X.2016.1207841
43. Ghiotto M, Gauthier L, Serriari N, Pastor S, Truneh A, Nunes JA, et al. PD-L1 and PD-L2 differ in their molecular mechanisms of interaction with PD-1. *Int Immunol*. (2010) 22:651–60. doi: 10.1093/intimm/dxq049
44. Zak KM, Grudnik P, Magiera K, Domling A, Dubin G, Holak TA. Structural biology of the immune checkpoint receptor PD-1 and its ligands PD-L1/PD-L2. *Structure*. (2017) 25:1163–74. doi: 10.1016/j.str.2017.06.011
45. Kamphorst AO, Wieland A, Nasti T, Yang S, Zhang R, Barber DL, et al. Rescue of exhausted CD8 T cells by PD-1-targeted therapies is CD28-dependent. *Science*. (2017) 355:1423–7. doi: 10.1126/science.aaf0683
46. Wang Q, He J, Flies DB, Luo L, Chen L. Programmed death one homolog maintains the pool size of regulatory T cells by promoting their differentiation and stability. *Sci Rep*. (2017) 7:6086. doi: 10.1038/s41598-017-06410-w
47. Liu J, Yuan Y, Chen W, Putra J, Suriawinata AA, Schenk AD, et al. Immune-checkpoint proteins VISTA and PD-1 nonredundantly regulate murine T-cell responses. *Proc Natl Acad Sci USA*. (2015) 112:6682–7. doi: 10.1073/pnas.1420370112
48. Chew V, Lai L, Pan L, Lim CJ, Li J, Ong R, et al. Delineation of an immunosuppressive gradient in hepatocellular carcinoma using high-dimensional proteomic and transcriptomic analyses. *Proc Natl Acad Sci USA*. (2017) 114:E5900–9. doi: 10.1073/pnas.1706559114
49. Zheng C, Zheng L, Yoo JK, Guo H, Zhang Y, Guo X, et al. Landscape of infiltrating T cells in liver cancer revealed by single-cell sequencing. *Cell*. (2017) 169:1342–56 e1316. doi: 10.1016/j.cell.2017.05.035
50. Kalathil SG, Lugade AA, Miller A, Iyer R, Thanavala Y. PD-1(+) and Foxp3(+) T cell reduction correlates with survival of HCC patients after sorafenib therapy. *JCI Insight*. (2016) 2016:e86182. doi: 10.1172/jci.insight.86182
51. Johnson TS, Munn DH. Host indoleamine 2,3-dioxygenase: contribution to systemic acquired tumor tolerance. *Immunol Invest*. (2012) 41:765–97. doi: 10.3109/08820139.2012.689405
52. Han Y, Chen Z, Yang Y, Jiang Z, Gu Y, Liu Y, et al. Human CD14+ CTLA-4+ regulatory dendritic cells suppress T-cell response by cytotoxic T-lymphocyte antigen-4-dependent IL-10 and indoleamine-2,3-dioxygenase production in hepatocellular carcinoma. *Hepatology*. (2014) 59:567–79. doi: 10.1002/hep.26694
53. Mukhopadhyay B, Schuebel K, Mukhopadhyay P, Cinar R, Godlewski G, Xiong K, et al. Cannabinoid receptor 1 promotes hepatocellular carcinoma initiation and progression through multiple mechanisms. *Hepatology*. (2015) 61:1615–26. doi: 10.1002/hep.27686
54. Platten M, Wick W, Van Den Eynde BJ. Tryptophan catabolism in cancer: beyond IDO and tryptophan depletion. *Cancer Res*. (2012) 72:5435–40. doi: 10.1158/0008-5472.CAN-12-0569
55. Dill EA, Dillon PM, Bullock TN, Mills AM. IDO expression in breast cancer: an assessment of 281 primary and metastatic cases with comparison to PD-L1. *Mod Pathol*. (2018) 31:1513–22. doi: 10.1038/s41379-018-0061-3
56. Mills AM, Peres LC, Meiss A, Ring KL, Modesitt SC, Abbott SE, et al. Targetable immune regulatory molecule expression in high-grade serous ovarian carcinomas in african american women: a study of PD-L1 and IDO in 112 cases from the African American Cancer Epidemiology Study (AACES). *Int J Gynecol Pathol*. (2018) 38:157–70. doi: 10.1097/PGP.0000000000000494
57. Rosenberg AJ, Wainwright DA, Rademaker A, Galvez C, Genet M, Zhai L, et al. Indoleamine 2,3-dioxygenase 1 and overall survival of patients diagnosed with esophageal cancer. *Oncotarget*. (2018) 9:23482–93. doi: 10.18632/oncotarget.25235
58. Holmgaard RB, Zamarin D, Munn DH, Wolchok JD, Allison JP. Indoleamine 2,3-dioxygenase is a critical resistance mechanism in antitumor T cell

immunotherapy targeting CTLA-4. *J Exp Med*. (2013) 210:1389–402. doi: 10.1084/jem.20130066
59. Brown ZJ, Yu SJ, Heinrich B, Ma C, Fu Q, Sandhu M, et al. Indoleamine 2,3-dioxygenase provides adaptive resistance to immune checkpoint inhibitors in hepatocellular carcinoma. *Cancer Immunol Immunother*. (2018) 67:1305–15. doi: 10.1007/s00262-018-2190-4
60. Long GV, Dummer R, Hamid O, Gajewski T, Caglevic C, Dalle S, et al. Epacadostat. (E) plus pembrolizumab. (P) versus pembrolizumab alone in patients. (pts) with unresectable or metastatic melanoma: Results of the phase 3 ECHO-301/KEYNOTE-252 study. *J Clin Oncol*. (2018) 36:108–108. doi: 10.1016/S1470-2045(19)30274-8
61. Voskoboinik I, Whisstock JC, Trapani JA. Perforin and granzymes: function, dysfunction and human pathology. *Nat Rev Immunol*. (2015) 15:388–400. doi: 10.1038/nri3839
62. Durgeau A, Virk Y, Corgnac S, Mami-Chouaib F. Recent advances in targeting CD8 T-cell immunity for more effective cancer immunotherapy. *Front Immunol*. (2018) 9:14. doi: 10.3389/fimmu.2018.00014
63. Ding W, Xu X, Qian Y, Xue W, Wang Y, Du J, et al. Prognostic value of tumor-infiltrating lymphocytes in hepatocellular carcinoma: a meta-analysis. *Medicine*. (2018) 97:e13301. doi: 10.1097/MD.0000000000013301
64. Long J, Qu T, Pan XF, Tang X, Wan HH, Qiu P, et al. Expression of programmed death ligand-1 and programmed death 1 in hepatocellular carcinoma and its clinical significance. *J Cancer Res Ther*. (2018) 14:S1188–92. doi: 10.4103/0973-1482.204850
65. Nelson A. The social life of DNA: racial reconciliation and institutional morality after the genome - a response. *Br J Sociol*. (2018) 69:575–9. doi: 10.1111/1468-4446.12612
66. Liao H, Chen W, Dai Y, Richardson JJ, Guo J, Yuan K, et al. Expression of programmed cell death-ligands in hepatocellular carcinoma: correlation with immune microenvironment and survival outcomes. *Front Oncol*. (2019) 9:883. doi: 10.3389/fonc.2019.00883
67. Kim HD, Song GW, Park S, Jung MK, Kim MH, Kang HJ, et al. Association between expression level of PD1 by tumor-infiltrating CD8(+) T cells and features of hepatocellular carcinoma. *Gastroenterology*. (2018) 155:1936–50 e1917. doi: 10.1053/j.gastro.2018.08.030
68. Zheng Y, Liao N, Wu Y, Gao J, Li Z, Liu W, et al. High expression of B7H2 or B7H3 is associated with poor prognosis in hepatocellular carcinoma. *Mol Med Rep*. (2019) 19:4315–25. doi: 10.3892/mmr.2019.10080
69. Sun TW, Gao Q, Qiu SJ, Zhou J, Wang XY, Yi Y, et al. B7-H3 is expressed in human hepatocellular carcinoma and is associated with tumor aggressiveness and postoperative recurrence. *Cancer Immunol Immunother*. (2012) 61:2171–82. doi: 10.1007/s00262-012-1278-5
70. Wang Y, Yao R, Zhang L, Xie X, Chen R, Ren Z. IDO and intratumoral neutrophils were independent prognostic factors for overall survival for hepatocellular carcinoma. *J Clin Lab Anal*. (2019) 33:e22872. doi: 10.1002/jcla.22872
71. Chinnadurai R, Sands J, Rajan D, Liu X, Arafat D, Das R, et al. Molecular genetic and immune functional responses distinguish bone marrow mesenchymal stromal cells from hepatic stellate cells. *Stem Cells*. (2019) 37:1075–82. doi: 10.1002/stem.3028
72. Wu K, Kryczek I, Chen L, Zou W, Welling TH. Kupffer cell suppression of CD8++ T cells in human hepatocellular carcinoma is mediated by B7-H1/programmed death-1 interactions. *Cancer Res*. (2009) 69:8067–75. doi: 10.1158/0008-5472.CAN-09-0901

Conflict of Interest: The authors declare that the research was conducted in the absence of any commercial or financial relationships that could be construed as a potential conflict of interest.

frontiers in Immunology

REVIEW
published: 24 September 2020
doi: 10.3389/fimmu.2020.531491

IDO Expression in Cancer: Different Compartment, Different Functionality?

Annabel Meireson[1,2], *Michael Devos*[1] *and Lieve Brochez*[1,2]*

[1] Department of Dermatology, Ghent University Hospital, Ghent, Belgium, [2] Cancer Research Institute Ghent, Ghent, Belgium

Indoleamine 2,3-dioxygenase 1 (IDO1) is a cytosolic haem-containing enzyme involved in the degradation of tryptophan to kynurenine. Although initially thought to be solely implicated in the modulation of innate immune responses during infection, subsequent discoveries demonstrated IDO1 as a mechanism of acquired immune tolerance. In cancer, IDO1 expression/activity has been observed in tumor cells as well as in the tumor-surrounding stroma, which is composed of endothelial cells, immune cells, fibroblasts, and mesenchymal cells. IDO1 expression/activity has also been reported in the peripheral blood. This manuscript reviews available data on IDO1 expression, mechanisms of its induction, and its function in cancer for each of these compartments. In-depth study of the biological function of IDO1 according to the expressing (tumor) cell can help to understand if and when IDO1 inhibition can play a role in cancer therapy.

Keywords: IDO, kynurenine, tryptophan, cancer, indoleamine (2,3)-dioxygenase, tumor immunity

OPEN ACCESS

Edited by:
Giovanna Schiavoni,
National Institute of Health (ISS), Italy

Reviewed by:
Chai K. Lim,
Macquarie University, Australia
Francesca Fallarino,
University of Perugia, Italy

***Correspondence:**
Lieve Brochez
lieve.brochez@ugent.be

Specialty section:
This article was submitted to Cancer Immunity and Immunotherapy, a section of the journal Frontiers in Immunology

Received: *31 January 2020*
Accepted: *25 August 2020*
Published: *24 September 2020*

Citation:
Meireson A, Devos M and Brochez L (2020) IDO Expression in Cancer: Different Compartment, Different Functionality? Front. Immunol. 11:531491. doi: 10.3389/fimmu.2020.531491

INTRODUCTION

Indoleamine 2, 3-dioxygenase 1 (IDO1, hereafter referred to as IDO) is a 403 amino acid cytosolic haem-containing enzyme involved in the first, rate-limiting step of the tryptophan (Trp) metabolism to kynurenine (Kyn) (1, 2). Trp is an essential amino acid for which both neuropsychological as well as immunological functions have been described. Despite their shared function in Trp degradation, the IDO2 isoform and tryptophan 2, 3-dioxygenase (TDO2) have distinct inducers and patterns of tissue expression (3, 4).

IDO (human chromosome 8p22) is recognized as an interferon (IFN)-inducible gene. Indeed, the promoter region of *IDO* consists of several IFN-stimulated response elements (ISREs) and gamma activation sequences (GAS), permitting a controlled and context-dependent transcriptional process (2, 5, 6).

Although initially thought to be solely implicated in the modulation of innate immune responses in parasitic/viral conditions (7–9), subsequent discoveries demonstrated IDO to be a mechanism of acquired immune tolerance (4). In cancer, IDO expression has not only been documented in tumor cells but also in endothelial cells, fibroblasts and immune cells infiltrating the tumor microenvironment (**Figure 1**). In addition to the local tumor microenvironment, IDO expression was detected in peripheral blood mononuclear cells (PBMCs) in blood samples of cancer patients. Although IDO expression has been reported in these different compartments, the exact mechanisms for its distinct expression patterns and their functions are far from completely understood. In view of the complex interplay between malignant cells and their microenvironment, understanding IDO activation and its particular function in the different compartments may be of the outmost importance. This review summarizes the available scientific data.

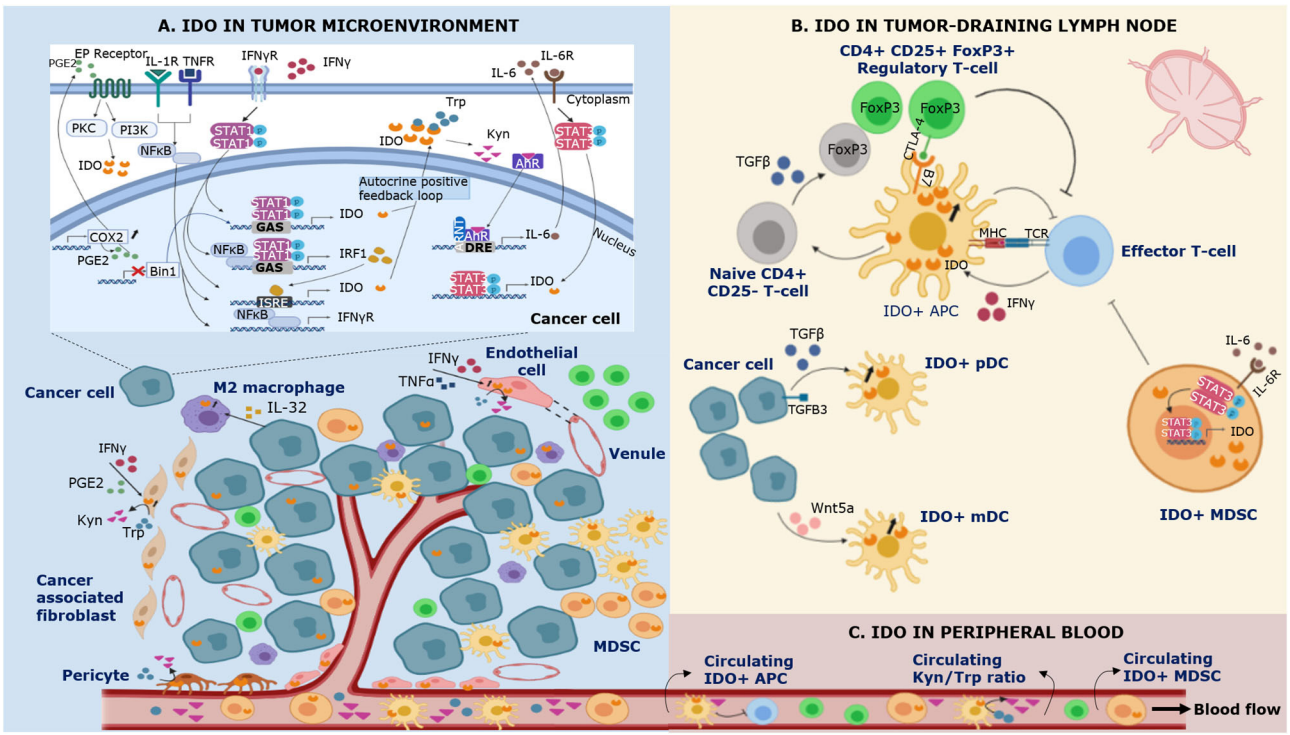

FIGURE 1 | Schematic representation of IDO expression in different compartments of the immune system during cancer. IDO is expressed by multiple cell types in the tumor microenvironment **(A)**, the tumor-draining lymph node **(B)** and the peripheral blood **(C)**. **(A)** Bin1 attenuation results in STAT1- and NFκB-dependent constitutive expression of IDO in cancer cells. In addition, COX2 overexpression facilitates constitutive IDO expression via PGE2-mediated activation of the PKC/PI3K pathways. IFNγ is recognized as a highly potent inducer of IDO expression. Binding of IFNγ to its receptor (IFNγR) leads to (i) tyrosine phosphorylation of STAT-1, triggering its dimerization and binding to the GAS sequence in *IDO1* and (ii) NF-κB and STAT-1 dependent synthesis of IFNγ-regulated factor 1 (IRF1), which binds to the ISRE sequences in *IDO1*. Tumor IDO expression activates the cytosolic transcription factor aryl hydrocarbon receptor (AhR) by kynurenine (Kyn), stimulating an autocrine positive feedback loop via IL-6 dependent STAT-3 signaling which maintains IDO expression. In addition to IFNγ, IDO expression can be induced by other proinflammatory cytokines such as tumor necrosis factor α (TNFα) and IL-1 who enhance the expression of IFNγR on cancer cells. IFNγ and TNFα can also induce IDO expression in endothelial cells of venules in the tumor microenvironment. In the tumor-surrounding stroma, IDO is expressed by cancer associated-fibroblasts, pericytes, and infiltrating immune cells. **(B)** Regulatory T-cells (Tregs) induce IDO expression by antigen-presenting cells (APCs) via CTLA-4/B7 ligation in the tumor-draining lymph node. In addition, cancer cells are involved in the upregulation of IDO expression in plasmacytoid dendritic cells (pDCs) by shedding of the extracellular domain of the type III TGF-B receptor (sTGFBR3). IDO expression in myeloid DCs (mDCs) can be induced by cancer cell-secreted Wnt5a, which triggers binding of β-catenin to its responsive elements. IDO$^+$ APCs inhibit T-cell responses and polarize naïve CD4$^+$ T-cell differentiation toward the phenotype of suppressive Tregs via TGFβ-mediated FoxP3 upregulation. Myeloid derived suppressor cells (MDSCs) upregulate IDO via IL-6 triggered STAT-3 activation. **(C)** IDO$^+$ APCs and IDO$^+$ MDSCs infiltrate the tumor microenvironment and the peripheral blood, contributing to local and systemic immune escape.

IDO IN THE TUMOR MICROENVIRONMENT

IDO expression in the tumor microenvironment has been described in tumor cells, immune cells, endothelial cells, and stromal fibroblasts (**Table 1**).

Tumor Cells

The majority of literature reports on IDO positivity in neoplastic cells. Strong expression in tumor tissue is identified as an independent negative prognostic factor in multiple cancers (4, 35, 87, 105, 106). It is well-documented that tumoral IDO expression is associated with tumor-infiltrating forkhead box P3 positive regulatory T-cells (FoxP3$^+$ Tregs) and IDO-expressing mononuclear cells, while a negative association with CD8$^+$ cytotoxic T-cells in the primary tumor and metastatic tissue has been reported (23–30, 107). These observations in human samples are consistent with earlier mechanistic studies elucidating the involvement of IDO in impairing cytotoxic effector T-cell function/proliferation via downregulation of the T-cell receptor ζ chain as well as its stimulatory role in enhancing Treg generation (31, 47, 54, 108, 109). In diffuse-type gastric cancer, elevated tumoral IDO expression correlated with decreased expression of CD107a and granzyme B in tumor-infiltrating CD8$^+$ T-cells, reflecting T-cell dysfunction (32). IDO expressed by pancreatic ductal adenocarcinoma cells was observed to support immune escape of cancer cells by impairing cytotoxicity and degranulation of γδ T-cells (33). In addition to FoxP3, tumoral IDO expression has been evidenced to be strongly correlated with other immunosuppressive molecules such as programmed cell death protein 1 (PD-1) and its ligand PD-L1 (29, 30, 44–46).

The extent of tumoral IDO expression has been investigated in the context of deficiencies in the DNA mismatch repair system. The microsatellite instable (MSI-H) subgroup of colorectal

TABLE 1 | Regulatory mechanisms and functions of IDO expressing cells in the tumor microenvironment.

		Human studies	Animal studies
Tumor cells	Regulatory mechanisms	- **Constitutive expression** (10, 11) dependent on COX2 and PGE2 (12) - **Induction by type I,II IFNs** (13), mediated by STAT-1 and NF-κB signaling (2, 5, 6, 14, 15) - Expression inversely correlated with Bin expression (16, 17) - Synergism between IFNγ and TNFα/IL1 on expression (18–20) - **Autocrine positive feedback loop** through Kyn-AhR-IL6-STAT3 (11)	- STAT-1- and NF-κB-dependent expression as a consequence of loss of Bin (21) - LPS induces systemic activity dependent on TNF (22)
	Functions	- Associated with **increased intratumoral Treg** infiltration and **impaired cytotoxic T-cell function** (23–30) - Conversion of $CD4^+CD25^-$Treg into $CD4^+CD25^+$ cells (31) - Prevents degranulation of $CD8^+$ and γδ T-cells (32, 33) - Associated with **MDSC infiltration** (34) - Promotes **proliferation of HUVEC cells** (35) - Associated with metastasis (35–42) - Drives **dormancy** of tumor repopulating cells (11, 43) - Correlates with PD-1 and PD-L1 expression (29, 30, 44–46)	- Trp depletion/catabolites drive TCR ζ-chain downregulation in $CD8^+$ cells and induce FoxP3 in $CD4^+$ cells (47) - Drives IL-6 dependent MDSC-mediated immune escape (36) - Associated with enhanced VEGF-C expression and lymphangiogenesis (48–50) - Promotes tumor vascularization (36) - Drives dormancy of tumor repopulating cells (43) - Drives tumorigenesis through NAD^+-depletion induced DNA damage (51)
Immune cells	Regulatory mechanisms	- Induction by PGE2 and activated by TNFα/TLR signaling in moDC (52, 53) - Induction by synergystic combination of IFNγ and CD40L in monocyte-derived macrophages (54) - Induction by IL-32γ depending on NF-κB and STAT-3 in macrophages (55) - Induction in MDSCs requires phosphorylation of STAT-3, but not STAT-1 (39) and non-canonical NF-κB (56)	- Expression in splenic DCs induced by CpGs and dependent on IFN type I signaling (57) - Expression in DCs induced by Tregs through CTLA-4/B7 (58) - Expression in pDCs induced by CpG, TGFβ, CD200 (59–61) - Expression in mDCs induced by Wnt5a (62, 63) and IFNγ in an IRF8-dependent way, functionally active in cDC1 (64, 65)
	Functions	- **DCs decrease antigen uptake and downregulate CD40/CD80** under low Trp conditions (66) - Expression in moDCs induces regulatory activity in T-cells (67, 68) - Expression is associated with distinct profile of cytokines and surface markers in moDCs (69, 70) - Mediates IFNγ-induced differentiation of monocytes into **M2-macrophages** (71–74) - Expression in macrophages halts cell cycle progression in T-cells (54, 55) - Expressing MDSCs associated with **$FoxP3^+$ Tregs and impaired $CD8^+$ T-cell function** (39, 75, 76)	- Expression in pDCs suppresses T-cell responses in TDLN (77) and activates Tregs in tumor microenvironment and TDLN (60, 61, 78) - Expression in DCs and MDSCs implicated in anti-PD-1 resistance (79) - Expression in MDSCs impairs AMPK and mTOR function (80)
Endothelial cells	Regulatory mechanisms	Induction and synergism by IFNγ (81, 82) and TNF (81)	- Induced by IFNγ through non-canonical NF-κB activation (83) - Induced by agonistic CD40 mAb through IFNγ secretion by $CD8^+$ T-cells (84)
	Functions	- Expression in $CD31^+$ HEV in peritumoral stroma: sentinel LN and metastatic tissue associated with **reduced $CD8^+$ T-cells** and **increased $FoxP3^+$ Tregs** (85) - Expression in sentinel LN associated with enhanced IDO expression in peripheral blood (86) - Expression associated with microsatellite instability in CRC (87) - Expression associated with responsiveness to anti-PD-1 (88, 89) - Drives tumor dormancy through Trp depletion-induced TSLP expression/secretion (90) - Expression in LECs **impairs $CD4^+$ T-cell proliferation** (91)	

(Continued)

TABLE 1 | Continued

		Human studies	Animal studies
Stromal cells	Regulatory mechanisms	- Induction in CAFs (92, 93), mesenchymal stem cells (94–96) and pericytes (82) by IFNγ - Expression in CAFS mediated by COX2/PGE2 (97)	
	Functions	- Expression in CAFs **suppresses NK cell activity** (98, 99) - Expression in dermal fibroblasts induces **apoptosis in T-cells, B cells and monocytes** (100) - Expression in mesenchymal stem cells involved in **inhibition of T-cell function** (96) and conversion of monocytes into **M2-macrophages** (101) - Expression in pericytes **negatively regulates T-cell proliferation** (102)	Expression in CAFs (103) and mesenchymal stem cells (104) involved in Treg activation

cancer is characterized by a strong infiltration of activated cytotoxic T-lymphocytes, which is a positive prognostic factor (110–113). Despite this highly inflamed environment, MSI-H tumors persist in such hostile climate due to overexpression of immune checkpoint molecules as cytotoxic T-lymphocyte-associated protein 4 (CTLA-4), lymphocyte-activation gene 3 (LAG-3), PD-1/PD-L1, and IDO, hampering an efficient anti-tumor T-cell response (87, 114, 115). It is hypothesized that the active tumor microenvironment is stimulated by an increased neoantigen load in MSI-H tumors, which is counterbalanced by the upregulation of immune checkpoints, such as IDO, as a negative feedback mechanism. This immunosuppressive climate mediates evasion of the tumor from the host immune system.

Besides the suppression of anti-tumor immune responses, tumoral IDO is involved in tumor vascularization. IDO-deficiency was observed to significantly decrease pulmonary vascular density in lung cancer mouse models, predominantly reducing small to medium size vessels, unaltering large vessels (36). In breast cancer, a cancer cell line (MCF-7) with strong IDO expression promoted proliferation of human umbilical vein endothelial cells (35). In murine metastasized melanoma lymph nodes, tumoral IDO expression was associated with enhanced expression of VEGF-C, an inducer of lymphangiogenesis, previously linked to the occurrence of regional lymph node metastasis (48–50). This observation suggests tumoral IDO expression is involved in the expansion of lymphatic vessels. Furthermore, tumoral IDO expression has been proposed to stimulate the metastasic process. An association between strong IDO expression at the primary tumor and development of lymph node and/or metachronous metastases is described in various malignancies (36–42). Studies detecting IDO in the primary tumor and the corresponding lymph node and metastatic tissue reported a highly consistent expression pattern of IDO throughout the disease course (44, 87). Altogether, these data define tumoral IDO as a modulator that bridges inflammation, vascularization, and immune escape to promote primary and metastatic tumor outgrowth.

Although it is widely accepted that tumor cells are capable of expressing IDO, the critical signals directing its expression and activity are only partially revealed. There are indications for constitutive/intrinsic as well as induced/extrinsic tumor IDO expression. Constitutive expression of *IDO* mRNA in the absence of any IFNγ exposure has been demonstrated in several cancer cell lines (10). This study also investigated *in vivo* IDO expression in multiple malignancies and normal cells in the stroma were observed to be IDO-negative in contrast to the tumor cells. The authors concluded that this tumoral IDO expression could not be the result of IFNγ exposure, as this would have induced IDO in the surrounding stroma too. Another study in ovarian and adeno-squamous lung cancer cell lines demonstrated that cancer cells expressed *IDO1* mRNA and constitutively released Kyn into the supernatant (11).

Loss of the tumor suppressor Bridging Integrator 1 (Bin1) and overexpression of cyclooxygenase-2 (COX2) are both linked to intrinsic upregulation of IDO. Bin1 loss in a knockout mouse model was associated with elevated STAT1- and NFκB-dependent expression of IDO, driving tumor immune escape (21). This is supported *in vivo* by the observation that tumor expression of Bin1 is inversely correlated with IDO expression in esophageal squamous cell cancer and lung cancer (16, 17). COX2 has been implicated in the pathogenesis of several cancers, in particular colorectal cancer, where it impacts oncogenic signaling, invasion and metastasis, survival and angiogenesis (116–118). In a series of tumor cell lines, it was demonstrated that constitutive IDO expression depends on COX2 and prostaglandin E2 (PGE2), which upon autocrine signaling through the EP receptor activates IDO transcription via the PKC and PI3K pathways. Oncogenic mutations were identified in the signaling pathways involved in this autocrine loop, favoring constitutive IDO expression (12).

Type I and especially type II IFNs are known to be potent IDO-inducers (13). As tumor-infiltrating lymphocytes (TILs) are a predominant source of IFNγ, they might upregulate IDO as a negative feedback signal, hereby potentially contributing to tumor immune escape. This is in line with the observation that human hepatoma cell lines express IDO once T-lymphocytes and monocytes are added, subsequently upregulating IFNγ in the co-culture (18). IFNγ-dependent induction of tumoral IDO expression has been extensively analyzed in various malignancies (38, 88, 119, 120). IFNγ-mediated signal transduction leads to (i) tyrosine phosphorylation of STAT-1, triggering its dimerization and binding to the GAS sequence in *IDO* and (ii) NFκB- and

STAT-1-dependent synthesis of IFNγ-regulated factor 1 (IRF1), which binds to the ISRE sequences in *IDO*. Combined STAT-1 and IRF-1 binding to GAS and ISRE sequences in the *IDO1* gene promoter is necessary for maximal IFNγ-mediated induction of IDO transcription (2, 5, 6, 14, 15). Tumoral IDO expression was suggested to stimulate an autocrine positive feedback loop via the activation of the cytosolic transcription factor aryl hydrocarbon receptor (AhR) by Kyn. AhR activation subsequently upregulates IL-6, which mediates STAT-3 signaling driving IDO expression (11). In addition, the IDO-Kyn-AhR pathway has been evidenced to drive dormancy in tumor repopulating cells (TRCs), a highly tumorigenic subpopulation of cancer cells involved in the initiation and progression of tumorigenesis. When TRCs were stimulated *in vitro* with IFNγ, phosphorylated STAT-1 rapidly upregulated IDO expression, subsequently elevating Kyn levels and activating AhR. This pathway triggers G0/G1 cell cycle arrest by p27 and TRC dormancy (43).

IFNγ-mediated IDO induction can be potentiated by other proinflammatory cytokines, such as tumor necrosis factor α (TNFα) (18, 19), IL-1 (20), lipopolysaccharide (LPS) (7, 22), CpG oligodoxynucleotides (57) and PGE2 (52). The combination of these inflammatory stimuli results in synergistic enhancement of *IDO* transcription. For instance, IL-1 and TNFα enhance the expression of IFNγ receptors (IFNγRs) via the transcription factor NFκB, lowering the threshold for IFNγ-directed IDO upregulation (121). In addition to IFNγ, TNFα synergistically induces IDO expression by increasing both STAT-1 activation and NFκB -dependent IRF-1 expression (19).

Immunohistochemical analysis of biopsies of melanoma metastases detected IDO, PD-L1, and FoxP3 in $CD8^+$ T-cell inflamed regions (29). In contrast, non-T-cell inflamed melanomas lacked these factors, suggesting that immune suppression might not be a property of tumor cells but rather an immune-intrinsic negative feedback process that follows the infiltration of activated $CD8^+$ T-cells. These data indicate that IFNγ produced by $CD8^+$ T-cells is a requisite factor for PD-L1 and IDO expression in melanoma metastatic tissue (29). Such T-cell inflamed–also termed immunologically "hot" –tumors have been associated with higher response rates to anti-PD-1 immunotherapy (122). This is in contrast to T-cell non-inflamed tumors–also referred to as "cold" tumors–which might constitute a group of tumors expressing IDO in absence of any inflammation and T-cell infiltration, representing a state of intrinsic immune resistance.

$CD8^+$ T-cell-mediated IDO expression via IFNγ in immunologically "hot" tumors could be one of the explanations why studies in breast cancer (123, 124), gastric adenocarcinoma (125), hepatocellular (126), pancreatic cancer (127), adenosquamous lung carcinoma (128), and prostate cancer (129) observed a positive prognostic effect for tumoral IDO expression. Another explanation–apart from technicalities such as the use of different antibody clones that could result in distinct staining patterns–could be Trp shortage caused by IDO activity. Trp is the only endogenous precursor for *de novo* biosynthesis of nicotinamide adenine dinucleotide (NAD^+), which is a co-enzyme of redox reactions for adenosine triphosphate (ATP) production. Enhanced IDO activity results in downregulated Trp and NAD^+ levels, the latter being a vital co-factor in energy production, DNA synthesis, and cellular homeostasis. NAD^+ depletion-induced DNA damage has been evidenced to play a role in liver tumorigenesis (51, 130).

Immune Cells

The most extensively studied IDO-expressing immune cell types in the tumor microenvironment are antigen presenting cells (APCs) and myeloid derived suppressor cells (MDSCs).

Immunohistochemical analysis of the local tumor microenvironment identified IDO expression in human dendritic cells (DCs) in melanoma (131), breast cancer (45), squamous cell carcinoma (132), Hodgkin lymphoma (71), and esophageal cancer (133). It is well-known that DCs acquire a strong tolerogenic capacity when cultivated under low Trp conditions as they decrease antigen uptake and downregulate the expression of the costimulatory molecules CD40 and CD80 (66). Munn et al. (77) detected IDO expression in murine plasmacytoid dendritic cell (pDCs) subsets upon CTLA4-Ig exposure. Although human $CD11c^-$ $CD123^+$ pDCs constitute a minor part of the tumor infiltrate, *in vitro* experiments in murine tumor draining lymph nodes (TDLNs) demonstrated that pDCs potently suppress $CD8^+$ T-cell responses to (i) antigens presented by the pDCs themselves, but also to (ii) third-party antigens presented by non-suppressive APCs (78). Notably, all of the T-cells achieved anergy when cultivated *in vitro* with a low quantity of IDO-expressing DCs, suggesting that *in vivo* levels (estimated at 0.5% of all TDLN cells) are sufficient to direct the entire TDLN toward a tolerogenic climate. The immunosuppressive effects of IDO^+ pDCs are elicited by inhibitory effects on $CD8^+$ T-cell responses, but also by GCN2-dependent activation of mature $CD4^+$ $CD25^+$ Tregs. *In vitro* CTLA-4 blockade significantly inhibited IDO-induced activation of Tregs in co-cultures, underlining the essential role of CTLA-4 in this pathway. Importantly, Tregs can trigger upregulation of IDO expression in DCs via CTLA-4 ligation with B7 receptor molecules on DCs (58). Fully activated Tregs reciprocally upregulate PD-L1 and PD-L2 expression on target DCs, suggesting IDO-induced Treg activation proceeds via a self-amplifying loop. Reverse signaling via other ligand-receptor pathways than CTLA-4/B7 interaction to induce IDO expression on DCs such as GITR, ICOS and CD200 has also been reported (59, 134, 135). In addition to the described rapid and potent mechanism of activating mature Tregs, IDO^+ pDCs also upregulate TGFβ-mediated FoxP3 expression in naïve $CD4^+$ $CD25^-$ cells, hereby polarizing $CD4^+$ T-cell differentiation toward the phenotype of suppressive Tregs. IL-6 production is simultaneously blocked in these naïve $CD4^+$ $CD25^-$ cells which prevents their conversion into Th17-like effector T-cells (47, 60). Intriguingly, tumor cells are involved in the upregulation of IDO expression in pDCs by shedding of the extracellular domain of the type III TGF-B receptor (sTGFBR3). A decrease in tumor-associated TGFBR3 expression increased TGFβ-dependent upregulation of IDO in pDCs within the primary tumor and TDLN of murine models of breast cancer and melanoma (61).

Myeloid conventional DCs (mDCs, characterized by $CD11c^+$ $CD123^-$) are also documented to express IDO. Despite the

fact that both murine CD8α$^+$ and CD8α$^-$ dendritic cells (resp. cDC1 and cDC2) express IDO upon *in vitro* stimulation with IFNγ, only IDO expression on cDC1s seems to be functionally active as evidenced by the Kyn concentration in the supernatant. Addition of IFNγ-stimulated cDC1s to Th1 cells caused up to 40% of Th1 cells to undergo apoptosis. In case of cDC2s, the proportion of Th1 cells undergoing apoptosis was equally low when co-cultured with unstimulated or IFNγ-stimulated cDC2s (64, 65). Besides IFNγ-mediated upregulation of IDO expression in mDCs, tumor cells promote mDC tolerization in the tumor microenvironment via paracrine Wnt-mediated signaling. Wnt5a secreted by melanoma cells activates β-catenin in DCs which upon nuclear translocation binds the TCF/LEF1 transcription factor responsive elements subsequently inducing IDO expression in an IFNγ-independent manner (62, 63). IDO expression in murine lung cancer models was uniquely observed in CD11b$^+$ CD11c$^-$ DCs, which were predominantly CD8α$^-$ (79). IDO expression has also been detected in a rare murine splenic cell type having phenotypic attributes of cDC1s (CD8α$^+$, CD80/CD86, MHCII) combined with expression of markers of the B-cell lineage (CD19$^+$, Pax5 and surface Ig) (136).

In addition to DCs differentiating from common dendritic progenitor cells (pDCs and mDCs), human monocyte-derived DCs (moDCs) are identified as IDO-competent APCs. Immunomodulatory properties of IDO$^+$ moDCs are identical to those described for pDCs and mDCs, including stimulation of Treg differentiation from naïve CD4$^+$ CD25$^-$ cells and suppression of T-cell responses (53, 67, 68). IDO expression seems to be dependent on the maturity status of moDCs and is limited to CD83$^+$ moDCs. Compared to IDO$^-$ moDCs, IDO$^+$ moDCs release a different pattern of cytokines (less IL-6 & IL-10, more IL-1β & IL-15) and upregulate surface markers as CD80, CD86, PD-L1, and PD-L2 (69). The different cytokine expression profile suggests altered functionality in IDO$^+$ moDCs. Remarkably, direct cell-contact between immature moDCs and mast cells has been observed to upregulate IDO in moDCs. This depends on interaction between PD-1, expressed by tissue resident mast cells, and PD-L1/PD-L2 on moDCs (70).

A role for IDO in the IFNγ-mediated differentiation of monocytes into M2-type macrophages has also been proposed (72, 73). M2-macrophages are associated with tumor progression in prostate, colon, breast cancer, gastric and ovarian cancer (137–144). *In vitro* stimulation of monocytes with IFNγ increased the M2/M1 ratio, while silencing of IDO in monocytes resulted in upregulation of pro-inflammatory M1-macrophages (74). In melanoma, macrophages constituted the predominant source of IDO expression in brain metastases (145). In agreement with these observations, IDO expression was detected in CD163$^+$ (M2-type) macrophages infiltrating the tumor microenvironment in Hodgkin lymphoma, and associated with shortened survival in these patients (71). A negative prognostic effect was confirmed in an independent Hodgkin lymphoma cohort, and the proportion of macrophages expressing both IDO and PD-L1 correlated with IFNγ gene expression (146). *In vitro* stimulation of human monocyte-derived macrophages showed that the early T-cell activation marker CD40L synergized with IFNγ for IDO upregulation (54). IDO-expressing macrophages interfered with T-cell activation, halting cell-cycle progression in the G1-phase. In multiple myeloma patients, tumor cells were described to secrete IL-32, triggering phosphorylation of STAT-3 and nuclear translocation of NFkB, subsequently inducing IDO expression in macrophages (55). Moreover, IDO$^+$ IL-32-educated macrophages suppressed proliferation of CD4$^+$ T-cells when co-cultured *in vitro*.

Strong expression of IDO by tumor cells associates with a higher level of tumor-infiltrating MDSCs in melanoma (34). MDSCs are myeloid cells with potent suppressive activities against effector lymphocytes in tumor immunology (147). IL-6 was found to be critical as an effector cytokine of IDO-driven MDSC activity and subsequent metastasis in lung cancer (36). MDSCs are also capable of expressing IDO, promoting tumor growth, and T-cell inhibition. The frequency of IDO$^+$ MDSCs was positively associated with the amount of FoxP3$^+$ Tregs and had a negative impact on patient outcome in breast cancer patients receiving neoadjuvant chemotherapy (75). In the tumor microenvironment of murine lung cancer models a subgroup of monocytic (Gr1^{int} CD11b$^+$) MDSCs were defined as the main source of IDO expression (79). IDO$^+$ MDSCs in a lung cancer mouse model were evidenced to impair AMPK and mTOR function, which are metabolic regulators in energy homeostasis during cellular stress (80). Because of reduced signaling of these regulators, tumor-residing CD8$^+$ T-cells upregulate checkpoint molecules, such as PD-1, CTLA-4, LAG-3, and TIM-3, reflecting the exhausted state of these cells. The molecular mechanisms underlying aberrant expression of IDO in MDSCs remain partially unclear. As described above, IFNγ is the most potent inducer of IDO expression in DCs and macrophages. IFNγ-triggered IDO expression mainly occurs trough the STAT-1 pathway (5, 57, 148). However, in human breast cancer or hematological cancer no changed IFNγ expression or STAT-1 signaling in MDSCs could be observed (39, 76). IDO was upregulated in breast cancer-derived MDSCs via IL-6-triggered STAT-3 activation, which activated the non-canonical NFκB pathway resulting in enhanced transcriptional activity of the IDO promoter (56).

Endothelial Cells

Physiological expression of IDO in endothelial cells (ECs) is limited, but has been extensively demonstrated in vessels of the villous chorion and in the spiral arteries of the decidua in humans during pregnancy (149). During the course of pregnancy endothelial IDO expression extends from the subtrophoblastic capillaries to larger vessels in the villi and the chorionic plate (150). Gestational age is associated with an increased Kyn/Trp ratio in the placenta, reflecting enhanced IDO activity. Endothelial IDO expression during pregnancy has been implicated in various important functions such as immune tolerance, antimicrobial protection, and optimization of placental perfusion (151–155). Antimicrobial as well as immunoregulatory properties have been designated to IDO-positive ECs. Stimulation of human brain microvascular ECs with IFNγ restricted growth/replication of viruses, bacteria, and parasites (153, 156, 157). In addition to these antimicrobial effects, IDO-mediated degradation of Trp in brain microvascular

ECs is responsible for a significant reduction of T-lymphocyte proliferation. This is in line with observations made in IDO-transfected ECs, which failed to stimulate allogeneic T-cell responses while anergy was induced in allospecific T-cells (81). A role for IDO-expressing ECs in the regulation of blood pressure has been observed, as IDO activity in murine ECs—measured by Kyn and Trp concentrations in plasma—resulted in arterial vessel relaxation through involvement of adenylate and soluble guanylate cyclase pathways (158). Furthermore, increased plasma Kyn/Trp has been associated with endothelial dysfunction and dysregulated immune responses during human sepsis (159, 160). Intriguingly, a recent study reported that patients with microvascular endothelial dysfunction had a >2-fold increased risk of developing solid-tumor cancer over a median follow-up period of 6 years (161).

Endothelial IDO expression has been described in several malignancies (71, 85, 87, 88, 90, 162, 163). In melanoma, IDO expression was prominent in $CD31^+$ high endothelial venules (HEV) in the stroma surrounding the tumor (85). Endothelial IDO expression in the peritumoral stroma of the primary tumor was consistent with expression in the corresponding sentinel node. Notably, IDO positivity in ECs persisted in metastatic melanoma tissue developing at a median time of 3.4 years (41.5 months) after first surgery. Its expression was a negative independent prognostic marker for recurrent-free survival and overall survival. Furthermore, endothelial IDO expression was associated with reduced $CD8^+$ T-cells and increased $FoxP3^+$ Tregs in the tumor microenvironment. Interestingly, in patients with IDO^+ ECs in the sentinel node enhanced IDO expression in the peripheral blood was detected, suggesting that endothelial IDO expression impacts systemic immunity (86). Similar observations were made in colorectal cancer, including a highly consistent expression pattern in the primary tumor, TDLNs (both tumor-invaded and tumor-uninvaded) and distant metastases (87). Endothelial IDO expression was more prevalent in MSI-H tumors compared to microsatellite stable (MSS) tumors. A negative effect on recurrence-free survival was observed for endothelial IDO expression, independent from disease stage, MMR status and CD8 count in the primary tumor.

In contrast, low IDO mRNA in the primary tumor of renal cell cancer patients was an independent unfavorable prognostic marker (88). Immunohistochemical analyses revealed that IDO was exclusively expressed by ECs, in contrast to the tumor cells which were IDO-negative. Another study in renal cell carcinoma confirmed absence of tumoral IDO expression and revealed that responders to anti-PD-1 therapy had stronger endothelial IDO expression compared to non-responders (89).

Little is known on the signaling pathways inducing IDO expression in ECs. Human umbilical vein ECs were reported to induce IDO upon stimulation with IFNγ (82) or TNFα, and these act synergistically when combined (81). IFNγ was also evidenced to upregulate IDO expression in human saphenous endothelial cells (164) and human corneal endothelial cells (165). In rats, IDO expression was induced in ECs by IFNγ-mediated activation of IKKα, which in turn stimulates the non-canonical NFκB pathway (83). In human invasive ductal carcinoma, IFNγ was demonstrated to be a potent inducer of endothelial IDO expression, which subsequently negatively affected the synthesis and secretion of stromal thrombospondin 1 (TSP1) via Trp deprivation. Reduced expression of TSP1, which is a large matricellular glycoprotein, supports cancer cells to evade tumor dormancy (90). Intriguingly, IDO was also induced when ECs were co-cultured with a tumorigenic metastatic triple negative breast cancer cell line (MDA-MB231). Tumor cells were a source of IFNγ in the co-culture, inducing IDO expression in ECs. Similarly, mRNA expression of IDO in lymphatic EC was significantly upregulated when co-cultured with $CD4^+$ T-lymphocytes and a gastric cancer cell line (OCUM12) (162). Treatment of murine experimental melanoma with CD40 immunotherapy resulted in upregulation of IFNγ signaling and subsequent expression of IDO by ECs (84). Interestingly, CD40 mAb combined with an IDO inhibitor (epacadostat) delayed tumor growth in these mice, while activation of TILs was increased.

Lymphatic endothelial cells (LECs) have been implicated to attribute to a climate of systemic peripheral tolerance. Lymphatic vessels transport antigens and DCs to lymph nodes, where naïve cells are primed via cross-reaction. Despite their facilitating role in the migration and homeostasis of naïve T-cells, it has been described that LECs are involved in the induction of anergy of activated T-cells. An *in vitro* study observed that human LECs in lymph nodes induced IDO expression upon IFNγ-stimulation and impaired $CD4^+$ T-cell proliferation when co-cultured (91). It is hypothesized that LECs promote $CD8^+$ T-cell tolerance by the upregulation of inhibitory molecules including PD-L1 and IDO (166–168).

Stromal Fibroblasts and Mesenchymal Cells

Tumor-surrounding stroma consists of fibroblasts, mesenchymal stromal cells, inflammatory cells, endothelial cells, and pericytes, which are all embedded in the extracellular matrix produced by fibroblasts (169, 170). Cancer associated-fibroblasts (CAFs) are the dominant stromal cell type and promote an immunosuppressive tumor microenvironment and tumor growth. IDO expression by CAFs was reported to be increased in the stroma of human esophageal cancers compared to non-tumor esophageal tissues (163). CAFs isolated from human metastatic melanoma and hepatocellular carcinomas have been documented to interfere with NK-cell mediated cancer cell killing (98, 99). CAFs expressed IDO and PGE2 when co-cultured with NK-cells, and impaired NK-cell secretion of granzyme B and perforin. Moreover, expression of NK-cell activation receptors such as NKp30 and NKp44 was downregulated. In addition to its suppressive effects on NK-cells, IFNγ-stimulated expression of IDO by dermal fibroblasts has been observed to induce apoptosis in $CD4^+$ and $CD8^+$ T-cells, B-cells and monocytes (100). In contrast to immune cells in the Trp-depleted microenvironment in this study, keratinocytes and endothelial cells were resistant and their proliferation was not altered. Another study highlighted low survival of the overall $CD4^+$ T-cell population when co-cultured with IDO^+ (compared to IDO^-) fibroblasts (103). However, the frequency of the $CD25^+$ $FoxP3^+$ $CD4^+$ subset

was increased and these T-cells exhibited classic functional characteristics of Tregs (CTLA-4, IL10, and TGFβ). IFNγ is recognized as a potent inducer of IDO in fibroblasts (92, 93, 103). Additionally, the COX2/PGE2 pathway was suggested to mediate IDO induction in CAFs. Overexpression of COX2 by breast cancer cells was documented to trigger PGE2 secretion, subsequently upregulating STAT3-mediated transcription of IDO in fibroblasts (97). Strong expression of IDO by CAFs was associated with decreased disease-free and metastasis-free survival in breast cancer patients.

In addition to CAFs, mesenchymal cells are able to express IDO in the tumor-surrounding stroma. Bone marrow-derived mesenchymal stem cells [also known as multipotent mesenchymal stromal cells (171), both abbreviated MSCs] are recruited to sites of tissue injury, where they have the potential to differentiate into osteoblasts, adipocytes, and chondrocytes and mediate tissue repair (172). In cancer, bone marrow-derived mesenchymal stem cells are recruited to the primary tumor where they differentiate into CAFs (173–175). Similar to CAFs, IDO can be induced in mesenchymal stem cells by IFNγ (94–96). IDO expressing mesenchymal stem cells are also involved in inhibition of T-cell function (96) and expansion of Tregs (104). Mesenchymal stromal cells were demonstrated to be involved in the differentiation of monocytes into immunosuppressive M2-macrophages (101).

Besides CAFs and MSCs, the tumor-surrounding stroma also consists of pericytes. In normal conditions, pericytes participate in the regulation of blood flow and vessel permeability, and provide important mechanical and physiological support to ECs (176–178). The reciprocal communication between ECs and pericytes is crucial for vessel remodeling, maturation, and stabilization (177, 179, 180). Pericytes promote tumor angiogenesis, and once detached from tumor vessels they are able to differentiate into CAFs, thereby mediating an immunosuppressive tumor microenvironment (181). Intriguingly, resting pericytes were reported to activate alloreactive T-cells while IFNγ-stimulated pericytes suppress T-cell proliferation. Immunophenotyping of IFNγ-stimulated pericytes revealed IDO as one of the most upregulated gene transcripts, together with other inhibitory molecules such as PD-L1, PD-L2, and CAECAM1 (82). In this study, IDO expression in pericytes was verified as the principal mechanism accounting for negative regulation of T-cell proliferation. In primary ovarian cancer, IDO-positive tumor-associated vessels were predominantly mature blood vessels covered by pericytes (102).

IDO IN THE PERIPHERAL BLOOD

IDO expression in the peripheral blood can be measured by direct methods such as single-cell RNA sequencing and flow cytometry allowing intracellular detection of IDO in specific PBMC subsets. Another method is quantification of Trp and Kyn in plasma/serum via ultra-performance liquid chromatography–tandem mass spectrometry (UPLC-MS/MS). Since enzymatic activity of IDO is involved in the first and rate-limiting step of the catabolism of Trp to Kyn and its downstream metabolites, increased Kyn/Trp is regarded as a surrogate for enhanced IDO activity. Several studies in different solid and hematological cancer types have related increased serum (or plasma) Kyn/Trp ratio to worse survival outcome (4, 182–186). A higher Kyn/Trp ratio has been linked to metastasis, higher tumor size, and advanced disease stages (4, 187, 188). Furthermore, a role for serum Kyn/Trp in predicting resistance to systemic treatment has been reported in several malignancies (79, 187, 189–192). In a large number of stage IV melanoma and renal cell cancer patients treated with anti-PD-1 therapy, a high increase in Kyn/Trp during therapy compared to baseline was associated with significantly reduced progression-free survival (193).

Although Kyn/Trp seems to have clinical relevance, the exact source of this IDO expression is unclear since its detection in serum/plasma is an indirect method measuring enzymatic IDO activity. Serum Kyn/Trp in human penile squamous cell carcinoma patients correlated with IDO expression in cancer cells but not with IDO expression on tumor-infiltrating immune cells (194). A recent study profiling Kyn/Trp in more than 900 human cancer cell lines demonstrated that secreted Kyn can be attributed to both IDO and TDO expression by tumor cells (195). However, another study observed a correlation of the Kyn/Trp ratio with PD-L1 and IDO but not with TDO mRNA levels in melanoma samples after 4 cycles of anti-PD-1 immunotherapy (193). Nevertheless, the authors argued that additional sources of Trp to Kyn degradation outside the tumor may exist. In support of this, ovarian cancer patients with high serum Kyn/Trp had strong IDO expression in both tumor cells and pericytes (102). In glioblastoma, diminished therapeutic response to CTLA-4/PD-L1 mAbs in $IDO^{-/-}$ mice compared to WT mice was observed, indicating the requirement for germline IDO to achieve maximal survival benefit from immune checkpoint therapy against brain tumors (196). Serum Kyn/Trp levels were significantly lower in $IDO^{-/-}$ mice compared to WT mice. Notably, no change in Kyn/Trp levels of isolated brain from glioblastoma WT mice and $IDO^{-/-}$ mice was noted. These findings suggest that non-tumor cell IDO activity contributes to a pool of Kyn in serum that facilitates responsiveness to immune checkpoint blockade. In line with these observations, serum Kyn/Trp measured by UPLC-MS/MS correlated with IDO expression in PBMCs measured by flow cytometric analysis of peripheral blood samples of melanoma patients (86). This correlation suggests that serum Kyn/Trp reflects metabolic activity of IDO-expressing circulating immune cells.

Only a few studies report on *in vivo* expression of IDO by specific subsets of immune cells in the peripheral blood. Munn et al. (197) observed low to undetectable levels of IDO in monocytes isolated from fresh PBMCs. Monocyte-derived $CD123^{+}$ macrophages upregulated IDO expression when stimulated with IFNγ *in vitro*. Surprisingly, IDO was constitutively expressed in human $CD123^{+}$ DCs in peripheral blood, but activation with IFNγ was still required for functional enzymatic activity. IDO^{+} $CD123^{+}$ DCs expressed MHC II and costimulatory molecules and were effective stimulators of T-cell proliferation when incubated with an IDO-inhibitor, suggesting that these cells could act as competent APCs.

DCs are observed to constitutively express IDO, but an additional set of triggering signals during antigen-presentation is required for its activity. Monocyte-derived DCs obtained from peripheral blood of melanoma patients were demonstrated to upregulate IDO expression upon *in vitro* activation by CD40L and IFNγ. During an immune response, activated DCs interact with IFNγ-expressing $CD8^+$ T-cells via CD40-CD40L ligation, subsequently mediating NFκB-dependent IDO upregulation in DCs (108, 198). Furthermore, IDO activity during DC activation was observed to be involved in the maturation of DCs, as Trp deprivation regulated expression of CCR5 and CXCR4 and DC responsiveness to chemokines (199). Another IDO-triggering signal can be elicited by DC B7-1/B7-2 ligation with CTLA-4/CD28, the latter being predominantly expressed by Tregs (200). Subsequent to the activation of IDO on DCs by activated Tregs, IDO^+ DCs drive differentiation of naïve $CD4^+$ $CD25^-$ T-cells into mature Tregs (201–204).

Expression of IDO by DCs has been demonstrated in peripheral blood of melanoma patients. IDO expression was predominantly found in $CD123^+$ pDCs in addition to monocytic MDSCs (mMDSCs), and to a lesser extent in polymorphonuclear MDSCs (pmnMDSCs) (86). Circulating pDCs and MDSCs were key players in the systemic response in melanoma, as they had an independent prognostic effect on survival of melanoma patients (205). Furthermore, IDO activity in peripheral blood was positively correlated with levels of circulating PD-$L1^+$ $CD8^+$ T-cells and CTLA-4^+ Tregs, underlining the close interconnection between these immunosuppressive markers in the blood circulation (86, 206). In early epithelial ovarian cancer, the level of IDO^+ mMDSCs and IDO^+ pmnMDSCs was significantly higher in the peripheral blood compared to the tumor microenvironment (207).

DISCUSSION

IDO expression in cancer has been described in a wide variety of cells both at the level of the tumor microenvironment and the peripheral blood. Depending on the exact location of expression, different induction pathways and effector functions have been observed. Several inflammatory cytokines such as IFNγ, IL-1, IL-6, IL-32, TNFα, and TGFβ were evidenced to drive IDO induction. Soluble factors excreted by tumor cells such as Wnt5a and sTGFBR3 are capable of inducing IDO in immune cells. Vice versa, immune cells such as $CD8^+$ T-cells in highly inflamed tumors were found to mediate induction of IDO in tumor cells via IFNγ signaling. The mechanisms that induce IDO expression and its various physiological and pathophysiological roles are currently incompletely understood but may be important in human biology in general and medical oncology in specific.

There is ample evidence on the role of IDO in tumor immune escape. The suppressive effects on T-cell responses in the different compartments of the tumor microenvironment are well-documented in both animal and human studies. Enzymatic activity of IDO in tumor cells, as well as in endothelial cells, APCs, MDSCs, and fibroblasts has been reported to stimulate anergy of effector T-cells, while Treg activity is enhanced. In addition, naïve $CD25^-$ $CD4^+$ T-cells are polarized toward the immunosuppressive $FoxP3^+$ $CD25^-$ $CD4^+$ phenotype while their conversion into Th17-like T-cells is blocked. In addition to the inhibition of antitumor immune responses, tumoral IDO expression promotes lymphangiogenesis and neovascularization, further facilitating tumor progression.

In the different compartments, IDO expression is closely interconnected with other immune checkpoint molecules already targeted by current immunotherapies. In the local tumor microenvironment, CTLA-4 expression in Tregs upregulates IDO in DCs, which reciprocally promotes Treg activation. This interplay of immune checkpoints is also evidenced in the peripheral blood, where IDO expression by PBMCs was demonstrated to be associated with increased circulating PD-$L1^+$ $CD8^+$ T-cells and CTLA-4^+ Tregs. In addition, blockade of CTLA-4 and/or PD-1 has been reported to upregulate IDO expression as a result of the increased IFNγ-production by reactivated effector T-cells. Immunomonitoring of blood samples can highlight such dynamic shifts in ongoing immune responses. In NSCLC, RCC and melanoma patients the baseline value of systemic Kyn/Trp as well as its dynamics during treatment course were associated with patient outcome (189, 193). In this way the Kyn/Trp ratio could be a marker best capturing IDO activity at a specific moment and perhaps could have relevance in therapeutic monitoring.

In the context of immunotherapy, the immunosuppressive role of host cell expressed IDO is supported by a striking delay in tumor growth in anti-CTLA-4 treated IDO knockout mice compared to WT mice (208). Pharmacological inhibition of IDO by 1-methyl-tryptophan (1MT) combined with anti-CTLA-4 resulted in rejection of established tumors and resistance to secondary challenge in mice inoculated with B16 melanoma. Tumor rejection by anti-CTLA-4/1MT therapy was associated with enhanced infiltration of functional $CD8^+$ and $CD4^+$ T-cells in the tumor. Notably, the combination therapy is synergistic irrespective of detectable IDO expression in tumor cells, though therapeutic efficacy was reduced against B16 melanoma cells engineered to overexpress IDO. Synergistic retardation of tumor outgrowth by anti-CTLA-4, anti-PD-L1 and/or IDO inhibition (INCB23843) was confirmed in a murine B16.SIY melanoma model (209). In preclinical models, IDO blockade has been demonstrated to be effective as part of combination therapy including immune checkpoint therapy, DNA-damaging chemotherapy and radiotherapy (21, 210). In a 4T1 breast tumor bearing mouse model, local radiotherapy combined with intratumoral CpG upregulated IDO expression in neoplastic epithelial cells. Systemic 1MT significantly decreased IDO activity (as measured by serum Kyn/Trp) and augmented the antitumor efficacy of local radiotherapy and intratumoral CpG (210).

Several IDO inhibitors tested in phase 1/2 clinical trials showed promising results. INCB024360 (epacadostat), a competitive, selective inhibitor of IDO, was well-tolerated in a first-in-human phase 1 study with near maximal inhibition achieved (measured by decreases in plasma Kyn levels) at doses $\geq$100 mg twice daily (BID) (211). Phase 1/2 studies evaluated epacadostat in combination with anti-CTLA-4

(ipilimumab) (212) and anti-PD-1 [nivolumab (213) and pembrolizumab (214)] and showed encouraging antitumor activity in multiple advanced solid tumors. However, a phase 3 trial in unresectable or metastatic melanoma (ECHO-301/KEYNOTE-252) failed to show any benefit of the addition of epacadostat to pembrolizumab (215). Results of this trial raised questions concerning IDO inhibition strategies in cancer treatment, however there are certain caveats (216). The dose of epacadostat used in ECHO-301 is debated as a maximum reduction in Kyn levels of only 50% was seen for this 100 mg dose in phase 1 studies. In addition, pharmacodynamic data reported for epacadostat were based on plasma measurements of Kyn, while IDO expression in the tumor microenvironment was not investigated (211). Baseline IDO expression or Kyn/Trp levels were not employed as inclusion criteria in the ECHO-301 study, and patients who previously received an adjuvant CTLA-4-inhibitor or interferon treatment were also included. Importantly, in a melanoma cohort receiving adjuvant IFN-α2b enhanced Kyn/Trp levels were detected compared to untreated patients (217). Furthermore, melanoma patients who did not respond to anti-CTLA-4 (ipilimumab) combined with stereotactic body radiotherapy showed an increase in the Kyn/Trp ratio during treatment compared to baseline Kyn/Trp (191). These data indicate that certain (immuno-) therapies may upregulate IDO activity, raising the question whether an enhanced dose of epacadostat would have been needed in the ECHO-301 study in order to fully block IDO activity.

BMS-986205, an irreversible IDO1 inhibitor, was demonstrated to reduce both serum (>60% mean reduction at a dose from 100 to 200 mg) and intratumoral (up to 90% reduction) Kyn levels (218). Currently, BMS-986205 in combination with anti-PD-1 therapy is investigated in several phase 2 trials (219–221). Besides IDO-specific inhibitors, other approaches to inhibit this pathway continue to be considered. Indoximod, a Trp mimetic, restores the activity of master metabolic kinase mTORC1 in effector T-cells, reversing autophagy triggered by Trp depletion (222). By targeting a downstream convergent effector mechanism used by IDO, as well as IDO2 and TDO, indoximod might prove less sensitive to negative feedback mechanisms that may result in treatment resistance (223).

Further research is needed to better understand the exact biological functions of IDO but also of the two other Trp-degrading enzymes IDO2 and TDO in the different compartments in cancer (224, 225). Increased insights in how these enzymes affect cancer immune escape and disease outcome could facilitate patient stratification in future clinical studies. The next step would be to investigate how these insights can be used to reverse this negative immune climate, thereby paving the way to personalized immuno-oncology possibly already in an early stage of cancer.

AUTHOR CONTRIBUTIONS

All authors had a substantial contribution to the manuscript, and approved the submitted version. AM and LB wrote the manuscript. AM generated the figure and MD assisted in the revision and made the table.

FUNDING

AM was funded by a grant of Ghent University Hospital.

REFERENCES

1. Shimizu T, Nomiyama S, Hirata F, Hayaishi O. Indoleamine 2,3-dioxygenase. Purification and some properties. *J Biol Chem*. (1978) 253:4700–6.
2. Taylor MW, Feng GS. Relationship between interferon-gamma, indoleamine 2,3-dioxygenase, and tryptophan catabolism. *FASEB J*. (1991) 5:2516–22. doi: 10.1096/fasebj.5.11.1907934
3. Prendergast GC, Malachowski WP, DuHadaway JB, Muller AJ. Discovery of IDO1 inhibitors: from bench to bedside. *Cancer Res*. (2017) 77:6795–811. doi: 10.1158/0008-5472.CAN-17-2285
4. Brochez L, Chevolet I, Kruse V. The rationale of indoleamine 2,3-dioxygenase inhibition for cancer therapy. *Eur J Cancer*. (2017) 76:167–82. doi: 10.1016/j.ejca.2017.01.011
5. Chon SY, Hassanain HH, Pine R, Gupta SL. Involvement of two regulatory elements in interferon-gamma-regulated expression of human indoleamine 2,3-dioxygenase gene. *J Interferon Cytokine Res Off J Int Soc Interferon Cytokine Res*. (1995) 15:517–26. doi: 10.1089/jir.1995.15.517
6. Konan KV, Taylor MW. Importance of the two interferon-stimulated response element (ISRE) sequences in the regulation of the human indoleamine 2,3-dioxygenase gene. *J Biol Chem*. (1996) 271:19140–5. doi: 10.1074/jbc.271.32.19140
7. Yoshida R, Hayaishi O. Induction of pulmonary indoleamine 2,3-dioxygenase by intraperitoneal injection of bacterial lipopolysaccharide. *Proc Natl Acad Sci USA*. (1978) 75:3998–4000. doi: 10.1073/pnas.75.8.3998
8. Yoshida R, Urade Y, Tokuda M, Hayaishi O. Induction of indoleamine 2,3-dioxygenase in mouse lung during virus infection. *Proc Natl Acad Sci USA*. (1979) 76:4084–6. doi: 10.1073/pnas.76.8.4084
9. Pfefferkorn ER. Interferon gamma blocks the growth of *Toxoplasma gondii* in human fibroblasts by inducing the host cells to degrade tryptophan. *Proc Natl Acad Sci USA*. (1984) 81:908–12. doi: 10.1073/pnas.81.3.908
10. Uyttenhove C, Pilotte L, Théate I, Stroobant V, Colau D, Parmentier N, et al. Evidence for a tumoral immune resistance mechanism based on tryptophan degradation by indoleamine 2,3-dioxygenase. *Nat Med*. (2003) 9:1269–74. doi: 10.1038/nm934
11. Litzenburger UM, Opitz CA, Sahm F, Rauschenbach KJ, Trump S, Winter M, et al. Constitutive IDO expression in human cancer is sustained by an autocrine signaling loop involving IL-6, STAT3 and the AHR. *Oncotarget*. (2014) 5:1038–51. doi: 10.18632/oncotarget.1637
12. Hennequart M, Pilotte L, Cane S, Hoffmann D, Stroobant V, Plaen ED, et al. Constitutive IDO1 expression in human tumors is driven by cyclooxygenase-2 and mediates intrinsic immune resistance. *Cancer Immunol Res*. (2017) 5:695–709. doi: 10.1158/2326-6066.CIR-16-0400
13. Takikawa O, Kuroiwa T, Yamazaki F, Kido R. Mechanism of interferon-gamma action. Characterization of indoleamine 2,3-dioxygenase in cultured human cells induced by interferon-gamma and evaluation of the enzyme-mediated tryptophan degradation in its anticellular activity. *J Biol Chem*. (1988) 263:2041–2048.
14. Hassanain HH, Chon SY, Gupta SL. Differential regulation of human indoleamine 2,3-dioxygenase gene expression by interferons-gamma and -alpha. Analysis of the regulatory region of the gene and identification of an interferon-gamma-inducible DNA-binding factor. *J Biol Chem*. (1993) 268:5077–84.
15. Du MX, Sotero-Esteva WD, Taylor MW. Analysis of transcription factors regulating induction of indoleamine 2,3-dioxygenase by IFN-gamma.

J Interferon Cytokine Res. (2000) 20:133–42. doi: 10.1089/107999000312531
16. Jia Y, Wang H, Wang Y, Wang T, Wang M, Ma M, et al. Low expression of Bin1, along with high expression of IDO in tumor tissue and draining lymph nodes, are predictors of poor prognosis for esophageal squamous cell cancer patients. *Int J Cancer*. (2015) 137:1095–106. doi: 10.1002/ijc.29481
17. Ahmadzada T, Lee K, Clarke C, Cooper WA, Linton A, McCaughan B, et al. High BIN1 expression has a favorable prognosis in malignant pleural mesothelioma and is associated with tumor infiltrating lymphocytes. *Lung Cancer*. (2019) 130:35–41. doi: 10.1016/j.lungcan.2019.02.005
18. Zhao Q, Wang P, Huang Z, Peng L, Lin C, Gao Z, et al. Tumoral indoleamine 2, 3-dioxygenase 1 is regulated by monocytes and T lymphocytes collaboration in hepatocellular carcinoma. *Oncotarget*. (2016) 7:14781–90. doi: 10.18632/oncotarget.7438
19. Robinson CM, Hale PT, Carlin JM. The role of IFN-γ and TNF-α-responsive regulatory elements in the synergistic induction of indoleamine dioxygenase. *J Interferon Cytokine Res Off J Int Soc Interferon Cytokine Res*. (2005) 25:20–30. doi: 10.1089/jir.2005.25.20
20. Babcock TA, Carlin JM. Transcriptional activation of indoleamine dioxygenase by interleukin 1 and tumor necrosis factor alpha in interferon-treated epithelial cells. *Cytokine*. (2000) 12:588–94. doi: 10.1006/cyto.1999.0661
21. Muller AJ, DuHadaway JB, Donover PS, Sutanto-Ward E, Prendergast GC. Inhibition of indoleamine 2,3-dioxygenase, an immunoregulatory target of the cancer suppression gene Bin1, potentiates cancer chemotherapy. *Nat Med NY*. (2005) 11:312–9. doi: 10.1038/nm1196
22. Fujigaki S, Saito K, Sekikawa K, Tone S, Takikawa O, Fujii H, et al. Lipopolysaccharide induction of indoleamine 2,3-dioxygenase is mediated dominantly by an IFN-gamma-independent mechanism. *Eur J Immunol*. (2001) 31:2313–8. doi: 10.1002/1521-4141(200108)31:8<2313::AID-IMMU2313>3.0.CO;2-S
23. Brody JR, Costantino CL, Berger AC, Sato T, Lisanti MP, Yeo CJ, et al. Expression of indoleamine 2,3-dioxygenase in metastatic malignant melanoma recruits regulatory T cells to avoid immune detection and affects survival. *Cell Cycle Georget Tex*. (2009) 8:1930–4. doi: 10.4161/cc.8.12.8745
24. Inaba T, Ino K, Kajiyama H, Shibata K, Yamamoto E, Kondo S, et al. Indoleamine 2,3-dioxygenase expression predicts impaired survival of invasive cervical cancer patients treated with radical hysterectomy. *Gynecol Oncol*. (2010) 117:423–8. doi: 10.1016/j.ygyno.2010.02.028
25. Zhang G, Liu W-L, Zhang L, Wang J-Y, Kuang M-H, Liu P, et al. Involvement of indoleamine 2,3-dioxygenase in impairing tumor-infiltrating CD8 T-cell functions in esophageal squamous cell carcinoma. *Clin Dev Immunol*. (2011) 2011:384726. doi: 10.1155/2011/384726
26. Ye J, Liu H, Hu Y, Li P, Zhang G, Li Y. Tumoral indoleamine 2,3-dioxygenase expression predicts poor outcome in laryngeal squamous cell carcinoma. *Virchows Arch Int J Pathol*. (2013) 462:73–81. doi: 10.1007/s00428-012-1340-x
27. Moretti S, Menicali E, Voce P, Morelli S, Cantarelli S, Sponziello M, et al. Indoleamine 2,3-dioxygenase 1 (IDO1) is up-regulated in thyroid carcinoma and drives the development of an immunosuppressant tumor microenvironment. *J Clin Endocrinol Metab*. (2014) 99:832–40. doi: 10.1210/jc.2013-3351
28. Ino K, Yamamoto E, Shibata K, Kajiyama H, Yoshida N, Terauchi M, et al. Inverse correlation between tumoral indoleamine 2,3-dioxygenase expression and tumor-infiltrating lymphocytes in endometrial cancer: its association with disease progression and survival. *Clin Cancer Res Off J Am Assoc Cancer Res*. (2008) 14:2310–7. doi: 10.1158/1078-0432.CCR-07-4144
29. Spranger S, Spaapen RM, Zha Y, Williams J, Meng Y, Ha TT, et al. Up-regulation of PD-L1, IDO, and Tregs in the melanoma tumor microenvironment is driven by CD8+ T cells. *Sci Transl Med*. (2013) 5:200ra116. doi: 10.1126/scitranslmed.3006504
30. Gide TN, Allanson BM, Menzies AM, Ferguson PM, Madore J, Saw RPM, et al. Inter- and intrapatient heterogeneity of indoleamine 2,3-dioxygenase expression in primary and metastatic melanoma cells and the tumour microenvironment. *Histopathology*. (2019) 74:817–28. doi: 10.1111/his.13814
31. Curti A, Pandolfi S, Valzasina B, Aluigi M, Isidori A, Ferri E, et al. Modulation of tryptophan catabolism by human leukemic cells results in the conversion of CD25– into CD25+ T regulatory cells. *Blood*. (2007) 109:2871–7. doi: 10.1182/blood-2006-07-036863
32. Li R, Zhang H, Cao Y, Liu X, Chen Y, Qi Y, et al. Lauren classification identifies distinct prognostic value and functional status of intratumoral CD8+ T cells in gastric cancer. *Cancer Immunol Immunother*. (2020) 69:1327–36. doi: 10.1007/s00262-020-02550-7
33. Jonescheit H, Oberg H-H, Gonnermann D, Hermes M, Sulaj V, Peters C, et al. Influence of indoleamine-2,3-dioxygenase and its metabolite kynurenine on γδ T cell cytotoxicity against ductal pancreatic adenocarcinoma cells. *Cells*. (2020) 9:1140. doi: 10.3390/cells9051140
34. Holmgaard RB, Zamarin D, Li Y, Gasmi B, Munn DH, Allison JP, et al. Tumor-expressed IDO recruits and activates MDSCs in a Treg-dependent manner. *Cell Rep*. (2015) 13:412–24. doi: 10.1016/j.celrep.2015.08.077
35. Wei L, Zhu S, Li M, Li F, Wei F, Liu J, et al. High indoleamine 2,3-dioxygenase is correlated with microvessel density and worse prognosis in breast cancer. *Front Immunol*. (2018) 9:724. doi: 10.3389/fimmu.2018.00724
36. Smith C, Chang M-Y, Parker K, Beury D, DuHadaway JB, Flick HE, et al. IDO is a nodal pathogenic driver of lung cancer and metastasis development. *Cancer Discov*. (2012) 2:722–35. doi: 10.1158/2159-8290.CD-12-0014
37. Yu J, Sun J, Wang SE, Li H, Cao S, Cong Y, et al. Upregulated expression of indoleamine 2, 3-dioxygenase in primary breast cancer correlates with increase of infiltrated regulatory T cells *in situ* and lymph node metastasis. *Clin Dev Immunol*. (2011) 2011:469135. doi: 10.1155/2011/469135
38. Ferdinande L, Decaestecker C, Verset L, Mathieu A, Moles Lopez X, Negulescu A-M, et al. Clinicopathological significance of indoleamine 2,3-dioxygenase 1 expression in colorectal cancer. *Br J Cancer*. (2012) 106:141–7. doi: 10.1038/bjc.2011.513
39. Yu J, Du W, Yan F, Wang Y, Li H, Cao S, et al. Myeloid-derived suppressor cells suppress antitumor immune responses through ido expression and correlate with lymph node metastasis in patients with breast cancer. *J Immunol*. (2013) 190:3783–97. doi: 10.4049/jimmunol.1201449
40. Engin A, Gonul II, Engin AB, Karamercan A, Sepici Dincel A, Dursun A. Relationship between indoleamine 2,3-dioxygenase activity and lymphatic invasion propensity of colorectal carcinoma. *World J Gastroenterol*. (2016) 22:3592–601. doi: 10.3748/wjg.v22.i13.3592
41. Tang D, Yue L, Yao R, Zhou L, Yang Y, Lu L, et al. P53 prevent tumor invasion and metastasis by down-regulating IDO in lung cancer. *Oncotarget*. (2017) 8:54548–57. doi: 10.18632/oncotarget.17408
42. Ogawa M, Watanabe M, Hasegawa T, Ichihara K, Yoshida K, Yanaga K. Expression of CXCR-4 and IDO in human colorectal cancer: an immunohistochemical approach. *Mol Clin Oncol*. (2017) 6:701–4. doi: 10.3892/mco.2017.1207
43. Liu Y, Liang X, Yin X, Lv J, Tang K, Ma J, et al. Blockade of IDO-kynurenine-AhR metabolic circuitry abrogates IFN-γ-induced immunologic dormancy of tumor-repopulating cells. *Nat Commun*. (2017) 8:1–15. doi: 10.1038/ncomms15207
44. Dill EA, Dillon PM, Bullock TN, Mills AM. IDO expression in breast cancer: an assessment of 281 primary and metastatic cases with comparison to PD-L1. *Mod Pathol*. (2018) 31:1513–22. doi: 10.1038/s41379-018-0061-3
45. Ye Q, Wang C, Xian J, Zhang M, Cao Y, Cao Y. Expression of programmed cell death protein 1 (PD-1) and indoleamine 2,3-dioxygenase (IDO) in the tumor microenvironment and in tumor-draining lymph nodes of breast cancer. *Hum Pathol*. (2018) 75:81–90. doi: 10.1016/j.humpath.2018.02.004
46. Mandarano M, Bellezza G, Belladonna ML, Van den Eynde BJ, Chiari R, Vannucci J, et al. Assessment of TILs, IDO-1, and PD-L1 in resected non-small cell lung cancer: an immunohistochemical study with clinicopathological and prognostic implications. *Virchows Arch*. (2019) 474:159–68. doi: 10.1007/s00428-018-2483-1
47. Fallarino F, Grohmann U, You S, McGrath BC, Cavener DR, Vacca C, et al. The combined effects of tryptophan starvation and tryptophan catabolites down-regulate T cell receptor ζ-chain and induce a regulatory phenotype in naive T cells. *J Immunol*. (2006) 176:6752–61. doi: 10.4049/jimmunol.176.11.6752
48. He Y, Rajantie I, Pajusola K, Jeltsch M, Holopainen T, Yla-Herttuala S, et al. Vascular endothelial cell growth factor receptor 3–mediated activation of lymphatic endothelium is crucial for tumor

cell entry and spread via lymphatic vessels. *Cancer Res*. (2005) 65:4739–46. doi: 10.1158/0008-5472.CAN-04-4576
49. Boone B, Blokx W, De Bacquer D, Lambert J, Ruiter D, Brochez L. The role of VEGF-C staining in predicting regional metastasis in melanoma. *Virchows Arch*. (2008) 453:257–65. doi: 10.1007/s00428-008-0641-6
50. Massi D, Puig S, Franchi A, Malvehy J, Vidal-Sicart S, Gonzalez-Cao M, et al. Tumour lymphangiogenesis is a possible predictor of sentinel lymph node status in cutaneous melanoma: a case–control study. *J Clin Pathol*. (2006) 59:166–73. doi: 10.1136/jcp.2005.028431
51. Tummala KS, Gomes AL, Yilmaz M, Graña O, Bakiri L, Ruppen I, et al. Inhibition of *de novo* NAD(+) synthesis by oncogenic URI causes liver tumorigenesis through DNA damage. *Cancer Cell*. (2014) 26:826–39. doi: 10.1016/j.ccell.2014.10.002
52. Braun D, Longman RS, Albert ML. A two-step induction of indoleamine 2,3 dioxygenase (IDO) activity during dendritic-cell maturation. *Blood*. (2005) 106:2375–81. doi: 10.1182/blood-2005-03-0979
53. Lanzinger M, Jürgens B, Hainz U, Dillinger B, Raberger J, Fuchs D, et al. Ambivalent effects of dendritic cells displaying prostaglandin E2-induced indoleamine 2,3-dioxygenase. *Eur J Immunol*. (2012) 42:1117–28. doi: 10.1002/eji.201141765
54. Munn DH, Shafizadeh E, Attwood JT, Bondarev I, Pashine A, Mellor AL. Inhibition of T cell proliferation by macrophage tryptophan catabolism. *J Exp Med*. (1999) 189:1363–72. doi: 10.1084/jem.189.9.1363
55. Yan H, Dong M, Liu X, Shen Q, He D, Huang X, et al. Multiple myeloma cell-derived IL-32γ increases the immunosuppressive function of macrophages by promoting indoleamine 2,3-dioxygenase (IDO) expression. *Cancer Lett*. (2019) 446:38–48. doi: 10.1016/j.canlet.2019.01.012
56. Yu J, Wang Y, Yan F, Zhang P, Li H, Zhao H, et al. Noncanonical NF-κB activation mediates STAT3-stimulated IDO upregulation in myeloid-derived suppressor cells in breast cancer. *J Immunol*. (2014) 193:2574–86. doi: 10.4049/jimmunol.1400833
57. Mellor AL, Baban B, Chandler PR, Manlapat A, Kahler DJ, Munn DH. Cutting edge: CpG oligonucleotides induce splenic CD19+ dendritic cells to acquire potent indoleamine 2,3-dioxygenase-dependent T cell regulatory functions via IFN Type 1 signaling. *J Immunol Baltim Md 1950*. (2005) 175:5601–5. doi: 10.4049/jimmunol.175.9.5601
58. Fallarino F, Grohmann U, Hwang KW, Orabona C, Vacca C, Bianchi R, et al. Modulation of tryptophan catabolism by regulatory T cells. *Nat Immunol*. (2003) 4:1206–12. doi: 10.1038/ni1003
59. Fallarino F, Asselin-Paturel C, Vacca C, Bianchi R, Gizzi S, Fioretti MC, et al. Murine plasmacytoid dendritic cells initiate the immunosuppressive pathway of tryptophan catabolism in response to CD200 receptor engagement. *J Immunol*. (2004) 173:3748–54. doi: 10.4049/jimmunol.173.6.3748
60. Baban B, Chandler PR, Sharma MD, Pihkala J, Koni PA, Munn DH, et al. IDO activates regulatory T cells and blocks their conversion into Th17-like T cells. *J Immunol Baltim Md 1950*. (2009) 183:2475–83. doi: 10.4049/jimmunol.0900986
61. Hanks BA, Holtzhausen A, Evans KS, Jamieson R, Gimpel P, Campbell OM, et al. Type III TGF-β receptor downregulation generates an immunotolerant tumor microenvironment. *J Clin Invest*. (2013) 123:3925–40. doi: 10.1172/JCI65745
62. Holtzhausen A, Zhao F, Evans KS, Tsutsui M, Orabona C, Tyler DS, et al. Melanoma-derived Wnt5a promotes local dendritic-cell expression of IDO and immunotolerance: opportunities for pharmacologic enhancement of immunotherapy. *Cancer Immunol Res*. (2015) 3:1082–95. doi: 10.1158/2326-6066.CIR-14-0167
63. Zhao F, Xiao C, Evans KS, Theivanthiran T, DeVito N, Holtzhausen A, et al. Paracrine Wnt5a-β-catenin signaling triggers a metabolic program that drives dendritic cell tolerization. *Immunity*. (2018) 48:147–60. doi: 10.1016/j.immuni.2017.12.004
64. Fallarino F, Vacca C, Orabona C, Belladonna ML, Bianchi R, Marshall B, et al. Functional expression of indoleamine 2,3-dioxygenase by murine CD8α+ dendritic cells. *Int Immunol*. (2002) 14:65–8. doi: 10.1093/intimm/14.1.65
65. Orabona C, Puccetti P, Vacca C, Bicciato S, Luchini A, Fallarino F, et al. Toward the identification of a tolerogenic signature in IDO-competent dendritic cells. *Blood*. (2006) 107:2846–54. doi: 10.1182/blood-2005-10-4077
66. Brenk M, Scheler M, Koch S, Neumann J, Takikawa O, Häcker G, et al. Tryptophan deprivation induces inhibitory receptors ILT3 and ILT4 on dendritic cells favoring the induction of human CD4+CD25+ Foxp3+ T regulatory cells. *J Immunol*. (2009) 183:145–54. doi: 10.4049/jimmunol.0803277
67. Jürgens B, Hainz U, Fuchs D, Felzmann T, Heitger A. Interferon-γ-triggered indoleamine 2,3-dioxygenase competence in human monocyte-derived dendritic cells induces regulatory activity in allogeneic T cells. *Blood*. (2009) 114:3235–43. doi: 10.1182/blood-2008-12-195073
68. Chung DJ, Rossi M, Romano E, Ghith J, Yuan J, Munn DH, et al. Indoleamine 2,3-dioxygenase–expressing mature human monocyte-derived dendritic cells expand potent autologous regulatory T cells. *Blood*. (2009) 114:555–63. doi: 10.1182/blood-2008-11-191197
69. Von Bubnoff D, Scheler M, Wilms H, Fimmers R, Bieber T. Identification of IDO-positive and IDO-negative human dendritic cells after activation by various proinflammatory stimuli. *J Immunol Baltim Md 1950*. (2011) 186:6701–9. doi: 10.4049/jimmunol.1003151
70. Rodrigues CP, Ferreira ACF, Pinho MP, de Moraes CJ, Bergami-Santos PC, Barbuto JAM. Tolerogenic IDO+ dendritic cells are induced by PD-1-expressing mast cells. *Front Immunol*. (2016) 7:9. doi: 10.3389/fimmu.2016.00009
71. Choe J-Y, Yun JY, Jeon YK, Kim SH, Park G, Huh JR, et al. Indoleamine 2,3-dioxygenase (IDO) is frequently expressed in stromal cells of Hodgkin lymphoma and is associated with adverse clinical features: a retrospective cohort study. *BMC Cancer*. (2014) 14:335. doi: 10.1186/1471-2407-14-335
72. Carlin JM, Borden EC, Sondel PM, Byrne GI. Interferon-induced indoleamine 2,3-dioxygenase activity in human mononuclear phagocytes. *J Leukoc Biol*. (1989) 45:29–34. doi: 10.1002/jlb.45.1.29
73. Werner ER, Bitterlich G, Fuchs D, Hausen A, Reibnegger G, Szabo G, et al. Human macrophages degrade tryptophan upon induction by interferon-gamma. *Life Sci*. (1987) 41:273–80. doi: 10.1016/0024-3205(87)90149-4
74. Wang X-F, Wang H-S, Wang H, Zhang F, Wang K-F, Guo Q, et al. The role of indoleamine 2,3-dioxygenase (IDO) in immune tolerance: focus on macrophage polarization of THP-1 cells. *Cell Immunol*. (2014) 289:42–8. doi: 10.1016/j.cellimm.2014.02.005
75. Li F, Zhao Y, Wei L, Li S, Liu J. Tumor-infiltrating Treg, MDSC, and IDO expression associated with outcomes of neoadjuvant chemotherapy of breast cancer. *Cancer Biol Ther*. (2018) 19:695–705. doi: 10.1080/15384047.2018.1450116
76. Mougiakakos D, Jitschin R, von Bahr L, Poschke I, Gary R, Sundberg B, et al. Immunosuppressive CD14 + HLA-DR low/neg IDO + myeloid cells in patients following allogeneic hematopoietic stem cell transplantation. *Leukemia*. (2013) 27:377–88. doi: 10.1038/leu.2012.215
77. Munn DH, Sharma MD, Hou D, Baban B, Lee JR, Antonia SJ, et al. Expression of indoleamine 2,3-dioxygenase by plasmacytoid dendritic cells in tumor-draining lymph nodes. *J Clin Invest*. (2004) 114:280–90. doi: 10.1172/JCI21583
78. Sharma MD, Baban B, Chandler P, Hou D-Y, Singh N, Yagita H, et al. Plasmacytoid dendritic cells from mouse tumor-draining lymph nodes directly activate mature Tregs via indoleamine 2,3-dioxygenase. *J Clin Invest*. (2007) 117:2570–82. doi: 10.1172/JCI31911
79. Li A, Barsoumian HB, Schoenhals JE, Cushman TR, Caetano MS, Wang X, et al. Indoleamine 2,3-dioxygenase 1 inhibition targets anti-PD1-resistant lung tumors by blocking myeloid-derived suppressor cells. *Cancer Lett*. (2018) 431:54–63. doi: 10.1016/j.canlet.2018.05.005
80. Schafer CC, Wang Y, Hough KP, Sawant A, Grant SC, Thannickal VJ, et al. Indoleamine 2,3-dioxygenase regulates anti-tumor immunity in lung cancer by metabolic reprogramming of immune cells in the tumor microenvironment. *Oncotarget*. (2016) 7:75407–24. doi: 10.18632/oncotarget.12249
81. Beutelspacher SC, Tan PH, McClure MO, Larkin DFP, Lechler RI, George AJT. Expression of indoleamine 2,3-dioxygenase (IDO) by endothelial cells: implications for the control of alloresponses. *Am J Transplant*. (2006) 6:1320–30. doi: 10.1111/j.1600-6143.2006.01324.x
82. Liu R, Merola J, Manes TD, Qin L, Tietjen GT, López-Giráldez F, et al. Interferon-γ converts human microvascular pericytes into negative regulators of alloimmunity through induction of indoleamine 2,3-dioxygenase 1. *JCI Insight*. (2018) 3:e97881. doi: 10.1172/jci.insight.97881

83. Liang Y, Yu Z, Song Y, Wang T, Xiao B. Indoleamine 2,3-dioxygenase activation by interferon gamma in vascular endothelial rat cells requires noncanonical nf-κb signaling. *Transplant Proc*. (2019) 51:2141–5. doi: 10.1016/j.transproceed.2019.03.043
84. Georganaki M, Ramachandran M, Tuit S, Núñez NG, Karampatzakis A, Fotaki G, et al. Tumor endothelial cell up-regulation of IDO1 is an immunosuppressive feed-back mechanism that reduces the response to CD40-stimulating immunotherapy. *OncoImmunology*. (2020) 9:1730538. doi: 10.1080/2162402X.2020.1730538
85. Chevolet I, Speeckaert R, Haspeslagh M, Neyns B, Krüse V, Schreuer M, Gele MV, et al. Peritumoral indoleamine 2,3-dioxygenase expression in melanoma: an early marker of resistance to immune control? *Br J Dermatol*. (2014) 171:987–95. doi: 10.1111/bjd.13100
86. Chevolet I, Speeckaert R, Schreuer M, Neyns B, Krysko O, Bachert C, et al. Characterization of the *in vivo* immune network of IDO, tryptophan metabolism, PD-L1, and CTLA-4 in circulating immune cells in melanoma. *OncoImmunology*. (2015) 4:e982382. doi: 10.4161/2162402X.2014.982382
87. Meireson A, Chevolet I, Hulstaert E, Ferdinande L, Ost P, Geboes K, et al. Peritumoral endothelial indoleamine 2, 3-dioxygenase expression is an early independent marker of disease relapse in colorectal cancer and is influenced by DNA mismatch repair profile. *Oncotarget*. (2018) 9:25216–24. doi: 10.18632/oncotarget.25393
88. Riesenberg R, Weiler C, Spring O, Eder M, Buchner A, Popp T, et al. Expression of indoleamine 2,3-dioxygenase in tumor endothelial cells correlates with long-term survival of patients with renal cell carcinoma. *Clin Cancer Res*. (2007) 13:6993–7002. doi: 10.1158/1078-0432.CCR-07-0942
89. Seeber A, Klinglmair G, Fritz J, Steinkohl F, Zimmer K-C, Aigner F, et al. High IDO-1 expression in tumor endothelial cells is associated with response to immunotherapy in metastatic renal cell carcinoma. *Cancer Sci*. (2018) 109:1583–91. doi: 10.1111/cas.13560
90. Lopes-Bastos B, Jin L, Ruge F, Owen S, Sanders A, Cogle C, et al. Association of breast carcinoma growth with a non-canonical axis of IFNγ/IDO1/TSP1. *Oncotarget*. (2017) 8:85024–39. doi: 10.18632/oncotarget.18781
91. Nörder M, Gutierrez MG, Zicari S, Cervi E, Caruso A, Guzmán CA. Lymph node-derived lymphatic endothelial cells express functional costimulatory molecules and impair dendritic cell-induced allogenic T-cell proliferation. *FASEB J*. (2012) 26:2835–46. doi: 10.1096/fj.12-205278
92. Yufit T, Vining V, Brown RR, Varga J, Wang L. Inhibition of type I collagen mRNA expression independent of tryptophan depletion in interferon-γ-treated human dermal fibroblasts. *J Invest Dermatol*. (1995) 105:388–93. doi: 10.1111/1523-1747.ep12320990
93. Ryu Y-H, Kim J-C. Expression of indoleamine 2,3-dioxygenase in human corneal cells as a local immunosuppressive factor. *Invest Ophthalmol Vis Sci*. (2007) 48:4148–52. doi: 10.1167/iovs.05-1336
94. Meisel R, Zibert A, Laryea M, Göbel U, Däubener W, Dilloo D. Human bone marrow stromal cells inhibit allogeneic T-cell responses by indoleamine 2,3-dioxygenase-mediated tryptophan degradation. *Blood*. (2004) 103:4619–21. doi: 10.1182/blood-2003-11-3909
95. Ryan JM, Barry F, Murphy JM, Mahon BP. Interferon-γ does not break, but promotes the immunosuppressive capacity of adult human mesenchymal stem cells. *Clin Exp Immunol*. (2007) 149:353–63. doi: 10.1111/j.1365-2249.2007.03422.x
96. Ren G, Su J, Zhang L, Zhao X, Ling W, L'huillie A, et al. Species variation in the mechanisms of mesenchymal stem cell-mediated immunosuppression. *Stem Cells*. (2009) 27:1954–62. doi: 10.1002/stem.118
97. Chen J-Y, Li C-F, Kuo C-C, Tsai KK, Hou M-F, Hung W-C. Cancer/stroma interplay via cyclooxygenase-2 and indoleamine 2,3-dioxygenase promotes breast cancer progression. *Breast Cancer Res*. (2014) 16:410. doi: 10.1186/s13058-014-0410-1
98. Balsamo M, Scordamaglia F, Pietra G, Manzini C, Cantoni C, Boitano M, et al. Melanoma-associated fibroblasts modulate NK cell phenotype and antitumor cytotoxicity. *Proc Natl Acad Sci USA*. (2009) 106:20847–52. doi: 10.1073/pnas.0906481106
99. Li T, Yang Y, Hua X, Wang G, Liu W, Jia C, et al. Hepatocellular carcinoma-associated fibroblasts trigger NK cell dysfunction via PGE2 and IDO. *Cancer Lett*. (2012) 318:154–61. doi: 10.1016/j.canlet.2011.12.020
100. Li Y, Tredget EE, Kilani RT, Iwashina T, Karami A, Lin X, et al. Expression of indoleamine 2,3-dioxygenase in dermal fibroblasts functions as a local immunosuppressive factor. *J Invest Dermatol*. (2004) 122:953–64. doi: 10.1111/j.0022-202X.2004.22409.x
101. François M, Romieu-Mourez R, Li M, Galipeau J. Human MSC suppression correlates with cytokine induction of indoleamine 2,3-dioxygenase and bystander M2 macrophage differentiation. *Mol Ther*. (2012) 20:187–95. doi: 10.1038/mt.2011.189
102. Heeren AM, van Dijk I, Berry DRAI, Khelil M, Ferns D, Kole J, et al. Indoleamine 2,3-dioxygenase expression pattern in the tumor microenvironment predicts clinical outcome in early stage cervical cancer. *Front Immunol*. (2018) 9:1598. doi: 10.3389/fimmu.2018.01598
103. Curran T-A, Jalili RB, Farrokhi A, Ghahary A. IDO expressing fibroblasts promote the expansion of antigen specific regulatory T cells. *Immunobiology*. (2014) 219:17–24. doi: 10.1016/j.imbio.2013.06.008
104. Kadle RL, Abdou SA, Villarreal-Ponce AP, Soares MA, Sultan DL, David JA, et al. Microenvironmental cues enhance mesenchymal stem cell-mediated immunomodulation and regulatory T-cell expansion. *PLoS ONE*. (2018) 13:e0193178. doi: 10.1371/journal.pone.0193178
105. Yu C-P, Fu S-F, Chen X, Ye J, Ye Y, Kong L-D,et al. The clinicopathological and prognostic significance of IDO1 expression in human solid tumors: evidence from a systematic review and meta-analysis. *Cell Physiol Biochem*. (2018) 49:134–43. doi: 10.1159/000492849
106. Kim D, Kim JM, Kim J-S, Kim S, Kim K-H. Differential expression and clinicopathological significance of HER2, indoleamine 2,3-dioxygenase and PD-L1 in urothelial carcinoma of the bladder. *J Clin Med*. (2020) 9:1265. doi: 10.3390/jcm9051265
107. Wang S, Wu J, Shen H, Wang J. The prognostic value of IDO expression in solid tumors: a systematic review and meta-analysis. *BMC Cancer*. (2020) 20:471. doi: 10.1186/s12885-020-06956-5
108. Hwu P, Du MX, Lapointe R, Do M, Taylor MW, Young HA. Indoleamine 2,3-dioxygenase production by human dendritic cells results in the inhibition of T cell proliferation. *J Immunol*. (2000) 164:3596–9. doi: 10.4049/jimmunol.164.7.3596
109. Chen W, Liang X, Peterson AJ, Munn DH, Blazar BR. The indoleamine 2,3-dioxygenase pathway is essential for human plasmacytoid dendritic cell-induced adaptive T regulatory cell generation. *J Immunol*. (2008) 181:5396–404. doi: 10.4049/jimmunol.181.8.5396
110. Dolcetti R, Viel A, Doglioni C, Russo A, Guidoboni M, Capozzi E, et al. High prevalence of activated intraepithelial cytotoxic T lymphocytes and increased neoplastic cell apoptosis in colorectal carcinomas with microsatellite instability. *Am J Pathol*. (1999) 154:1805–13. doi: 10.1016/S0002-9440(10)65436-3
111. Smyrk TC, Watson P, Kaul K, Lynch HT. Tumor-infiltrating lymphocytes are a marker for microsatellite instability in colorectal carcinoma. *Cancer*. (2001) 91:2417–22. doi: 10.1002/1097-0142(20010615)91:12<2417::AID-CNCR1276>3.0.CO;2-U
112. Phillips SM, Banerjea A, Feakins R, Li SR, Bustin SA, Dorudi S. Tumour-infiltrating lymphocytes in colorectal cancer with microsatellite instability are activated and cytotoxic. *BJS Br J Surg*. (2004) 91:469–75. doi: 10.1002/bjs.4472
113. Pagès F, Galon J, Dieu-Nosjean M-C, Tartour E, Sautès-Fridman C, Fridman W-H. Immune infiltration in human tumors: a prognostic factor that should not be ignored. *Oncogene*. (2010) 29:1093–102. doi: 10.1038/onc.2009.416
114. Llosa NJ, Cruise M, Tam A, Wick EC, Hechenbleikner EM, Taube JM, et al. The vigorous immune microenvironment of microsatellite instable colon cancer is balanced by multiple counter-inhibitory checkpoints. *Cancer Discov*. (2015) 5:43–51. doi: 10.1158/2159-8290.CD-14-0863
115. Loupakis F, Maddalena G, Depetris I, Murgioni S, Bergamo F, Dei Tos AP, et al. Treatment with checkpoint inhibitors in a metastatic colorectal cancer patient with molecular and immunohistochemical heterogeneity in MSI/dMMR status. *J Immunother Cancer*. (2019) 7:297. doi: 10.1186/s40425-019-0788-5
116. Tsujii M, Kawano S, DuBois RN. Cyclooxygenase-2 expression in human colon cancer cells increases metastatic potential. *Proc Natl Acad Sci USA*. (1997) 94:3336–40. doi: 10.1073/pnas.94.7.3336
117. Iñiguez MA, Rodriguez A, Volpert OV, Fresno M, Redondo JM. Cyclooxygenase-2: a therapeutic target in angiogenesis. *Trends Mol Med*. (2003) 9:73–8. doi: 10.1016/S1471-4914(02)00011-4

118. Kaidi A, Qualtrough D, Williams AC, Paraskeva C. Direct transcriptional up-regulation of cyclooxygenase-2 by hypoxia-inducible factor (HIF)-1 promotes colorectal tumor cell survival and enhances HIF-1 transcriptional activity during hypoxia. *Cancer Res*. (2006) 66:6683–91. doi: 10.1158/0008-5472.CAN-06-0425
119. Brandacher G, Perathoner A, Ladurner R, Schneeberger S, Obrist P, Winkler C, et al. Prognostic value of indoleamine 2,3-dioxygenase expression in colorectal cancer: effect on tumor-infiltrating T cells. *Clin Cancer Res*. (2006) 12:1144–51. doi: 10.1158/1078-0432.CCR-05-1966
120. Banzola I, Mengus C, Wyler S, Hudolin T, Manzella G, Chiarugi A, et al. Expression of indoleamine 2,3-dioxygenase induced by IFN-γ and TNF-α as potential biomarker of prostate cancer progression. *Front Immunol*. (2018) 9:51. doi: 10.3389/fimmu.2018.01051
121. Shirey KA, Jung J-Y, Maeder GS, Carlin JM. Upregulation of IFN-γ receptor expression by proinflammatory cytokines influences IDO activation in epithelial cells. *J Interferon Cytokine Res Off J Int Soc Interferon Cytokine Res*. (2006) 26:53–62. doi: 10.1089/jir.2006.26.53
122. Tumeh PC, Harview CL, Yearley JH, Shintaku IP, Taylor EJM, Robert L, et al. PD-1 blockade induces responses by inhibiting adaptive immune resistance. *Nature*. (2014) 515:568–71. doi: 10.1038/nature13954
123. Jacquemier J, Bertucci F, Finetti P, Esterni B, Charafe-Jauffret E, Thibult M-L, et al. High expression of indoleamine 2,3-dioxygenase in the tumour is associated with medullary features and favourable outcome in basal-like breast carcinoma. *Int J Cancer*. (2012) 130:96–104. doi: 10.1002/ijc.25979
124. Soliman H, Rawal B, Fulp J, Lee J-H, Lopez A, Bui MM, et al. Analysis of indoleamine 2-3 dioxygenase (IDO1) expression in breast cancer tissue by immunohistochemistry. *Cancer Immunol Immunother*. (2013) 62:829–37. doi: 10.1007/s00262-013-1393-y
125. Patil PA, Blakely AM, Lombardo KA, Machan JT, Miner TJ, Wang L-J, et al. Expression of PD-L1, indoleamine 2,3-dioxygenase and the immune microenvironment in gastric adenocarcinoma. *Histopathology*. (2018) 73:124–36. doi: 10.1111/his.13504
126. Ishio T, Goto S, Tahara K, Tone S, Kawano K, Kitano S. Immunoactivative role of indoleamine 2,3-dioxygenase in human hepatocellular carcinoma. *J Gastroenterol Hepatol*. (2004) 19:319–26. doi: 10.1111/j.1440-1746.2003.03259.x
127. Sideras K, Biermann K, Yap K, Mancham S, Boor PPC, Hansen BE, et al. Tumor cell expression of immune inhibitory molecules and tumor-infiltrating lymphocyte count predict cancer-specific survival in pancreatic and ampullary cancer. *Int J Cancer*. (2017) 141:572–82. doi: 10.1002/ijc.30760
128. Ma W, Duan H, Zhang R, Wang X, Xu H, Zhou Q, et al. High expression of indoleamine 2, 3-dioxygenase in adenosquamous lung carcinoma correlates with favorable patient outcome. *J Cancer*. (2019) 10:267–76. doi: 10.7150/jca.27507
129. Ferreira JM, Dellê H, Camacho CP, Almeida RJ, Reis ST, Matos YST, et al. Indoleamine 2,3-dioxygenase expression in the prognosis of the localized prostate cancer. *Int Urol Nephrol*. (2020) 52:1477–82. doi: 10.1007/s11255-020-02414-0
130. Reinhardt HC, Schumacher B. The p53 network: cellular and systemic DNA damage responses in aging and cancer. *Trends Genet TIG*. (2012) 28:128–136. doi: 10.1016/j.tig.2011.12.002
131. Rubel F, Kern JS, Technau-Hafsi K, Uhrich S, Thoma K, Häcker G, et al. Indoleamine 2,3-dioxygenase expression in primary cutaneous melanoma correlates with breslow thickness and is of significant prognostic value for progression-free survival. *J Invest Dermatol*. (2018) 138:679–87. doi: 10.1016/j.jid.2017.09.036
132. Kuales MA, Wenzel J, Schmid-Wendtner M-H, Bieber T, von Bubnoff D. Myeloid CD11c+ S100+ dendritic cells express indoleamine 2,3-dioxygenase at the inflammatory border to invasive lower lip squamous cell carcinoma. *Histol Histopathol*. (2011) 26:997–1006. doi: 10.14670/HH-26.997
133. Liu J, Lu G, Tang F, Liu Y, Cui G. Localization of indoleamine 2,3-dioxygenase in human esophageal squamous cell carcinomas. *Virchows Arch*. (2009) 455:441–8. doi: 10.1007/s00428-009-0846-3
134. Grohmann U, Volpi C, Fallarino F, Bozza S, Bianchi R, Vacca C, et al. Reverse signaling through GITR ligand enables dexamethasone to activate IDO in allergy. *Nat Med*. (2007) 13:579–86. doi: 10.1038/nm1563
135. Coquerelle C, Oldenhove G, Acolty V, Denoeud J, Vansanten G, Verdebout J-M, et al. Anti-CTLA-4 treatment induces IL-10-producing ICOS+ regulatory T cells displaying IDO-dependent anti-inflammatory properties in a mouse model of colitis. *Gut*. (2009) 58:1363–73. doi: 10.1136/gut.2008.162842
136. Johnson BA, Kahler DJ, Baban B, Chandler PR, Kang B, Shimoda M, et al. B-lymphoid cells with attributes of dendritic cells regulate T cells via indoleamine 2,3-dioxygenase. *Proc Natl Acad Sci USA*. (2010) 107:10644–8. doi: 10.1073/pnas.0914347107
137. Shimura S, Yang G, Ebara S, Wheeler TM, Frolov A, Thompson TC. Reduced infiltration of tumor-associated macrophages in human prostate cancer: association with cancer progression. *Cancer Res*. (2000) 60:5857–61.
138. Forssell J, Öberg Å, Henriksson ML, Stenling R, Jung A, Palmqvist R. High macrophage infiltration along the tumor front correlates with improved survival in colon cancer. *Clin Cancer Res*. (2007) 13:1472–9. doi: 10.1158/1078-0432.CCR-06-2073
139. Tsutsui S, Yasuda K, Suzuki K, Tahara K, Higashi H, Era S. Macrophage infiltration and its prognostic implications in breast cancer: the relationship with VEGF expression and microvessel density. *Oncol Rep*. (2005) 14:425–31. doi: 10.3892/or.14.2.425
140. Herrera M, Herrera A, Domínguez G, Silva J, García V, García JM, et al. Cancer-associated fibroblast and M2 macrophage markers together predict outcome in colorectal cancer patients. *Cancer Sci*. (2013) 104:437–44. doi: 10.1111/cas.12096
141. Zhang H, Wang X, Shen Z, Xu J, Qin J, Sun Y. Infiltration of diametrically polarized macrophages predicts overall survival of patients with gastric cancer after surgical resection. *Gastric Cancer*. (2015) 18:740–50. doi: 10.1007/s10120-014-0422-7
142. Lan C, Huang X, Lin S, Huang H, Cai Q, Wan T, et al. Expression of M2-polarized macrophages is associated with poor prognosis for advanced epithelial ovarian cancer. *Technol Cancer Res Treat*. (2013) 12:259–67. doi: 10.7785/tcrt.2012.500312
143. Honkanen TJ, Tikkanen A, Karihtala P, Mäkinen M, Väyrynen JP, Koivunen JP. Prognostic and predictive role of tumour-associated macrophages in HER2 positive breast cancer. *Sci Rep*. (2019) 9:1–9. doi: 10.1038/s41598-019-47375-2
144. Adu-Gyamfi CG, Savulescu D, George JA, Suchard MS. Indoleamine 2, 3-dioxygenase-mediated tryptophan catabolism: a leading star or supporting act in the tuberculosis and HIV Pas-de-Deux? *Front Cell Infect Microbiol*. (2019) 9:372. doi: 10.3389/fcimb.2019.00372
145. Herrera-Rios D, Mughal SS, Teuber-Hanselmann S, Pierscianek D, Sucker A, Jansen P, et al. Macrophages/microglia represent the major source of indolamine 2,3-dioxygenase expression in melanoma metastases of the brain. *Front Immunol*. (2020) 11:120. doi: 10.3389/fimmu.2020.00120
146. Karihtala K, Leivonen S-K, Brück O, Karjalainen-Lindsberg M-L, Mustjoki S, Pellinen T, et al. Prognostic impact of tumor-associated macrophages on survival is checkpoint dependent in classical hodgkin lymphoma. *Cancers*. (2020) 12:877. doi: 10.3390/cancers12040877
147. Nakamura K, Smyth MJ. Myeloid immunosuppression and immune checkpoints in the tumor microenvironment. *Cell Mol Immunol*. (2019) 17:1–12. doi: 10.1038/s41423-019-0306-1
148. Chon SY, Hassanain HH, Gupta SL. Cooperative role of interferon regulatory factor 1 and p91 (STAT1) response elements in interferon-γ-inducible expression of human indoleamine 2,3-dioxygenase gene. *J Biol Chem*. (1996) 271:17247–52. doi: 10.1074/jbc.271.29.17247
149. Sedlmayr P, Blaschitz A, Stocker R. The role of placental tryptophan catabolism. *Front Immunol*. (2014) 5:230. doi: 10.3389/fimmu.2014.00230
150. Blaschitz A, Gauster M, Fuchs D, Lang I, Maschke P, Ulrich D, et al. Vascular endothelial expression of indoleamine 2,3-dioxygenase 1 forms a positive gradient towards the feto-maternal interface. *PLoS ONE*. (2011) 6:e0021774. doi: 10.1371/journal.pone.0021774
151. Munn DH, Zhou M, Attwood JT, Bondarev I, Conway SJ, Marshall B, et al. Prevention of allogeneic fetal rejection by tryptophan catabolism. *Science*. (1998) 281:1191–3. doi: 10.1126/science.281.5380.1191
152. Mellor AL, Sivakumar J, Chandler P, Smith K, Molina H, Mao D, et al. Prevention of T cell–driven complement activation and inflammation by tryptophan catabolism during pregnancy. *Nat Immunol*. (2001) 2:64–8. doi: 10.1038/83183

153. Däubener W, Schmidt SK, Heseler K, Spekker KH, MacKenzie CR. Antimicrobial and immunoregulatory effector mechanisms in human endothelial cells. *Thromb Haemost*. (2009) 102:1110–6. doi: 10.1160/TH09-04-0250
154. Santoso DIS, Rogers P, Wallace EM, Manuelpillai U, Walker D, Subakir SB. Localization of indoleamine 2,3-dioxygenase and 4-hydroxynonenal in normal and pre-eclamptic placentae. *Placenta*. (2002) 23:373–9. doi: 10.1053/plac.2002.0818
155. Kudo Y, Boyd CAR, Sargent IL, Redman CWG. Decreased tryptophan catabolism by placental indoleamine 2,3-dioxygenase in preeclampsia. *Am J Obstet Gynecol*. (2003) 188:719–26. doi: 10.1067/mob.2003.156
156. Adam R, Rüssing D, Adams O, Ailyati A, Kim KS, Schroten H, et al. Role of human brain microvascular endothelial cells during central nervous system infection. *Thromb Haemost*. (2005) 94:341–6. doi: 10.1160/TH05-01-0053
157. Däubener W, Spors B, Hucke C, Adam R, Stins M, Kim KS, et al. Restriction of *Toxoplasma gondii* growth in human brain microvascular endothelial cells by activation of indoleamine 2,3-dioxygenase. *Infect Immun*. (2001) 69:6527–31. doi: 10.1128/IAI.69.10.6527-6531.2001
158. Wang Y, Liu H, McKenzie G, Witting PK, Stasch J-P, Hahn M, et al. Kynurenine is an endothelium-derived relaxing factor produced during inflammation. *Nat Med*. (2010) 16:279–85. doi: 10.1038/nm.2092
159. Darcy CJ, Davis JS, Woodberry T, McNeil YR, Stephens DP, Yeo TW, et al. An observational cohort study of the kynurenine to tryptophan ratio in sepsis: association with impaired immune and microvascular function. *PLoS ONE*. (2011) 6:e21185. doi: 10.1371/journal.pone.0021185
160. Padberg J-S, Van Meurs M, Kielstein JT, Martens-Lobenhoffer J, Bode-Böger SM, Zijlstra JG, et al. Indoleamine-2,3-dioxygenase activity in experimental human endotoxemia. *Exp Transl Stroke Med*. (2012) 4:24. doi: 10.1186/2040-7378-4-24
161. Toya T, Sara JD, Corban MT, Taher R, Godo S, Herrmann J, et al. Assessment of peripheral endothelial function predicts future risk of solid-tumor cancer. *Eur J Prev Cardiol*. (2019) 27:608–18. doi: 10.1177/2047487319884246
162. Tokumoto M, Tanaka H, Tauchi Y, Tamura T, Toyokawa T, Kimura K, et al. Immunoregulatory function of lymphatic endothelial cells in tumor-draining lymph nodes of human gastric cancer. *Anticancer Res*. (2017) 37:2875–83. doi: 10.21873/anticanres.11640
163. Cui G, Li C, Xu G, Sun Z, Zhu L, Li Z, et al. Tumor-associated fibroblasts and microvessels contribute to the expression of immunosuppressive factor indoleamine 2, 3-dioxygenase in human esophageal cancers. *Pathol Oncol Res*. (2018) 24:269–75. doi: 10.1007/s12253-017-0244-0
164. Mouratidis PX, George AJ. Regulation of indoleamine 2,3-dioxygenase in primary human saphenous vein endothelial cells. *J Inflamm Res*. (2015) 8:97–106. doi: 10.2147/JIR.S82202
165. Lahdou I, Engler C, Mehrle S, Daniel V, Sadeghi M, Opelz G, et al. Role of human corneal endothelial cells in T-cell–mediated alloimmune attack *in vitro*. *Invest Ophthalmol Vis Sci*. (2014) 55:1213–21. doi: 10.1167/iovs.13-11930
166. Tewalt EF, Cohen JN, Rouhani SJ, Guidi CJ, Qiao H, Fahl SP, et al. Lymphatic endothelial cells induce tolerance via PD-L1 and lack of costimulation leading to high-level PD-1 expression on CD8 T cells. *Blood*. (2012) 120:4772–82. doi: 10.1182/blood-2012-04-427013
167. Rouhani SJ, Eccles JD, Riccardi P, Peske JD, Tewalt EF, Cohen JN, et al. Roles of lymphatic endothelial cells expressing peripheral tissue antigens in CD4 T-cell tolerance induction. *Nat Commun*. (2015) 6:1–13. doi: 10.1038/ncomms7771
168. Lane RS, Femel J, Breazeale AP, Loo CP, Thibault G, Kaempf A, et al. IFNγ-activated dermal lymphatic vessels inhibit cytotoxic T cells in melanoma and inflamed skin. *J Exp Med*. (2018) 215:3057–74. doi: 10.1084/jem.20180654
169. Valkenburg KC, de Groot AE, Pienta KJ. Targeting the tumour stroma to improve cancer therapy. *Nat Rev Clin Oncol*. (2018) 15:366–81. doi: 10.1038/s41571-018-0007-1
170. Chen X, Song E. Turning foes to friends: targeting cancer-associated fibroblasts. *Nat Rev Drug Discov*. (2019) 18:99–115. doi: 10.1038/s41573-018-0004-1
171. Horwitz EM, Le Blanc K, Dominici M, Mueller I, Slaper-Cortenbach I, Marini FC, et al. Clarification of the nomenclature for MSC: the International Society for Cellular Therapy position statement. *Cytotherapy*. (2005) 7:393–5. doi: 10.1080/14653240500319234
172. Phinney DG, Prockop DJ. Concise review: mesenchymal stem/multipotent stromal cells: the state of transdifferentiation and modes of tissue repair—current views. *Stem Cells*. (2007) 25:2896–902. doi: 10.1634/stemcells.2007-0637
173. Direkze NC, Hodivala-Dilke K, Jeffery R, Hunt T, Poulsom R, Oukrif D, et al. Bone marrow contribution to tumor-associated myofibroblasts and fibroblasts. *Cancer Res*. (2004) 64:8492–5. doi: 10.1158/0008-5472.CAN-04-1708
174. Mishra PJ, Mishra PJ, Humeniuk R, Medina DJ, Alexe G, Mesirov JP, et al. Carcinoma associated fibroblast like differentiation of human mesenchymal stem cells. *Cancer Res*. (2008) 68:4331–9. doi: 10.1158/0008-5472.CAN-08-0943
175. Spaeth EL, Dembinski JL, Sasser AK, Watson K, Klopp A, Hall B, et al. Mesenchymal stem cell transition to tumor-associated fibroblasts contributes to fibrovascular network expansion and tumor progression. *PLoS ONE*. (2009) 4:e4992. doi: 10.1371/journal.pone.0004992
176. Rucker HK, Wynder HJ, Thomas WE. Cellular mechanisms of CNS pericytes. *Brain Res Bull*. (2000) 51:363–9. doi: 10.1016/S0361-9230(99)00260-9
177. Sims DE. Diversity within pericytes. *Clin Exp Pharmacol Physiol*. (2000) 27:842–6. doi: 10.1046/j.1440-1681.2000.03343.x
178. Bergers G, Song S. The role of pericytes in blood-vessel formation and maintenance. *Neuro-Oncol*. (2005) 7:452–64. doi: 10.1215/S1152851705000232
179. Gerhardt H, Betsholtz C. Endothelial-pericyte interactions in angiogenesis. *Cell Tissue Res*. (2003) 314:15–23. doi: 10.1007/s00441-003-0745-x
180. Armulik A, Abramsson A, Betsholtz C. Endothelial/pericyte interactions. *Circ Res*. (2005) 97:512–23. doi: 10.1161/01.RES.0000182903.16652.d7
181. Hosaka K, Yang Y, Seki T, Fischer C, Dubey O, Fredlund E, et al. Pericyte–fibroblast transition promotes tumor growth and metastasis. *Proc Natl Acad Sci USA*. (2016) 113:5618–27. doi: 10.1073/pnas.1608384113
182. Weinlich G, Murr C, Richardsen L, Winkler C, Fuchs D. Decreased serum tryptophan concentration predicts poor prognosis in malignant melanoma patients. *Dermatology*. (2007) 214:8–14. doi: 10.1159/000096906
183. Corm S, Berthon C, Imbenotte M, Biggio V, Lhermitte M, Dupont C, et al. Indoleamine 2,3-dioxygenase activity of acute myeloid leukemia cells can be measured from patients' sera by HPLC and is inducible by IFN-γ. *Leuk Res*. (2009) 33:490–4. doi: 10.1016/j.leukres.2008.06.014
184. Folgiero V, Goffredo BM, Filippini P, Masetti R, Bonanno G, Caruso R, et al. Indoleamine 2,3-dioxygenase 1 (IDO1) activity in leukemia blasts correlates with poor outcome in childhood acute myeloid leukemia. *Oncotarget*. (2013) 5:2052–64. doi: 10.18632/oncotarget.1504
185. Mabuchi R, Hara T, Matsumoto T, Shibata Y, Nakamura N, Nakamura H, et al. High serum concentration of L-kynurenine predicts unfavorable outcomes in patients with acute myeloid leukemia. *Leuk Lymphoma*. (2016) 57:92–8. doi: 10.3109/10428194.2015.1041388
186. Zhai L, Dey M, Lauing KL, Gritsina G, Kaur R, Lukas RV, et al. The kynurenine to tryptophan ratio as a prognostic tool for glioblastoma patients enrolling in immunotherapy. *J Clin Neurosci*. (2015) 22:1964–8. doi: 10.1016/j.jocn.2015.06.018
187. Ferns DM, Kema IP, Buist MR, Nijman HW, Kenter GG, Jordanova ES. Indoleamine-2,3-dioxygenase (IDO) metabolic activity is detrimental for cervical cancer patient survival. *OncoImmunology*. (2015) 4:e981457. doi: 10.4161/2162402X.2014.981457
188. Suzuki Y, Suda T, Furuhashi K, Suzuki M, Fujie M, Hahimoto D, et al. Increased serum kynurenine/tryptophan ratio correlates with disease progression in lung cancer. *Lung Cancer*. (2010) 67:361–5. doi: 10.1016/j.lungcan.2009.05.001
189. Wang W, Huang L, Jin J-Y, Jolly S, Zang Y, Wu H, et al. IDO immune status after chemoradiation may predict survival in lung cancer patients. *Cancer Res*. (2018) 78:809–16. doi: 10.1158/0008-5472.CAN-17-2995
190. Botticelli A, Cerbelli B, Lionetto L, Zizzari I, Salati M, Pisano A, et al. Can IDO activity predict primary resistance to anti-PD-1 treatment in NSCLC? *J Transl Med*. (2018) 16:219. doi: 10.1186/s12967-018-1595-3
191. Sundahl N, De Wolf K, Kruse V, Meireson A, Reynders D, Goetghebeur E, et al. Phase 1 dose escalation trial of ipilimumab and stereotactic body radiation therapy in metastatic melanoma. *Int J Radiat Oncol*. (2018) 100:906–15. doi: 10.1016/j.ijrobp.2017.11.029

192. Botticelli A, Mezi S, Pomati G, Cerbelli B, Cerbelli E, Roberto M, et al. Tryptophan catabolism as immune mechanism of primary resistance to anti-PD-1. *Front Immunol*. (2020) 11:1243. doi: 10.3389/fimmu.2020.01243
193. Li H, Bullock K, Gurjao C, Braun D, Shukla SA, Bossé D, et al. Metabolomic adaptations and correlates of survival to immune checkpoint blockade. *Nat Commun*. (2019) 10:1–6. doi: 10.1038/s41467-019-12361-9
194. Zhou Q-H, Han H, Lu J-B, Liu T-Y, Huang K-B, Deng C-Z, et al. Up-regulation of indoleamine 2,3-dioxygenase 1 (IDO1) expression and catalytic activity is associated with immunosuppression and poor prognosis in penile squamous cell carcinoma patients. *Cancer Commun Lond Engl*. (2020) 40:3–15. doi: 10.1002/cac2.12001
195. Li H, Ning S, Ghandi M, Kryukov GV, Gopal S, Deik A, et al. The landscape of cancer cell line metabolism. *Nat Med*. (2019) 25:850–60. doi: 10.1038/s41591-019-0404-8
196. Zhai L, Ladomersky E, Dostal CR, Lauing KL, Swoap K, Billingham LK, et al. Non-tumor cell IDO1 predominantly contributes to enzyme activity and response to CTLA-4/PD-L1 inhibition in mouse glioblastoma. *Brain Behav Immun*. (2017) 62:24–9. doi: 10.1016/j.bbi.2017.01.022
197. Munn DH, Sharma MD, Lee JR, Jhaver KG, Johnson TS, Keskin DB, et al. Potential regulatory function of human dendritic cells expressing indoleamine 2,3-dioxygenase. *Science*. (2002) 297:1867–70. doi: 10.1126/science.1073514
198. Tas SW, Vervoordeldonk MJ, Hajji N, Schuitemaker JHN, van der Sluijs KF, May MJ, et al. Noncanonical NF-κB signaling in dendritic cells is required for indoleamine 2,3-dioxygenase (IDO) induction and immune regulation. *Blood*. (2007) 110:1540–9. doi: 10.1182/blood-2006-11-056010
199. Hwang SL, Chung NP-Y, Chan JK-Y, Lin C-LS. Indoleamine 2, 3-dioxygenase (IDO) is essential for dendritic cell activation and chemotactic responsiveness to chemokines. *Cell Res*. (2005) 15:167–75. doi: 10.1038/sj.cr.7290282
200. Munn DH, Sharma MD, Mellor AL. Ligation of B7-1/B7-2 by Human CD4+ T cells triggers indoleamine 2,3-dioxygenase activity in dendritic cells. *J Immunol*. (2004) 172:4100–10. doi: 10.4049/jimmunol.172.7.4100
201. Boasso A, Herbeuval J-P, Hardy AW, Anderson SA, Dolan MJ, Fuchs D, et al. HIV inhibits CD4+ T-cell proliferation by inducing indoleamine 2,3-dioxygenase in plasmacytoid dendritic cells. *Blood*. (2007) 109:3351–9. doi: 10.1182/blood-2006-07-034785
202. Kavousanaki M, Makrigiannakis A, Boumpas D, Verginis P. Novel role of plasmacytoid dendritic cells in humans: induction of interleukin-10–producing treg cells by plasmacytoid dendritic cells in patients with rheumatoid arthritis responding to therapy. *Arthritis Rheum*. (2010) 62:53–63. doi: 10.1002/art.25037
203. Yun TJ, Lee JS, Machmach K, Shim D, Choi J, Wi YJ, et al. Indoleamine 2,3-dioxygenase-expressing aortic plasmacytoid dendritic cells protect against atherosclerosis by induction of regulatory T cells. *Cell Metab*. (2016) 23:852–66. doi: 10.1016/j.cmet.2016.04.010
204. Zhang H, Gregorio JD, Iwahori T, Zhang X, Choi O, Tolentino LL, et al. A distinct subset of plasmacytoid dendritic cells induces activation and differentiation of B and T lymphocytes. *Proc Natl Acad Sci USA*. (2017) 114:1988–93. doi: 10.1073/pnas.1610630114
205. Chevolet I, Speeckaert R, Schreuer M, Neyns B, Krysko O, Bachert C, et al. Clinical significance of plasmacytoid dendritic cells and myeloid-derived suppressor cells in melanoma. *J Transl Med*. (2015) 13:9. doi: 10.1186/s12967-014-0376-x
206. Brochez L, Meireson A, Chevolet I, Sundahl N, Ost P, Kruse V. Challenging PD-L1 expressing cytotoxic T cells as a predictor for response to immunotherapy in melanoma. *Nat Commun*. (2018) 9:2921. doi: 10.1038/s41467-018-05047-1
207. Okła K, Czerwonka A, Wawruszak A, Bobiński M, Bilska M, Tarkowski R, et al. Clinical relevance and immunosuppressive pattern of circulating and infiltrating subsets of myeloid-derived suppressor cells (MDSCs) in epithelial ovarian cancer. *Front Immunol*. (2019) 10:691. doi: 10.3389/fimmu.2019.00691
208. Holmgaard RB, Zamarin D, Munn DH, Wolchok JD, Allison JP. Indoleamine 2,3-dioxygenase is a critical resistance mechanism in antitumor T cell immunotherapy targeting CTLA-4. *J Exp Med*. (2013) 210:1389–402. doi: 10.1084/jem.20130066
209. Spranger S, Koblish HK, Horton B, Scherle PA, Newton R, Gajewski TF. Mechanism of tumor rejection with doublets of CTLA-4, PD-1/PD-L1, or IDO blockade involves restored IL-2 production and proliferation of CD8+ T cells directly within the tumor microenvironment. *J Immunother Cancer*. (2014) 2:3. doi: 10.1186/2051-1426-2-3
210. Monjazeb AM, Kent MS, Grossenbacher SK, Mall C, Zamora AE, Mirsoian A, et al. Blocking indolamine-2,3-dioxygenase rebound immune suppression boosts antitumor effects of radio-immunotherapy in murine models and spontaneous canine malignancies. *Clin Cancer Res*. (2016) 22:4328–40. doi: 10.1158/1078-0432.CCR-15-3026
211. Beatty GL, O'Dwyer PJ, Clark J, Shi JG, Bowman KJ, Scherle PA, et al. First-in-human phase I study of the oral inhibitor of indoleamine 2,3-dioxygenase-1 epacadostat (INCB024360) in patients with advanced solid malignancies. *Clin Cancer Res Off J Am Assoc Cancer Res*. (2017) 23:3269–76. doi: 10.1158/1078-0432.CCR-16-2272
212. Gibney GT, Hamid O, Lutzky J, Olszanski AJ, Mitchell TC, Gajewski TF, et al. Phase 1/2 study of epacadostat in combination with ipilimumab in patients with unresectable or metastatic melanoma. *J Immunother Cancer*. (2019) 7:80. doi: 10.1186/s40425-019-0562-8
213. Perez RP, Riese MJ, Lewis KD, Saleh MN, Daud A, Berlin J, et al. Epacadostat plus nivolumab in patients with advanced solid tumors: preliminary phase I/II results of ECHO-204. *J Clin Oncol*. (2017) 35:3003. doi: 10.1200/JCO.2017.35.15_suppl.3003
214. Mitchell TC, Hamid O, Smith DC, Bauer TM, Wasser JS, Olszanski AJ, et al. Epacadostat plus pembrolizumab in patients with advanced solid tumors: phase I results from a multicenter, open-label phase I/II trial (ECHO-202/KEYNOTE-037). *J Clin Oncol*. (2018) 36:3223–30. doi: 10.1200/JCO.2018.78.9602
215. Long GV, Dummer R, Hamid O, Gajewski TF, Caglevic C, Dalle S, et al. Epacadostat plus pembrolizumab versus placebo plus pembrolizumab in patients with unresectable or metastatic melanoma (ECHO-301/KEYNOTE-252): a phase 3, randomised, double-blind study. *Lancet Oncol*. (2019) 20:1083–97. doi: 10.1016/S1470-2045(19)30274-8
216. Muller AJ, Manfredi MG, Zakharia Y, Prendergast GC. Inhibiting IDO pathways to treat cancer: lessons from the ECHO-301 trial and beyond. *Semin Immunopathol*. (2019) 41:41–8. doi: 10.1007/s00281-018-0702-0
217. Chevolet I, Schreuer M, Speeckaert R, Neyns B, Hoorens I, van Geel N, et al. Systemic immune changes associated with adjuvant interferon-α2b-therapy in stage III melanoma patients: failure at the effector phase? *Melanoma Res*. (2015) 25:357–61. doi: 10.1097/CMR.0000000000000171
218. Siu L, Gelmon K, Chu Q, Pachynski R, Alese O, Basciano P, et al. BMS-986205, an optimized indoleamine 2,3-dioxygenase 1 (IDO1) inhibitor, is well tolerated with potent pharmacodynamic (PD) activity, alone and in combination with nivolumab (nivo) in advanced cancers in a phase 1/2a trial. *Cancer Res*. (2017) 77:CT116. doi: 10.1158/1538-7445.AM2017-CT116
219. *BMS-986205 and Nivolumab as First or Second Line Therapy in Treating Patients With Liver Cancer*. Available online at: https://clinicaltrials.gov/ct2/show/NCT03695250 (accessed June 18, 2020).
220. *Study of BMS-986205 and Nivolumab in Endometrial Cancer or Endometrial Carcinosarcoma That Has Not Responded to Treatment*. Available online at: https://clinicaltrials.gov/ct2/show/NCT04106414 (accessed June 18, 2020).

221. *Nivolumab and BMS986205 in Treating Patients With Stage II-IV Squamous Cell Cancer of the Head and Neck*. Available online at: https://clinicaltrials.gov/ct2/show/NCT03854032 (accessed June 18, 2020).
222. Metz R, Rust S, DuHadaway JB, Mautino MR, Munn DH, Vahanian NN, et al. IDO inhibits a tryptophan sufficiency signal that stimulates mTOR. *Oncoimmunology*. (2012) 1:1460–8. doi: 10.4161/onci.21716
223. Fox E, Oliver T, Rowe M, Thomas S, Zakharia Y, Gilman PB, et al. Indoximod: an immunometabolic adjuvant that empowers T cell activity in cancer. *Front Oncol*. (2018) 8:370. doi: 10.3389/fonc.2018.00370
224. Prendergast GC, Malachowski WJ, Mondal A, Scherle P, Muller AJ. Indoleamine 2,3-dioxygenase and its therapeutic inhibition in cancer. *Int Rev Cell Mol Biol*. (2018) 336:175–203. doi: 10.1016/bs.ircmb.2017.07.004
225. Ye Z, Yue L, Shi J, Shao M, Wu T. Role of IDO and TDO in cancers and related diseases and the therapeutic implications. *J Cancer*. (2019) 10:2771–82. doi: 10.7150/jca.31727

Conflict of Interest: LB was participant in advisory board Incyte, München, Germany, June 2017 and gave an internal training for Incyte European division, Amsterdam, October 2017.

The remaining authors declare that the research was conducted in the absence of any commercial or financial relationships that could be construed as a potential conflict of interest.

Advantages of publishing in Frontiers

OPEN ACCESS
Articles are free to read for greatest visibility and readership

FAST PUBLICATION
Around 90 days from submission to decision

HIGH QUALITY PEER-REVIEW
Rigorous, collaborative, and constructive peer-review

TRANSPARENT PEER-REVIEW
Editors and reviewers acknowledged by name on published articles

Frontiers
Avenue du Tribunal-Fédéral 34
1005 Lausanne | Switzerland

Visit us: www.frontiersin.org
Contact us: frontiersin.org/about/contact

REPRODUCIBILITY OF RESEARCH
Support open data and methods to enhance research reproducibility

DIGITAL PUBLISHING
Articles designed for optimal readership across devices

FOLLOW US
@frontiersin

IMPACT METRICS
Advanced article metrics track visibility across digital media

EXTENSIVE PROMOTION
Marketing and promotion of impactful research

LOOP RESEARCH NETWORK
Our network increases your article's readership